Addis Ababa University

College of Technology and Built Environment

School of Civil and Environmental Engineering

Green-Grey Infrastructure Development for Sustainable Stormwater Management in Addis Ababa, Ethiopia

Dissertation for the Degree of Doctor of Philosophy

By Bilal Kemal Harun

May 2026

Addis Ababa

Green-Grey Infrastructure Development for Sustainable Stormwater Management in Addis Ababa, Ethiopia

Ph.D. Dissertation

By Bilal Kemal Harun

Main Supervisor

Professor Dr. Ing. Geremew Sahilu Gebre

School of Civil and Environmental Engineering, College of Technology and Bult Environment,

Addis Ababa University, Ethiopia

A Ph.D. Dissertation Submitted in Partial Fulfillment of the Requirements for the Degree of Doctor of Philosophy (Ph.D.) in Civil and Environmental Engineering (Hydraulic Engineering)

Declaration of Authorship

I, the undersigned, declare that this doctoral dissertation is my original work and has not been presented for any degree in any other university, and that all sources of materials used in this dissertation have been duly acknowledged.

Bilal Kemal Harun	____________	5/8/2026
PhD Candidate	Signature	Date

This doctoral dissertation has been submitted for examination with my approval (main advisor) and co-advisors as university advisors:

Prof. Dr. -Ing. Geremew Sahilu	____________	5/8/2026
Main Advisor	Signature	Date
Prof. Dr. -Ing. Dereje Hailu	Dereje Hailu	5/8/2026
Co–Advisor	Signature	Date
Dr. Daneal Fikeresilassie (Assist. Prof.)	Daneal Fls	5/8/2026
Co–Advisor	Signature	Date
Dr. Solomon Seyoum (Assist. Prof.)	____________	5/8/2026
Co–Advisor	Signature	Date

Doctoral Dissertation Approval Sheet

We, the undersigned, have examined the dissertation entitled ***"Green-Grey Infrastructure Development for Sustainable Stormwater Management in Addis Ababa, Ethiopia",*** submitted by Bilal Kemal Harun, a candidate for the degree of Doctor of Philosophy at the School of Civil and Environmental Engineering, College of Technology and Built Environment, Addis Ababa University. We hereby certify that the dissertation meets the standards required for acceptance.

Bilal Kemal Harun ______________ 5/8/2026

PhD Candidate Signature Date

Approved By Board of Examiners

Prof. Dr. -Ing. Esayas Alemayehu ______________ 5/8/2026

External Examiner Signature Date

Dr. Agizew Nigussie (Assoc. Prof.) ______________ 5/8/2026

Internal Examiner Signature Date

Yenesew Mengiste (Dr.-Ing.)
Head, Scclool of Civil &
Environmental Engineering

Dr. Yenesew Mengiste (Assist. Prof.) ______________ 5/8/2026

Dean, School of Civil and Environmental Engineering Signature Date

Chairperson of the Examining Board

Acknowledgement

First and foremost, I express my deepest gratitude to Allah, the Almighty, for His guidance, blessings, and strength, without which this research would not have been possible.

I am profoundly grateful to my major advisor, Prof. Dr. Ing. Geremew Sahilu, for his continuous guidance, invaluable insights, and unwavering support throughout all stages of this study. My sincere thanks also go to my co-advisors, Prof. Dr. Ing. Dereje Hailu, Dr. Daneal Fekeresellassie, and Dr. Solomon Seyoum, for their constructive feedback, encouragement, and expert advice, which greatly enriched this dissertation.

I extend my heartfelt appreciation to my beloved wife, whose patience, encouragement, and constant support provided me with motivation and comfort during this demanding journey.

I would like to acknowledge the School of Civil and Environmental Engineering, Addis Ababa University, for providing the essential facilities and resources needed to conduct this research. I am also grateful to the Nefas Silk Lafto Sub-City of Addis Ababa for their cooperation in granting access to the pilot study area for the Integrated Green and Grey Infrastructure (IGGI) intervention.

My gratitude goes to the Ethiopian Meteorology Agency, Addis Ababa Road Authority, and the Ministry of Agriculture, as well as to the experts who responded to my questionnaires and provided crucial input for this study. I also acknowledge the support of the Water Quality Laboratories at Addis Ababa University and Addis Ababa Science and Technology University for their assistance in conducting laboratory analyses.

Special thanks are due to Computational Hydraulics International for providing student licenses for PCSWMM Professional Version, which enabled essential hydrological modeling for this research.

Finally, I extend my appreciation to family members, all individuals and institutions who contributed directly or indirectly to the successful completion of this dissertation.

Dedication

I dedicate this dissertation first and foremost to Allah, the Almighty, whose guidance, mercy, and blessings have made this work possible. Thereafter, I honor my beloved wife, my sweet daughter, and family, creations of Allah, whose love, patience, and unwavering support have been a source of strength, inspiration, and motivation throughout this journey.

List of Publications: Journal Articles

1 Kemal, B., Hailu, D., Fekersillassie, D., Seyoum, S., & Sahilu, G. (2025). Assessing green and grey infrastructure suitability in Addis Ababa, Ethiopia using GIS-based multi-criteria analysis. *Environmental Earth Sciences*, *84*(16), 455. https://doi.org/10.1007/s12665-025-12441-8

2 Kemal, B., Hailu, D., Fekersillassie, D., Seyoum, S., Sahilu, G., & Tariq, A. (2025). Stormwater modeling in a steep, poorly drained contributing micro-watershed zone of Addis Ababa. *Earth Systems and Environment*, *10*(3), 3029-3049. https://doi.org/10.1007/s41748-025-00765-1

3 Kemal, B., Hailu, D., Fekersillassie, D., Seyoum, S., & Sahilu, G. (2026). Multi-criteria performance evaluation of stormwater infrastructure in a micro urban watershed, Addis Ababa, Ethiopia. *PLOS Water*, *5*(6), e0000494. https://doi.org/10.1371/journal.pwat.0000494

4 Kemal, B., Hailu, D., Fekersillassie, D., Seyoum, S., & Sahilu, G. (2026). A novel integration of green-grey infrastructure in steep slope micro-watersheds: PCSWMM modeling for non-draining soils in Addis Ababa. *Environmental Systems Research*, *15*(1), 3. https://doi.org/10.1186/s40068-025-00435-1

Table of Contents

List of Tables

List of Figures

List of Appendix Tables

List of Appendix Figures

Abbreviations

AHP Analytical Hierarchy Process

ALOS-PALSAR Advanced Land Observing Satellite – Phased Array type L-band Synthetic Aperture Radar

ANP Analytic Network Process

AUC Area Under the Curve

BMP Best Management Practice

BOD Biochemical Oxygen Demand

CC Climate Change

CHI Computational Hydraulics International

CI Consistency Index

Ci Consistency Measure of Criterion i

CMIP Coupled Model Intercomparison Project

COD Chemical Oxygen Demand

CR Consistency Ratio

CSS Central Statistical Service

DEM Digital Elevation Model

ELECTRE ELimination Et Choix Traduisant la REalité (a multi-criteria decision method)

EMC Event Mean Concentration

EPA Environmental Protection Agency

ESS Ecosystem Services

ETB Ethiopian Birr

FAO Food and Agriculture Organization

GCM Global Climate Model

GEV Generalized Extreme Value

GI Green Infrastructure

GIS Geographic Information System

GPD Generalized Pareto Distribution

GPS Global Positioning System

IDF Intensity-Duration-Frequency

IGGI Integrated Green-Grey Infrastructure

IMD	India Meteorological Department (used for rainfall reference)
ISE	Integral Square Error
IUWM	Integrated Urban Water Management
K	Frequency Factor
KGE	Kling–Gupta Efficiency
LID	Low Impact Development
LULC	Land Use / Land Cover
LUV	Land Use and Vegetation
MAUT	Multi-Attribute Utility Theory
MCDA	Multi-Criteria Decision Analysis
MCDM	Multi-Criteria Decision-Making
MOALOA	Multi-Objective Adaptive Learning Optimization Algorithm
MOPSO	Multi-Objective Particle Swarm Optimization
NBS	Nature-Based Solutions
NDVI	Normalized Difference Vegetation Index
NMA	National Meteorological Agency (Ethiopia)
NSE	Nash–Sutcliffe Efficiency
NSGA	Non-dominated Sorting Genetic Algorithm
O&M	Operation and Maintenance
OAT	One-at-a-Time Sensitivity Analysis
OF	Outfall
PBIAS	Percent Bias
PCSWMM	Personal Computer Storm Water Management Model
PROMETHEE	Preference Ranking Organization Method for Enrichment Evaluation
QGIS	Quantum Geographic Information System
RB	Rain Barrel
RG	Rain Garden
RI	Random Index
RMSE	Root Mean Square Error
RSR	RMSE-Standard Deviation Ratio
SDG	Sustainable Development Goals

SMA	Simple Moving Average
SRTC	Sensitivity-Based Radio Tuning Calibration
SSA	Socio-Spatial and Accessibility
SSP	Shared Socioeconomic Pathway
SuDS	Sustainable Drainage Systems
SUSM	Sustainable Urban Stormwater Management
SUSTAIN	System for Urban Stormwater Treatment and Analysis INtegration
SWMM	Storm Water Management Model
TDS	Total Dissolved Solids
TH	Topographical and Hydrological
TN	Total Nitrogen
TOPSIS	Technique for Order of Preference by Similarity to Ideal Solution
TP	Total Phosphorus
TPI	Topographic Position Index
TRI	Topographic Ruggedness Index
TSS	Total Suspended Solids
TWI	Topographic Wetness Index
UGS	Urban Green Space
UN	United Nations
UNESCO	United Nations Educational, Scientific and Cultural Organization
US	United States
USA	United States of America
USD	United States Dollar
USDA	United States Department of Agriculture
USEPA	United States Environmental Protection Agency
USGS	United States Geological Survey
WLC	Weighted Linear Combination
WSUD	Water Sensitive Urban Design

Abstract

Rapid urbanization and climate change intensify stormwater challenges in developing cities. Conventional grey systems fail under extreme events, and green infrastructure alone is insufficient on steep slopes and poorly draining Vertisol soils. This dissertation develops an Integrated Green-Grey Infrastructure (IGGI) framework for Addis Ababa, Ethiopia, through four interlinked studies.

First, a GIS-based Multi-Criteria Decision Analysis (AHP and ANP) maps IGGI suitability across the city. The ANP model (AUC = 0.92, RMSE = 0.12) outperforms AHP, identifying 59.86% of Addis Ababa as suitable for IGGI. Second, PCSWMM modeling of a 30-ha steep, Vertisol-dominated micro-watershed shows that under climate change (SSP5-8.5, mid-term) peak flows increase up to 83%, while urbanization (80% imperviousness) raises pollutant loads by 7–12%. Urbanization is the dominant driver of water quality decline. Third, a TOPSIS-AHP-PCSWMM evaluation of 30 stormwater infrastructure units reveals that 42.3% are ready for GI retrofitting, with sediment accumulation and conveyance capacity as key performance determinants. Fourth, a novel IGGI system integrating buried rain barrels with conventional rain gardens is field-tested in a steep, Vertisol-dominated contributing zone. The system achieves 43.5% peak-flow reduction, 36.7% runoff-volume reduction, and 37.2–42.4% pollutant-load reduction – substantially outperforming conventional systems.

The findings provide a scalable, climate-resilient, and context-sensitive IGGI framework for Addis Ababa and comparable Global South cities, contributing directly to SDGs 6 (Clean Water and Sanitation), 11 (Sustainable Cities and Communities), and 13 (Climate Action).

Keywords: IGGI, stormwater management, AHP, ANP, TOPSIS, PCSWMM, runoff, pollutant load, climate change, Addis Ababa.

Chapter 1

1 Introduction

1.1 Background of the Study

Urban stormwater management has emerged as one of the defining sustainability and resilience challenges of the twenty-first century. As urbanization accelerates, the conversion of vegetated and permeable land surfaces into impervious structures—such as roads, pavements, and rooftops—has fundamentally altered natural hydrological processes. This transformation disrupts the balance between infiltration, evapotranspiration, and surface runoff, leading to higher peak discharges, reduced groundwater recharge, and increased pollutant transport (Barbosa et al., 2012; Oudin et al., 2018; Zhou et al., 2019). Climate change further amplifies these effects by increasing the frequency and intensity of extreme precipitation events and altering rainfall patterns, thereby exacerbating flooding risks, degrading water quality, and threatening urban ecosystems and public health (Almaliki et al., 2023; Moisa et al., 2023; Zerouali et al., 2022).

Historically, stormwater management has relied on conventional grey infrastructure—engineered systems such as culverts, pipes, detention tanks, and concrete channels—designed primarily to control stormwater quantity through rapid collection and conveyance. While such systems have proven effective in managing peak flows in the short term, they are increasingly recognized as unsustainable due to their rigidity, limited adaptability, high maintenance costs, and environmental drawbacks. Grey infrastructure disrupts natural hydrological connectivity, transfers flood risks downstream, and provides no ecological and social co-benefits (Butler et al., 2016; Holm et al., 2014; McFarland et al., 2019). As climate and land-use pressures intensify, the inability of these systems to adapt to dynamic hydrological conditions and urban growth has become a major urban planning and environmental challenge.

In response, a paradigm shift has occurred toward Green Infrastructure (GI)—approaches that mimic natural hydrologic functions through infiltration, retention, evapotranspiration, and stormwater reuse. GI measures—such as bio-retention cell, infiltration trench, permeable pavement, rain barrel, vegetative swale, rain garden, green roof, and rooftop disconnection—have demonstrated significant capacity for reducing runoff volumes, improving water quality, and providing multiple co-benefits including urban cooling, biodiversity enhancement, and aesthetic value (Fletcher et al., 2015; Hua et al., 2020; Qiu et al., 2020). However, GI alone is insufficient to manage intense storm events especially under climate change and rapid urbanization effect. Conversely, grey infrastructure lacks flexibility and ecosystem functionality. This recognition has led to the emergence of IGGI—a hybrid approach that seeks to combine the reliability of engineered systems with the multifunctionality of green, nature-based interventions (Rodríguez et al., 2021; Bai et al., 2018).

IGGI frameworks have been operationalized globally under different terminologies: Low Impact Development (LID) in North America, Sustainable Urban Drainage Systems (SuDS) in the United Kingdom, Water Sensitive Urban Design (WSUD) in Australia, and Sponge City initiatives in China. While the principles differ contextually, they share a common goal—to integrate hydrological, ecological, and engineering perspectives for managing stormwater at its source, restoring natural water pathways, and improving urban resilience. However, their widespread and context-sensitive adoption in developing regions remains limited. In the Global South, including rapidly expanding cities such as Addis Ababa (Ethiopia)**,** Nairobi (Kenya), and Dar es Salaam (Tanzania), stormwater management is constrained by outdated infrastructure, insufficient maintenance, fragmented governance, and limited data availability (Mguni et al., 2015; Mulligan et al., 2020; Kumar et al., 2023).

Addis Ababa exemplifies these challenges. The city has undergone rapid spatial growth—over 20% expansion in urbanized area within the past two decades (Woldegerima et al., 2016; World Bank, 2015)—outpacing infrastructure development and institutional capacity. The existing stormwater drainage system is characterized by undersized and poorly maintained open channels and non-separated sewer networks (Jemberie et al., 2023). This deficiency, coupled with unregulated land development and informal settlements encroaching on natural waterways, has made the city increasingly prone to urban flooding. In 2017 alone, 76 flood events were recorded, disproportionately affecting low-income communities in flood-prone areas along the Akaki River (Birhanu et al., 2016; Jemberie and Melesse, 2021). Furthermore, in watersheds characterized by steep topography and clayey Vertisol soils, limited infiltration leads to rapid surface runoff and sediment-laden flows, which degrade both water quality and infrastructure.

While global advances in IGGI demonstrate its promise, its applicability in steep and poorly draining soil urban environments—like few of Addis Ababa's micro-watersheds—remains poorly understood. Most existing green infrastructure systems are designed for flat or moderately sloping terrain and well-drained soils (EPA, 2014), limiting their effectiveness in Vertisol-dominated landscapes. Consequently, there is an urgent need to develop terrain-sensitive, data-informed, and spatially optimized IGGI strategies that can perform effectively under the city's unique hydrological and geotechnical constraints. Achieving this requires an integrated approach that accounts for land use, slope, soil, and hydrological processes at micro-watershed scale—particularly focusing on contributing zones, which generate the majority of surface runoff and significantly influence downstream flooding dynamics (McFarland et al., 2019; Speak et al., 2013).

1.2 Problem Statement

Despite growing global efforts to implement IGGI as a sustainable solution to urban stormwater challenges, its effective application in environments characterized by steep topography and poorly draining soils remains a persistent and underexplored challenge. In such conditions, steep slopes accelerate overland flow and reduce the time available for infiltration, while low-permeability soils—such as Vertisols (clay)—further restrict infiltration, and percolation, exacerbating surface runoff generation. This hydrological imbalance increases the frequency and severity of flash flooding and elevates pollutant loads in runoff (Barbosa et al., 2012; Zhou et al., 2019; Oudin et al., 2018). These environments demand specialized stormwater management approaches that can both attenuate runoffs, enhance infiltration, and improve water quality under such physical constraints. However, conventional retrofittable GI systems—such as bio-retention cells, infiltration trenches, permeable pavement, rain barrels, vegetative swales, rain gardens, green roofs, and rooftop disconnections—often fail to achieve their design functions under such conditions due to limited infiltration capacity and structural instability on steep gradients. Similarly, grey infrastructure, while hydraulically efficient, often lacks flexibility, adaptability, and ecological functionality (Butler et al., 2017; Holm et al., 2014; McFarland et al., 2019).

This challenge becomes particularly critical within the contributing zones of urban micro-watersheds, which play a decisive role in generating and routing stormwater to downstream collecting and conveyance areas (Marsh, 2010; McFarland et al., 2019; Speak et al., 2013). Nevertheless, current research and practice often focus on the collecting and conveyance zones—where flooding is most visible—rather than the contributing zones where hydrological control is most effective.

In Addis Ababa, Ethiopia, this problem is increasingly evident. The city's complex urban morphology—comprising highland plateaus, mid-slope zones, and low-lying floodplains—creates distinct hydrological behaviors across different sub-watersheds. Although Addis Ababa is not uniformly characterized by steep slopes and poorly draining soils, few micro-watersheds exhibit these conditions, particularly where steep gradients intersect with poorly draining Vertisols (clay) soil. These areas generate rapid surface runoff during high-intensity rainfall events, overwhelming the underdeveloped, poorly maintained, and fragmented drainage infrastructure. The result is recurrent urban flooding, infrastructure damage, and pollution of receiving rivers (Angello et al., 2021; Jemberie et al., 2023; Jemberie and Melesse, 2021).

Conventional grey drainage systems in Addis Ababa—primarily open ditches, pipes, and culverts—have proven insufficient to handle these pressures, while isolated applications of GI remain limited in scale and constrained by space, design, and maintenance challenges (Jemberie et al., 2023; Moisa et al., 2023). Integrating green and grey systems therefore offers a promising but underdeveloped pathway toward urban flood resilience, particularly in micro watersheds characterized by steep slopes and poorly draining soils. Additionally, the city currently lacks a scientifically grounded framework to guide such integration based on spatial suitability, hydrologic dynamics, and infrastructure performance. Furthermore, the effectiveness of integrating most GI systems with grey infrastructure is globally limited to slopes of less than 7% and well-drained soils (EPA, 2014; McFarland et al., 2019; Omitaomu et al., 2021).

Research and planning gaps persist in four critical dimensions:

Spatial Suitability: Absence of GIS-based multi-criteria spatial analyses to identify technically and environmentally appropriate sites for IGGI implementation in heterogeneous urban landscapes.

Hydrologic Understanding: Limited modeling of runoff and pollutant behavior under the combined influences of steep slopes, low-permeability soils, and changing rainfall and land-use conditions in micro-watershed contributing zones.

Infrastructure Performance: Lack of documented assessment on the hydraulic condition, structural performance, and maintenance needs of existing drainage networks to guide IGGI retrofitting priorities.

Integrated Design Framework: There is no established methodology for integrating green and grey infrastructure to function synergistically within topographically steep, poorly draining soils and contributing zones of urban micro-watersheds.

Addressing these gaps is essential for developing resilient, adaptive, and context-sensitive stormwater management strategies in Addis Ababa and similar rapidly urbanizing cities across the

Global South. This study therefore proposes an IGGI framework that combines geospatial analysis, hydrologic modeling, and multi-criteria decision analysis to identify suitable locations, assess the hydrologic dynamics, evaluate existing infrastructure, and design improved integrated systems. By focusing on the contributing zones of micro-watersheds, the research aims to demonstrate that targeted upstream interventions can significantly enhance downstream resilience, reduce flooding risk, and contribute to achieving sustainable, climate-resilient urban water management (Qiu et al., 2020; Rodriguez et al., 2021; Hua et al., 2020; Yang and Zhang, 2021).

1.3 Research Objective

1.3.1 General Objective

To improve the methodology for integrating green and grey infrastructure for sustainable urban stormwater management within Addis Ababa**,** with a particular focus on steep-slope, poorly draining soil, and contributing zone of micro-watersheds**.**

1.3.2 Specific Objectives

- To develop a GIS-based spatial suitability map for IGGI implementation using AHP and ANP, integrating key hydrological, topographical, socio-spatial, and accessibility parameters.
- To quantify surface runoff and pollutant loading in steep slope, poorly draining, soil and contributing zone of micro-watersheds under both current and projected land-use and climatic conditions using hydrologic modeling.
- To evaluate the performance of existing stormwater infrastructure using MCDA and hydrologic evaluation to determine maintenance needs and readiness for IGGI retrofitting.
- To develop and validate a novel IGGI system that integrates buried rain barrels with rain gardens to enable improved flood-mitigation performance and pollutant load reduction in steep, low-infiltration urban micro-watersheds.

1.4 Research Questions (RQ)

1.4.1 RQ1 – IGGI Spatial Suitability (supports Specific Objective 1)

- Which watershed zones exhibit the highest spatial suitability for IGGI deployment, considering topographical, socio-spatial, hydrological, and accessibility criteria?
- How do weighting variations in AHP/ANP influence suitability rankings across hydrological, topographical, socio-spatial, and accessibility dimensions?
- What spatial trade-offs emerge when evaluating topographical, socio-spatial, and accessibility factors for IGGI implementation feasibility?

1.4.2 RQ_2 – Runoff Dynamics and Pollution (supports Specific Objective 2)

- How do land-use change, steep slope, and Vertisol (clay) dominated soil characteristics impact stormwater runoff generation and pollutant transport within urban micro-watershed contributing zones?
- How will projected climate extremes alter peak discharge, total runoff volume, and pollutant loading in these terrain systems?
- What thresholds of rainfall intensity and duration trigger critical runoff surges in steeply sloped, poorly draining Vertisol-dominated micro-watersheds?

1.4.3 RQ_3 – Existing Infrastructure Performance and Retrofit Readiness (supports Specific Objective 3)

- What is the current performance state of stormwater drainage infrastructure in terms of conveyance capacity, structural integrity, erosion control efficiency, sediment accumulation, and accessibility?
- Which system components exhibit the greatest urgency for retrofit intervention versus standard maintenance cycles?
- How do climate-related stressors constrain IGGI retrofit feasibility under existing infrastructure conditions?

1.4.4 RQ_4 – Innovation: Novel IGGI System Effectiveness (supports Specific Objective 4)

- How effectively does the buried rain-barrel and rain-garden configuration control runoff from rooftops and adjacent impervious surfaces compared with conventional systems?
- Which performance indicators—peak-flow mitigation, runoff volume reduction, and pollutant load attenuation—show statistically significant improvement in steep, Vertisol-dominated micro-watershed?
- How do climate-event intensities, soil conditions, topographical gradients, and land-use transitions influence the operational reliability of the subsurface-integrated IGGI system?

1.5 Research Significance

This dissertation carries both scientific and practical significance by bridging a critical gap between sustainable stormwater management research and urban planning practice. Scientifically, it advances the understanding of urban stormwater sustainability by introducing a novel IGGI configuration that exceeds the operational limits of conventional systems in runoff control and water-quality improvement. By combining GIS-based spatial modeling, MCDA, and hydrological simulation using PCSWMM, the study introduces a scalable and adaptable methodology suited to complex urban topographies, poorly draining soils, and data-scarce micro-watershed environments—particularly in rapidly urbanizing cities of the Global South, such as Addis Ababa. Practically, the research delivers evidence-based insights and a decision-support framework that enable municipal authorities to prioritize IGGI interventions, enhance drainage network design, and optimize resource allocation. Furthermore, the study aligns with global sustainability agendas, notably the SDGs, by contributing directly to SDG 6 (Clean Water and Sanitation), SDG 11 (Sustainable Cities and Communities), and SDG 13 (Climate Action). Through its context-sensitive and interdisciplinary approach, the research strengthens urban resilience, improves environmental quality, and enhances the livability of rapidly developing Global South cities—offering a replicable model for other regions facing similar stormwater management challenges.

1.6 Scope of the Study

This study focuses on Addis Ababa, Ethiopia, and its selected micro-watersheds characterized by steep slopes, poorly draining soils, and urban contributing zones. It integrates hydrologic, spatial, and decision-support modeling to enhance sustainable stormwater management. The temporal scope spans the period from 1983 to 2083, employing rainfall and temperature datasets to simulate stormwater dynamics under varying climatic conditions. Methodologically, the study combines GIS-based spatial analysis for suitability mapping at the city scale, PCSWMM-based hydrologic modeling for runoff and pollutant estimation at the micro-watershed level, and performance evaluation of green and grey infrastructure systems within these catchments. Furthermore, it develops an improved IGGI integration framework to support effective implementation within selected portions of the micro-watersheds. The study excludes groundwater recharge simulation and detailed cost–benefit analyses, focusing instead on spatial, hydrologic, and decision-support aspects of stormwater management to advance IGGI integration for sustainable urban infrastructure in complex terrains. The spatial suitability mapping covered all ten sub-cities of Addis Ababa. The hydrologic modeling, performance evaluation, and novel IGGI integration were conducted on a representative micro-watershed where slopes >10% cover 42.6% of the city and Vertisols cover 61.0%. Hence, the study area's steep, Vertisol-dominated conditions are representative of a substantial portion of Addis Ababa, supporting broader applicability of the IGGI framework.

1.7 Outline of the Dissertation

This dissertation is structured into seven main chapters, followed by references and appendices, as summarized below:

Chapter 1: Introduction — Presents the background, problem statement, research objectives, research questions, and significance of the study. This chapter contextualizes the challenges of urban stormwater management in Addis Ababa and the rationale for integrating green and grey infrastructure.

Chapter 2: Literature Review — Reviews key literature on sustainable stormwater management, emphasizing integrated green-grey infrastructure, hydrologic principles, and modeling approaches. It covers hillslope hydrology, climate change, urbanization, and the Sponge City concept, concluding with five research gaps.

Chapter 3: Assessing Green and Grey Infrastructure Suitability — First article. Uses GIS-based MCDA (AHP and ANP) for spatial suitability mapping of IGGI across Addis Ababa.

Chapter 4: Stormwater Modeling in a Steep, Poorly Drained Contributing Micro-Watershed — Second article. Details PCSWMM hydrologic modeling, scenario analysis for climate change and urbanization, and runoff and pollutant load simulations.

Chapter 5: Performance Evaluation of Existing Stormwater Infrastructure — Third article. Assesses operational performance of existing stormwater systems using TOPSIS, AHP-weighted criteria, field inspections, and sensitivity analysis to identify maintenance and retrofitting priorities.

Chapter 6: A Novel Integration of Green-Grey Infrastructure in Steep Slope Micro-Watersheds — Fourth article. Introduces an innovative IGGI design combining buried rain barrels and rain gardens, with model-based evaluation of hydrological performance and water quality improvement.

Chapter 7: Conclusions and Recommendations — Summarizes key findings across all studies, highlights scientific and practical contributions, discusses policy and planning implications, and proposes directions for future research.

References and Appendices — Include supplementary data, methodological details, and supporting figures and tables.

Chapter 2

2 Literature Review

2.1 Introduction to Stormwater Management and Urban Hydrology

Urban stormwater management has emerged as one of the defining sustainability and resilience challenges of the twenty-first century. As urbanization accelerates and climate patterns shift, the ability to manage rainfall-runoff effectively determines not only flood risk but also water quality, public health, and urban livability (Karamoutsou et al., 2024; McGrane, 2016; Qiao et al., 2020). Stormwater, defined by the U.S. Environmental Protection Agency as surface runoff generated from precipitation that flows over impervious surfaces before entering receiving waters (USEPA, 2025), was historically viewed as a nuisance to be conveyed away as quickly as possible. This perspective, however, ignores the fundamental hydrological functions that stormwater performs in natural landscapes: infiltration, groundwater recharge, baseflow maintenance, and evapotranspiration.

Under pre-development conditions, vegetated and permeable landscapes absorb a significant portion of incident rainfall. Depending on soil type, vegetation cover, and topography, infiltration rates typically range from 25-100 mm/hr in natural catchments, allowing 50-80% of annual precipitation to percolate into subsurface storage (Barbosa et al., 2012; Jacobson, 2011). The remaining precipitation is returned to the atmosphere through evaporation and transpiration (20-40%), with only 5-15% becoming surface runoff during most rainfall events (Oudin et al., 2018; Shuster et al., 2005). This natural water balance maintains hydrological stability, sustains baseflow in streams during dry periods, recharges aquifers, and filters pollutants through soil and vegetation. Urbanization fundamentally disrupts this balance through two primary mechanisms. First, the conversion of pervious, vegetated surfaces to impervious structures—rooftops, roads, parking lots, and pavements—reduces infiltration capacity dramatically. Where natural soils may infiltrate 50-100 mm/hr, compacted urban soils and impervious surfaces may infiltrate less than 1-5 mm/hr or zero, respectively (Jacobson, 2011; Zhou et al., 2019). Second, urbanization alters the timing and magnitude of runoff through the construction of drainage networks (pipes, channels, culverts) that convey water efficiently from impervious surfaces to receiving waters, bypassing natural detention and infiltration zones (Fletcher et al., 2013; Walsh et al., 2005).

The hydrological consequences of urbanization are well-documented and severe. Peak discharges in urban catchments increase by factors of 2-5 for frequent storm events (2- to 5-year return periods) and by 1.5-2.5 for rare events (100-year return periods), depending on imperviousness levels and drainage efficiency (Oudin et al., 2018; Zhou et al., 2019). Time to peak—the interval between rainfall maximum and peak discharge—decreases by 30-70% in urban catchments, producing flashier hydrographs with more rapid rises and recessions (McGrane, 2016; Shuster et al., 2005). Total annual runoff volume increases by 2-6 times pre-development levels at imperviousness of 30-75%, the typical range for residential and commercial urban land uses (Barbosa et al., 2012; Jacobson, 2011).

Simultaneously, climate change is altering precipitation regimes across most of the globe. The Intergovernmental Panel on Climate Change (IPCC) Sixth Assessment Report (2023) concludes with high confidence that the frequency and intensity of extreme precipitation events have increased since the 1950s and will continue to increase with each increment of global warming. For East Africa, including Ethiopia, climate projections indicate a 10-30% increase in extreme rainfall intensity by 2050, with longer dry spells punctuated by more intense storms (Rettie et al., 2023; Gebrechorkos et al., 2019). This pattern—more intense rainfall falling on increasingly impervious urban surfaces—creates a compound flood risk that exceeds the design capacity of most conventional drainage systems.

The combined effects of urbanization and climate change disproportionately impact cities in the Global South, where infrastructure development has lagged population growth and where institutional capacity for stormwater management is often limited (Kumar et al., 2023; Parkinson and Mark, 2015; Mguni et al., 2015). Cities such as Nairobi (Kenya), Dar es Salaam (Tanzania), Dhaka (Bangladesh), Jakarta (Indonesia), and Addis Ababa (Ethiopia) experience recurrent flooding during rainy seasons, with disproportionate impacts on low-income communities in informal settlements located in flood-prone areas (Mulligan et al., 2020; Jemberie and Melesse, 2021; Birhanu et al., 2016). These compounding pressures—hydrological disruption from urbanization, intensifying rainfall from climate change, and institutional constraints on infrastructure investment—motivate the search for more sustainable, adaptive, and context-sensitive approaches to urban stormwater management.

2.2 Evolution from Conventional to Sustainable Stormwater Management

Historically, stormwater management was conceived as an engineering problem requiring hydraulic solutions. From the late nineteenth through the late twentieth centuries, cities in industrialized nations constructed extensive networks of pipes, culverts, open channels, and detention basins designed to collect and convey stormwater runoff as rapidly as possible to receiving water bodies (Butler and Davies, 2011; Marsalek, 2006). These systems, now termed "grey infrastructure," were remarkably effective at controlling localized flooding during design storm events and were credited with enabling urban expansion, reducing waterborne disease, and protecting property in developed cities (Grigg, 2024; Chocat et al., 2001).

However, grey infrastructure operates on a fundamental assumption that has proven increasingly untenable: hydrological stationarity—the idea that statistical properties of historical rainfall adequately represent future conditions (Milly et al., 2008). Grey systems are designed for specific return periods (typically 2- to 25-year storms) using historical rainfall records. When rainfall intensities exceed design thresholds—as they increasingly do under climate change—grey systems surcharge, flood, and fail (Arnbjerg-Nielsen et al., 2013; Abebe and Tesfamariam, 2019). Furthermore, grey infrastructure transfers flood risk downstream rather than reducing it: runoff captured and conveyed from upstream areas is released at higher velocities and volumes, exacerbating flooding and erosion in downstream reaches (Fletcher et al., 2013; Zhou et al., 2019).

Beginning in the 1980s, growing awareness of environmental degradation, urban heat island effects, rising infrastructure costs, and the limitations of purely engineered solutions catalyzed a paradigm shift in stormwater management (Fletcher et al., 2015). The United States pioneered the concept of Best Management Practices (BMPs)—structural and non-structural measures to control non-point source pollution from urban runoff (USEPA, 1993). BMPs included detention ponds, constructed wetlands, vegetative filter strips, and infiltration basins, marking the first systematic integration of water quality objectives into stormwater management.

The BMP framework evolved into Low Impact Development (LID) in North America during the 1990s and 2000s. LID emphasized distributed, site-scale controls designed to mimic pre-development hydrology by maintaining infiltration, detention, and evapotranspiration at the source (Dietz, 2007; Prince George's County, 1999). Key LID practices include bioretention cells (rain gardens), permeable pavements, green roofs, rain barrels, cisterns, vegetative swales, and rooftop disconnection. Unlike BMPs, which were often implemented as end-of-pipe solutions, LID interventions are distributed throughout the catchment, reducing runoff volume at its origin (Fletcher et al., 2015).

Concurrently, the United Kingdom developed Sustainable Drainage Systems (SuDS), which added water quality and amenity/biodiversity objectives to water quantity management. The SuDS "treatment train" approach sequences interventions—from source control (rainwater harvesting, green roofs) through site control (permeable pavements, swales) to regional control (detention basins, constructed wetlands)—to achieve progressive runoff reduction and pollutant removal (Woods-Ballard et al., 2015; O'Donnell et al., 2017). SuDS also explicitly incorporated social and ecological co-benefits, including urban greening, habitat creation, and public amenity.

Australia's Water Sensitive Urban Design (WSUD) framework, emerging in the 1990s, integrated stormwater management with broader urban water cycle considerations. WSUD aims to protect natural water systems, integrate stormwater treatment into the landscape, reduce potable water demand through stormwater harvesting and reuse, and enhance urban amenity through vegetated water features (Fletcher et al., 2015; Mitchell, 2006). WSUD's holistic perspective—considering stormwater, wastewater, potable water, and urban design as an integrated system—represented a significant conceptual advance.

Most recently, China launched the Sponge City initiative in 2013, representing the largest-scale implementation of nature-based stormwater management globally. Sponge Cities are designed to "absorb, store, infiltrate, and purify" stormwater using green infrastructure, rather than relying solely on grey drainage systems (Chan et al., 2018; Li et al., 2019; Qiao et al., 2020). By 2020, 30 pilot Sponge Cities had been designated, with a national target that 80% of urban built-up areas achieve 70% stormwater capture and reuse by 2030 (WWAP, 2018). Early evaluations report significant benefits, including 50-90% reduction in annual runoff volume and 30-70% peak flow attenuation in pilot districts (Jiang et al., 2018; Wang et al., 2020).

Despite conceptual and terminological differences, these paradigms share core principles: (1) decentralized, source-control approaches; (2) mimicking pre-development hydrology; (3) integrating water quality and water quantity objectives; (4) providing ecological and social co-benefits beyond flood control; and (5) adapting to climate change and urbanization pressures (Fletcher et al., 2015; Hua et al., 2020; Yang and Zhang, 2021). The term "Integrated Green-Grey Infrastructure" (IGGI) is used throughout this dissertation as an umbrella term encompassing these principles, with explicit emphasis on the integration of green and grey systems rather than purely green approaches.

2.3 Theoretical Underpinnings of IGGI

The IGGI concept is grounded in several complementary theoretical frameworks that together provide a robust intellectual foundation for sustainable urban stormwater management: resilience theory, systems thinking, and ecosystem services.

Resilience Theory views urban hydrological systems as complex adaptive systems capable of absorbing disturbances while retaining essential functions (Meerow et al., 2016; Holling, 1973). Resilience in stormwater management has multiple dimensions: engineering resilience (speed of return to equilibrium after disturbance), ecological resilience (magnitude of disturbance that can be absorbed before system flips to an alternative state), and social-ecological resilience (capacity to adapt and transform in response to changing conditions) (Folke et al., 2010; Walker et al., 2004). Conventional grey infrastructure optimizes for engineering resilience—rapid return to normal function after design storms—but exhibits low ecological and social-ecological resilience. When rainfall exceeds design thresholds, grey systems fail catastrophically, causing flooding, property damage, and pollution (Abebe and Tesfamariam, 2019; Arnbjerg-Nielsen et al., 2013). By contrast, IGGI systems enhance multiple resilience dimensions through diversity (multiple types of intervention at multiple scales), redundancy (overlapping functions across green and grey components), modularity (independent units that can fail without system-wide collapse), and feedback (learning and adaptation from monitoring data) (Meerow et al., 2016; Dagenais et al., 2016).

Systems Thinking provides a complementary framework that emphasizes interconnections, feedback, and emergent properties. Urban stormwater systems are not isolated hydraulic networks but are embedded within broader social-ecological-technical systems (SETS) comprising hydrological processes, built infrastructure, governance institutions, and human behaviors (Walsh et al., 2005; Fletcher et al., 2013). Intervention in one subsystem inevitably produces consequences—intended and unintended—in others.

For example, increasing imperviousness in upstream areas reduces infiltration, increases peak flows, and exacerbates downstream flooding—a classic unintended consequence of land use decisions made without considering system-wide hydrologic effects (Jacobson, 2011; Zhou et al., 2019). Conversely, installing rain gardens or permeable pavements in a contributing zone not only reduces runoff from that site but also attenuates peak flows, reduces pollutant loads, and decreases stress on downstream grey infrastructure—positive cascading effects across the system (McFarland et al., 2019; Rodriguez et al., 2021). IGGI design explicitly incorporates systems thinking by considering hydrological connectivity, flow pathways, and cumulative effects across the watershed.

Ecosystem Services (ESS) theory provides a framework for valuing the multiple benefits that nature-based systems provide to human societies (Tzoulas et al., 2007; Millennium Ecosystem Assessment, 2005). The ESS framework classifies services into four categories: provisioning (water supply, food, fiber), regulating (flood control, water purification, climate regulation, pollination), supporting (soil formation, nutrient cycling, habitat provision), and cultural (recreation, aesthetic value, spiritual benefits).

Green infrastructure delivers multiple regulating services directly relevant to stormwater management. Bioretention systems and constructed wetlands remove 50-90% of total suspended solids (TSS), 30-70% of nutrients (nitrogen and phosphorus), and 40-80% of heavy metals from urban runoff (Davis et al., 2009; Hunt et al., 2012; Vymazal, 2011). Permeable pavements reduce peak flows by 30-60% and total runoff volumes by 40-80% (Scholz and Grabowiecki, 2007). Green roofs retain 40-80% of annual rainfall, reduce building energy consumption, and mitigate urban heat island effects (Czemiel Berndtsson, 2010). Vegetated swales and filter strips slow runoff, enhance infiltration, and remove sediments and attached pollutants (Fletcher et al., 2015).

Grey infrastructure, by contrast, provides primarily regulating services (flood conveyance) and does so with minimal co-benefits. Concrete channels and pipes convey runoff efficiently but do not filter pollutants, recharge groundwater, cool urban temperatures, provide wildlife habitat, or enhance aesthetics. Indeed, conventional grey infrastructure often produces disservices: channelization increases downstream flooding and erosion, impervious surfaces contribute to urban heat islands, and stormwater outfalls deliver pollutant loads to receiving waters (Barbosa et al., 2012; Fletcher et al., 2013).

IGGI approaches explicitly aim to maximize ecosystem service co-benefits while maintaining reliable flood conveyance. By integrating green elements—vegetation, permeable surfaces, bioretention media—with grey infrastructure, IGGI systems provide multiple services from the same spatial footprint. A vegetated swale adjacent to a paved road, for example, conveys stormwater (grey function) while filtering pollutants, recharging groundwater, providing habitat, and enhancing aesthetics (green co-benefits). This multi-functionality is the defining characteristic of IGGI and the source of its sustainability advantage over purely grey approaches.

2.4 Grey Infrastructure: Characteristics, Performance, and Limitations

Grey infrastructure constitutes the engineered backbone of conventional urban drainage systems, encompassing pipes, culverts, open channels, manholes, detention basins, and pumping stations designed to collect and convey stormwater runoff efficiently from developed areas (Butler and Davies, 2011; Marsalek, 2006). These systems are designed according to hydraulic principles governing flow capacity, velocity, roughness, and network connectivity, with design standards codified in municipal engineering manuals and national guidelines such as those of the American Society of Civil Engineers (ASCE) or the UK's Design and Analysis of Urban Drainage Systems.

Design Principles and Methods: Grey infrastructure design typically follows deterministic hydrological methods, most commonly the Rational Method (Q = CiA) for small catchments (<50 ha) or unit hydrograph methods for larger areas (Chow, 1988). Design storms are specified by return period (typically 2- to 25-year for drainage systems, 50- to 100-year for critical infrastructure) and duration (often the time of concentration of the catchment). Rainfall intensity-duration-frequency (IDF) curves, derived from historical rainfall records, provide the design intensity for each return period and duration. Conduits (pipes, channels) are sized using Manning's equation or similar hydraulic formulas to ensure that design flows do not exceed capacity, causing surcharging and surface flooding (Rossman, 2015).

Performance Characteristics: When properly designed, constructed, and maintained, grey infrastructure performs reliably for storm events up to the design return period. Piped networks convey runoff rapidly, reducing surface ponding and protecting property from inundation. Detention basins temporarily store floodwaters, releasing them at controlled rates to prevent downstream flooding. Culverts maintain road crossings and prevent washouts. Combined sewer systems, found in older cities, convey both stormwater and sanitary sewage to treatment plants, preventing untreated discharges under dry weather conditions (Butler and Davies, 2011; Marsalek, 2006).

Limitations: Despite these capabilities, grey infrastructure exhibits fundamental limitations that are increasingly problematic under urbanization and climate change pressures.

First, hydraulic stationarity assumption. Grey systems are designed based on historical rainfall records under the assumption of stationarity—that future rainfall extremes will resemble historical patterns (Milly et al., 2008). Climate change has rendered this assumption invalid across most of the globe. Rainfall intensities and frequencies are increasing in many regions, meaning that design storms occur more frequently than intended. A 10-year storm may now occur every 5-7 years, a 100-year storm every 50-70 years, progressively overwhelming systems designed for lower intensities (Arnbjerg-Nielsen et al., 2013; Jiang et al., 2023).

Second, lack of adaptability. Grey systems are rigid and difficult to modify after construction. Upsizing pipes, adding detention capacity, or reconfiguring networks requires major excavation, road closures, and substantial capital investment, often prohibitively expensive in built-out urban areas (Abebe and Tesfamariam, 2019; Rodriguez et al., 2021). This rigidity contrasts sharply with green infrastructure, which can be implemented incrementally, adjusted based on performance monitoring, and adapted to changing conditions.

Third, hydrological disconnection. Grey infrastructure disconnects urban landscapes from hydrological processes that sustain healthy ecosystems. By conveying runoff rapidly through pipes to receiving waters, grey systems bypass infiltration, groundwater recharge, and evapotranspiration—the very processes that maintain baseflow, water quality, and aquatic habitat (Fletcher et al., 2013; Walsh et al., 2005). The result is "urban stream syndrome": flashy hydrographs, elevated pollutant loads, channel erosion, and loss of sensitive aquatic species (Barbosa et al., 2012; McGrane, 2016).

Fourth, transfer of risk downstream. Because grey systems are designed primarily for conveyance, they do not reduce runoff volumes; they simply move water from upstream to downstream locations. Peak discharges from urban catchments are often 2-5 times higher than pre-development levels, exacerbating flooding and erosion in downstream reaches (Zhou et al., 2019; Oudin et al., 2018). Flood risk is transferred rather than reduced, shifting the burden from affluent upstream neighborhoods to often less affluent downstream communities.

Fifth, pollutant mobilization and transport. Grey infrastructure does not treat stormwater; it conveys pollutants—sediments, nutrients, heavy metals, hydrocarbons, pathogens—directly to receiving waters (Hatt et al., 2006; Barbosa et al., 2012). First-flush phenomena, where initial runoff carries the highest pollutant concentrations, deliver acute doses of contaminants to aquatic ecosystems during each storm event. Unlike natural landscapes, where soils and vegetation filter pollutants, grey infrastructure provides no treatment function.

Sixth, high life-cycle costs. Grey infrastructure requires substantial capital investment for construction and ongoing expenditure for inspection, cleaning, repair, and replacement. Concrete pipes deteriorate over time (design life typically 50-100 years), requiring rehabilitation or replacement at significant cost. Sediment accumulation reduces hydraulic capacity, requiring periodic cleaning. Pipe joints fail, causing infiltration and exfiltration (Butler and Davies, 2011). These costs are often underestimated in initial project budgets, leading to deferred maintenance and progressive system deterioration.

In the context of Addis Ababa, these limitations are acutely visible. The city's stormwater drainage system comprises primarily open roadside ditches and concrete-lined channels, many constructed decades ago without systematic design or maintenance (Jemberie et al., 2023; Adugna et al., 2019). Rapid urbanization has increased imperviousness and runoff volumes beyond system capacity, while sediment accumulation and solid waste clog channels, reducing conveyance. No systematic inspection or maintenance program exists, and design records are often unavailable. The result is recurrent flooding during rainy seasons, with 76 flood events recorded in 2017 alone (Jemberie and Melesse, 2021), damage to roads and property, and pollution of receiving rivers (Angello et al., 2021).

2.5 Green Infrastructure: Principles, Types, and Functional Performance

Green infrastructure (GI) refers to vegetated and permeable systems designed to manage stormwater at its source through infiltration, evapotranspiration, detention, and filtration (Benedict and McMahon, 2006; Fletcher et al., 2015). Unlike grey infrastructure, which conveys runoff rapidly off-site, GI aims to restore hydrological processes disrupted by urbanization, reducing runoff volumes, attenuating peak flows, improving water quality, and providing multiple ecosystem co-benefits.

Core Principles: GI design is guided by several principles derived from LID, SuDS, WSUD, and Sponge City frameworks. *Source control* prioritizes interventions as close to the rainfall origin as possible—on individual lots, at building rooftops, along roadsides—rather than end-of-pipe solutions (Dietz, 2007). *Decentralization* distributes interventions throughout the catchment rather than concentrating capacity at a single downstream location, enhancing resilience and redundancy (Fletcher et al., 2015). *Multi-functionality* designs each intervention to provide multiple services: flood control, water quality improvement, groundwater recharge, habitat provision, urban cooling, and aesthetics (Tzoulas et al., 2007). *Hydrological mimicry* seeks to restore pre-development hydrology by matching infiltration, runoff, and evapotranspiration rates to natural landscapes (Bai et al., 2018; Yang and Zhang, 2021).

GI Typologies: Numerous GI practices have been developed, each with specific hydrological functions, design requirements, and performance characteristics, as presented in Table 2.1.

Table 2.1: Common Types of GI

<table>
<tr>
<td>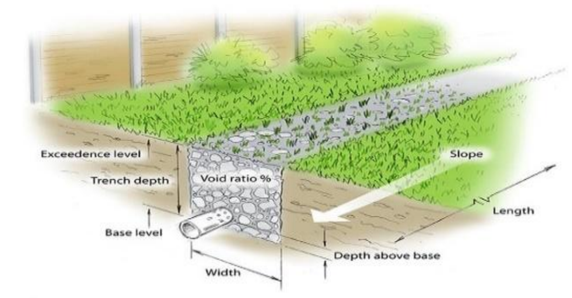

Infiltration Trench (Arch Students, 2023)</td>
<td>
Vegetated Swale (Regional Plan, 2023)</td>
</tr>
<tr>
<td>
Dry Well (Balkan Sewer, 2023)</td>
<td>
Pervious Pavement (Megan Geall, 2023)</td>
</tr>
<tr>
<td>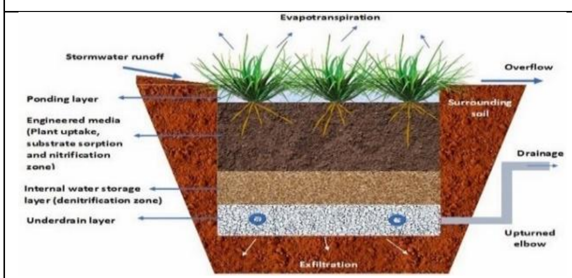

Bio-retention (Vijayaraghavan et al., 2021)</td>
<td>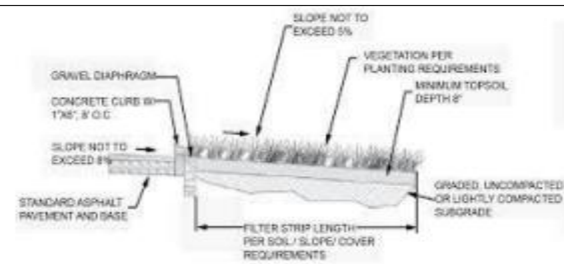

Vegetated Strips (Greater Vancouver, 2005)</td>
</tr>
<tr>
<td>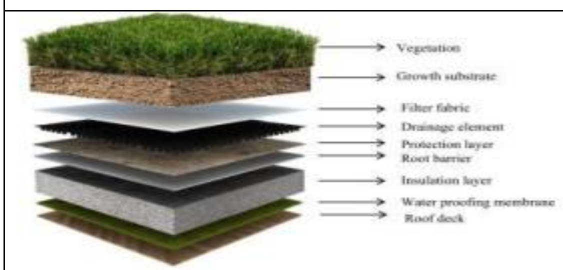

Green roofs detailed (Vijayaraghavan, 2016)</td>
<td>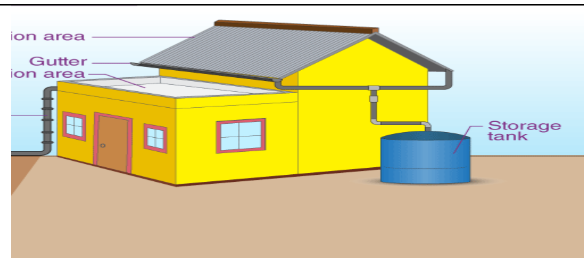

Rainwater Harvesting (Ju, 2023)</td>
</tr>
</table>

Bioretention systems (rain gardens) are shallow, vegetated depressions designed to capture, infiltrate, and filter runoff from small drainage areas (typically 0.1-2.0 ha). A typical bioretention system comprises a surface ponding zone (15-30 cm), a mulch layer (5-10 cm), an engineered soil media (30-90 cm of sandy loam with 2-5% organic matter), and a gravel drainage layer (15-30 cm) with an underdrain (optional) (Davis et al., 2009; Hunt et al., 2012). Runoff ponds temporarily in the surface depression, infiltrates through the soil media (infiltration rates typically 25-500 mm/hr depending on media composition), and is either exfiltrated to underlying native soil or collected in the underdrain. Bioretention systems remove 70-90% of TSS, 50-80% of total phosphorus, 30-70% of total nitrogen, and 60-90% of heavy metals (Li et al., 2009; Blecken et al., 2017). Peak flow reduction ranges from 40-80% for frequent storms, with some attenuation even for larger events (Davis et al., 2012).

Permeable pavements replace conventional impervious asphalt or concrete with porous materials that allow water to infiltrate through the surface into underlying storage and drainage layers. Permeable pavement types include porous asphalt (void space 15-20%), pervious concrete (void space 15-25%), permeable interlocking concrete pavers (void space 5-15% between pavers filled with aggregate), and plastic or concrete grid systems (Scholz and Grabowiecki, 2007; Weiss et al., 2017). A typical profile includes a permeable surface layer, an aggregate base course (30-60 cm) for storage, and optional underdrain. Permeable pavements reduce total runoff volume by 40-80% and peak flows by 50-90% for frequent storms (Brattebo and Booth, 2003; Bean et al., 2007). Water quality improvements include TSS removal of 70-95%, reductions in heavy metals (copper, zinc, lead) of 50-90%, and moderate nutrient removal (Weiss et al., 2017).

Green roofs are vegetated systems installed on building rooftops, comprising a waterproof membrane, drainage layer, growing media (5-30 cm depth for extensive green roofs; >30 cm for intensive green roofs), and vegetation (sedums, grasses, or other drought-tolerant plants for extensive roofs; shrubs and trees for intensive roofs) (Czemiel Berndtsson, 2010; Oberndorfer et al., 2007). Green roofs retain 40-80% of annual rainfall, with higher retention for thicker media and deeper vegetation. Peak flow reduction ranges from 50-90%, time to peak is delayed by 30-120 minutes, and total runoff volume is substantially reduced (Mentens et al., 2006; Stovin, 2010). Water quality effects are variable: green roofs may initially leach nutrients (particularly phosphorus) but typically become nutrient sinks after 1-3 years of establishment (Berndtsson et al., 2009). Secondary benefits include building energy savings (10-30% reduction in cooling demand, 5-15% reduction in heating demand), urban heat island mitigation (surface temperature reduction of 15-40°C compared to conventional roofs), noise reduction, biodiversity enhancement, and aesthetic value (Oberndorfer et al., 2007).

Rain gardens are a subset of bioretention systems, typically smaller (0.5-5% of drainage area) and designed for residential or small commercial applications. Rain gardens are planted with native, water-tolerant vegetation and positioned to capture runoff from rooftops, driveways, and lawns (Sharma and Malaviya, 2021; Dietz, 2007). Performance is similar to larger bioretention systems: 30-90% runoff volume reduction, 40-90% peak flow reduction, and 50-90% pollutant removal for TSS, metals, and nutrients (Davis et al., 2009; Hunt et al., 2012). Rain gardens are particularly suited to retrofitting in existing neighborhoods because they require minimal space, can be integrated into landscaping, and are relatively low-cost (Sharma and Malaviya, 2021).

Rain barrels and cisterns capture rooftop runoff for non-potable uses such as irrigation, toilet flushing, and car washing. Rain barrels (typically 150-400 L capacity) are the smallest-scale GI, suitable for individual households. Cisterns (1,000-50,000 L capacity) serve larger buildings, institutions, or neighborhoods (DeBusk et al., 2012; Teston et al., 2022). Rainwater harvesting reduces runoff volume by 20-60% depending on tank size, rainfall patterns, and water demand. Water quality benefits are indirect: captured water is used on-site rather than discharged to drainage systems, but stored water requires treatment (filtration, disinfection) for potable uses (Jones and Hunt, 2010; Eroksuz and Rahman, 2010). Rain barrels are inexpensive (USD 50-200 per unit) and easy to install, making them accessible for broad adoption (Ghodsi et al., 2021).

Vegetated swales and filter strips are linear, vegetated channels designed to convey, slow, and treat stormwater runoff. Swales are typically sized for the design flow, with gentle side slopes, flat bottoms (or parabolic cross-sections), and dense vegetation that increases hydraulic roughness and promotes settling of sediments (Fletcher et al., 2015; Hunt et al., 2012). Dry swales convey only storm flows; wet swales maintain base flow between events. Filter strips are gently sloping, vegetated areas over which runoff flows as sheet flow before entering swales or receiving waters. Swales and filter strips reduce peak flows by 30-80% depending on length, slope, vegetation, and soil infiltration rate (Stagge et al., 2012). Pollutant removal includes TSS (50-90%), metals (40-80%), and moderate nutrient removal (20-60% for phosphorus, 10-40% for nitrogen) (Deletic and Fletcher, 2006; Davis et al., 2012).

Constructed wetlands are engineered systems that mimic natural wetland hydrology, vegetation, and biogeochemical processes to treat stormwater runoff. A typical constructed wetland includes a forebay (sedimentation zone), a macrophyte zone (dense emergent vegetation), a microphyte zone (open water with submerged vegetation), and an outlet structure (Vymazal, 2011; Kadlec and Wallace, 2009). Constructed wetlands detain stormwater for 24-72 hours, allowing sedimentation, filtration by vegetation, nutrient uptake, and microbial transformation (nitrification, denitrification, phosphorus uptake). Pollutant removal is excellent: TSS reduction 70-95%, total phosphorus 40-80%, total nitrogen 30-70%, and heavy metals 50-90% (Vymazal, 2011; Mallin et al., 2002). Constructed wetlands also provide high-quality wildlife habitat, aesthetic value, and public amenity, making them particularly valuable for parks and greenways in urban areas (Tzoulas et al., 2007).

Barriers to GI Adoption: Despite demonstrated performance and co-benefits, GI adoption faces significant barriers, particularly in Global South cities. *Land availability* is often limited in dense urban areas, competing with housing, commercial development, and transportation infrastructure (Seidu et al., 2025). *Institutional fragmentation* disperses responsibility for stormwater, land use planning, and environmental regulation across multiple agencies with limited coordination (Dereje Fekadu et al., 2022; Azagew and Worku, 2020). *Technical capacity* for GI design, construction, and maintenance may be limited, particularly in municipal agencies accustomed to conventional grey infrastructure approaches (Eshetu et al., 2021; Ijara, 2020). *Financial constraints* include higher upfront costs for GI than conventional drainage, lack of dedicated funding mechanisms, and difficulty quantifying long-term benefits and co-benefits in cost-benefit analyses (Vineyard et al., 2015). *Maintenance requirements* for GI—vegetation management, sediment removal, inlet/outlet cleaning, media replacement—are often underestimated and underfunded, leading to performance decline and system failure (Lindsey et al., 1992; Shafique and Kim, 2015). *Regulatory barriers* include zoning codes that discourage GI (e.g., setback requirements, impervious surface maximums), lack of design standards for GI in municipal codes, and performance requirements that favor grey infrastructure (Jemberie and Melesse, 2021; Jemberie et al., 2023).

2.6 Comparative Analysis and Transition toward Integration

The preceding sections have characterized grey infrastructure as reliable but inflexible, hydraulically efficient but ecologically dysfunctional, and effective for design storms but vulnerable to extremes. Green infrastructure has been characterized as multi-functional but space-intensive, effective for water quality and frequent storms but potentially inadequate for extreme events, and rich in co-benefits but challenging to implement in dense urban contexts. These complementary strengths and weaknesses have led to the recognition that grey and green are not mutually exclusive alternatives but complementary components of an integrated urban water system (Wang et al., 2023; Rodriguez et al., 2021; Bai et al., 2018).

Comparative Performance: Table 2.2 synthesizes performance comparisons from multiple studies across key dimensions of stormwater management.

Table 2.2: Comparative Performance of Grey and Green Infrastructure

Parameter	Grey Infrastructure	Green Infrastructure	Integrated (IGGI)
Peak flow reduction (2-year event)	90-100% (up to capacity)	40-80%	60-95%
Peak flow reduction (100-year event)	0-100% (system fails beyond capacity)	0-40% (limited by storage)	20-60% (grey provides backup)
Total runoff volume reduction	0-10% (conveys, does not retain)	30-80%	30-80%
TSS removal (%)	0-10% (no treatment)	50-95%	50-95%
Nutrient removal (TN, TP) (%)	0-5%	30-80%	30-80%
Heavy metal removal (%)	0-10%	50-90%	50-90%
Groundwater recharge	None	Moderate to high	Moderate to high
Urban heat island mitigation	Negative (impervious surfaces increase heat)	Positive (evapotranspiration, shading)	Positive
Habitat provision	None	Moderate to high (wetlands, vegetated swales)	Moderate to high
Aesthetic value	Low (concrete channels, manholes)	High (vegetated features, gardens)	High
Capital cost (USD/m³ storage)	Low to moderate ($50-200)	Moderate to high ($100-500)	Moderate ($75-300)

Operation and maintenance cost (annual % of capital)	1-3% (inspection, cleaning, repair)	3-8% (vegetation, media, sediment removal)	2-5%
Design life (years)	50-100 (pipes, channels)	20-50 (vegetation, media requires renewal)	30-60
Adaptability to climate change	Low (rigid, difficult to modify)	High (modular, incremental)	Moderate to high
Land requirement	Low (underground or narrow corridors)	Moderate to high (surface area for bioretention, wetlands)	Moderate (shared space, multi-functional)

Sources: Compiled from Dietz (2007), Davis et al. (2009), Fletcher et al. (2015), Barbosa et al. (2012), Zhou et al. (2019), Vineyard et al. (2015), Ghodsi et al. (2021).

Integration Mechanisms: IGGI approaches integrate green and grey systems through several mechanisms. *Sequential integration* places green interventions upstream of grey infrastructure: runoff first encounters rain gardens, permeable pavements, or green roofs, where volume reduction and pollutant removal occur; excess flows then enter grey pipes and channels for conveyance to downstream storage or discharge (Wang et al., 2023; Dagenais et al., 2016). This arrangement reduces the hydraulic load on grey infrastructure, extending its effective capacity and reducing maintenance requirements. *Spatial integration* locates green and grey interventions within the same corridor or footprint. Vegetated swales alongside paved roads, for example, convey stormwater (grey function) while filtering pollutants and providing habitat (green functions). Permeable pavement overlays on conventional base courses provide infiltration (green) while supporting vehicle loads (grey). Green roofs on buildings reduce runoff (green) while protecting roofing membranes from UV degradation (grey) (Rodriguez et al., 2021; Bai et al., 2018).

Functional integration designs green and grey components to perform complementary functions. Wetlands provide detention (grey function) and water quality treatment (green function). Detention basins designed with vegetated slopes and benches provide flood storage (grey) and habitat/aesthetics (green). Rain gardens with underdrains (grey component) provide infiltration (green) during smaller storms and conveyance (grey) during larger events (Hunt et al., 2012; Davis et al., 2009). *Institutional integration* aligns governance, planning, and funding mechanisms across agencies responsible for stormwater, land use, transportation, parks, and environmental protection (Dereje Fekadu et al., 2022; Seidu et al., 2025).

Evidence for IGGI Effectiveness: Multiple modeling and field studies have demonstrated IGGI effectiveness. Qin et al. (2013) simulated IGGI combinations (bioretention + permeable pavement + green roof) in a Chinese urban catchment, finding 25-40% peak flow reduction and 30-50% runoff volume reduction compared to grey-only baseline. Li et al. (2018) evaluated IGGI in a Swedish catchment, reporting 35% peak reduction and 45% volume reduction for 2-year storms, with diminishing but still substantial (15-20%) benefits for 10-year events. Ben-Daoud et al. (2024) modeled bioretention with permeable pavement in a Moroccan catchment, finding 31% TSS reduction, 29% TN reduction, and 40% TP reduction. Lin et al. (2023) evaluated integrated rain barrel-rain garden systems in Japanese residential areas, reporting 29-36% peak flow reduction and 18-40% volume reduction. Ghodsi et al. (2021) assessed city-wide rain barrel implementation, finding 5-12% runoff volume reduction, which increased to 15-25% when rain barrels were integrated with downspout disconnection and rain gardens.

Despite this evidence, the examiners have correctly noted that most IGGI studies assume gentle slopes (<7%) and well-drained soils, leaving a critical gap for steep, Vertisol-dominated urban environments. This dissertation directly addresses that gap.

2.7 Hillslope Hydrology in Urban Catchments: Steep Slopes and Contributing Zones

Understanding hillslope hydrological processes is fundamental to stormwater management in topographically complex urban environments. In natural catchments, hillslope hydrology has been extensively studied, with established conceptual models of overland flow generation (Horton, 1933; Dunne and Black, 1970; Kirkby, 1978). Three primary runoff generation mechanisms operate on hillslopes. *Infiltration-excess (Hortonian) overland flow* occurs when rainfall intensity exceeds soil infiltration capacity, generating runoff on both vegetated and bare surfaces. This mechanism dominates in arid and semi-arid regions with high-intensity rainfall and/or low-infiltration soils (Horton, 1933; Dunne, 1978). *Saturation-excess overland flow* occurs when the soil profile becomes fully saturated—either by rainfall or by rising groundwater—and additional precipitation cannot infiltrate. This mechanism dominates in humid regions with shallow soils, convergent topography, and/or near-stream zones (Dunne and Black, 1970; Kirkby, 1978). *Subsurface stormflow* is lateral flow through the soil profile above less permeable layers, contributing to streamflow with longer lag times than overland flow (Kirkby, 1978; Weiler, 2017).

These hillslope processes have been intensively studied in agricultural, forested, and rangeland catchments across diverse climatic and topographic conditions. The literature includes hundreds of plot-scale rainfall simulation experiments (e.g., Bryan, 2000; Gomi et al., 2002), hillslope-scale tracer studies (e.g., McGuire and McDonnell, 2006; Weiler, 2017), and process-based modeling applications (e.g., Beven and Kirkby, 1979; Qu and Duffy, 2007). Consensus findings include slope gradient is a primary control on runoff velocity and erosion potential (Haggard et al., 2005); soil hydraulic conductivity controls the balance between infiltration and overland flow (Nimmo, 2004); upslope contributing area determines the volume of water converging on a point (Beven and Kirkby, 1979); and antecedent moisture conditions modulate hydrologic response to rainfall (Weiler, 2017).

However, the translation of these hillslope hydrological understandings to urban catchments—particularly those with steep gradients (>7%) and low-permeability soils (Vertisols)—remains limited and problematic. Urbanization fundamentally alters hillslope hydrology through several mechanisms. First, impervious surfaces (roofs, roads, parking lots) generate Hortonian overland flow even under low-intensity rainfall, bypassing natural infiltration pathways (Jacobson, 2011; Shuster et al., 2005). Second, the conversion of vegetated hillslopes to urban land uses reduces surface roughness (Manning's n decreases from 0.2-0.8 for forested slopes to 0.01-0.03 for asphalt), accelerating flow concentration and shortening time of concentration (Oudin et al., 2018; McGrane, 2016). Third, artificial drainage networks (pipes, channels, culverts) create hydrological connectivity that routes runoff efficiently from hillslopes to downstream channels, often bypassing natural detention and infiltration zones (Fletcher et al., 2013; Walsh et al., 2005). Fourth, soil compaction during construction reduces infiltration capacity of remaining pervious areas, further promoting overland flow (Yang and Zhang, 2011; Gregory et al., 2006).

The concept of the contributing zone is particularly relevant to urban stormwater management in steep catchments. In hillslope hydrology, the contributing zone refers to the uppermost area of a watershed where overland flow is initiated and shallow interflow occurs—the "source area" for runoff (Marsh, 2010; Speak et al., 2013). In natural catchments, contributing zones expand and contract with antecedent moisture, a phenomenon known as variable source area hydrology (Dunne and Black, 1970; Beven and Kirkby, 1979). In urban catchments, impervious surfaces create permanent contributing zones that generate runoff during every storm, irrespective of antecedent moisture. The contributing zone in an urban micro-watershed is thus the area that most strongly influences downstream flooding and water quality—yet it is often the least studied and least managed portion of the watershed (McFarland et al., 2019).

In steep urban catchments, contributing zones are particularly critical. Runoff generated on steep hillslopes accelerates rapidly, gaining erosive energy as it moves downslope. Sediment and attached pollutants are mobilized, vegetation is scoured, and concentrated flow channels (rills, gullies) may form (Omitaomu et al., 2021; EPA, 2014). By the time flow reaches downstream conveyance zones, it may have already caused substantial erosion and pollutant loading. Intervening at the contributing zone—upstream, near the runoff origin—is therefore more effective than downstream, after erosion and pollution have already occurred (McFarland et al., 2019; Speak et al., 2013).

Vertisol-Specific Hydrology: In the Ethiopian context, Vertisols present hydrological challenges that interact with steep slopes to produce unique stormwater management problems. Vertisols are clay-rich soils (>50% clay content, typically montmorillonite clay minerals) that exhibit high shrink-swell potential, low saturated hydraulic conductivity (typically <10 mm/hr, often <1 mm/hr.), and surface sealing during rainfall events (Berhanu, 1983; Srivastava et al., 1989; Debele and Deressa, 2016). When dry, Vertisols crack deeply (cracks up to 1-2 cm wide, 50-100 cm deep), providing infiltration pathways. When wet, clay minerals swell, closing cracks and dramatically reducing infiltration—a positive feedback that promotes Hortonian overland flow (FAO, 2006; Ahmad, 1983).

For stormwater management, Vertisol hydrology has profound implications. Even gentle slopes (3-7%) on Vertisols generate substantial overland flow during moderate-to-high intensity storms because infiltration capacity is quickly exceeded. When slopes exceed 7-15%—as in the study area of this dissertation—overland flow becomes rapid, erosive, and voluminous (EPA, 2014; Omitaomu et al., 2021). Conventional green infrastructure practices designed for well-drained soils (infiltration trenches, bioretention with underdrains, permeable pavements without impermeable liners) may fail on Vertisols because the underlying native soil cannot infiltrate treated water at sufficient rates. Indeed, this limitation motivated the design of the novel IGGI system in Chapter 7, which uses buried rain barrels (temporary storage) and rain gardens (engineered media above native soil) to manage runoff without relying on infiltration into Vertisol subgrade.

Research Gap: Despite the prevalence of steep slopes and Vertisols in the Ethiopian highlands and other tropical regions, few studies have explicitly modeled hydrologic processes in steep, Vertisol-dominated urban contributing zones using process-based models such as PCSWMM. The literature includes studies of GI on clay soils (e.g., Khan et al., 2020; Sharma and Malaviya, 2021) and studies of hillslope hydrology on steep terrain (e.g., Gomi et al., 2002; Weiler, 2017), but rarely both in combination. This dissertation addresses that gap by focusing explicitly on a steep, Vertisol-dominated contributing zone in Addis Ababa.

2.8 Review of Hydrological Models for Urban Stormwater Management

Hydrological models are essential tools for urban stormwater management, enabling simulation of rainfall-runoff processes, flow routing, pollutant transport, and performance evaluation of infrastructure alternatives. Models range from simple empirical equations to complex, physically based distributed simulations. This section reviews the major models used in urban stormwater applications, compares their capabilities and limitations, and justifies the selection of PCSWMM for this dissertation.

Model Classification: Hydrological models can be classified along several dimensions. *Conceptual vs. physically based* distinguishes models that represent processes through simplified, lumped parameters (e.g., runoff coefficient, time of concentration) from those that solve fundamental physical equations (e.g., Richard's equation for infiltration, Saint-Venant equations for flow routing) (Singh and Woolhiser, 2002; Chow et al., 1988). *Lumped vs. distributed* distinguishes models that treat the catchment as a single unit with average properties from those that discretize space into grid cells or sub-catchments with spatially varying parameters (Beven, 2012). *Event-based vs. continuous* distinguishes models that simulate individual storm events (requiring initial conditions as input) from those that simulate long periods (allowing soil moisture, groundwater, and other state variables to evolve between storms) (Rossman, 2015). *Quantity-only vs. quantity-quality* distinguishes models that simulate only water flow from those that also simulate pollutant buildup, washoff, and transport (Rossman and Huber, 2016).

Urban Stormwater Models: Several models have been widely used in urban stormwater applications.

SWMM (Storm Water Management Model), developed by the U.S. Environmental Protection Agency (USEPA) since 1971, is the most widely used urban drainage model globally (Rossman, 2015; Huber and Dickinson, 1988). SWMM is a dynamic, distributed, continuous simulation model that represents catchments as sub-catchment units with user-specified area, width, slope, imperviousness, and infiltration parameters. Surface runoff is calculated using non-linear reservoir routing (with Manning's equation for outflow). Flow routing through pipes, channels, pumps, and storage units uses full dynamic wave, kinematic wave, or diffusive wave solutions to the Saint-Venant equations. Water quality simulation includes pollutant buildup (exponential, power, or saturation functions), washoff (exponential rating curve or event mean concentration), and routing through the drainage network with optional treatment functions. SWMM's open-source code, extensive documentation, large user community, and integration with proprietary interfaces (e.g., PCSWMM, InfoWorks ICM) have made it the standard tool for urban stormwater modeling (Rossman, 2015; James and Rossman, 2010).

PCSWMM is a commercial software package developed by Computational Hydraulics International (CHI) that wraps the USEPA SWMM computational engine with a geographic information system (GIS) interface, advanced visualization, calibration tools, and decision-support features (CHI, 2023). PCSWMM retains SWMM's full hydrologic, hydraulic, and water quality simulation capabilities while adding: (1) direct integration with GIS data (shapefiles, rasters, CAD files) for model building and results visualization; (2) automated sensitivity analysis and calibration tools (SRTC - Sensitivity-based Radio Tuning Calibration); (3) scenario management for comparing alternatives; (4) low impact development (LID) controls module with detailed representation of green infrastructure practices (rain barrels, rain gardens, permeable pavements, green roofs, etc.); (5) climate change scenario generation using global climate model outputs; and (6) uncertainty analysis and risk assessment. PCSWMM is particularly suited to complex urban catchments where spatial heterogeneity in land use, topography, and drainage infrastructure is significant (CHI, 2023; Akhter and Hewa, 2016).

SUSTAIN (System for Urban Stormwater Treatment and Analysis INtegration), developed by USEPA, is a decision-support system specifically designed for evaluating and optimizing BMP/LID placement at watershed scale (USEPA, 2009; Lee et al., 2012). SUSTAIN couples a watershed runoff model (based on SWMM) with a GIS-based BMP siting tool and optimization algorithms (genetic algorithms, simulated annealing) to identify cost-effective BMP/LID combinations. SUSTAIN's strengths include sophisticated optimization capabilities and explicit representation of BMP/LID performance curves. However, SUSTAIN is less widely used than

SWMM/PCSWMM, has a steeper learning curve, and is not as well-suited for detailed hydraulic modeling of pipe networks (Lee et al., 2012).

InfoWorks ICM (Integrated Catchment Modeling), developed by Innovyze (now Autodesk), is a commercial software package that integrates urban drainage and river system modeling. InfoWorks ICM uses a 1D/2D coupled engine capable of simulating both pipe network flow (1D) and surface overland flow (2D) simultaneously, making it particularly suitable for floodplain mapping and surface flooding studies (Autodesk, 2023). However, InfoWorks ICM is more expensive than PCSWMM, has a steeper learning curve, and is less commonly used in academic research on LID/IGGI performance (Zhou et al., 2019).

MIKE URBAN (formerly MOUSE), developed by DHI, is a commercial modeling package for urban drainage and water distribution systems (DHI, 2020). MIKE URBAN includes pipe flow modeling, rainfall-runoff simulation, water quality modeling, and real-time control. Like ***InfoWorks ICM***, MIKE URBAN is widely used in engineering consulting but less common in academic research on green infrastructure (DHI, 2020).

HEC-HMS (Hydrologic Modeling System), developed by the U.S. Army Corps of Engineers, is a hydrologic model for watershed runoff simulation (USACE, 2022). While HEC-HMS is widely used for flood hydrology and reservoir operations, it is less suited to urban drainage because it lacks the detailed hydraulic routing (open channel, pipe, pump) that characterizes urban drainage networks. HEC-HMS is primarily used for natural and agricultural catchments (USACE, 2022).

Model Comparison and Selection for This Study: Table 2.3 compares the relevant models across criteria important for this dissertation: capability for urban drainage networks, LID/IGGI representation, water quality simulation, climate change scenario integration, sensitivity/calibration tools, GIS integration, cost, and learning curve.

Table 2.3: Comparison of Urban Stormwater Models

Criterion	PCSWMM	SWMM (standalone)	SUSTAIN	InfoWorks ICM	MIKE URBAN	HEC-HMS
Urban drainage network (pipes, channels)	Excellent	Excellent	Moderate	Excellent	Excellent	Poor

LID/IGGI representation	Excellent (LID module)	Good (LID module in v5.1+)	Excellent (BMP/LID curves)	Good	Moderate	Poor
Water quality simulation	Excellent	Excellent	Good	Good	Good	Poor
Climate change scenario integration	Excellent (built-in GCM downscaling)	Manual	Manual	Manual	Manual	Manual
Sensitivity analysis/calibration	Excellent (SRTC automated)	Manual	Good	Moderate	Moderate	Moderate
GIS integration	Excellent (native)	Moderate (through external GIS)	Good (ArcGIS-based)	Good	Moderate	Moderate
Cost	Moderate (student/educational licenses available)	Free (open source)	Free (USEPA)	High (commercial)	High (commercial)	Free (USACE)
Learning curve	Moderate	Moderate	Steep	Steep	Steep	Moderate
Peer-reviewed LID/IGGI studies	Extensive (1000+)	Extensive (5000+)	Moderate (50-100)	Moderate (100-200)	Moderate (100-200)	Limited

Sources: CHI (2023), Rossman (2015), USEPA (2009), Autodesk (2023), DHI (2020), USACE (2022).

Justification for PCSWMM Selection: PCSWMM was selected for this dissertation for the following reasons, which align with the study objectives and constraints:

First, PCSWMM's LID module provides explicit representation of the IGGI components evaluated in Chapter 7 (rain barrels, rain gardens). The module requires parameters (storage depth, surface roughness, soil media properties, underdrain characteristics) that can be measured or estimated from literature, enabling simulation of pre- and post-IGGI conditions. No other model provides such detailed, process-based representation of LID/IGGI practices (CHI, 2023; Rossman, 2015).

Second, PCSWMM's climate change module directly integrates downscaled GCM outputs (CMIP5, CMIP6) into IDF curve development and continuous simulation. The study uses downscaled CMIP6 projections from Rettie et al. (2023), which can be directly imported into PCSWMM, eliminating manual processing steps required for other models.

Third, PCSWMM's SRTC (Sensitivity-based Radio Tuning Calibration) tool automates sensitivity analysis and calibration, which is particularly valuable given the data-scarce context of Addis Ababa. SRTC identifies influential parameters, optimizes parameter values, and quantifies uncertainty—functions that would be laborious or infeasible using manual calibration (Wagener and Wheater, 2006; CHI, 2023).

Fourth, PCSWMM's GIS integration enables direct use of spatial data (DEM, land use, soil maps) for sub-catchment delineation, parameter assignment, and results visualization. Given that this dissertation includes city-wide spatial suitability mapping (Chapter 4) and micro-watershed modeling (Chapters 5-7), seamless GIS integration is essential.

Fifth, PCSWMM's widespread use in peer-reviewed LID/IGGI research (1000+ studies) provides a basis for comparing results with other catchments and practices (Akhter and Hewa, 2016; Bibi et al., 2023; Zakizadeh et al., 2022). Computational Hydraulics International (CHI) provided student licenses for PCSWMM Professional Version, making the software accessible within the dissertation budget and timeline.

Sixth, while SWMM is free, it lacks PCSWMM's calibration tools, climate module, and GIS integration, requiring substantial manual processing for equivalent analyses. SUSTAIN's optimization capabilities exceed PCSWMM's but SUSTAIN is weaker in hydraulic modeling of complex pipe networks—a requirement for Chapter 6 (existing infrastructure performance evaluation). InfoWorks ICM and MIKE URBAN are cost-prohibitive for this dissertation and less common in academic IGGI research.

2.9 Climate Change Impacts on Urban Stormwater Systems

Climate change is unequivocally altering precipitation regimes, temperature patterns, and extreme event frequencies across the globe, with profound implications for urban stormwater management (IPCC, 2023; Arnbjerg-Nielsen et al., 2013). The most recent Coupled Model Intercomparison Project Phase 6 (CMIP6) provides updated climate projections under Shared Socioeconomic

Pathways (SSPs), which replace the Representative Concentration Pathways (RCPs) used in previous assessments (Eyring et al., 2016; O'Neill et al., 2016). SSPs combine socioeconomic development narratives with radiative forcing levels: SSP1-1.9 (sustainability, low emissions), SSP1-2.6 (sustainability, medium-low), SSP2-4.5 (middle-of-the-road, medium), SSP3-7.0 (regional rivalry, high), and SSP5-8.5 (fossil-fueled development, very high) (Riahi et al., 2017).

Precipitation Extremes: Climate models consistently project increases in extreme precipitation intensity and frequency across most land areas, including East Africa. For the Ethiopian highlands, CMIP6 projections indicate the following changes by 2050-2080 under medium-to-high emissions scenarios (SSP2-4.5 and SSP5-8.5): (1) Annual maximum 1-day precipitation (Rx1day) increases by 10-25% (Rettie et al., 2023; Gebrechorkos et al., 2019); (2) Annual maximum 5-day precipitation (Rx5day) increases by 15-30% (Dile et al., 2018); (3) Simple daily intensity index (SDII) increases by 5-15% (Rettie et al., 2023); (4) Consecutive dry days (CDD) increase by 10-30%, indicating longer dry spells punctuated by more intense storms (Wagesho and Yohannes, 2021). This pattern—more intense rainfall falling on increasingly impervious urban surfaces—creates compounding flood risk that exceeds the design capacity of most conventional drainage systems (Zhou et al., 2019; Arnbjerg-Nielsen et al., 2013).

IDF Curve Updating: Intensity-Duration-Frequency (IDF) curves, which relate rainfall intensity to duration and return period, are fundamental inputs for stormwater infrastructure design. Climate change alters IDF curves by increasing intensities for given return periods and/or reducing the return period for given intensities. A 10-year storm in the historical record may become a 5-year storm in future climate; a 100-year storm may become a 30–50-year storm (Arnbjerg-Nielsen et al., 2013; Ewea et al., 2018). Methods for updating IDF curves under climate change include: ***(1) delta change approach***—applying GCM-derived change factors to historical IDF curves; ***(2) quantile mapping***—using GCM outputs to directly estimate quantile-quantile relationships; and ***(3) stationary assumption rejection***—modeling IDF parameters as non-stationary functions of climate variables (Milly et al., 2008; Mailhot et al., 2012).

This dissertation uses the delta change approach, applying change factors derived from downscaled CMIP6 GCMs (Rettie et al., 2023) to historical IDF curves for the Ayertena station (1994-2023 baseline). Historical IDF curves were developed using the Indian Meteorological Department disaggregation method (Al Mamun et al., 2018) and Gumbel distribution for extreme value analysis (see Chapter 5, Section 5.2.2.1 for justification). The delta change method was selected because it is computationally efficient, widely used in engineering practice, and conservatively assumes that the relative change in rainfall intensity applies uniformly across durations and return periods—a simplification that is acceptable for comparing scenarios but may underestimate changes in tail extremes (Milly et al., 2008; Mailhot et al., 2012).

Urban Drainage Vulnerability: Climate change increases the vulnerability of urban drainage systems through several mechanisms (Arnbjerg-Nielsen et al., 2013; Semadeni-Davies et al., 2008). *Increased flooding* occurs when rainfall intensities exceed the hydraulic capacity of pipes, channels, and pumps, causing surcharging, manhole overflows, and surface flooding. Systems designed for 2–10-year storms may experience flooding annually or more frequently under climate change (Zhou et al., 2019; Abebe and Tesfamariam, 2019). *Higher pollutant loads* result because washoff and erosion increase with flow velocity and volume; sediments, nutrients, heavy metals, and pathogens are mobilized in higher concentrations during more intense storms (Dong et al., 2021; Yang et al., 2024). *Reduced infiltration* occurs when intense rainfall exceeds soil infiltration capacity, generating Hortonian overland flow even on pervious surfaces and reducing groundwater recharge (Jacobson, 2011). *Combined sewer overflow (CSO) frequency* increases as storm volumes exceed interceptor and treatment plant capacity, discharging untreated sewage and stormwater to receiving waters (Arnbjerg-Nielsen et al., 2013). *Maintenance costs* increase as sediment loading, debris, and structural damage accelerate, requiring more frequent cleaning and repair (Semadeni-Davies et al., 2008).

Adaptation Pathways: Adaptation to climate change in urban stormwater management requires moving beyond stationary design to flexible, adaptive approaches (Arnbjerg-Nielsen et al., 2013; Abebe and Tesfamariam, 2019). *Design under uncertainty* uses scenario planning, real options analysis, and dynamic adaptive policy pathways (DAPP) to identify strategies that perform well across a range of plausible futures (Walker et al., 2001; Haasnoot et al., 2013). *Green infrastructure* provides adaptive capacity because GI can be implemented incrementally, expanded based on performance monitoring, and modified in response to changing conditions—unlike rigid grey infrastructure (Fletcher et al., 2015; Dagenais et al., 2016). *IGGI* combines the adaptive capacity of GI with the reliability of GI, offering redundancy and diversity that enhance system resilience (Wang et al., 2023; Rodriguez et al., 2021). *Climate-informed IDF curves* incorporate GCM projections into design standards, adjusting return periods and intensities to account for future conditions (Milly et al., 2008; Mailhot et al., 2012).

This dissertation explicitly models climate change impacts by simulating baseline (historical 1994-2023), near-term (2024-2053), and midterm (2054-2083) periods under SSP2-4.5 and SSP5-8.5 scenarios (Chapter 5). This approach allows quantification of climate-driven increases in runoff and pollutant loads and evaluation of IGGI effectiveness under future climates (Chapter 7).

2.10 Urbanization and Land Use Change Effects on Runoff and Water Quality

Urbanization—the conversion of natural and agricultural land to build uses—is one of the most significant drivers of hydrological change globally (Jacobson, 2011; McGrane, 2016). Urbanization alters stormwater runoff through multiple mechanisms: increasing impervious surfaces, compacting remaining pervious soils, modifying drainage networks, and introducing new pollutant sources.

Imperviousness and Runoff Generation: Impervious surfaces (roofs, roads, parking lots, sidewalks, driveways) prevent infiltration of rainfall into underlying soils, converting precipitation directly to surface runoff. The relationship between impervious cover and runoff volume is strongly nonlinear: at low imperviousness (5-10%), runoff volume increases modestly (1.5-2× pre-development); at moderate imperviousness (20-40%), runoff volume increases substantially (3-5× pre-development); at high imperviousness (50-80%), runoff volume approaches total precipitation minus evaporation (8-12× pre-development) (Shuster et al., 2005; Oudin et al., 2018). This nonlinearity occurs because imperviousness not only reduces infiltration but also creates connectivity between impervious surfaces and drainage networks, routing runoff efficiently off-site (Jacobson, 2011; Zhou et al., 2019).

Peak discharge increases even more dramatically than runoff volume. For a 2-year return period storm, a catchment with 10-20% imperviousness may experience 2-4× pre-development peak flows; at 40-60% imperviousness, peak flows may increase 5-10×; at >70% imperviousness, peak flows can exceed 15× pre-development (Oudin et al., 2018; Zhou et al., 2019). Time to peak decreases correspondingly, from hours in natural catchments to minutes in highly urbanized catchments, producing flashy hydrographs with little baseflow between storms (McGrane, 2016; Barbosa et al., 2012).

Soil Compaction and Reduced Infiltration: Even pervious areas in urban catchments are often compacted during construction, reducing their infiltration capacity by 70-90% compared to undisturbed natural soils (Gregory et al., 2006; Yang and Zhang, 2011). Compaction increases bulk density (from 1.2-1.4 g/cm³ in natural soils to 1.6-1.9 g/cm³ in urban soils), reduces porosity (from 40-50% to 20-30%), and decreases saturated hydraulic conductivity (from 10-100 mm/hr to 0.1-10 mm/hr) (Gregory et al., 2006). Compacted urban soils behave hydrologically more like impervious surfaces than natural soils, generating overland flow even during moderate rainfall events (Pitt et al., 1999). Remediating compaction through soil restoration (deep tillage, compost amendment, vegetation establishment) can partially restore infiltration but is rarely implemented in routine landscaping (Yang and Zhang, 2011).

Pollutant Sources and Buildup-Wash-off: Urbanization introduces a wide range of pollutants to stormwater runoff, with concentrations and loads correlated with land use type, traffic intensity, and anthropogenic activities (Hatt et al., 2006; Barbosa et al., 2012). Major pollutant categories and sources include:

- ***Sediments (TSS):*** soil erosion from exposed and compacted surfaces, vehicle-induced road dust, construction activities, atmospheric deposition. TSS concentrations in urban runoff range from 20-500 mg/L for residential areas to 100-1,500 mg/L for construction sites and high-traffic roads (Hatt et al., 2006; Davis et al., 2012).
- ***Nutrients (nitrogen, phosphorus):*** fertilizer application (residential lawns, golf courses, parks), atmospheric deposition (NOx from vehicle emissions), detergents (car washing), pet waste, decomposing organic matter (leaves, grass clippings). Total nitrogen (TN) concentrations range from 1-10 mg/L; total phosphorus (TP) from 0.1-2 mg/L (Taylor et al., 2005; Line et al., 2002).
- ***Heavy metals (copper, lead, zinc, cadmium, chromium):*** vehicle emissions (past use of leaded gasoline), tire wear (zinc), brake pad wear (copper, antimony), building materials (galvanized roofs, gutters—zinc; copper pipes, electrical wiring—copper), atmospheric deposition. Copper concentrations range from 10-100 μg/L, lead 5-200 μg/L, zinc 50-500 μg/L (Davis et al., 2001; Brown and Peake, 2006).
- ***Organic pollutants (hydrocarbons, pesticides, PAHs):*** vehicle emissions (oil, grease, unburned fuel), road surface degradation, pesticide application (lawns, gardens), atmospheric deposition. Oil and grease concentrations range from 1-20 mg/L; PAHs from 0.1-10 μg/L (Hatt et al., 2006; Brown and Peake, 2006).
- ***Pathogens (bacteria, viruses):*** pet and wildlife waste, leaking sanitary sewers, illicit connections. Fecal coliform concentrations range from 100-10,000 CFU/100mL; E. coli from 50-5,000 CFU/100mL (Mallin et al., 2000; Line et al., 2002).

Pollutant *buildup* occurs during dry periods (antecedent dry days) as particles and adsorbed pollutants accumulate on impervious surfaces. Buildup rates follow exponential (first order) or power functions, asymptotically approaching maximum accumulation (Huber et al., 1979; Rossman and Huber, 2016). Pollutant *wash-off* during storm events follows exponential (exponential decay of remaining buildup) or rating curve (wash-off load proportional to runoff velocity or volume raised to a power) relationships (Temprano et al., 2006; Tu and Smith, 2018). *First flush*—the phenomenon where initial runoff carries disproportionately high pollutant loads—occurs for TSS, heavy metals, and particle-bound pollutants but may not occur for dissolved pollutants, which are more uniformly distributed throughout the event (Saget et al., 1996; Lee et al., 2002).

Land Use-Pollutant Relationships: Land use type strongly influences pollutant concentrations and loads (Hatt et al., 2006; Barbosa et al., 2012). *Residential areas* typically have moderate TSS (30-100 mg/L), higher nutrients (TN 2-8 mg/L, TP 0.3-1 mg/L) due to fertilizer use, and moderate metals (Cu 10-30 μg/L, Zn 50-150 μg/L) (Taylor et al., 2005). *Commercial areas* show higher TSS (50-200 mg/L), moderate nutrients (TN 1-5 mg/L), and higher metals from parking lot runoff and vehicle traffic (Cu 20-50 μg/L, Zn 100-300 μg/L) (Line et al., 2002). *Industrial areas* produce the highest TSS (100-1,000 mg/L), highest metals (Cu 50-200 μg/L, Zn 200-1,000 μg/L, Pb 50-500 μg/L), and may include site-specific pollutants (solvents, acids, alkalis) (Brown and Peake, 2006). *Transportation corridors (roads, highways)* produce high TSS (50-300 mg/L from tire wear, brake dust, road degradation), high metals (Cu 20-100 μg/L, Zn 100-400 μg/L, Pb 50-200 μg/L from legacy leaded gasoline and current brake pad wear), and hydrocarbons (oil, grease 5-20 mg/L) (Davis et al., 2001). *High-density mixed-use (residential-commercial)* sites produce the most variable pollutant signatures, reflecting the combination of sources.

Urbanization Trends in Addis Ababa: Addis Ababa has experienced rapid urbanization over the past three decades. Between 1991 and 2021, built-up area in the city increased by approximately 187%, from 78 km² to 224 km² (Moisa et al., 2022). Between 1993 and 2023, built-up area increased by 224% (Hailu et al., 2024). The city's population, approximately 3.95 million in 2023 (ESS, 2023), has doubled since 2000 and is projected to double again by 2035 (Koroso et al., 2021). This growth has increased imperviousness in many sub-catchments from 30-50% historically to 60-80% currently (Jemberie and Melesse, 2021; Adugna et al., 2019). Continued urbanization is projected to increase imperviousness further, with 15-20% reduction in pervious area over the next two decades under current land use policies (Hailu et al., 2024).

This dissertation explicitly models urbanization impacts by simulating an 80% imperviousness scenario (increase from baseline 70% imperviousness) under historical climate (Chapter 5). This scenario represents continued urban expansion consistent with observed trends and projections. The combined climate-urbanization scenario (SSP2-4.5 or SSP5-8.5 + 80% imperviousness) represents the most challenging future condition and provides the basis for evaluating IGGI resilience (Chapter 7).

2.11 Sponge City Concept: Principles, Implementation, and Comparison with IGGI

The Sponge City concept, pioneered in China since 2013, represents one of the most ambitious and large-scale applications of nature-based stormwater management globally (Chan et al., 2018; Li et al., 2019; Nguyen et al., 2019). A Sponge City is defined as an urban planning model designed to “absorb, store, infiltrate, and purify” stormwater using green infrastructure—parks, permeable pavements, rain gardens, green roofs, constructed wetlands, detention basins—rather than relying solely on conventional grey drainage systems (Jia et al., 2017; Qiao et al., 2020; Xu et al., 2019).

Core Principles: The Sponge City concept operationalizes several key principles. *Source control* places green infrastructure at the location of runoff generation—rooftops, courtyards, streets, parking lots—to capture and treat stormwater at its origin (Li et al., 2018; Liu et al., 2021). *Slow down* uses vegetated swales, terraced landscapes, check dams, and meandering channels to reduce flow velocity, increasing contact time with vegetation and soil for infiltration and treatment (Zevenbergen et al., 2018). *Store* incorporates temporary retention in rain barrels, cisterns, ponds, wetlands, and underground storage tanks, capturing stormwater for non-potable uses (irrigation, toilet flushing, street cleaning) (Jia et al., 2017). *Treat* removes pollutants through bioretention (filtration, adsorption, plant uptake), sedimentation, and microbial transformation (nitrification, denitrification, phosphorus uptake) (Nguyen et al., 2019). *Reuse* harvests captured stormwater for irrigation, toilet flushing, car washing, and other non-potable applications, reducing potable water demand and maintaining baseflow (Qiao et al., 2020). *Release* controls discharge of excess runoff to grey infrastructure (pipes, channels) or receiving waters, with flow regulation to prevent downstream flooding (Chan et al., 2018).

Implementation Scale and Performance: By 2020, China had designated 30 Sponge City pilot municipalities, with investments exceeding USD 10 billion. The national target, set by the State

Council, requires that 80% of urban built-up areas achieve 70% stormwater capture and reuse by 2030 (WWAP, 2018). Pilot projects have been implemented at multiple scales, from neighborhood-level retrofits (e.g., Yueliangwan in Zhenjiang) to district-scale development (e.g., Lingang in Shanghai) to municipal-wide programs (e.g., Shenzhen, Xiamen, Wuhan) (Li et al., 2018; Qiao et al., 2020).

Early evaluations of Sponge City pilots report significant stormwater management benefits. In the Lingang Sponge City district (Shanghai), annual runoff volume reduction reached 65-75%, peak flow reduction for 2-year storms was 50-70%, and pollutant load reductions (TSS, TP, TN) ranged from 40-60% (Wang et al., 2020). In the Yueliangwan neighborhood (Zhenjiang), annual runoff capture exceeded 85%, and surface flooding was eliminated during storms up to the 10-year return period (Jiang et al., 2018). In Shenzhen, Sponge City retrofits reduced annual runoff volume by 55-70%, reduced peak flows by 45-65%, and reduced TSS loads by 60-80% across 50 km² of built area (Liu et al., 2021).

Beyond stormwater benefits, Sponge City projects have generated measurable co-benefits: urban surface temperatures decreased by 2-5°C in vegetated areas; property values near Sponge City parks increased by 5-15%; and residential satisfaction with flood risk, aesthetics, and recreational amenities increased significantly (Qiao et al., 2020; Wang et al., 2020).

Comparison with IGGI and Related Paradigms: The Sponge City concept shares fundamental principles with other sustainable stormwater management paradigms, though with distinct emphases and contexts (Table 2.4).

Table 2.4: Comparison of Sponge City with IGGI and Related Paradigms

Paradigm	Origin	Primary Focus	Scale	Key Features	Typical Slope/Soil Assumption
Sponge City	China	Stormwater capture, storage, reuse, flood mitigation	City/district (10-100 km²)	Government-led, large-scale investment (USD billions), integrated with urban planning, 70% capture target	Gentle slopes (<5%), variable soils (loam, clay, reclaimed)

IGGI (this study)	Global South (Ethiopia)	Hybrid green-grey systems for challenging terrain	Micro-watershed/contributing zone (0.2-30 ha)	Terrain-sensitive, modular, low-cost, adaptable to data-scarce contexts, buried infrastructure for space efficiency	Steep slopes (>7%), poorly draining soils (Vertisols)
LID	USA	Mimicking pre-development hydrology	Site/neighborhood (0.1-10 ha)	Decentralized, infiltration-based, design-storm focused, site-scale	Gentle to moderate slopes (1-7%), well-drained soils (loam, sand)
SUDS	UK	Water quantity, quality, amenity, biodiversity	Site to catchment (0.1-100 ha)	Treatment train approach, multi-objective, regulatory driver (planning policy)	Gentle slopes (<7%), variable soils
WSUD	Australia	Integrating water cycle into urban design	Precinct/city (1-50 km^2)	Interdisciplinary (engineers + planners + landscape architects), water-sensitive cities vision	Gentle to moderate slopes (<10%), variable soils

Sources: *Compiled from Fletcher et al. (2015), Chan et al. (2018), Qiao et al. (2020), Hua et al. (2020), Yang and Zhang (2021).*

Relevance to This Dissertation: The Sponge City concept offers several lessons for IGGI implementation in Addis Ababa and other Global South cities (Dereje Fekadu et al., 2022; Azagew and Worku, 2020). First, institutional integration—creating cross-agency coordination mechanisms—is essential for scaling IGGI from pilot projects to city-wide programs. Second, performance standards (e.g., Shanghai's 70% capture target) provide clear, measurable objectives that can be incorporated into municipal codes and development approvals. Third, dedicated financing mechanisms (central government subsidies, municipal bonds, developer exactions) are necessary for upfront capital investment. Fourth, public engagement and communication (education campaigns, demonstration projects, citizen science monitoring) build support and compliance.

However, direct transferability of the Sponge City model to Addis Ababa is limited by differences in institutional capacity, land tenure systems, available financial resources, and biophysical conditions (Eshetu et al., 2021; Ijara, 2020). The Sponge City program is state-led with central government financing exceeding USD 10 billion; Addis Ababa operates with municipal budgets two to three orders of magnitude smaller. Land tenure in China is state ownership with long-term leases, facilitating land acquisition for GI; Addis Ababa has complex customary, leasehold, and informal tenure systems that complicate coordinated GI implementation (Koroso et al., 2021). Most Sponge City pilots have been implemented on gentle slopes (<5%) and variable soils; Addis Ababa's steep slopes and Vertisols pose more challenging conditions. The IGGI framework developed in this dissertation—modular, low-cost, terrain-sensitive, and adaptable to data-scarce contexts—represents a context-sensitive adaptation of Sponge City principles to Ethiopian realities.

2.12 The Need for Innovative IGGI Approaches

The preceding literature review has established that conventional grey infrastructure is insufficient under climate change and urbanization pressures (Section 2.4), that green infrastructure provides co-benefits but faces implementation barriers in dense urban areas (Section 2.5), that hillslope hydrology research has focused on natural catchments rather than steep, Vertisol-dominated urban contributing zones (Section 2.7), and that existing IGGI frameworks (including Sponge City) assume gentle slopes and well-drained soils (Section 2.11). A persistent gap remains: IGGI approaches suited to steep slopes (>7%) and poorly draining Vertisol soils in rapidly urbanizing Global South cities with limited data and budgets.

Hydrological Complexity in Steep, Vertisol-Dominated Catchments: Steep slopes (>7-15%) generate rapid overland flow with short concentration times (often <10-30 minutes), reducing the time available for infiltration, storage, and treatment (Omitaomu et al., 2021; EPA, 2014). Soils with low permeability (<10 mm/hr, often <1 mm/hr for Vertisols) cannot infiltrate runoff at rates sufficient to prevent overland flow, even on gentle slopes (Berhanu, 1983; Debele and Deressa, 2016). The combination of steep slopes and low-permeability soils creates a "double constraint" that renders conventional GI practices ineffective: bioretention systems and infiltration trenches pond water that cannot infiltrate rapidly enough, leading to increased mosquito habitat, plant stress, and potential failure (Sharma and Malaviya, 2021; EPA, 2014). Permeable pavements may collapse under wheel loads if subgrade saturation occurs (Weiss et al., 2017). Rain gardens require engineered media and underdrains to function, increasing costs beyond typical household budgets in lower-income contexts (Ghodsi et al., 2021).

Innovations Required: Addressing the double constraint requires innovative IGGI designs that: (1) provide temporary storage for runoff until infiltration into low-permeability native soils can occur (delayed infiltration); (2) capture runoff from multiple impervious surfaces (rooftops, roads, parking lots, yards) rather than relying on single-source capture; (3) combine green and grey functions in space-efficient configurations suitable for dense urban areas where surface space is limited; (4) use locally available, low-cost materials and construction techniques; (5) require minimal maintenance and can function even if maintenance is deferred; and (6) provide measurable performance (peak flow reduction, volume reduction, pollutant load reduction) under climate-urbanization pressures.

The Buried Rain Barrel + Rain Garden IGGI System: This dissertation introduces a novel IGGI configuration specifically designed for the double constraint (Chapter 7). The system integrates:

- ***Rain gardens (RGs):*** vegetated bioretention cells with engineered sandy-loam media (35 mm/hr. infiltration rate, 0.2 effective porosity) and underdrains, designed to capture, infiltrate, and treat runoff from contributing zone surfaces. The RGs provide rapid infiltration and pollutant removal for the frequent, smaller storms (2-year return period).
- ***Buried rain barrels (RBs):*** standard 400 L barrels buried in sand filtration beds along the lower boundary of the contributing zone, capturing runoff from multiple surfaces (roofs, roads, vegetation, yards, parking areas) that bypasses or exceeds RG capacity. The buried RBs provide additional temporary storage (collectively ≥ 2 m^3) and delayed infiltration to native Vertisol subgrade via sand bed and ball-tanker check valve control; excess water bypasses through a 75 cm outlet with 45° elbow to grey drainage network.
- ***Integration:*** The RG and buried RBs are hydraulically connected, forming a treatment train: runoff first enters the RG (for frequent storms), excess flow is conveyed to the buried RBs (for moderate storms), and bypass beyond RB capacity enters the grey drainage network (for extreme events). This configuration ensures that (1) even small storms are treated (RG only);

(2) moderate storms are detained and infiltrated (RG + RB); (3) extreme storms are conveyed without system failure (grey bypass); and (4) infiltration into native Vertisol occurs at controlled rates, avoiding ponding and saturation.

Hypothesis: The dissertation tests the hypothesis that the buried RB + RG IGGI system can reduce stormwater runoff volume, peak flow, and pollutant loads by approximately 30% under a typical 2-year return-period design storm, relative to baseline (grey-only) conditions, even on steep slopes and Vertisol soils.

Contribution to Knowledge: This IGGI innovation advances beyond existing LID, SUDS, WSUD, and Sponge City practices by explicitly addressing the double constraint. To the best of our knowledge, no previous study has: (1) evaluated buried rain barrels (as distinct from above-ground rain barrels) as a stormwater management practice; (2) integrated buried rain barrels with rain gardens in a treatment train; (3) quantified hydrological and water-quality performance of such a system in a steep, Vertisol-dominated urban contributing zone; or (4) applied PCSWMM to model pre- and post-IGGI conditions in this context. This dissertation thus contributes novel empirical evidence and a replicable IGGI framework for challenging urban environments in the Global South.

2.13 Central Role of PCSWMM in Modeling Complex Urban Catchments

As established in Section 2.8, PCSWMM is the selected modeling platform for this dissertation. This section elaborates PCSWMM's specific capabilities relevant to the study objectives and justifies its use for the integrated analysis presented in Chapters 5, 6, and 7.

Hydrologic and Hydraulic Representation: PCSWMM's hydrologic module represents sub-catchments as non-linear reservoirs, with runoff generated as the excess of precipitation over infiltration, evaporation, and depression storage (Rossman, 2015; CHI, 2023). Infiltration can be modeled using three methods: Horton (exponential decay of infiltration capacity), Green-Ampt (physics-based infiltration based on soil properties and moisture deficit), or Curve Number (empirical NRCS method). This dissertation uses the Modified Green-Ampt method because it provides more physically realistic representation of infiltration in low-permeability Vertisols than Horton's empirical decay curve or the NRCS curve number (which was developed for agricultural, not urban, conditions) (Lee et al., 2018; Rossman, 2015).

PCSWMM's hydraulic module routes flow through pipes, channels, pumps, and storage units using full dynamic wave solutions to the Saint-Venant equations (Rossman, 2015; CHI, 2023).

The dynamic wave method accounts for backwater effects, surcharging, pressurized flow, and looped networks—essential for urban drainage systems where pipe networks are interconnected, and surcharging occurs during high-flow events. This dissertation uses dynamic wave routing (Chapters 5-7) to accurately represent surcharging and flooding in the study area's drainage network. Kinematic wave routing (simplified, neglecting backwater) was rejected because it cannot simulate surcharging and may underestimate flood risk (Rossman, 2015).

LID Controls Module for IGGI Representation: PCSWMM's LID controls module provides explicit representation of nine GI practices: rain barrels, rain gardens, bioretention cells, permeable pavements, green roofs, infiltration trenches, vegetative swales, rooftop disconnection, and constructed wetlands (Rossman, 2015; CHI, 2023). Each LID type is represented as a vertical profile of layers (surface, soil, storage, pavement, drainage) with user-specified parameters (layer thickness, porosity, conductivity, roughness, etc.). LIDs can be placed on pervious or impervious fractions of sub-catchments, with runoff from the sub-catchment directed to the LID for treatment. This dissertation uses PCSWMM's LID module to represent rain gardens (bioretention cells) and rain barrels. For rain gardens, the LID module requires parameters for: surface layer (ponding depth, roughness, slope), soil layer (thickness, porosity, conductivity, hydraulic conductivity slope, suction head, and initial moisture deficit), storage layer (thickness, porosity, conductivity, clogging factor), and underdrain (drain coefficient, exponent, offset, opening height, and flow coefficient). These parameters were assigned based on design specifications (Section 7.2.4) and calibrated using observed field data (Section 7.2.7). For rain barrels, the LID module requires storage capacity (m^3), drain time (hours), and barrel count per treatment area. The buried RBs in this study (Section 7.2.4) required adaptation of standard rain barrel parameters to represent subsurface placement and sand filtration bed.

Pollutant Buildup and Wash-off: PCSWMM's water quality module simulates pollutant buildup during dry periods and wash-off during storms (Rossman and Huber, 2016; CHI, 2023). Buildup can be modeled using power, exponential, or saturation functions; wash-off using exponential (buildup decay) or rating curve. The Event Mean Concentration (EMC) method (constant pollutant concentration during runoff) was used in this dissertation for initial model setup, with subsequent calibration using observed water quality data from the study area (Sections 5.2.2.3, 5.2.4). EMC was selected because it is simpler and has fewer parameters than buildup-wash-off functions, which is advantageous in data-scarce contexts (Temprano et al., 2006; Tu and Smith, 2018).

However, this simplification introduces uncertainty that is addressed through sensitivity analysis (Section 5.2.4.2) and acknowledged as a limitation (Section 5.4.2).

Climate Change Scenario Generation: PCSWMM's climate change module directly imports downscaled GCM outputs (CMIP5, CMIP6) and applies change factors to historical IDF curves or continuous precipitation/temperature time series (CHI, 2023). The module supports multiple scenarios (e.g., RCPs, SSPs), time horizons (e.g., near-term, mid-term, far-term), and GCM ensemble averaging. This dissertation uses downscaled CMIP6 projections from Rettie et al. (2023) for SSP2-4.5 and SSP5-8.5 scenarios, near-term (2024-2053) and mid-term (2054-2083) time horizons (Section 4.2.2.1). The PCSWMM climate module was used to generate delta change factors for IDF curves and to adjust continuous precipitation for future periods in scenario simulations.

Calibration and Validation Tools: PCSWMM's Sensitivity-based Radio Tuning Calibration (SRTC) tool automates sensitivity analysis, calibration, and validation (CHI, 2023; Wagener and Wheater, 2006). SRTC uses a one-at-a-time (OAT) approach for sensitivity analysis (varying each parameter while holding others constant) and a multi-parameter optimization algorithm (pattern search, genetic algorithm, or simplex) for calibration. SRTC was used in this dissertation to:

- Identify influential parameters (imperviousness, sub-catchment width, Manning's n, LID parameters) (Sections 4.2.4.1, 6.2.6)
- Calibrate the baseline model using observed runoff depth and water quality data (Sections 5.2.3, 5.2.4, 7.2.3)
- Validate baseline and IGGI models using independent storm events (Sections 4.2.4, 6.2.7)

2.14 Decision-Support and Multi-Objective Optimization (MCDA)

Multi-Criteria Decision Analysis (MCDA) provides a systematic framework for integrating multiple, often conflicting criteria into transparent, defensible decisions (Hwang and Yoon, 1981; Saaty, 1980). In stormwater management, MCDA has been applied to site selection for GI (Chapter 4), infrastructure prioritization (Chapter 6), and design optimization (Luan et al., 2019; Omidi Arjenaki et al., 2020). Key MCDA methods include:

AHP (Analytic Hierarchy Process): A hierarchical method that decomposes decisions into criteria and sub-criteria, obtains pairwise comparisons from experts, and calculates weights as principal eigenvectors of comparison matrices (Saaty, 1980, 2008). AHP assumes independence among criteria—criteria are compared pairwise but do not influence each other.

ANP (Analytic Network Process): An extension of AHP that allows feedback and interdependencies among criteria using a supermatrix approach (Saaty, 2005). ANP is superior for problems where criteria influence each other in complex ways—for example, slope influencing soil moisture (TWI), which influences vegetation cover (NDVI), which influences runoff generation (Saaty and Vargas, 2012; Yüksel and Dağdeviren, 2007).

TOPSIS (Technique for Order of Preference by Similarity to Ideal Solution): A method that ranks alternatives based on their distance to the ideal (best) and anti-ideal (worst) solutions (Hwang and Yoon, 1981; Behzadian et al., 2012). TOPSIS does not require criteria independence, can accommodate both benefit and cost criteria, and produces cardinal (not just ordinal) rankings.

Other MCDA methods include Weighted Sum Model (WSM) — simple additive weighting but requires criteria to be commensurate; ELECTRE (ELimination Et Choix Traduisant la REalité) — outranking methods for problems with non-commensurable criteria; PROMETHEE — preference function-based outranking; and Multi-Attribute Utility Theory (MAUT) — utility function-based but requires more information from decision-makers (Huang et al., 2011; Linkov et al., 2006).

Application to IGGI Suitability (Chapter 3): Chapter 3 applies AHP and ANP to map IGGI suitability across Addis Ababa. Twelve attributes were grouped into three clusters: Topographical-Hydrological (slope, TWI, elevation, TPI, TRI), Land Use-Vegetation (LULC, soil, NDVI, hillshade), and Socio-Spatial-Accessibility (proximity to rivers, proximity to roads, population density). AHP (independence assumption) and ANP (interdependence allowed) were compared. ANP was expected to provide more accurate suitability mapping because the attributes are interdependent—for example, slope influences TWI (Beven and Kirkby, 1979), elevation influences temperature which influences NDVI, LULC influences runoff which influences flood risk captured by proximity to rivers (Mobarak et al., 2022; Waheeb et al., 2023). ANP's superior performance (AUC = 0.92 vs. 0.87 for AHP, RMSE = 0.12 vs. 0.16) confirmed that accounting for interdependencies improves spatial decision accuracy.

Application to Infrastructure Performance (Chapter 5): Chapter 5 applies AHP-weighted TOPSIS to rank five spatial blocks based on six performance criteria: flood conveyance capacity (C_1), structural integrity (C_2), erosion control effectiveness (C_3), sediment accumulation (C_4 — cost criterion), maintenance accessibility (C_5), and flood control effectiveness from PCSWMM (C_6). AHP provided expert-derived weights based on pairwise comparisons from 12 experts. TOPSIS then normalized the decision matrix, defined ideal and anti-ideal solutions, computed

Euclidean distances, and ranked blocks by relative closeness (C_i). Sensitivity analysis (varying weights across five scenarios) confirmed ranking robustness (Spearman's $\rho > 0.92$), with Blocks 3 and 4 remaining top and bottom performers regardless of weight changes.

Why AHP and TOPSIS Specifically? AHP was selected for weighting because it is the most widely used MCDA weighting method in environmental applications, has well-established consistency checks ($CR \leq 0.1$), and can be implemented with modest expert participation (12 experts in this study) (Saaty, 2008; Amjad et al., 2024; Asefa et al., 2021). TOPSIS was selected for ranking because it produces intuitive rankings based on distances to ideal solutions, handles benefit and cost criteria without transformation, and has been validated in numerous stormwater prioritization studies (Behzadian et al., 2012; Luan et al., 2019; Omidi Arjenaki et al., 2020). Other MCDA methods were rejected: WSM cannot handle cost criteria without transformation; ELECTRE and PROMETHEE require more information from decision-makers (preference thresholds, indifference thresholds) that may be arbitrary in data-scarce contexts; MAUT requires utility function elicitation, which is more cognitively demanding for experts than pairwise comparisons (Huang et al., 2011; Linkov et al., 2006).

2.15 Identification of Research Gaps

Based on the critical review of literature presented in Sections 2.1-2.14, four distinct research gaps are identified that collectively motivate this dissertation. Each gap is formulated as a specific deficiency in current knowledge that this dissertation directly addresses.

2.15.1 Gap 1: Spatial suitability mapping for IGGI in Global South cities

While GIS-based MCDA has been applied to urban green space planning (Moisa et al., 2023; Gelan, 2021; Anteneh et al., 2023), landfill site selection (Bakolo et al., 2024; Asefa et al., 2021), and flood risk mapping (Mukhtar et al., 2024; Zhran et al., 2024), no study has developed a spatially explicit suitability map specifically for IGGI—as distinguished from conventional green spaces—in a rapidly urbanizing African city. Furthermore, existing studies predominantly employ AHP assuming attribute independence, without systematically evaluating whether ANP (accounting for interdependencies) provides improved spatial accuracy. The comparative performance of AHP vs. ANP for IGGI suitability has not been reported in the literature.

2.15.2 Gap 2: Hydrologic modeling in steep, poorly draining urban contributing zones

Hillslope hydrology has been extensively studied in natural and agricultural catchments (Horton, 1933; Dunne and Black, 1970; Kirkby, 1978; Weiler, 2017), and process-based modeling using tools such as SWMM and PCSWMM has been widely applied to urban catchments. However, the specific combination of (a) an urban contributing zone (the uppermost runoff-generating area), (b) steep slopes (>7%), and (c) low-permeability Vertisol soils remains rare in the literature (Section 2.7). Moreover, few studies have quantified the combined impacts of climate change and urbanization on both runoff quantity and pollutant loading in such terrain- and soil-constrained urban environments, especially in data-scarce Global South contexts. Studies that do exist (e.g., Bibi et al., 2023; Abd-Elhamid et al., 2020) focus on gentle slopes and well-drained soils or do not explicitly model contributing zones.

2.15.3 Gap 3: Systematic performance assessment of existing stormwater infrastructure

In many Global South cities, including Addis Ababa, there is no regulatory framework mandating regular infrastructure inspection or performance documentation (Adugna et al., 2019; Jemberie et al., 2023). Consequently, no systematic assessment exists of existing stormwater infrastructure hydraulic condition, structural integrity, erosion control effectiveness, sediment accumulation, or maintenance accessibility. This absence of baseline data impedes evidence-based prioritization of maintenance and IGGI retrofitting interventions. Even where studies exist (e.g., Jemberie et al., 2023 for Addis Ababa; Ntakiyimana et al., 2022 for Kigali), they typically assess a few infrastructure units anecdotally rather than systematically applying MCDA frameworks to rank and classify performance.

2.15.4 Gap 4: IGGI design for steep slopes and poorly draining soils

Existing IGGI, LID, SUDS, WSUD, and Sponge City frameworks assume gentle slopes (<7%) and well-drained soils (loam, sand, loess) for most infiltration-based practices (EPA, 2014; Omitaomu et al., 2021; Seidu et al., 2025). There is no established methodology for harmonizing green and grey infrastructure specifically for steep slopes (>7%) and Vertisol (clay) soils—nor one that focuses explicitly on contributing zones of urban micro-watersheds where runoff generation is most active. Conventional rain barrels capture only rooftop runoff; their integration with rain gardens and burial for multi-source capture (rooftops + roads + parking lots + yards) has not been evaluated in steep, low-infiltration settings. Where GI on clay soils has been studied (Khan et al., 2020; Sharma and Malaviya, 2021), evaluations focus on bioretention or rain gardens alone, not integrated IGGI systems.

2.15.5 Gap 5 (Methodological integration)

While individual studies have used GIS-MCDA for suitability mapping (e.g., Moisa et al., 2023), PCSWMM for hydrologic modeling (e.g., Bibi et al., 2023), and TOPSIS-AHP for infrastructure prioritization (e.g., Omidi Arjenaki et al., 2020), no study has integrated these three methodological streams—spatial suitability assessment, hydrologic modeling under climate/urbanization scenarios, performance-based infrastructure ranking, and novel IGGI intervention design—within a unified, sequential framework for a single case study area. This sequential integration (suitability → modeling → performance → intervention) represents a methodological innovation with potential for replication in other Global South cities. This dissertation addresses Gap 5 across all chapters, with synthesis in Chapter 8.

2.16 How This Dissertation Addresses the Identified Gaps

The four specific objectives of this dissertation (Section 1.3.2) are directly mapped to the identified gaps, as shown in Table 2.5.

Table 2.5: Mapping of Dissertation Objectives to Research Gaps

Gap	Addressed by	Chapter	Specific Contribution
Gap 1 (Spatial suitability)	Specific Objective 1	Chapter 3	First IGGI-specific suitability map for Addis Ababa; compares AHP and ANP; validates with AUC/RMSE; identifies 59.86% of city as suitable
Gap 2 (Hydrologic modeling in steep/Vertisol contributing zones)	Specific Objective 2	Chapter 4	First PCSWMM application addressing the specific combination of steep slope (>7%), Vertisol soil, and contributing zone in a data-scarce Global South city; quantifies climate-urbanization combined impacts; calibrates/validates with field data
Gap 3 (Infrastructure performance assessment)	Specific Objective 3	Chapter 5	First systematic, multi-criteria performance assessment of existing stormwater infrastructure in Addis Ababa; provides evidence-based retrofit/maintenance prioritization using TOPSIS-AHP
Gap 4 (IGGI design for steep	Specific Objective 4	Chapter 6	Novel buried RB + RG IGGI configuration specifically designed for Vertisol soils and steep

slopes/poorly draining soils)			slopes; field implementation (0.836 ha) and PCSWWM modeling; cost-effectiveness analysis
Gap 5 (Methodological integration)	All objectives	Chapters 3-7	Sequential integration of GIS-MCDA (AHP/ANP) → PCSWMM modeling (climate-urbanization scenarios) → TOPSIS-AHP infrastructure ranking → novel IGGI intervention in a single case study framework

Chapter 3

3 Assessing Green and Grey Infrastructure Suitability in Addis Ababa, Ethiopia Using GIS-Based Multi-Criteria Analysis

Abstract

Rapid urbanization and climate change intensified stormwater management challenges in urban areas, highlighting the need for sustainable alternatives like IGGI. This study assessed IGGI's spatial suitability in Addis Ababa, Ethiopia, using a GIS-based MCDA framework combining the AHP and ANP. Twelve attributes across hydrological, topographical, socio-spatial, and accessibility domains were analyzed. Results showed that ANP model identified 59.86% of the city as suitable and 33.82% as potentially suitable for IGGI, while AHP marked 42.24% as suitable and 52.2% as potentially suitable, indicating a more conservative approach. Less than 7% of the area was non-suitable in both models. Spatial analysis indicated highly suitable zones were near roads and rivers, with moderate slopes, well-drained soils, and low population densities—emphasizing the role of topography and accessibility. Validation revealed ANP's superior performance with an AUC of 0.92 and RMSE of 0.12, compared to AHP's AUC of 0.87 and RMSE of 0.16. These findings demonstrate ANP's enhanced spatial accuracy due to inter-attribute relationships. The study highlights the complementary strengths of AHP and ANP, offering a robust approach to urban infrastructure suitability analysis. It emphasizes IGGI's potential to boost urban resilience and promote sustainability, contributing to SDGs 6, 11, and 13. Future research should include economic factors—such as land acquisition, construction and maintenance costs—and community acceptance to refine IGGI implementation frameworks.

Keywords: IGGI, AHP, ANP, AUC, Suitability Analysis, Addis Ababa.

3.1 Introduction

Global urbanization is growing rapidly; more than half of the world's population lives in urban areas (Girma et al., 2019; United Nations, 2014; Wang et al., 2022). Increased impermeable surfaces have disrupted natural hydrological processes, leading to a decrease in infiltration and enhancing frequent and severe urban floods (Oudin et al., 2018; Wang et al., 2022). These impacts were aggravated by climate change, which may further add to these impacts due to increases in extreme precipitation events that threaten infrastructure and ecosystems (Almaliki et al., 2023; Moisa et al., 2023; Zerouali et al., 2022). In addition, pollution from urban areas is mobilized due to stormwater runoff, which then causes the discharge of these pollutants into water bodies degrading their quality and posing threats to human health (Dong et al., 2021; Shrestha et al., 2018; Zhou et al., 2019).

Traditional grey infrastructure is an engineering system which was designed mainly to deal with runoff quantity. They work by quickly collecting and moving stormwater further downstream. However, they are increasingly seen as unsustainable for future cities because these systems are rigid and non-adaptive. Moreover, they cannot cope with the multifaceted urbanization and climate change problems (Cheng et al., 2022; McFarland et al., 2019; Senes et al., 2021). Many countries are responding to these events by adopting climate change adaptations that advocate for nature-based integrated solutions. Emphasizing source control and resilience to improve sustainability. Notably, LID in North America, SuDS in the UK, WSUD in Australia and China's Sponge City (Fletcher et al., 2015; Hua et al., 2020; Yang and Zhang, 2021). Although there is some variation in terms and emphasis, these strategies support retrofitting of conventional infrastructure with green infrastructure- bioswales, rain gardens, rain barrels, permeable pavements, infiltration trenches, green roofs- to increase infiltration, water quality, flood mitigation and ecosystem service. Together, they are emerging the newest hybrid approach combined grey and green systems, popularly called IGGI. It brings reliability of grey and ecological benefit of green. In sharp contrast, cities such as Warangal in Andhra Pradesh, India (Parkinson and Mark, 2015), Nairobi, Kenya (Mulligan et al., 2020), Delhi, India (Kumar et al., 2023), Dar es Salaam, Tanzania (Mguni et al., 2015), and Addis Ababa continue to depend on fragmented, under-maintained grey infrastructure.

Addis Ababa has expanded rapidly over the past few decades, with the areas of the city growing by over 20% (Woldegerima et al., 2016; World Bank, 2015). Such rapid expansion has basically outpaced the city's stormwater and sanitary systems. The drainage system in Addis Ababa is poorly separated and generally not well maintained, and most areas are dependent on poorly functioning open channels and clogged pipes (Jemberie et al., 2023). Because of this, flooding during the rainy season is a regular occurrence, with 76 flood events occurring in 2017 alone (Jemberie and Melesse, 2021). Informal settlements near flood-prone rivers are more likely to be impacted (Birhanu et al., 2016). Many fast-growing cities in the Global South experience infrastructural and hydrological challenges like the one illustrated here. For this reason, Addis Ababa is a relevant case for the evaluation of integrated urban stormwater management solutions

(Kumar et al., 2023; Lemes de Oliveira et al., 2025). The lack of integrated planning and maintenance and uncontrolled land use also contributed to flooding and pollution, which increased health risks (Angello et al., 2021; Jemberie and Melesse, 2021). As developed nations migrate towards source-control-based IGGI, cities like Addis Ababa are still struggling with fundamental infrastructure shortcomings. Even so, incorporating green infrastructure into current grey networks provides a powerful means of managing runoff, enhancing water quality, and strengthening resilience.

A number of studies have been done on urban green spaces (UGS), which have concentrated on ecological, recreational, and social objectives (Girma et al., 2019; Mensah, 2014; Moisa et al., 2023; Waheeb et al., 2023). Nonetheless, this is not yet reflected in the planning at the local level, which often ignores the more contextual understanding of land-use, hydrological, infrastructural, and socio-spatial dynamics (McFarland et al., 2019; Tansar et al., 2024). Not taking these complexities into account will bring about system malfunctioning and underperformance (Lindsey et al., 1992). In addition to the above, many papers have employed the AHP in estimating the suitability of UGS (Abebe and Megento, 2017; Anteneh et al., 2023; Bakolo et al., 2024; Gelan, 2021; Hailemariam, 2021; Mobarak et al., 2022; Moisa et al., 2023; Waheeb et al., 2023). However, AHP by assumption considers all factors to be independent. Overall, IGGI planning is a multidimensional effort with interdependencies that AHP alone may miss.

In response to these gaps, this study presents an evaluation of the IGGI site suitability map to enhance sustainable urban stormwater management (SUSM) using AHP (considering independence between attributes) and ANP (considering interdependence between attributes). The joint application of AHP and ANP presents an effective way of analyzing independent and interrelated attributes. Both analyses are part of a GIS-based MCDA framework, which allows for joint spatial evaluation of technical suitability in Addis Ababa. Previously, efforts have been made to develop a GIS-based MCDA to support decision-making related to infrastructure, agriculture, environmental plans, and so on (Achu et al., 2020; Allende-Prieto et al., 2024; Azizi et al., 2014; Degefu and Asefa, 2024; Harlis and Seo, 2024; Mukhtar et al., 2024; Özkan et al., 2019; Pathan et al., 2022; Trupti L. et al., 2020; Zhran et al., 2024), without particular focus on IGGI suitability. The aim of this study is to create GIS-based technical site suitability maps for IGGI implementation in Addis Ababa using AHP and ANP for comparative analysis based on the evaluation of land use, hydrological, topographical, socio-spatial and accessibility factors using

Saaty's pairwise comparison matrix. Although the analysis included the technical feasibility, it does not consider all other aspects including Policy, economic (land acquisition/construction/maintenance cost), and community acceptance may still need to be assessed. However, the technical analysis is useful and may lay the foundation for additional studies that will analyze these further components. The findings ultimately contribute to urban resilience with a replicable framework for IGGI planning that promotes the transforming infrastructural planning towards sustainable stormwater systems in rapidly urbanizing cities. The research further contributes to the global pursuit of the SDGs, with particular emphasis on SDG targets 6, 11, and 13. It adopts the perspective of spatial sustainability and aims to contribute to enhancing integrated, climate-resilient, sustainable infrastructure in urban areas through spatially optimized IGGI application.

3.2 Materials and Methods

3.2.1 Description of the Study Area

Addis Ababa, Ethiopia's capital, covers approximately 527 km^2 and serves as the country's administrative, economic, and social center, with a population of about 3.95 million (CSS, 2023; Moisa et al., 2023). It lies between latitudes 8º1'15"–9º4'15" N and longitudes 38º38'0"–38º55'30" E (Moisa et al., 2023), with an average elevation of 2,600 m above sea level (Feyissa et al., 2018). Elevation ranges from 2,044 m in the Akaki plains to 3,140 m at Mount Entoto (Fig. 3.1). River systems such as Kebena and Akaki play vital roles in stormwater management (Feyissa et al., 2018; McFarland et al., 2019), while road networks enhance IGGI suitability and accessibility (Emagnu, 2018). The city receives an average annual rainfall of 1,184 mm, mainly from June to September, with temperatures ranging from 10.2°C to 22.9°C. Administratively, it comprises 10 sub-cities (Feyissa et al., 2018), including densely populated areas like Kolfe Keraniyo, Gulele, Arada, Chirkos, Addis Ketema, and Lideta, and moderately populated ones like Bole, Akaki Kality, Yeka, and Nefas Silk Lafto.

3.2.2 Data Acquisition and Preprocessing

We collected spatial datasets from open-access repositories and Ethiopian government agencies to enable method transparency and reproducibility. The topographic analysis relied on a Digital Elevation Model (DEM) from Advanced Land Observing Satellite Phased Array L-band Synthetic Aperture Radar (ALOS-PALSAR) (Shawky et al., 2019) with a resolution of 12.5 m (NASA Earth Data). Furthermore, the DEM permitted the extraction of water-related attributes. Esri's Sentinel-

2 imagery at a native 10 m resolution was used to obtain land use and land cover (LULC) data in 2023. Further datasets included soil types from the Ethiopian Ministry of Agriculture, river and road networks from DIVA-GIS, sub-city population statistics from the Ethiopian Statistical Service (ESS, 2023), and vegetation traits from Landsat 8/9 imagery from USGS Earth Explorer. All raster and vector layers were corrected with respect to one another and integrated on a common 12.5 m grid.

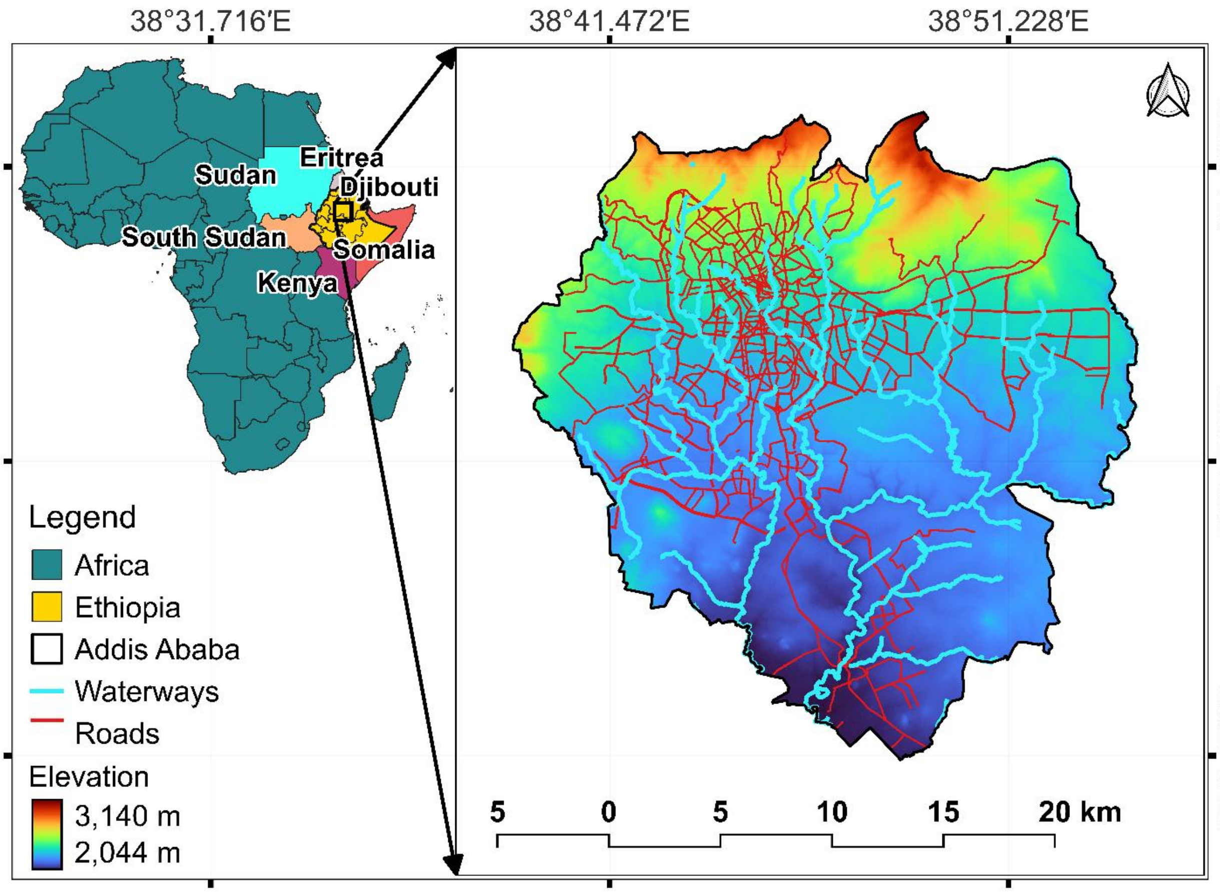

Figure 3.1: Study area: Addis Ababa map with major rivers, and road networks

3.2.3 Attribute Selection and Theoretical Clustering

Based on mechanistic closeness with IGGI functionality, and informed by water-related knowledge, land use constraints, and social spaces, twelve geospatial attributes have been selected. In this study, three independent clusters were identified to facilitate subsequent multi-attribute analysis. The Topographical and Hydrological (TH) cluster includes slope, TWI, elevation, TPI, and TRI. The above characteristics collectively quantify the terrain-mediated controls on runoff generation, flow concentration, and natural detention capacity for the placement of infiltration-based IGGI. In addition, LULC, soil type, NDVI, and hillshade, are features of the Land Use and

Vegetation (LUV) cluster. While hillshade is a visual derivative of slope and aspect rather than a direct hydrological variable, it was included as a proxy for solar exposure and evapotranspiration potential; this limitation is acknowledged in Section 3.4.4. Furthermore, LULC and NDVI capture complementary rather than redundant information. LULC is categorical (land use class: urban, crop, trees), indicating imperviousness and land function. NDVI is continuous (vegetation health/density), distinguishing, for example, a healthy tree canopy (high NDVI) from a stressed one (low NDVI) within the same LULC class. Both are standard in green infrastructure suitability studies (Anteneh et al., 2023; Moisa et al., 2023). Finally, the Socio-Spatial and Accessibility (SSA) cluster incorporates Euclidean distance to rivers and roads alongside population density. This grouping prioritizes sites experiencing flood risk, ensures maintenance accessibility, and addresses spatial IGGI distribution across varying urban population densities. Table 3.1 summarizes literatures consulted for attribute selection and their descriptions.

Table 3.1: Thematic clusters, attributes, and descriptions

Cluster	Attribute	Description	References
TH	Slope	Affects runoff and infiltration potential.	Haggard et al., 2005; Waheeb et al., 2023
	TWI	Identifies areas of moisture accumulation.	Beven and Kirkby, 1979; Mobarak et al., 2022
	Elevation	Influences runoff dynamics and accumulation.	Moisa et al., 2023; Wilson and Gallant, 2000
	TPI	Detects ridges and depressions.	Mobarak et al., 2022
	TRI	Measures surface ruggedness and accessibility.	Waheeb et al., 2023
LUV	LULC	Reflects imperviousness, infiltration, and land function.	Garg et al., 2013; Moisa et al., 2023
	Soil	Determines drainage capacity and infiltration.	FAO-UN, 2006; Moisa et al., 2023
	NDVI	Indicates vegetation health and IGGI potential.	Tucker, 1979; Anteneh et al., 2023
	Hillshade	Affects solar exposure and evapotranspiration.	Wilson and Gallant, 2000

SSA	Proximity-to-river	Assesses flood risk and water availability.	Ridolfi et al., 2021; Moisa et al., 2023
	Proximity-to-road	Supports maintenance and accessibility.	Kaur and Gupta, 2022
	Population Density	Highlights pressure zones for IGGI prioritization.	Browne et al., 2021

While slope, TWI, elevation, TPI, and TRI are derived from a common DEM, they capture distinct hydrological characteristics: slope quantifies runoff potential, TWI identifies moisture accumulation zones, elevation provides macro-topographic context, TPI distinguishes convergent/divergent positions, and TRI quantifies surface ruggedness (Mobarak et al., 2022; Waheeb et al., 2023). Multicollinearity diagnostics (VIF < 5) confirmed non-redundancy.

3.2.4 Thematic Layer Development and Scientific Rationale

Topographic parameterization employed the ALOS-PALSAR DEM to derive hydrologically significant attributes using established algorithms in QGIS version 3.40.4. Slope angle calculations identified surfaces conducive to rapid runoff versus infiltration-favorable low-gradient terrain. The TWI-derived upslope contributing area and local slope showed areas of natural moisture accumulation that can be good sites for vegetation-based IGGI (Mobarak et al., 2022). Elevation, TPI, and TRI are used to differentiate geomorphic settings further. Locations with low elevation, negative TPI (depressions), and low TRI (low ruggedness) were considered a priority for their inherent potential for stormwater retention, slow movement of surface runoff, and better constructability (Mobarak et al., 2022; Waheeb et al., 2023). Scientifically defined thresholds were used to classify land cover and environmental factors. The LULC map from Sentinel-2 was classified into five tiers of suitability, where permeable vegetated covers (water bodies, trees, vegetation) scored high and impervious urban fabrics scored low (FAO-UN, 2006; Gill et al., 2007; Harlis and Seo, 2024; Jha et al., 2012; Lourdes et al., 2022). Soil types were ranked according to drainage characteristics, with well-drained Eutric Nitisols deemed optimal for infiltration practices, while Pellic vertosol considered less favorable (Feyissa et al., 2018; Moisa et al., 2023; FAO-UNESCO, 1977). NDVI's values quantify the vigor of vegetation, hence, higher values are indicative of greater potential towards phytoremediation in IGGI. Derived from the ALOS-PALSAR DEM, the hill shade visualizes terrain illumination, with shaded areas being suitable for vegetation-based IGGI due to higher moisture content.

Socio-infrastructural layers employed Euclidean distance transforms. Proximity to rivers highlighted flood-prone corridors requiring mitigation and water availability making it primary candidate for IGGI interventions (Chen et al., 2021; Piran et al., 2013), while road accessibility ensured feasible construction and maintenance logistics (Moisa et al., 2023). Population density, though constraining available space in urban cores, guided retrofit prioritization in high-risk areas (Gelan, 2021). Computational formulas for these attributes are provided in Appendix A.

3.2.5 MCDA Framework: Integrating AHP and ANP

The weighting of attributes was accomplished via Saaty's AHP and network-based extension ANP. AHP and ANP were selected over alternative MCDA methods (e.g., Weighted Sum Model, 1000minds) because they provide explicit consistency checks (CR $\leq$ 0.1) and accommodate heterogeneous attribute units without transformation. The comparative application of AHP (independence assumption) and ANP (interdependence allowed) was designed to test whether accounting for inter-attribute relationships improves spatial prediction accuracy. The fundamental difference is that AHP assumes independence among criteria within a strict hierarchy, while ANP allows feedback and interdependencies through a super matrix approach (Saaty, 2005). ANP is superior for problems where criteria influence each other, as in IGGI suitability (e.g., slope influences TWI, which influences NDVI). Both approaches consulted experts to evaluate the relative significance of twelve geospatial attributes. In AHP, the attributes are considered independent and compared amongst themselves in pairs to derive the weight. The same attributes in ANP were grouped into three conceptual clusters TH, LUV, and SSA to allow for interdependencies and feedback. Twelve experts in water resources and environmental engineering (demographics in Appendix B) participated in digital (Kobe Toolbox) structured surveys. As per Saaty (1980), the fundamental scale is a 1−9 scale, which was used to carry out pairwise comparison, where the numbers 1, 3, 5, 7, and 9 represent equal to extreme importance, whereas numbers 2, 4, 6, and 8 denote intermediate values. Descriptions of attributes and background information were given to enable judgment. The expert responses generated comparison matrices as outlined in Table 3.2 (for more details, see Appendix C). The sample size is consistent with the practices of comparable studies (Alotaibi and Anzah, 2023; Amjad et al., 2024; Asefa et al., 2021; Das et al., 2024; Hisoglu et al., 2023; Marzuki et al., 2023).

Table 3.2: Pair-wise comparison matrices summary

Method	Component	Description

AHP	Attribute interaction	Twelve attributes compared pairwise to derive weights.
ANP	Inter-cluster interaction	Pairwise comparisons between clusters for the super-matrix.
ANP	Intra-cluster interaction	Feedback within clusters integrated into the super-matrix.

A pairwise comparison matrix is developed in AHP, and priority vectors were generated from the principal eigenvector. The Consistency Ratio (CR), as defined in Eq. 3.1-3.2, was used to assess the consistency of experts.

$$\mathrm{CR} = \frac{\mathrm{CI}}{\mathrm{RI}} \leq 0.1 \text{ , } \mathrm{CI} = \frac{\lambda_{\max} - \mathrm{n}}{\mathrm{n}-1} \quad (3.1\text{-}3.2)$$

where λ_{max} is the maximum eigenvalue of the matrix, n is the matrix size, and RI is the Random Index (Table 3.3).

Table 3.3: Saaty's RI values by matrix size

n	1	2	3	4	5	6	7	8	9	10	11	12	13	14	15
RI	0	0	0.58	0.9	1.12	1.24	1.33	1.4	1.45	1.49	1.51	1.54	1.56	1.57	1.59

To calculate the weights, we normalized the matrix, and then calculated the average of individual rows. A Weighted Linear Combination (WLC) of the above weights was applied to achieve a cumulative suitability score (Eq. 3.3).

$$S_{Total} = \sum_{i=1}^{n}(w_i * R_i) \quad (3.3)$$

Where w_i denotes the AHP model derived weight while the R_i is the normalized raster layer calculated as (Eq. 3.4).

$$\mathrm{R_i} = \frac{\mathrm{Raster\ Layer_i} - \mathrm{Min_i}}{\mathrm{Max_i} - \mathrm{Min_i}} \quad (3.4)$$

The ANP method was an enhancement of the AHP structure to include feedback and interdependencies within clusters as well as between clusters. Further pairwise comparisons were done between TH, LUV, and SSA clusters. The judgments were employed to create a super-matrix in SuperDecisions®, wherein consistency checks were conducted. The limit matrix that produced the global priority weights was obtained from the column normalized matrix by successive powering to a limit. The same WLC process (Eqs. 3.3 and 3.4) undertaken for AHP was used for the ANP-derived global weights. AHP and ANP models were comparatively assessed to understand the impact of interdependencies on the final suitability results. The assessment compared weights on attributes, spatial suitability maps, and classification results. With two methods, it balances analytical depth and straightforwardness and allows for more comprehensive context acquisition of IGGI.

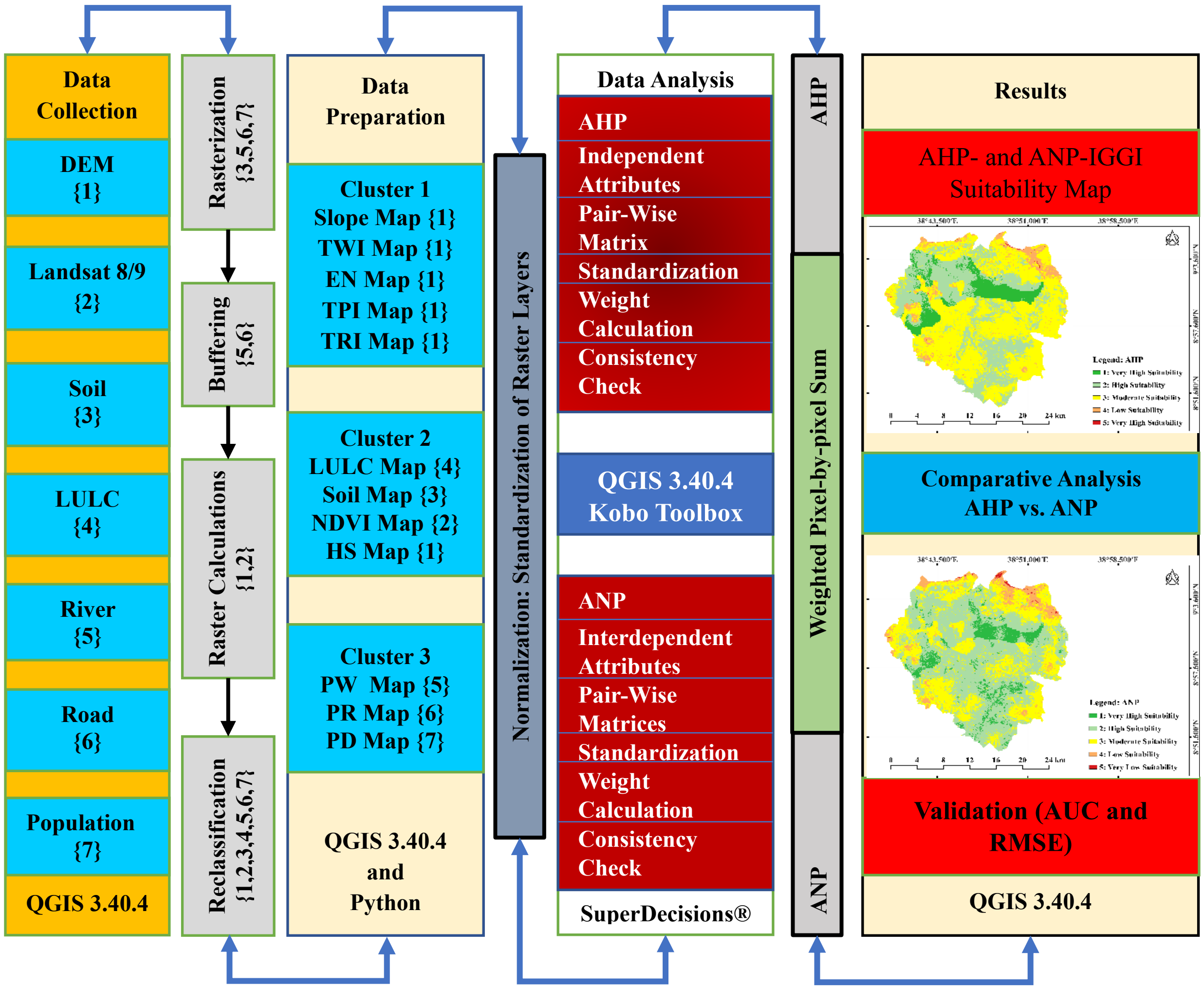

Figure 3.2: Methodological framework designed for this study

3.2.6 Validation and Analytical Workflow

3.2.6.1 Model Performance Evaluation

To evaluate the reliability of LULC classification and AHP and ANP-based IGGI-suitable maps, AUC and RMSE were employed. The metrics were analyzed using Python 3.11.4 using Seaborne, Matplotlib, and Scikit-learn. AUC is one of the metrics commonly used in spatial multi-criteria evaluation. AUC is used to calculate the model's accuracy based on true positive rates and false positive rates to have values ranging between 1 and 0. The closer the value is to 1, the stronger the predictive performance (Mugiyo et al., 2021; Senay and Worner, 2019; Zhran et al., 2024). The RMSE is the deviation of predicted values from the observed values (Moriasi et al., 2007; Singh et al., 2004). The validation made use of 206 georeferenced points, consisting of 103 utilized for field-based ground observation and 103 from Google Earth Pro high-resolution visual interpretation. Validation of LULC was performed using the Esri classification system (Appendix D), while IGGI suitability classes were further reclassified into suitable (1-3) and non-suitable (4-5) for AUC and RMSE computing, while agreement across all 206 validation points was also assessed. The combination of AUC and RMSE enabled a powerful assessment of spatial accuracy and model performance.

3.2.6.2 GIS-Based Suitability Map Analysis Framework

The analytical framework (Fig. 3.2) consists of four steps forming a spatial decision-support process. The first step was the acquisition of the geospatial data from different open access sources and the government agencies of Ethiopia. Subsequently, the data were preprocessed and standardized to 12.5 m resolution. Thematic layers were created using GIS in the second phase. The third phase involved multilayered weighting through both AHP and ANP based on expert evaluations. During the fourth stage, the thematic layers were combined using weighted raster overlay to produce spatial suitability maps, making use of these weights. To check the performance of the model, AUC and RMSE were used. Subsequently, the results of AHP and ANP were checked to see the effect of weighting.

3.3 Results

This section presents the results of the IGGI site suitability map analysis in Addis Ababa using GIS-based AHP and ANP methods for comparative assessment. The analysis evaluated spatial attributes, thematic suitability distributions, weighting schemes, consistency ratios, and suitability outcomes at both city-wide and sub-city levels. A summary of the spatial attributes is provided in (Appendix E), including unique IDs, sub-attributes, and suitability scores ranging from 1 (very high) to 5 (very low suitability). Areal coverage for each class is reported in square kilometers and as a percentage of the total study area.

The suitability of IGGI was significantly influenced by TH factors. Almost 50% of the area has slopes of less than 10%, which indicates high to moderate suitability. Steeper slopes need stabilization (Fig. 3.3a). The TWI evaluation depicted that about 60% of the area is moderately to highly suitable for water retention (Fig. 3.3b). According to Fig. 3.3c, elevation at over 2,040 m to 2,704 m have over 79% coverage of the city and support operational feasibility. The TPI classified 90 percent as moderately suitable (Fig. 3.3d), while TRI classified more than 98 percent as highly suitable (Fig. 3.3e). Nevertheless, there are issues with LUV patterns. Only 5.88%—mostly water bodies and tree cover—are highly suitable. Urban areas (70%) show very low suitability due to very little green space (Fig. 3.3f).

3.3.1 Individual Attribute Suitability: Thematic Maps

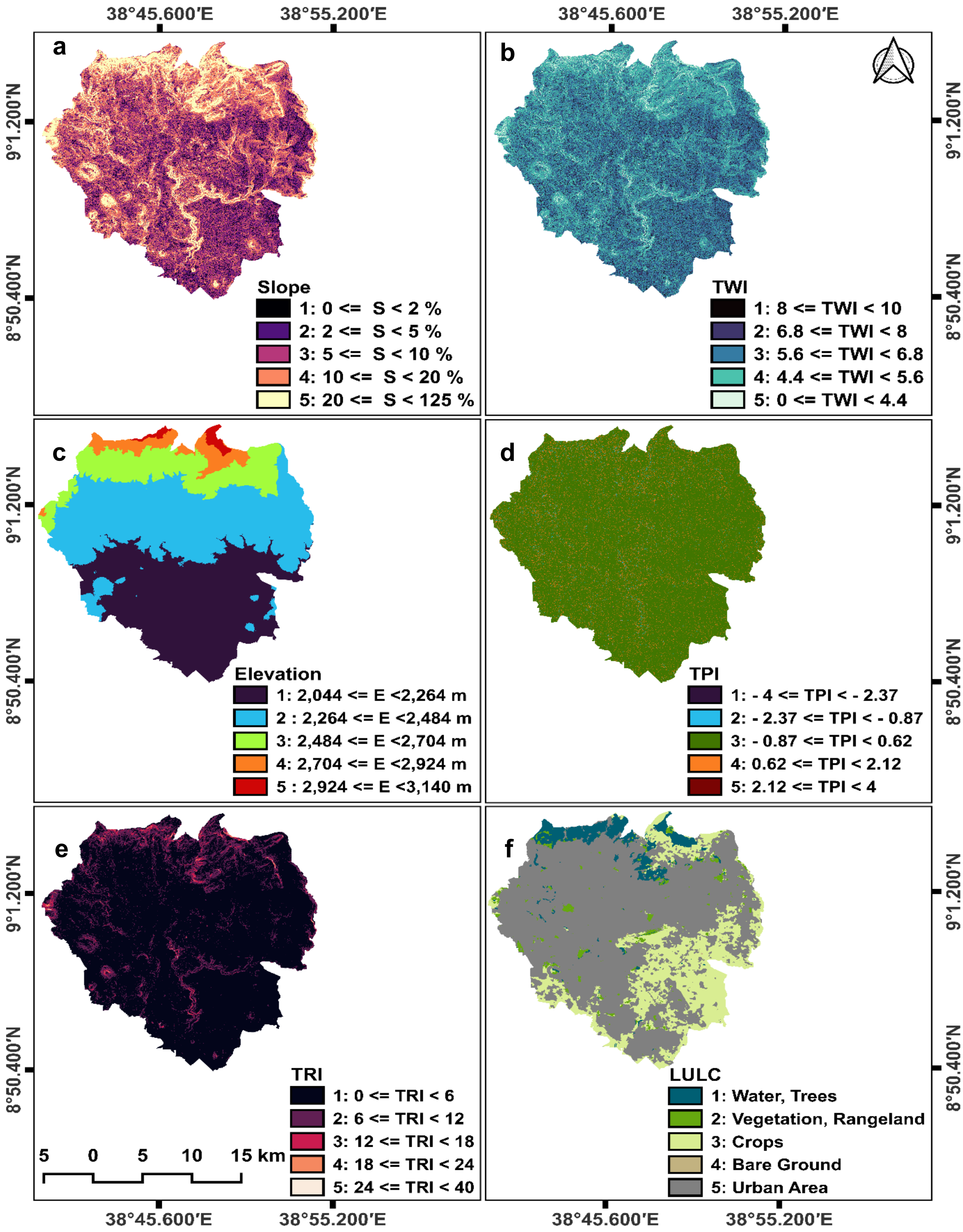

Figure 3.3: Thematic maps showing five-level suitability classifications for: (a) slope, (b) TWI, (c) elevation, (d) TPI, (e) TRI, and (f) LULC.

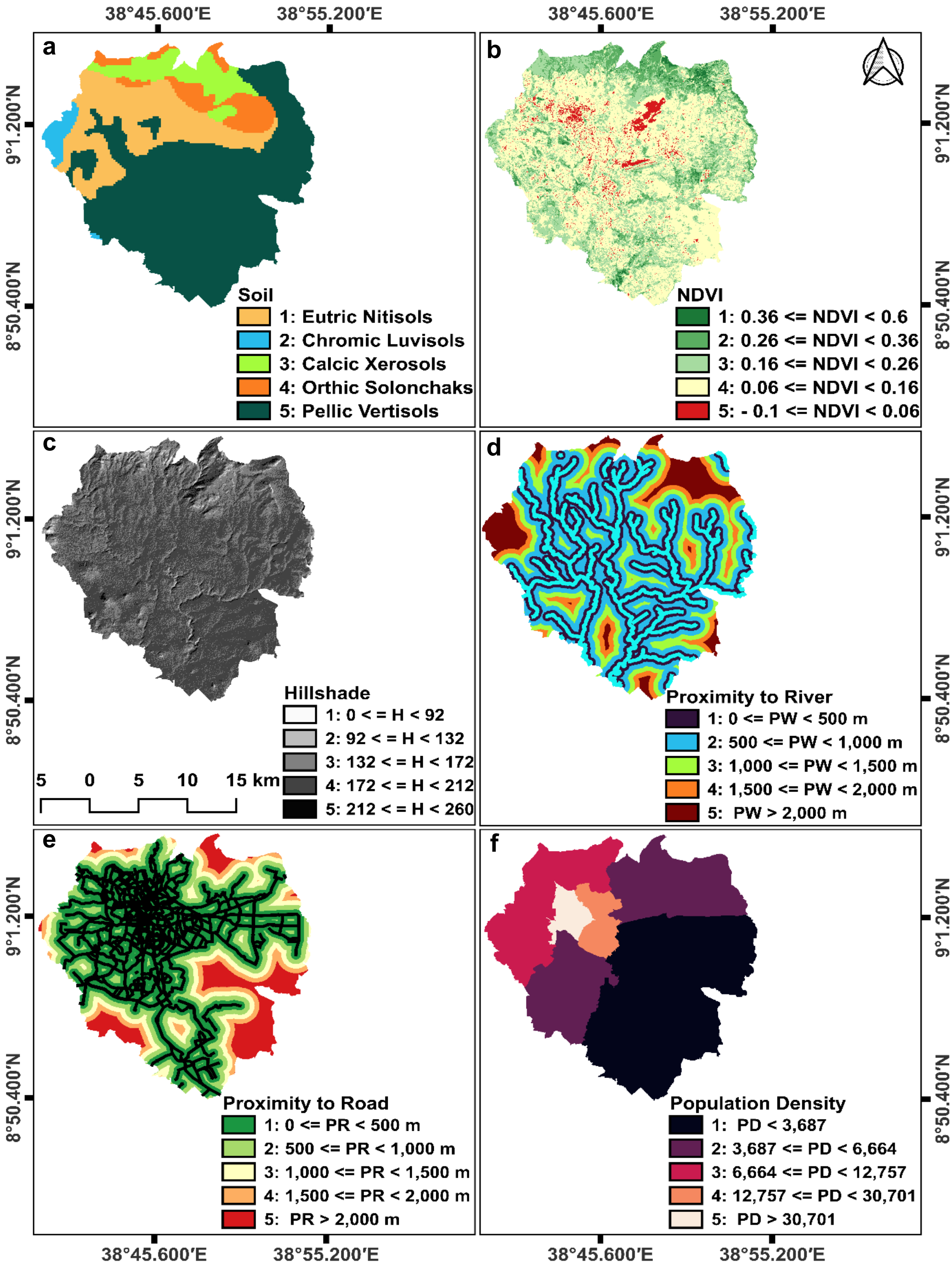

Figure 3.4: Thematic maps showing suitability classifications for: (a) soil, (b) NDVI, (c) hillshade, (d) proximity to river, (e) proximity to road, and (f) population density.

The soil types are rated differently in terms of suitability. Eutric Nitisols (21.17%) are rated very highly suitable, while Chromic and Pellic Vertisols (61.04%) have been rated with very low suitability (Fig. 3.4a). The NDVI analysis showed that the vegetation cover of the area was sparse, and 54.56% of the area came under low suitability, and only 1.33% came under very high suitability. Thus, greening strategies are needed for further vegetation in the area (Fig. 3.4b). The analysis of the hillshade has shown that 62.61% of the area has high solar exposure, and thus at limited shade, the suitability is very low (Fig. 3.4c). Being near rivers and roads improves the suitability, with 40.66% and 56.88% in that area. Conversely, much lower areas away from the river (16.79%) at greater than 1500 m and away from the road (10.7%) at 2000 m are less suitable. Population density analysis indicated that the low-density areas (density < 3,687 persons/km^2) were highly suitable while the highly dense zones (density > 30,701 persons/km^2) are less suitable (Fig. 3.4f).

3.3.2 Standardization, Attribute Weighting, and Consistency Evaluation

3.3.2.1 Factor Map Standardization

In IGGI suitability analysis, spatial attributes were standardized. Recognizing the newness of IGGI, there was limited literature that defined suitability thresholds. Thus, as stated in materials and methods (Section 3.2.4), the classification of attributes was based on functional relevance to IGGI and informed by UGS studies, it must be noted that the current study is focused on green infrastructure, land-use land cover, and stormwater management (e.g., McFarland et al., 2019; Omitaomu et al., 2021; Feyissa et al., 2018; Gelan, 2021; FAO-UNESCO, 1977). For instance, due to their capacity to infiltrate and retain water, flat slopes, permeable soils, and vegetated surfaces are rated highly suitable whereas, steep slopes and dense urban areas are rated unsuitable. This classification was further improved using expert opinion, field verification, and validation of suitability maps.

3.3.2.2 Weight Assignment and Comparison

As described in the materials and methods section (Section 3.2.5), the expert's judgment prioritized the attributes. Experts made comparisons against each attribute to determine its importance to IGGI. In AHP model, slope has the highest weight (0.2), followed by soil (0.15), TRI (0.1), and population density (0.09), implying focus on direct biophysical constraints. The ANP model managed interdependencies of attributes, which produced a more uniform distribution. The arrangement of importance was slope (0.11), TWI (0.095), TPI (0.095), elevation (0.09), and

NDVI (0.08). Furthermore, ANP gave higher weight to proximity-based factors such as proximity-to-river and road (0.08 each) due to their spatial connectivity and accessibility impact (Fig. 3.5).

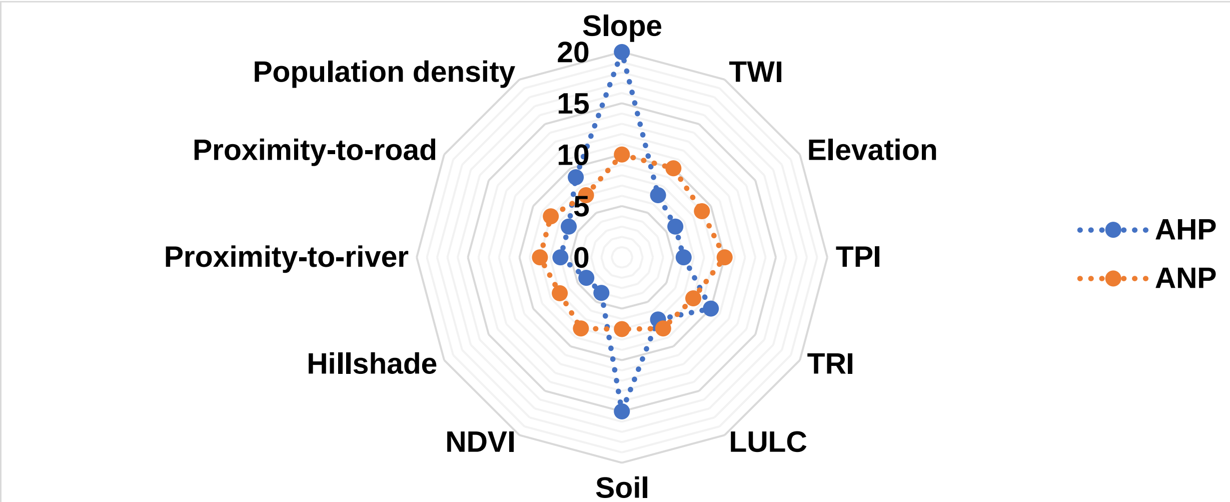

Figure 3.5: Pair-wise comparison matrix weightage result

3.3.2.3 Consistency Evaluation

The consistency of all pairwise comparison matrices was acceptable. For the AHP inconsistency values were 0.09 (Super Decisions) and 0.07 (Manual), both less than 0.1. The between-cluster matrix for the ANP showed a consistency of 0.03. The TH, LUV, and SSA clusters exhibited consistency ratios of 0.08, 0.05, and 0.09, respectively, all of which are within the acceptable range (Fig. 3.6).

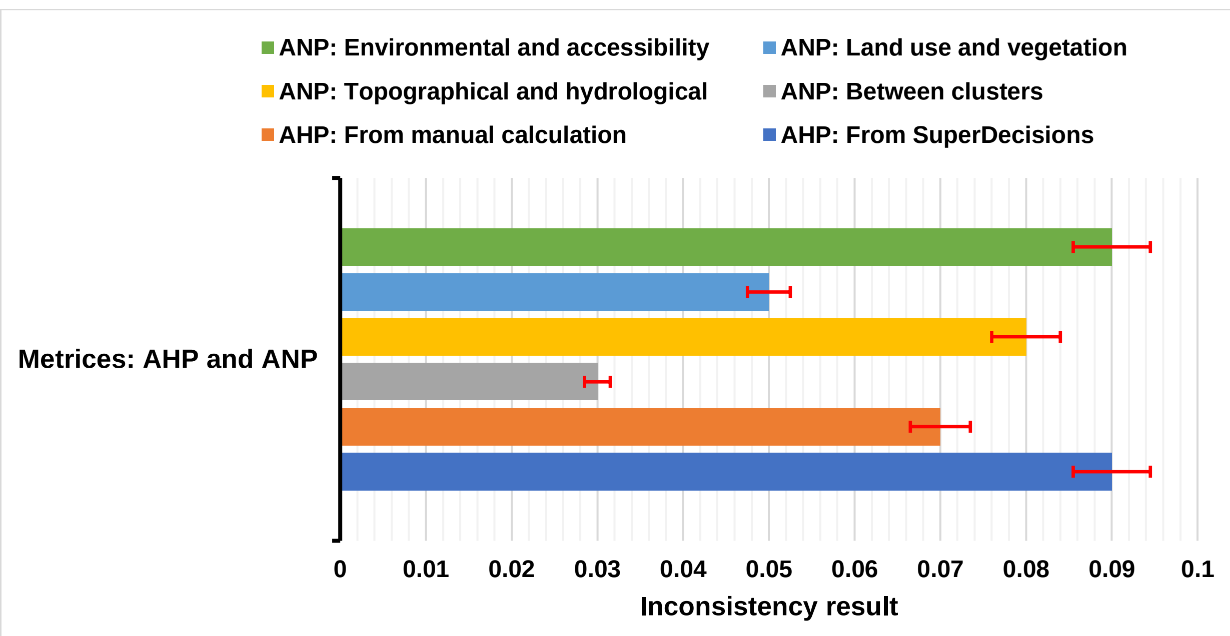

Figure 3.6: Results of the consistency check of pairwise comparison matrices

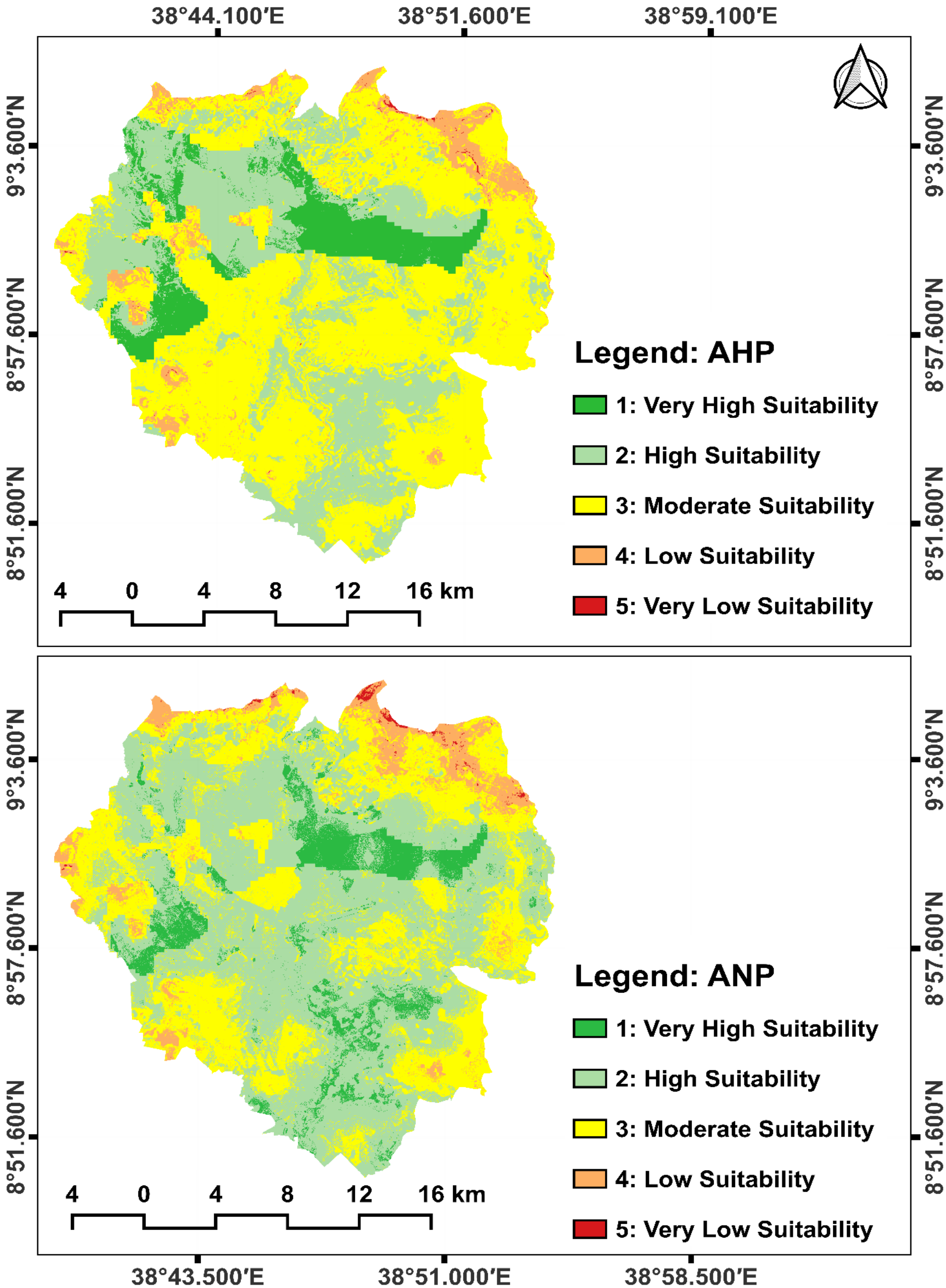

Figure 3.7: Suitability map reclassified raster layers

3.3.3 Comparative Suitability Analysis

3.3.3.1 Overall Suitability Maps

The methodology effect on the suitability classification was revealed in the city of Addis Ababa (Fig. 3.7). AHP indicated a moderate suitability (275.29 km^2, 52.2%), followed by the high suitability (173.12 km^2, 32.82%) and very high (49.7 km^2, 9.42%). According to ANP, the largest area under study is classified as highly suitable (271.61 km^2, 51.5%), followed by moderately suitable (178.35 km^2, 33.82%) and very highly suitable (44.1 km^2, 8.36%). Both methods categorized less than 7% areas as non-suitable, thus showing that there is considerable IGGI implementation potential.

3.3.3.2 Reclassified Suitability Scores

To account for wider interpretation, suitability scores were re-classified into three classes, namely, suitable (very high + high), potentially suitable (moderate), and non-suitable (low + very low). The suitable area from ANP results (315.71 km^2, 59.86%) was larger than from AHP (222.82 km^2, 42.24%) (Fig. 4.8). AHP designated a larger proportion potentially suitable (52.2% versus 33.82% for ANP) due to its more conservative weighting. AHP and ANP found a small amount of non-suitable area, which is 5.55% and 6.32%, respectively, which indicates good IGGI implementation potential.

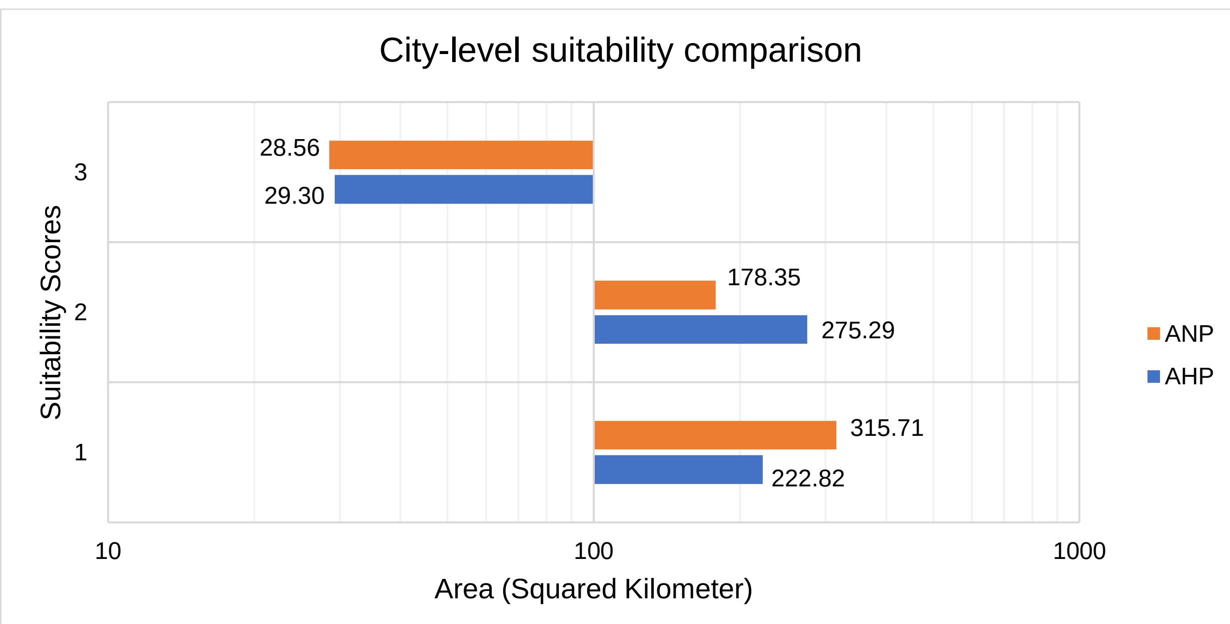

Figure 3.8: City-level suitability comparison: AHP and ANP

3.3.3.3 Sub-city Level Suitability Distribution

The suitability analysis of IGGI in Addis Ababa was conducted through AHP and ANP models of IGGI during a study across the ten sub-cities of Addis Ababa, and its findings were classified into three simplified categories: suitable (very high + high), potentially suitable (moderate), and non-suitable (very low + low), as shown in Fig 3.9. According to the AHP results, the most suitable ones are Arada (92.16%), followed by Addis Ketema (90.01%), Kolfe Keraniyo (66.23%), and Lideta (55.74%). The dominant potential suitability sub-cities were Akaki Kality (54.60%) and Bole (60.49%), whereas the non-suitable remained low for most sub-cities. Areas of non-suitability of Yeka and Lideta are relatively higher in percentage (16.74% and 17.96%).

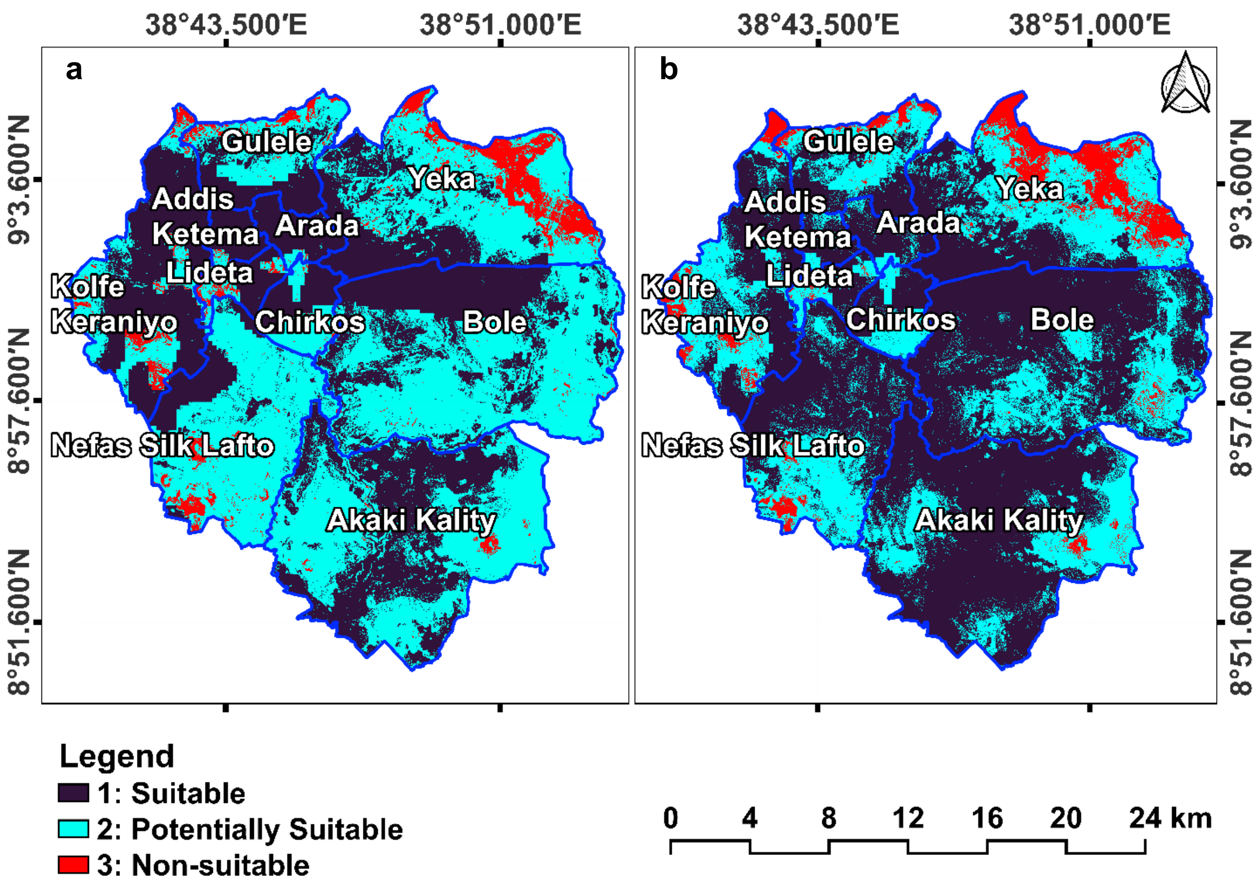

Figure 3.9: Sub-cities suitability map a) AHP, and b) ANP

The distribution was more balanced in the ANP model. Bole (72.29%), although somewhat diminished relative to AHP, was added to the remaining most suitable Arada (82.44%), and Addis Ketema (76.48%). Chirkos 47.11 and Gulele 47.33 have proven suitable. Specifically, Yeka (22.76%), Gulele (10.50%), and Kolfe Keraniyo (8.67%) had the highest non-suitable shares. Through the two models, as it can be seen, Yeka, Gulele and Kolfe Keraniyo have a lower suitability; thus, targeted interventions were needed for the improvement of IGGI implementation. However, Arada and Addis Ketema scored higher throughout.

3.3.3.4 Model Accuracy Assessment

With the help of 206 georeferenced reference points, the LULC validation recorded an AUC of 0.86 and an RMSE of 0.2 which shows a moderate agreement with those from the field and Google Earth. The initial findings confirm the utility of the Esri LULC dataset. AHP and ANP models were validated using the same reference points. The AUC (0.92) of ANP is higher than AHP (0.87), which shows strong power to discriminate suitable from unsuitable zones. In General, the ANP model picks out areas with high IGGI potential. Interestingly, many of these zones are also classified as flood-prone by the Addis Ababa Fire and Emergency Preparedness Office (Feyissa et al., 2018). There is a meaningfully spatial alignment between suitability and flood risk zones, which underscores the real-life importance of IGGI application on floods. Also, ANP has a lower RMSE equal to 0.12 as compared to AHP, which is 0.16. The lower RMSE indicates a lower prediction error of the model. It implies that ANP, through its prediction, gives only a 12% deviation from the actual suitability score on a 0 to 1 normalized scale. This illustrates the accuracy of the model and the confidence with which it can be used to support IGGI planning.

3.4 Discussion

Differences between AHP and ANP show how methods affect IGGI suitability outcomes. AHP has independence of factor structure in hierarchy while ANP has interdependencies, causing more integrated assessment. In the context of the study intended to select technically appropriate IGGI sites for stormwater use in Addis Ababa. The slope was the most important parameter in both models for site selection purposes. AHP gave prioritization clearly, while ANP took into account the feedback from attributes like slope and TWI and from clusters TH, LUV, and SSA.

The consistency ratios of both models were acceptable, indicating reliable weighting processes for urban planning. The analysis has shown that while technical feasibility is important, the degree of success also signals the need for economic and social-related dimensions to be factored into IGGI planning (Deely et al., 2020). The results are in line with SDGs 6, 11, and 13 by improving water quality, urban resilience, and climate adaptiveness (United Nations, 2015). The most suitable lands were found in areas with gentle slopes and high TWI values, and oppositely located steep zones may require adaptive design or an alternative to the actual design application. LUV finding recommends reforestation, green roofs, and soil enhancement. In denser areas, vertical greening and shared infrastructure are important. The need for joint IGGI strategies in dense urban areas is emphasized by SSA factors.

The historical flood data from 2010 to 2016 obtained from the Addis Ababa Fire and Emergency Preparedness Office was used to compare the suitability map created in this study. This data was used by a previously published, peer-reviewed study by Feyissa et al. (2018). The results indicate the zonation for flood risk aligns well with the category of suitability for urban development. Areas that are at very high risk of flooding are found either in the very high or high suitability category in this report. Similarly, high-risk areas are also found in the high suitability area. These results validate and show the relevance of the present research. Flood risk areas share significant IGGI potential; IGGI areas reveal significant overlap with areas of maximum flood risk. Giving priority to IGGI strategies in these zones, the urban planners and policymakers can manage flooding and pollution.

3.4.1 Urban Planning Implications

The suitability analysis gives crucial insight for urban planning in Addis Ababa and similarly rapidly urbanizing cities. Unlike Moisa et al. (2023), which analyzed UGS, the current research addresses IGGI for stormwater management by including topographic indices (TPI, TRI, and TWI), followed by the use of ANP to capture interdependencies among attributes. This strategy generated wider high-suitability areas as compared to Moisa's UGS model, which offered a mere 13%; the AHP approach generated a 42.24% and ANP 59.86% area, indicating a spatial potential for incorporating hydrology responsiveness into planning.

When it comes to policies, the findings have implications for zoning and infrastructure regulations. The outcomes show that there are areas with good IGGI conditions, moderate slopes, and more. The zoning helps avoid flooding; it would not be in an area with heavy flooding. Also, distance from population, road, and river. This is helpful for SDGs-6, 11, and 13. When looking from managerially, suitability classification would help in phased implementation. The zones that are highly suitable would be able to take up interventions like bioretention cells, bioswales, infiltration trenches, rain gardens, and more. These areas won't cause flooding to the nearby establishment. Moderately suitable areas may require some form of hybrid or structural solutions, such as rain barrels, green roofs, and green walls in built-up areas. Implementing IGGI project is much more difficult where it is not suitable. Infiltration-based GI performs best on flat, permeable ground, and vegetated swales function best on gentle slopes. Nonetheless, for all suitability categories, successful implementation will rely heavily on growing public awareness and community involvement, especially for green roofs and green walls, which are not popular in Addis Ababa (Eshetu et al., 2021; Ijara, 2020). Moreover, the study's finding assists the adjustment of IGGI in the long term by identifying reforesting and land-use zoning in various areas.

3.4.2 Sub-city Level Implications and Suitability-Based Planning

The two models indicated considerable area in Addis Ketema and Arada sub-cities show generally suitable area due to moderate slope, good access to roads and rivers, and Eutric Nitisol were dominant (92.5% for Addis Ketema and 90% for Arada). Their small, combined area of 3.15% of the study zone favoring IGGI retrofitting despite being highly populated, implies adoption of selected IGGI particularly green roofs and green walls on institutional and public buildings. Bole and Akaki Kality include expansive regions that are highly suitable. The low density of Bole enables interventions like bioswales, permeable pavements, and green corridors, while Akaki Kality's river accessibility is advantageous in spite of limited road infrastructure. The district around Lideta is a combination of suitable and potentially suitable areas and is well-connected. This makes it suitable for compact IGGI types, i.e., green roofs, curbside planters, and permeable surfaces. Chirkos and parts of Gulele combine a mix of suitable and potentially suitable zones. Common uses include street tree pits, rain gardens, and bioswales, preferably located along roads.

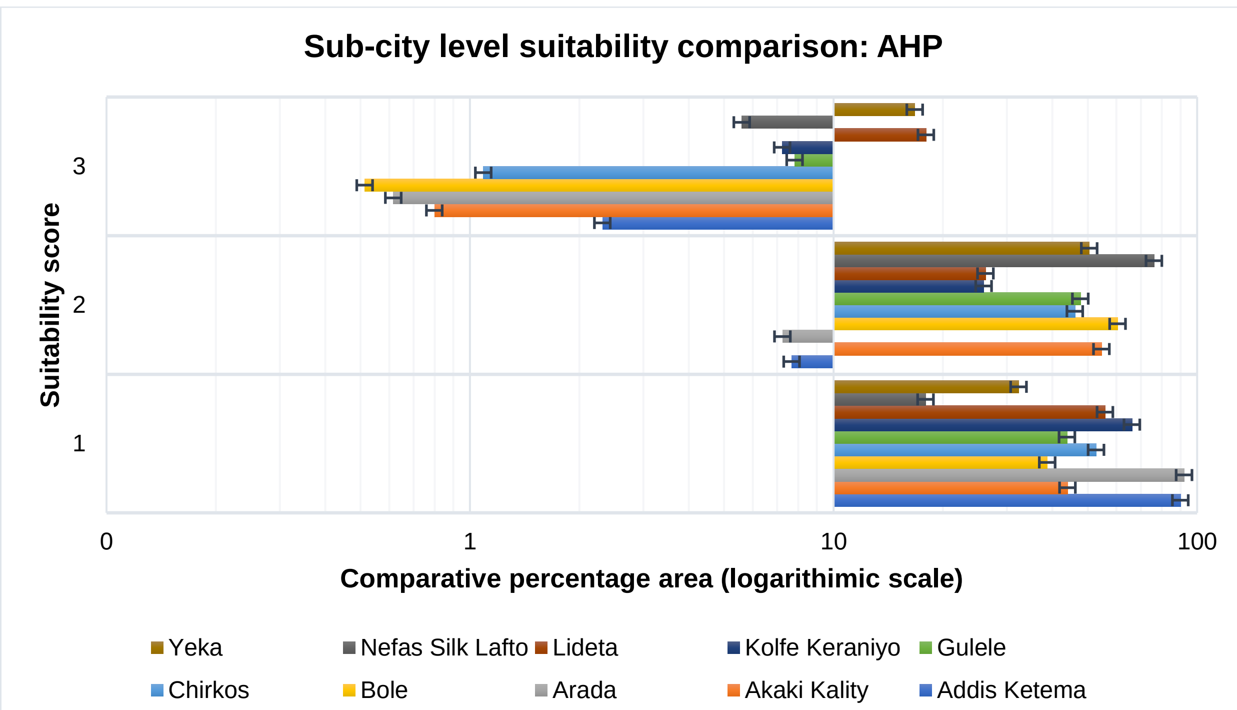

Figure 3.10: Sub-cities comparative score percentage: AHP

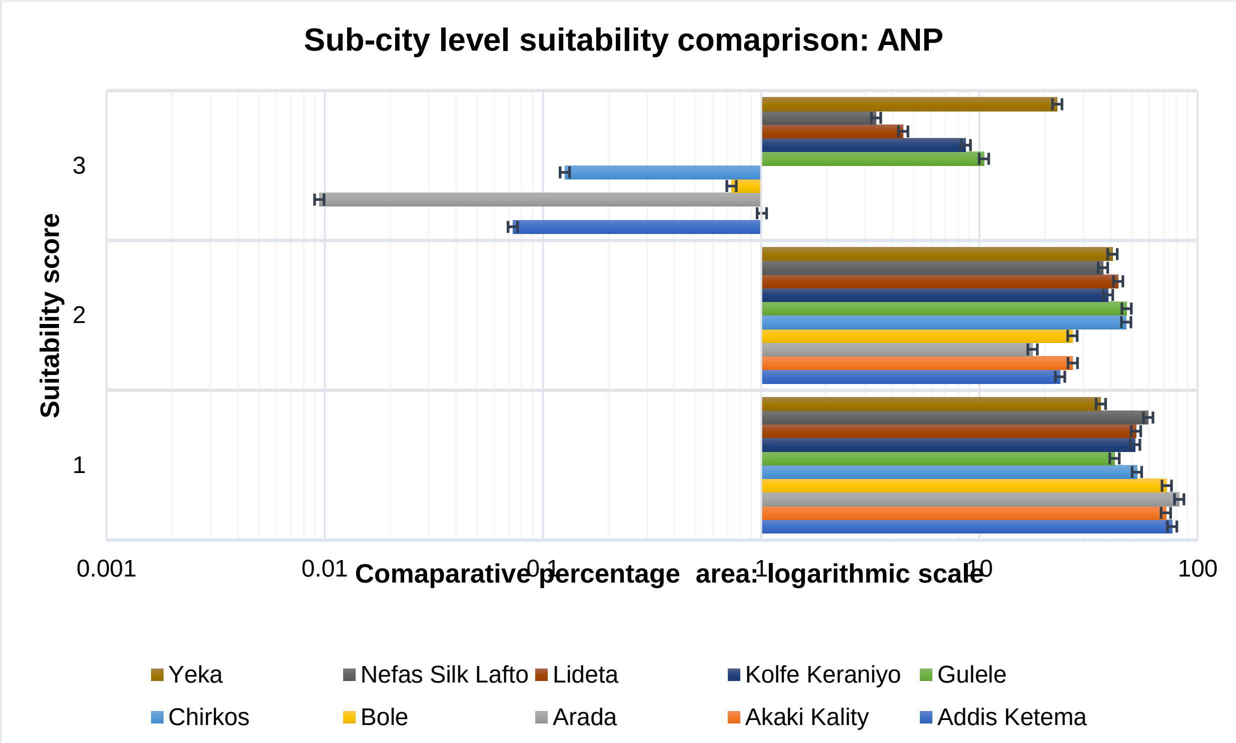

Figure 3.11: Sub-cities comparative suitability score percentage result from ANP analysis

In contrast, Yeka, Kolfe Keraniyo, and Nefas Silk Lafto have relatively more areas that are less suitable for IGGI placement, which need proper assessment and phased interventions due to limitations in slope, soil, and urban form. The Fig. 3.10 and 3.11 demonstrate the above-mentioned patterns and help in IGGI planning based on suitability.

3.4.3 Comparison with Earlier Studies

Numerous research efforts conducted across Africa and other regions in the Middle East are making concerted efforts to use GIS-based AHP-MCDA methods for UGS planning (Bakolo et al., 2024; Anteneh et al., 2023; Gelan, 2021; Mobarak et al. 2022; Moisa et al., 2023; Sahl et al., 2023). A lot is the same between the current study and that of Bakolo et al., (2024); Gelan, (2021), especially around using population density and accessibility as key suitability factors; however, regional and urban setting differences do set them apart. In line with past studies, the findings reveal that the application of GIS allows for better site selection, understanding spatial distribution and pattern data, and evidence-based decision-making (Bakolo et al., 2024; Gelan, 2021; Tripathi, 2021). The suitable zones for the application of IGGI in the peri-urban part of Addis Ababa correspond with the findings of Moisa et al. (2023) and Anteneh et al. (2023), by putting emphasis on the proximity to proper drainage and spatial accessibility. Integrating hydrological and topographic features, the present study builds upon prior work by providing a more detailed suitability assessment of IGGI.

In contrast to previous works that have only used AHP, our use of ANP also considers interdependencies such as slope and soil, echoing Sahl et al. (2023) and Mobarak et al. (2022), who also explored climatic and morphologic data but ignored how these different factors interrelate. According to our findings, which coincide with the findings of Ustaoglu and Aydinoglu (2019) and Hailemariam (2021), the factors of water access and slope limitations are major constraints for urban greening. In a similar vein, the identification of low-suitability zones due to very steep terrain and poor infrastructure can be found in the works of Gelan (2021) and Hordofa et al. (2024), who point out the importance of considering biophysical factors along with infrastructure development in planning.

The validation of the study in terms of field validated and Google Earth data was based on AUC and RMSE. Though Anteneh et al. (2023), Hordofa et al. (2024), and Zhran et al. (2024) considered checking model accuracy and performance, none have compared AHP with ANP directly. The results show that the modeling of interdependencies by ANP provides a more accurate prediction as measured by an enhanced AUC and RMSE. This research attempts to construct a GIS-based MCDA framework for IGGI planning based on scientific knowledge. This is an effort towards strengthening the role of greenery solutions for addressing urban flooding problems in Ethiopia and contributing towards the country's sustainable development. The approach can be duplicated in other rapidly urbanizing cities in Sub-Saharan Africa and cities of the Global South. Table 3.4 summarizes how AHP and ANP differ in methodology and that the ANP model can capture aspects that the AHP model cannot. Furthermore, the results can show different spatial trends as well.

Table 3.4: Comparative suitability results of Addis Ababa across different models

Aspect	AHP	ANP	Supporting Insight / Reference
Attribute Interaction	Independent	Interdependent	Yüksel and Dağdeviren (2007); Görener (2012)
Weighting Logic	Linear pairwise	Feedback-based super-matrix	Saaty (1980)
Top Attribute	Slope, Soil, TRI, and Population Density	Slope, TWI/TPI, elevation, NDVI, and Proximity-to-roads/rivers	Varies in topographical-hydrological sensitivity (Current study)

Suitability Trend	Dominantly moderate (52.2%, 46.9%)	Optimistic: high (51.5%) and moderate (33.8%)	Moisa et al. (2023); Current study
Access Sensitivity	Lower (e.g., roads/rivers < 0.05 each)	Higher (e.g., road/river = 0.08 each)	Current study
Context Fit	Simple, static hierarchies	Complex, dynamic systems (e.g., IGGI)	(Waheeb et al., 2023; Mobarak et al. 2022; Current study)
Tool Use	GIS + AHP	GIS + Super Decisions	Bakolo et al. (2024); Current study
Usability	Easier, transparent	Complex, nuanced	Görener (2012)

3.4.4 Limitation of the Study

There are some limitations to this study, notwithstanding a comprehensive and spatially explicit framework for IGGI suitability assessment. Because the LULC data and other input layers used in this study were public, there were some resolution limitations that may not allow for fine-scale precision. Weighting in the ANP model based on expert knowledge incorporated subjectivity, even after checking for consistency and validating the final output. In data-scarce settings, reproducibility may be affected. Also, the lack of dynamic stormwater flow modeling restricted the temporal simulation of runoff behavior. Finally, the model focused more on the technical, physical and spatial dimensions and, to a lesser extent, the economic, policy, and social factors that compromised its practical application: cost to implement, land tenure, and community acceptance. An economic, policy, and social factor should be included in future research that will enhance decision-making relevance and practical applicability. One more limitation is the inclusion of hillshade, which is a visual derivative of slope and aspect rather than a direct physical hydrological variable. Future studies may consider replacing it with physically based solar radiation or evapotranspiration indices.

3.5 Conclusion

This study established a GIS-based MCDA framework integrating AHP and ANP to evaluate spatial suitability for IGGI in SUSM across Addis Ababa. The methodological innovation centered on coupling geospatial analysis with hierarchical and network-based decision models explicitly designed for IGGI suitability assessment—distinct from conventional green space planning approaches. This tailored framework enabled a context-sensitive evaluation incorporating hydrological responsiveness, topographical constraints, land use characteristics, and socio-spatial attributes critical to urban stormwater dynamics.

Findings revealed that the ANP model—which accounts for interrelationships among suitability attributes—classified 59.86% of the city as highly suitable and 33.82% as moderately suitable for IGGI implementation. In contrast, the AHP model, treating attributes as independent, identified only 42.24% of the area as highly suitable and 52.2% as moderately suitable, indicating a more conservative spatial assessment. Notably, both models consistently identified less than 7% of Addis Ababa as unsuitable, underscoring the broad technical feasibility of citywide IGGI deployment. Key determinants of suitability included terrain slope, soil drainage capacity, TWI, population density distribution, and proximity to road and river infrastructure. Collectively, these factors pointed to peri-urban areas with moderate slopes and lower population densities as optimal zones for IGGI development, offering a balance between hydrological effectiveness and implementation practicality.

Validation metrics confirmed the superior predictive accuracy of the ANP approach (AUC = 0.92, RMSE = 0.12) over AHP (AUC = 0.87, RMSE = 0.16), underscoring ANP's capacity to capture complex spatial interdependencies inherent in urban hydrological systems. These results provide urban planners and policymakers with actionable geospatial intelligence to prioritize IGGI implementation zones, select context-appropriate infrastructure typologies, and enhance resilience planning across policy formulation, managerial coordination, and operational execution levels. The framework directly advances sustainable urban water management practices aligned with SDGs 6 (clean water), 11 (sustainable cities), and 13 (climate action), offering a replicable pathway for cities confronting rapid urbanization and climate volatility.

While this study delivers a robust spatial decision-support tool, limitations warrant consideration. These include resolution constraints from publicly available datasets, inherent subjectivity in expert-driven weight assignments, absence of dynamic rainfall-runoff modeling integration, and limited incorporation of economic viability and community acceptance factors. Future research should address these gaps through higher-resolution data acquisition, cost-benefit analysis of IGGI typologies, participatory social feasibility assessments, and coupled hydrodynamic modeling to strengthen practical applicability for city-scale stormwater management.

Chapter 4

4 Stormwater Modeling in a Steep, Poorly Drained Contributing Micro-Watershed Zone of Addis Ababa

Abstract

Urban micro-watersheds with steep slopes and poorly draining soils generate excessive runoff and pollutant loads, posing significant management challenges. This study introduces a novel focus on a contributing zone within a 30-ha micro-watershed in Addis Ababa to assess how climate change, urbanization and their combined effects influence stormwater runoff and water quality. The PCSWMM was employed to simulate four scenarios: baseline, climate change, urbanization, and combined impacts. The baseline model was calibrated and validated with observed storm data using the Sensitivity--Based Radio Tuning Calibration (SRTC) tool, achieving Nash-Sutcliffe Efficiency (NSE), RMSE-standard deviation ratio (RSR), and Integral Square Error (ISE) values within accepted thresholds. Over a 3-hour, 6,870 m^3 storm, 72% became surface runoff, 18.2% infiltrated, 2% evaporated, and 6.4% remained in storage, producing a peak flow of 3.6 m^3/s and localized node flooding. The climate change scenario employed an ensemble of Global Circulation Models (GCMs)—five for precipitation and seven for temperature—selected from twelve and sixteen models, respectively, based on their statistical performance. Under SSP2-4.5, 2-year return period peak flows increased to 3.8 m^3/s (2024–2053) and 4.7 m^3/s (2054–2083); under SSP5-8.5, they rose to 5.8 m^3/s and 6.6 m^3/s, respectively. An 80% imperviousness urbanization scenario increased peak flow to 4.1 m^3/s. The combined scenario yielded a peak of 7.2 m^3/s and a 10.3% pollutant load increase, which were (1.7%: climate change, and 7.1%: urbanization alone), highlighting urbanization as the principal driver of water quality decline. These findings highlight the need for IGGI and upgraded drainage systems to strengthen urban resilience. The study supports data-driven planning and advances SDGs 6 (clean water and sanitation), 11 (sustainable cities and communities), and 13 (climate action).

Keywords: Stormwater management; Pollutant loading; Green-grey infrastructure; PCSWMM; Climate change; Urbanization.

4.1 Introduction

The compounded effects of climate change and urban sprawl are further straining the management of urban stormwater, resulting in increasing occurrences of flooding and declining water quality

(Dong et al., 2021; Moisa et al., 2023; Oudin et al., 2018; Zerouali et al., 2022). The fast-growing cities of the Global South, such as Nairobi, Kenya, Dar es Salaam, Tanzania, and Addis Ababa, Ethiopia, are particularly challenged in this respect as their infrastructure systems have not kept pace with urban growth (Kumar et al., 2023; Mguni et al., 2015; Mulligan et al., 2020). The risks caused by stormwater in informal settlements of Addis Ababa and aging grey infrastructure further exacerbated were nearby riverine and flash flooding expose residents (Jemberie and Melesse, 2021; Angello et al., 2021; Birhanu et al., 2016). In the year 2017, the city recorded 76 floods, while the Little Aka River is one of the most polluted rivers of the country (Jemberie and Melesse, 2021; Angello et al., 2021).

Previous research has extensively modeled urban hydrology under the influences of climate and land use change, using tools like SWMM and PCSWMM to simulate runoff quantity, peak flow timing, and pollutant loading (Abd-Elhamid et al., 2020; Hussain et al., 2022; Zhang et al., 2018). These models often emphasize climate drivers over land use variables (Das and Sahoo, 2025; Sagar Kumar and Umamahesh, 2024). Additionally, IGGI frameworks—such as low impact development of North America, sustainable urban drainage systems of Europe, and sponge cities of China—have been widely adopted to mitigate stormwater impacts (Fletcher et al., 2015; Hua et al., 2020; Spahr et al., 2020).

However, a critical gap remains in stormwater studies at the micro-watershed scale, particularly regarding the contributing zone—the uppermost, often largest area of a micro-watershed, where overland flow is initiated and shallow interflow occurs (McFarland et al., 2019; Speak et al., 2013). This zone plays a pivotal role in stormwater response but is often overlooked in models that focus on broader catchments or average hydrological conditions. Its hydrological behavior becomes even more complex when it is characterized by steep slopes and poorly draining soils**,** which severely limit infiltration and accelerate runoff.

For instance, there is a work by Chanu et al., (2015) and Rejani et al., (2015) who applied curve number methods in micro-watersheds, but there is no study in the contributing zone of micro-watershed characterized by steep slope and poorly draining soil. Khan et al., (2020) focused on green infrastructure in low-permeability soils that does not focus on contributing zones. Huang et al., (2025) advocated for the implementation of low-impact development (LID) and best management practices (BMPs) at the micro-watershed scale. However, the authors did not consider slope or soil permeability constraints. According to Taylor, (1982), the effect of terrain and soil on contributing zones was not tested. These gaps highlight the lack of understanding of how localized topography and soil limitations affect runoff behavior, especially in future climates and land use.

This research looks into the contributing zone of an urban micro-watershed in Addis Ababa composed of steep slopes and poorly draining soils whose circumstances are not conducive to the implementation of IGGI. In contrast to earlier studies that evaluated the effectiveness of IGGI at the scale of a watershed (Ben-Daoud et al., 2024; Shrestha et al., 2014; Zakizadeh et al., 2022), the spatially focused approach captures fine-scale hydrologic responses, such as rapid runoff and short response times and minimal infiltration, which are masked at larger scales. Evidence generation at the micro-watershed level is crucial for tuning IGGI design in other constrained urban contexts. This is because the performance of IGGI is highly sensitive to small-scale hydrology that dominates urban stormwater runoff (Khan et al., 2020).

The objective of this study is to assess stormwater quantity and quality responses under baseline, climate change, urbanization, and combined scenarios in a contributing zone of micro-watershed characterized by steep slope and poorly draining soil. By explicitly modeling runoff and pollutant behavior under these interacting stressors, the study aims to inform terrain-sensitive IGGI planning for data-scarce and underrepresented urban settings. This contribution supports global efforts toward sustainable urban resilience, particularly aligned with SDG 6 (clean water and sanitation), SDG 11 (sustainable cities), and SDG 13 (climate action). The novel contribution is the application of PCSWMM to a steep (>7%), Vertisol-dominated contributing zone of an urban micro-watershed in a data-scarce Global South city, quantifying runoff and pollutant dynamics under combined climate change and urbanization scenarios.

4.2 Materials and Methods

4.2.1 Description of the Study Area

The study area (Fig. 4.1) is in Nefas Silk Lafto sub-city, a southwestern suburb of Addis Ababa, Ethiopia, within the small Akaki watershed. Geographically, the city is situated between 8°51’15” and 9°4’15” N latitude and 38°38’0” and 38°55’30” E longitude (Moisa et al., 2023), with an elevation ranging from 2,044 m to 3,140 m above mean sea level. The 30-ha study area, dominated by Vertosol soils, features mixed urban land uses—residential, commercial, roads, and green spaces. Selected for its critical role as a contributing zone within a micro-watershed, the site presents stormwater challenges due to steep slopes (7–15%) and low-permeability soils, which accelerate runoff and hinder infiltration (McFarland et al., 2019; Omitaomu et al., 2021). The site was selected based on QGIS overlay analysis of Addis Ababa's slope and soil maps, complemented by field observation. The 30-ha micro-watershed is representative of stormwater-challenged areas in Addis Ababa: its slope (7–15%) matches the modal class for southern/western sub-cities (42.6% of city area having slope greater than 10%); its Vertisol dominance affects ~61% of the city; its mixed land use mirrors most sub-cities; its undersized, poorly maintained drainage network is characteristic citywide (Jemberie et al., 2023). Chapter 4's city-wide suitability analysis confirms similar biophysical conditions occur across multiple sub-cities.

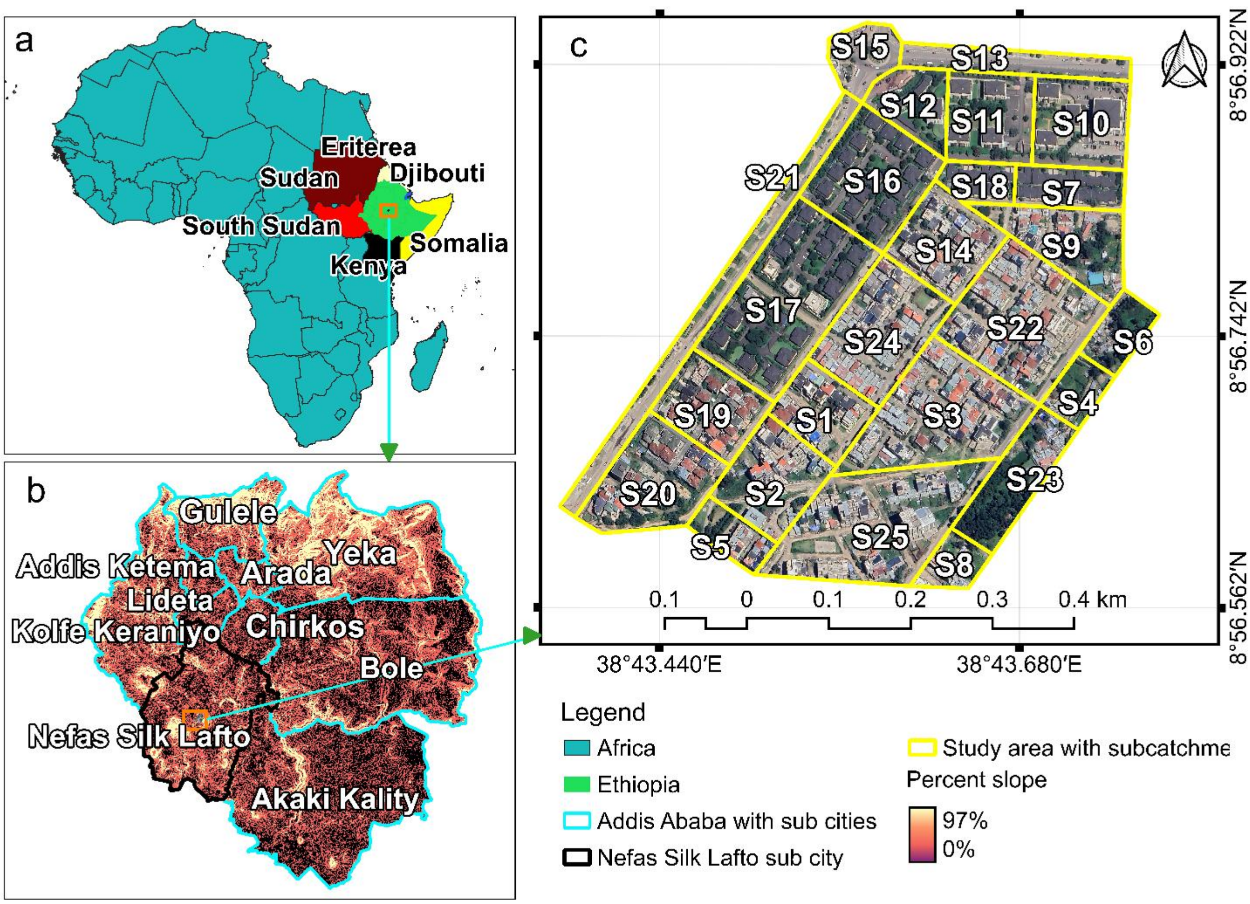

Figure 4.1: Study area map of a) Africa, b) Addis Ababa with sub-cities and elevation (percent), and c) typical study area with sub-catchments

4.2.2 Data Collection and Preparation

4.2.2.1 Climatic and Topographic Data

Rainfall and Temperature Data: Historical (1983–2023) climate data were obtained from the National Meteorological Agency, while future projections were sourced from CMIP6 GCMs, bias-corrected and downscaled by Rettie et al. (2023) using the bias correction constructed analogues with quantile mapping reordering method. This approach downscaled daily precipitation (12 GCMs) and maximum/minimum temperatures (16 GCMs) to 10 km resolution over Ethiopia, using a 5 km gridded dataset (1983–2012) for bias correction. Validation through a perfect sibling framework confirmed reduced bias and RMSE with improved correlation.

This study validated the downscaled data using observed records from Ayertena station (1983–2014), selected via Thiessen polygon analysis for its reliable long-term record, applying Pearson's correlation coefficient, RMSE, NSE, percent bias, and Kling–Gupta efficiency. Although Rettie et al. (2023) validated their downscaled product nationally, additional validation at the Ayertena station was performed because Ayertena was not individually reported in their validation, and this study extends the baseline to 2023, requiring verification of continued performance. Based on performance, five precipitation, four maximum temperature, and three minimum temperature GCMs were selected and ensembled under SSP2-4.5 and SSP5-8.5 scenarios using weighted average ensemble approach. Daily precipitation projections were used to construct intensity-duration-frequency (IDF) curves for climate impact simulations in PCSWMM. Historical data were preprocessed using the normal ratio method (Kemal and Adeba, 2021). Due to limited sub-daily data, IDF curves were derived from daily rainfall using disaggregation methods (Ewea et al., 2018; Krvavica and Rubinić, 2020). Ayertena station was selected via Thiessen polygon analysis as the most representative for the study area due to its proximity. Sub-daily data from alternative stations (Observatory, Bole) are not in proximity to the study area and lacked consistent temporal resolution for the required 30-year baseline, furthermore, they have considerable difference in magnitude. Therefore, daily rainfall from Ayertena was disaggregated using the IMD method (Al Mamun et al., 2018), a standard technique for data-scarce tropical regions (Bibi et al., 2023).

IDF Curve Development*:* IDF curves were generated using the Indian meteorological department equation (Al Mamun et al., 2018; Nwaogazie et al., 2021), which disaggregates daily maximum rainfall (P_{24}) into shorter durations (P_t) (Eq. 4.1):

$$P_t = P_{24} * \left(\frac{t}{24}\right)^{1/3} \quad (4.1)$$

Rainfall intensities for 2-, 5-, 10-, 25-, 50-, and 100-year return periods were estimated using the Gumbel distribution after computing return period rainfall depths (Eq. 4.2).

$$P_T = P_{ave} + KS \quad (4.2)$$

where P_{ave} is the mean of annual maxima, S is the standard deviation, and K is the frequency factor computed as:

$$K = \frac{\sqrt{2}}{\pi} + \left[0.5772 + \ln\left[ln\left[\frac{T}{(T-1]}\right]\right]\right]$$

The Gumbel distribution was selected after goodness-of-fit testing (Kolmogorov-Smirnov, Anderson-Darling, Chi-square) against GEV, Log-Pearson III, and Generalized Pareto distributions. Gumbel produced the lowest test statistics for all durations, consistent with other tropical highland studies (Badou et al., 2021).

Rainfall intensities (mm/hr.) were obtained by dividing P_T by duration t, forming the IDF curves, which were subsequently integrated into PCSWMM for baseline and future scenario simulations.

Topographical Data: A high-resolution DEM was developed for the study area using 1 × 1 m grid points generated in QGIS. Google Earth was used to collect elevation data for each of the points using the GPS visualizer (https://www.gpsvisualizer.com/elevation), an online tool that is free to use and has been validated in a number of studies (Bagheri et al., 2025; Chiteculo et al., 2022; Hussain, 2020; Khan et al., 2020; Saha et al., 2024). The inherent Google Earth vertical accuracy quality issue is acknowledged. QGIS was used to create a 1 m raster DEM layer of point elevations. The DEM and Bing satellite imagery built into PCSWMM assisted with slope generation, ground elevation profiles, flow direction maps, and the alignment of drainage pipes and channels in the study area.

4.2.2.2 Land Use and Soil Data

Land Use: Land use is at the core of how pollutants build up on surfaces and wash off. Drawing on field investigations and satellite images from Bing and Google Earth, the research area was found to have seven different land uses. Asphalt pavement, commercial area, multifamily residential area, single-family residential area, natural/forest area, cobblestone pavement area, and unpaved road. In PCSWMM's land use editor, the Event Mean Concentration (EMC) method was used to estimate wash off parameters. The wash off coefficient, cleaning efficiency, and exponent were necessary modeling parameters. The initial values of these parameters were derived from the literature review, which gave a range of values for the wash off parameters (Chow et al., 2012; Fernandez et al., 2019; Gaut et al., 2019; Temprano et al., 2006; Tu and Smith, 2018; Zakizadeh et al., 2022). The first model values were modified through sensitivity analysis and calibration.

Soil Data: Soil data helps to estimate the infiltration of soil, which is useful to estimate the stormwater runoff in PCSWMM. The soil map of the study area was extracted and analyzed from the study area from the Addis Ababa soil map prepared by the Ministry of Water and Energy in 2004 and has been used in the studies by Feyissa et al. (2018); Moisa et al. (2023). From the analysis, the dominant soil type in the study area was Pellic Vertosols, which is also supported in the study by Srivastava et al. (1989). Supported by the soil map extracted from the Food and Agriculture Organization (FAO) digital soil map of the world. The Ethiopian Vertisols are characterized by soil texture of more than 50% clay, less than 10% sand, and 40% silt (Berhanu, 1983; Debele and Deressa, 2016). Based on this proportion, the United States development association soil texture triangle reading shows a silty clay soil type. Typical value of parameter for the modified Green Ampt infiltration estimation method, including suction head (mm), hydraulic conductivity (mm/hr), and initial deficit for PCSWMM, was adopted from Rossman A. (2015) user manual, for the soil type.

4.2.2.3 Water Quality and Flow Data

Water Quality Parameter Selection: The study area lies within the Little Akaki River catchment, one of Ethiopia's most polluted urban waterways (Angello et al., 2021). Ten water quality parameters were selected based on their frequent presence in stormwater studies in Addis Ababa, relevance to dominant land uses, and known health and ecological risks (Adugna et al., 2019; Asnake et al., 2021; Gule et al., 2024; Mekuria et al., 2021; Solomon et al., 2024). These include nutrients (ammonia NH_3, nitrate NO_3^-, phosphate PO_4^{3-}), organic indicators (BOD, COD), and physicochemical parameters (calcium Ca^{2+}, chloride Cl^-, sulfate SO_4^{2-}, TDS, TSS). Collectively, these pollutants capture the pollution signature of densely populated, rapidly urbanizing catchments.

Initial Parameterization and Calibration: Due to the absence of routine water quality monitoring in Addis Ababa, initial pollutant parameters were sourced from PCSWMM defaults and urban stormwater literature (Angello et al., 2021; Beganskas et al., 2021; Brezonik, 1976; Charbeneau and Barrett, 1998; Cho and Seo, 2007; Gado et al., 2021; Huber et al., 1979; James and Rossman, 2010; Novotny et al., 1985; Rossman and Huber, 2016; Soonthornnonda and Christensen, 2008; Temprano et al., 2006; Tu and Smith, 2018; USEPA, 1983; Yu et al., 2011; Zakizadeh et al., 2022; Zambrano et al., 2017). These values were then calibrated against event-based field measurements to reflect local conditions.

Field Measurements – Flow Depth: The study site lacks continuous monitoring infrastructure. Therefore, event-based flow depth measurements were conducted at the main outlet (OF1, shown in Section 4.2.3, Fig. 5.2) during storm events. A graduated staff gauge (precision ±2 mm) was installed in the rectangular concrete channel (width 2.2 m, depth 2.4 m). During peak flow periods, depth readings were recorded manually every 5 minutes. The observed runoff depths were directly used in the PCSWMM SRTC (Sensitivity-based Radio Tuning Calibration) tool for model calibration and validation, as recommended by Rezaei et al. (2019), Basnayaka (2012), Bibi et al. (2023), and Yim et al. (2016).

Water Sampling and Laboratory Analysis: Stormwater grab samples were collected at the same outlet concurrently with flow depth measurements. Sampling was performed at 15-minute intervals from the onset of runoff until flow recession, using 1-L high-density polyethylene bottles previously rinsed with deionized water. Samples were stored on ice (4°C) in the field and transported to the laboratory within 6 hours. All analyses followed standard methods described in *APHA Standard Methods for the Examination of Water and Wastewater* (23rd edition, 2017). BOD was determined by 5-day incubation at 20°C (SM 5210 B). COD was measured by closed reflux colorimetric method (SM 5220 D) using a Hanna HI83399 multiparameter photometer. Ammonia, nitrate, and phosphate were analyzed by colorimetric methods (SM 4500-NH_3 F, SM 4500-NO_3^- E, SM 4500-P E, respectively) using the same photometer. TSS was determined by gravimetric analysis after filtration through Whatman GF/C filters (SM 2540 D). TDS was measured by evaporation (SM 2540 C). Calcium, chloride, and sulfate were analyzed by ion chromatography (SM 4110). Quality control included analysis of reagent blanks, duplicate samples (10% of total), and certified reference standards. Recovery rates ranged from 92% to 106% for all parameters.

Dry Weather Flow Estimation: In the absence of direct flow measurements, dry weather flow was estimated using the population of Nefas Silk Lafto sub-city and average per capita water consumption (70 L/cap/day, based on Addis Ababa Water and Sewerage Authority data). A return factor of 0.8 (i.e., 80% of supplied water becomes wastewater) was applied following established engineering practice (Tchobanoglous and Schroeder, 1985; Ghangrekar, 2022), supported by local studies in Addis Ababa. Although only ~22% of water is captured by the formal sewer network (van Rooijen et al., 2010), most greywater and wastewater from both connected and unconnected households are observed to enter storm drains. Accordingly, dry weather flow was calculated as:

$$Q = 0.8 * Population * Consumption\ rate \quad (4.3)$$

where Q is in m^3/day.

4.2.3 Model Setup in PCSWMM

SWMM is a dynamic simulation tool for single-event and long-term continuous runoff quantity and quality modeling in urban areas (Rossman and Huber, 2016). This research adopted PCSWMM, a GIS-based version of SWMM created by Computational Hydraulics Inc. for better spatial analysis integration. PCSWMM contains highly detailed hydrologic/hydraulic simulation capabilities, so users can visualize, configure, and assess stormwater systems. In this study, the software version 7.7.3920 with SWMM Engine 5.0.013-5.2.4 was used.

Model Structure: PCSWMM splits the study area into hydrologic and hydraulic components. The hydrologic part is the sub-catchments, and the hydraulic part is the nodes and conduits. The sub-catchment hydrologic processes infiltration, evaporation, and runoff, and the hydraulic module, which routes flow through pipes, channels, and nodes. It also simulates the processes whereby pollutants accumulate and are transported.

Model Inputs and Output Description: The inputs required include climate data such as rainfall time series, surface evaporation, or temperature. Hydrologic data: sub-catchment area, width, slope, imperviousness, roughness coefficients, infiltration parameters. Information regarding pipe diameters, slopes, invert and rim elevations, roughness coefficients, junction, and outfall attributes. Land use and soil data were used in estimating the pollutant wash-off parameter and finding infiltration behavior. The important outputs are runoff volume, infiltration, and ponding. Hydraulic: flow rates, velocities, depth, hydraulic grade lines. Concentrations and loads of the pollutants.

Hydraulic Configuration and Drainage Network Setup: In view of the limited secondary data, the drainage network was surveyed in the field for mapping purposes. Observation manholes were manually accessed to measure diameters, slopes, and roughness of conduits. Field monitoring and spatial data from Google Earth Pro and embedded Bing satellite image in PCSWMM georeferenced and assign elevation and attributes to the nodes (junctions). The drainage network had 25 sub-catchments, 142 junctions, 150 conduits, and one outfall (OF1), as illustrated in Fig. 4.2 of section 4.2.3. The boundary conditions, which incorporated rainfall inflow and outfall discharge, were set up to duplicate real-world hydrologic and hydraulic processes.

Simulation Options: The model is configured for simulating processes, such as rainfall runoff, flow routing, and water quality. Dynamic Wave Routing was chosen as the routing method because it can handle complex flow conditions, including backwater effects, pressurized flow, and other characteristics of urban systems. The infiltration model used for the simulation purpose was Modified Green-Amp because of its physical realism and satisfactory computational efficiency (Lee et al., 2018; Silva and Silva, 2020; Sun et al., 2014). The network performance during storms was simulated in detail through the dynamic wave routing process.

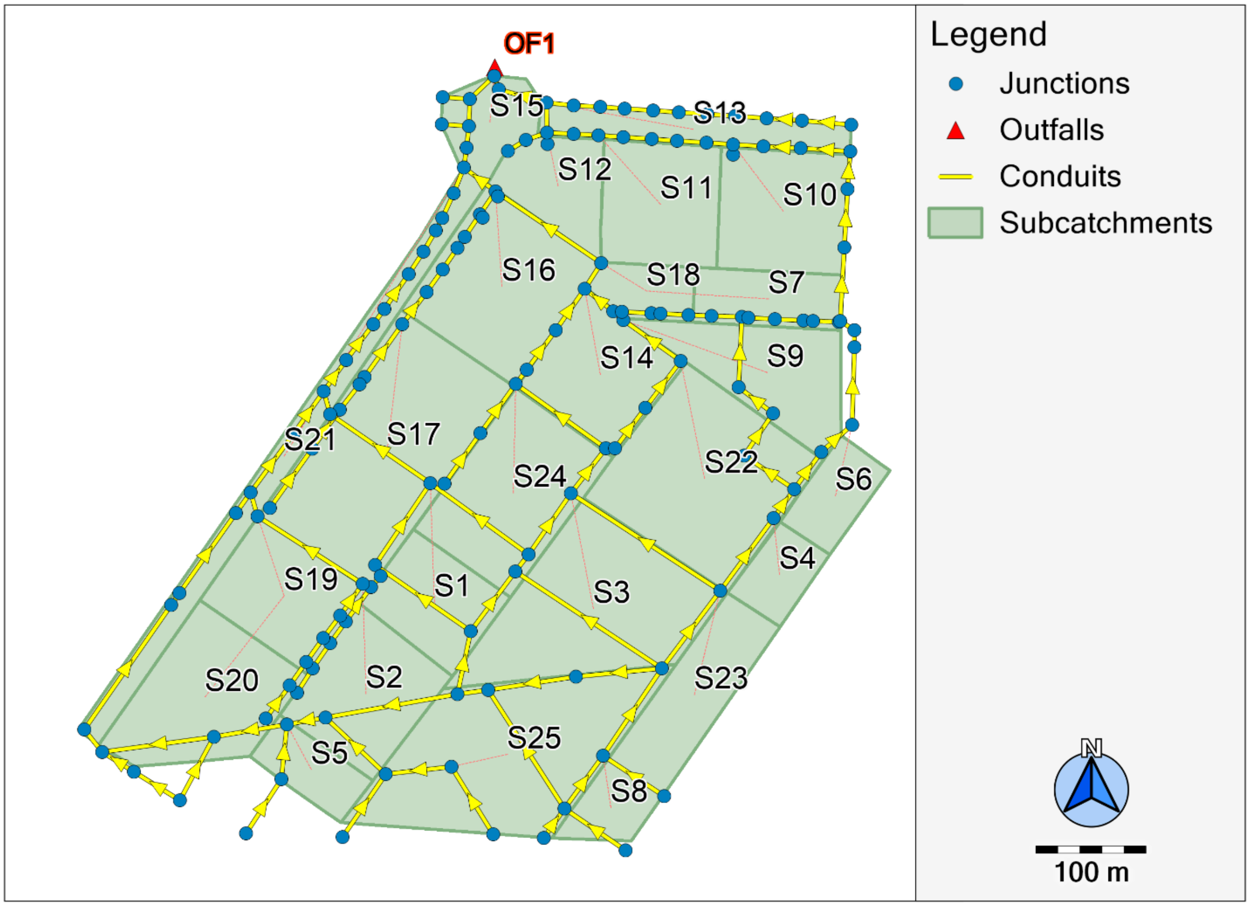

Figure 4.2: The drainage network of the study area with its junctions, conduits, sub-catchments, and outfalls

4.2.4 Model Performance

4.2.4.1 Sensitivity Analysis, Calibration, and Validation

Hydrologic-Hydraulic Sensitivity Analysis*:* Sensitivity analysis was carried out to identify the parameters of the model that most impact the output of the model. Table 4.1 summarizes relevant sensitive parameters with ranges of their uncertainties according to Akhter and Hewa (2016) and James (2005). Calibration used the SRTC method in PCSWMM, which varies sensitive parameters to minimize differences between the observed and modeled output (Wagener and Wheater, 2006). Stormwater runoff calibration parameters of the sensitivity analysis table.

Table 4.1: Sensitivity analysis parameters used in the calibration of stormwater runoff

Compartment	Notation	Calibration parameter	Uncertainty %
Surface	Area	Sub-catchment area	10
	Width	Sub-catchment width	100
	Imperv. %	Impervious Percentage	25
	N perv	Manning's roughness for a pervious area	25
	N Imperv	Manning's roughness for impervious area	25
Transport	Geom 1	Geometry and maximum depth of conduits	25
	Roughness	Manning's roughness of conduits	25

Depression storage, slope, and Green-Ampt infiltration parameters (Ks, suction head, initial deficit) were not included in the parametric sensitivity analysis because their values are constrained by literature for urban impervious surfaces and Vertisols. They are included in the baseline model and may be adjusted during SRTC calibration if identified as influential.

Water Quality Parameters Sensitivity Analysis: To assess the influence of parameter uncertainty due to the use of literature-based values, a one-at-a-time sensitivity analysis was performed for all ten simulated water quality parameters. Each pollutant's three input factors were varied independently by ±25% from the baseline values. The three input factors included rainfall event concentration, dry weather flow concentration, and initial concentration according to the acceptable practice in hydrologic modeling (Akhter and Hewa, 2016). Simulations in PCSWMM using a fixed hydrologic and hydraulic setup were carried out to assess the impact of changing pollutants on total event loads of pollutants. The percentage difference from baseline was utilized to identify the most sensitive parameters and to determine the level of uncertainty introduced using non-site-specific input data. This analysis supports both sensitivity interpretation and uncertainty acknowledgment in data-limited urban contexts. OAT sensitivity analysis was selected over global sensitivity analysis (GSA) because OAT requires fewer simulations (3n vs. 10,000+) and is standard in PCSWMM's SRTC module (CHI, 2023). The 25% uncertainty range follows prior studies (Akhter and Hewa, 2016; James, 2005).

Model Calibration and Validation: The model calibration and validation were carried out based on runoff depth data collected at outlet OF1 at a 5-minute time step during the peak flow periods of two storm events: August 12 and September 2, 2024. Although these storms persisted for 300 (August) and 360 (September) minutes, respectively, only the 115-minute and 110-minute periods of maximum runoff were used for calibration. The water quality samples were taken at the same time. For the purpose of validation, data from the storms of 23 August and 23 September 2024 were used. The storms had durations of 105 and 75 minutes, respectively. Runoff and pollutant measurements were recorded over the 75- and 60-minute duration, respectively, at 5-minute intervals. These four events were selected to capture peak flow dynamics and key pollutant transport phases, thereby enhancing model reliability despite limitations in data availability and budget.

4.2.4.2 Performance Metrics

NSE: NSE essentially assesses the proportion of the variance in the predicted values that may be explained by the independent variable. The NSE is used to measure how well the predicted and the observed data fit. Values of the coefficient are interpreted in the following way: NSE = 1 indicates a perfect fit, NSE = 0 means that "the model predictions are as accurate as using the mean of the observed data," and NSE < 0 means poor model performance. The model is considered to have good performance if its NSE is ≥ 0.8, adequate if its NSE is ≥ 0.6, and unsatisfactory if its NSE is < 0.6.

$$NSE = 1 - \left(\frac{\left(\left(\sum_{i=1}^{n} (Y_{obs}^{i} - Y_{sim}^{i} \right)^{2} \right)}{\left(\sum_{i=1}^{n} (Y_{obs}^{i} - Y_{obs}^{mean} \right)^{2}} \right) \tag{4.4}$$

RMSE: The mean magnitude of the error between predicted and observed value is given by RMSE (Eq. 4.5). Lower RMSE shows better performance of the model. The RSR (Eq. 4.6) gives dimensionless RMSE, where lower RSR means better performance. According to the rating, RMSE is very good when it is less than half times the standard deviation, whereas it is good if it is 10% above this and satisfactory if it is 20% above.

$$RMSE = \frac{\sqrt{\sum_{i=1}^{n} \left(Y_{obs}^{i} - Y_{sim}^{i}\right)^{2}}}{n} \tag{4.5}$$

$$RSR = \frac{RMSE}{STDEVA_{obs}} \tag{4.6}$$

ISE: ISE is the integral of the square of the error over time. Thus, a large error results in a larger ISE value because the error is squared. ISE performance is classified as Excellent if it ranges below 3, Very Good if 3 to 6, Good if 6 to 10, Fair if 10 to 25 and Poor if it is above 25.

$$ISE = \frac{\sum_{i=1}^{n} \left(Y_{obs}^{i} - Y_{sim}^{i}\right)^{2}}{\sum Y_{obs}^{i}} x100\% \tag{4.7}$$

Where: $STDEVA_{obs}$ = Standard deviation of observed values, Y_{obs}^{i} = Observed value at the i^{th} observation, Y_{sim}^{i} = Simulated value at the i^{th} observation, and Y_{obs}^{mean} = mean of observed values.

4.2.5 Development of Scenarios in PCSWMM

Four individual stormwater scenarios were created to analyze how stormwater will behave in baseline, climate change, urbanization, and combined scenarios.

Scenario 1 (Baseline Scenario): Under this scenario, the current land use (70% average imperviousness, 2023 conditions) with historical climate (1994–2023). The 30-year baseline follows World Meteorological Organization (WMO) climate normal standards. All scenario results are compared against this baseline.

In the following scenario, the impact of climate change, specifically the effect on rainfall and temperature, on urban drainage systems is examined using historical land use data, with the remaining model inputs unchanged. Downscaled ensembled GCMs were used to model the expected increase of extreme weather events (heavy rainfall). The near future and mid-century time frames (2024–2053 and 2054–2083, respectively) were used.

In the third scenario, the impact of increased urbanization was modeled by raising the impervious surface from 70% to 80%, although the climate data was kept to the baseline. It agrees with the observation of urban expansion in Addis Ababa. In relation to the built-up area, it grew around 187% between 1991 and 2021 (Moisa et al., 2022). Moreover, it grew 224% between 1993 and 2023 (Hailu et al., 2024). According to a study by Koroso et al. (2021), the city's population has "doubled since 2000, expected to double again in 2035." In micro-watersheds formed and already with 70% imperviousness, this scenario realistically predicts continuous urban expansion.

Lastly, the integrated impact scenario depicts the worst-case scenario by putting together the climate change projection scenarios (2024 – 2053 and 2054 – 2083), and the urbanization scenario (80 percent imperviousness). These two scenarios define the near term and midterm, respectively. This scenario characterizes the cumulative impacts of the two components in question, and so provides a suitable basis for urban stormwater management planning.

4.2.6 Conceptual Framework

Starting with data collection which refers to climatic, DEM, land use, soil, drainage, and stormwater quality (Fig. 4.3), the PCSWMM set-ups of sub-catchments hydraulic links and wash off parameters were carried out by these inputs during data preparation. The observed flow and pollutant data were used to calibrate and validate the model. An evaluation of simulation outputs in a baseline scenario, a climate change scenario, an urbanization scenario, and combined scenario is carried out which enabled the comparison of runoff dynamics and pollutants' behavior so that stormwater management can be made resilient.

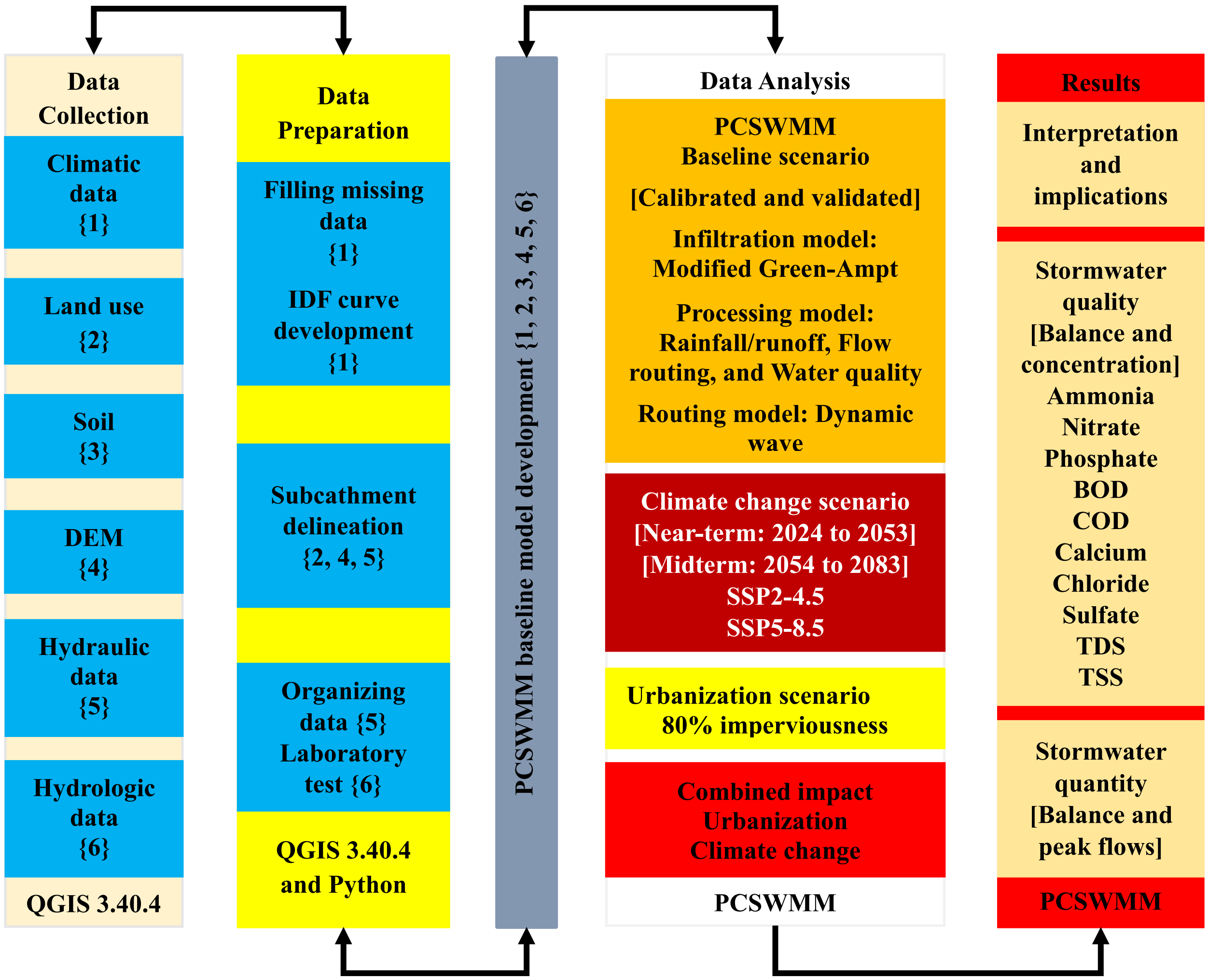

Figure 4.3: Methodological framework designed for this study

4.3 Results

4.3.1 IDF Curve and PCSWMM Model Performance Evaluation

PCSWMM was used to quantify stormwater runoff and pollutant-loading dynamics (expressed by 10-key water quality parameters) in a steep-slope, poorly draining soil micro-watershed in Addis Ababa under four scenarios: baseline, climate change, urbanization, and their combined impacts. The Results section is organized into seven subsections: 1) model performance evaluation, 2) sensitivity analysis result, 3) runoff quantity and quality balance, 4) baseline scenario, 5) impact of climate change, 6) urbanization effect, and 7) combined impact scenario outcomes. IDF curves generated from historical and ensembled GCM used in this study are presented in (Fig. 4.4) showing the increase in rainfall intensity across climate change scenarios as we go from historical to near- and mid-term projections.

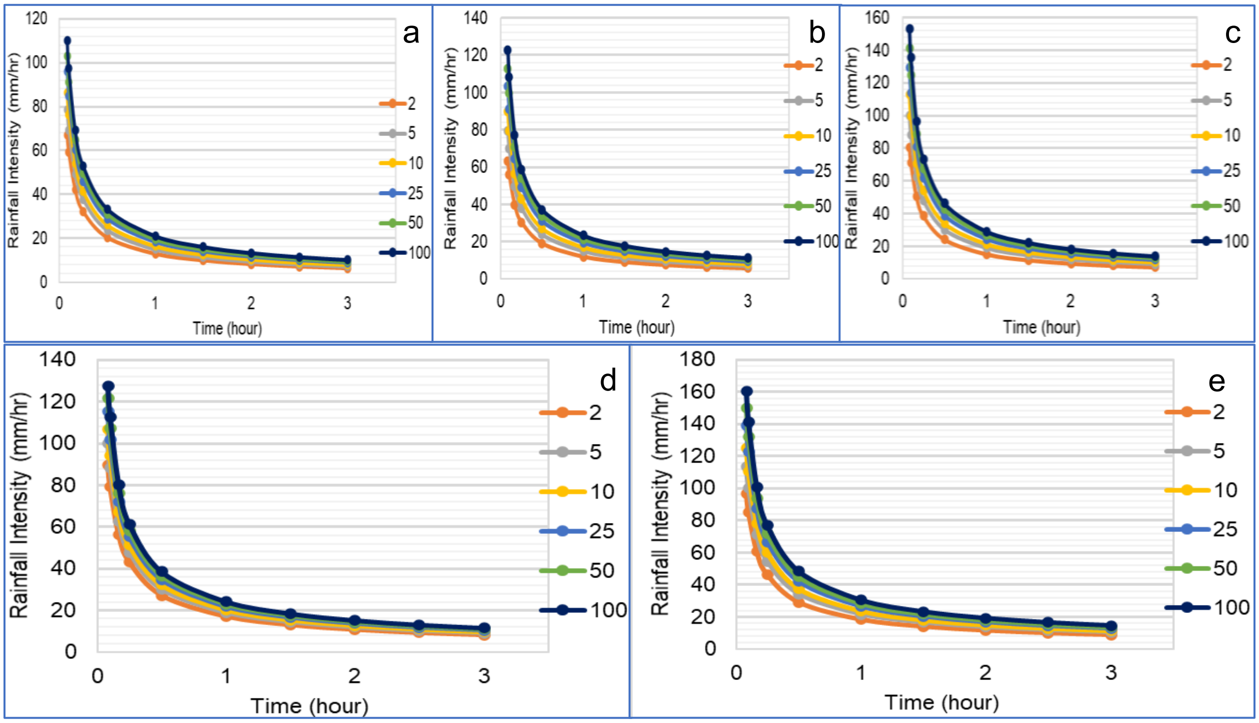

Figure 4.4: IDF curve for a) historical rainfall data of Ayertena station (1994–2023), and projected rainfall data of SSP2-4.5 b) near-term and c) midterm, and SSP5-8.5 d) near-term, and e) midterm

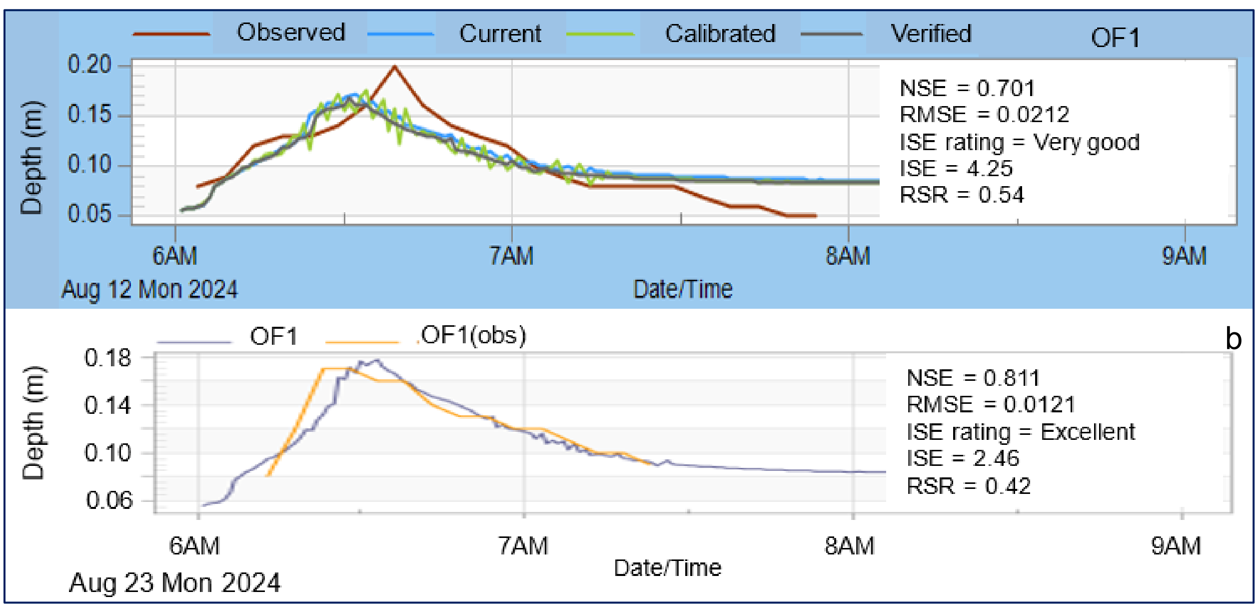

Figure 4.5: Performance evaluation metrics—NSE, RMSE, and ISE—for model calibration and validation. Results are shown for the first round (a: calibration, b: validation), highlighting model accuracy across both phases

The model performance evaluation showed that key metrics—NSE, RSR, and the ISE—all fell within acceptable thresholds. This indicates a strong agreement between observed and simulated values. As shown in (Fig. 4.5 and 4.6), the model accurately reproduced runoff depths, while (Fig. 4.7 and 4.8) illustrate the close match between observed and simulated concentrations of water quality parameters at outfall OF1 (see Fig. 4.2 at section 4.2.3) during the specified storm event. Furthermore, the RSR result at the baseline scenario for the ten-water quality parameter ranged from 0.45 to 0.62. These results confirm the reliability of the model in simulating both hydrologic and water quality components.

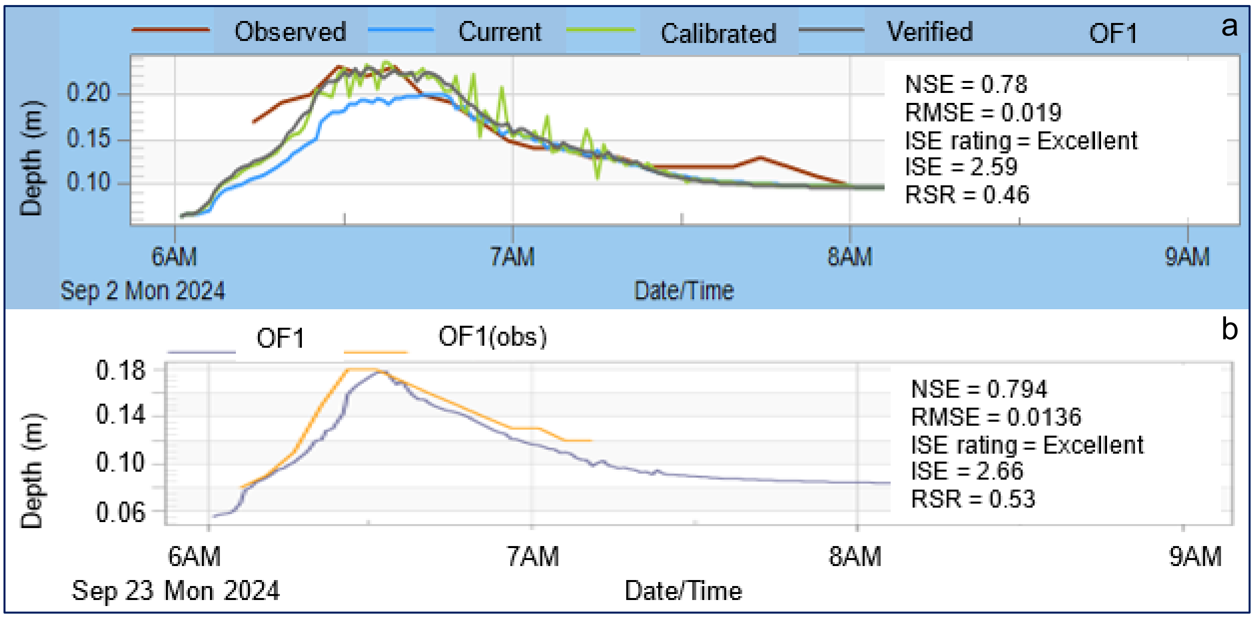

Figure 4.6: Performance evaluation metrics—NSE, RMSE, and ISE—for model calibration and validation. Results are shown for the second round (a: calibration, b: validation), highlighting model accuracy across both phases

4.3.2 Sensitivity Analysis Result

Hydrologic-Hydraulic Sensitivity Results: Sensitivity analysis using the SRTC method in PCSWMM identified impervious percentage, sub-catchment width, and Manning's roughness for pervious areas as the most influential parameters affecting peak flow. Sub-catchment area, impervious surface roughness, and conduit geometry and roughness showed moderate sensitivity. These results, derived using the parameter uncertainty ranges listed in Table 4.1 of Section 4.2.4, informed the prioritization of parameters during the calibration process.

Water Quality Parameters Sensitivity Results: A sensitivity analysis was performed for all ten modeled water quality parameters by varying rainfall concentration, dry weather flow concentration, and initial concentration by ±25%. As illustrated in Fig. 4.9, COD, TDS, and TSS emerged as the most sensitive pollutants, showing load variations of up to 35%, 32%, and 27%, respectively. BOD, nitrate, ammonia, and phosphate exhibited moderate sensitivity, while calcium, sulphate, and chloride showed relatively minor responses. Overall, the analysis indicated that dry weather flow concentration and initial concentration exerted a stronger influence on pollutant load estimates compared to rainfall concentration across all pollutants. These findings highlight the relative importance of parameter sources and underscore the need for accurate representation of base and antecedent pollutant conditions in stormwater quality modeling.

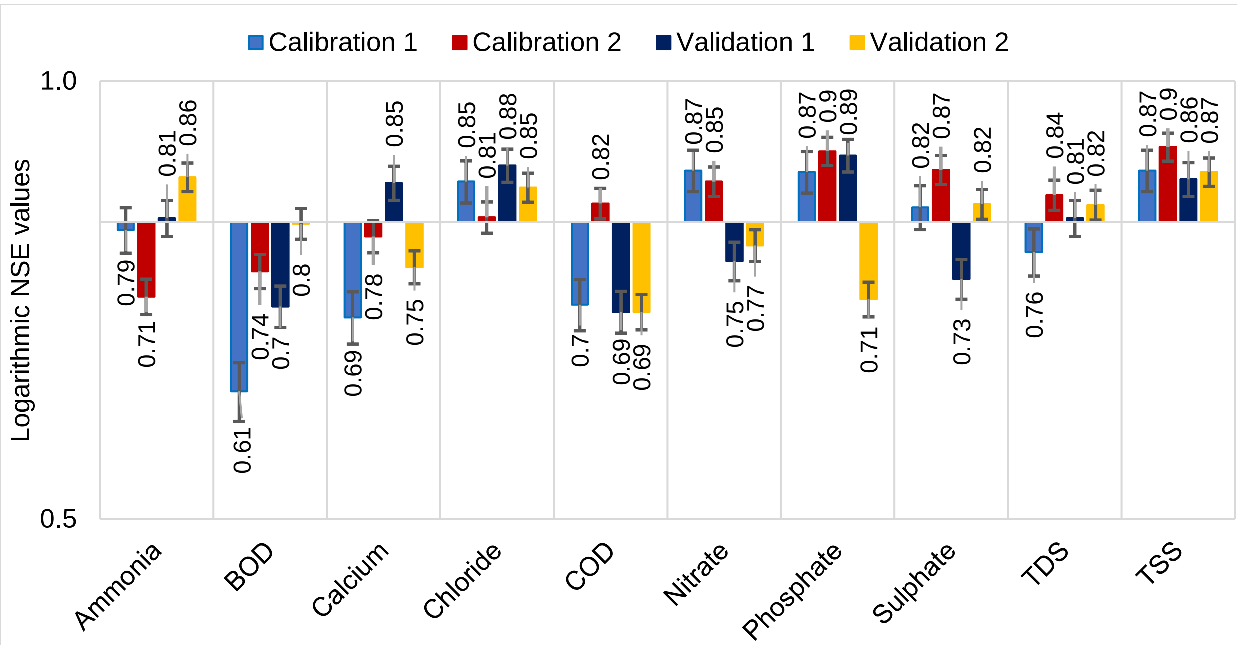

Figure 4.7: NSE values for model calibration (calibration 1: 12 August, calibration 2: 2 September) and validation (validation 1: 23 August, validation 2: 23 September) of ten water quality parameter concentrations during four storm events in 2024, illustrating model performance under varying storm conditions

4.3.3 Runoff Quantity and Quality Balance

Water Quantity Balance: According to the runoff quantity balance, the total precipitation that converted to surface runoff during the simulation period was very large compared to evaporation, infiltration, and storage. Out of total precipitation volume 6,870 m^3 over 3 hours, surface runoff generated 4,960 m^3 (72%) depicting that the area is dominated by non-permeable land, steep slopes, and the clayey characteristics of soil. The location of the study area in the contributing zone of the micro-watershed resulted in increased runoff generation because rainfall flows in quickly due to its hydrology and topography. Of the remaining precipitation, 140 m^3 (2%) evaporated, 1,250 m^3 (18.2%) infiltrated, and 440 m^3 (6.4%) remained in final storage. The overall continuity error of 80 m^3 (1.2%) of the model is acceptable. The low infiltration percentage of 18.2% indicates the non-draining soil characteristics as well as a lack of green infrastructure to facilitate the percolation of water.

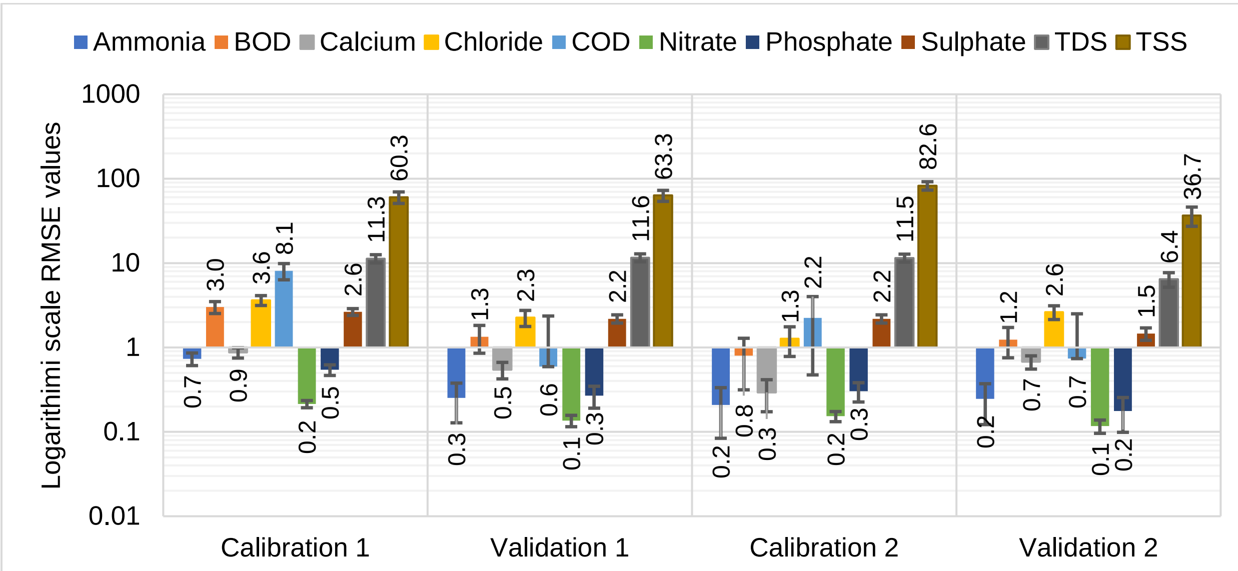

Figure 4.8: RMSE values for model calibration 1: 12 August, and validation 1: 23 August and calibration 2: 2 September, and validation 2: 23 September of ten water quality parameter concentrations during four storm events in 2024, illustrating model performance under varying storm conditions

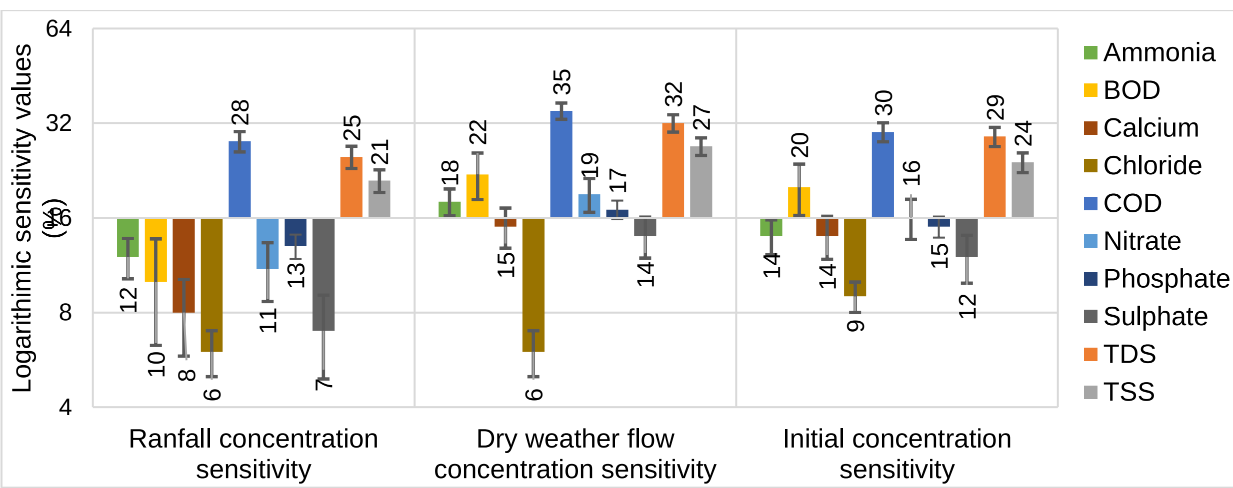

Figure 4.9: Sensitivity analysis results for the ten key stormwater quality parameters (pollutants), illustrating the responsiveness of each pollutant to variations in sensitivity parameters

Water Quality Balance: The pollutant continuity analysis shows how important parameters (buildup, deposition, infiltration losses, and surface runoff) are transformed in runoff quality. Most pollutants are transported by way of surface runoff, as buildup, deposition, and infiltration losses are negligible because of the steep slope nature of the study area and the low drainage capacity of soils (refer to Fig 4.10). Given the substantial runoff generation, the surface runoff was found to transport considerable quantities of pollutants into the waterways and water bodies. The continuity errors for all contaminants were within a limit of 1%.

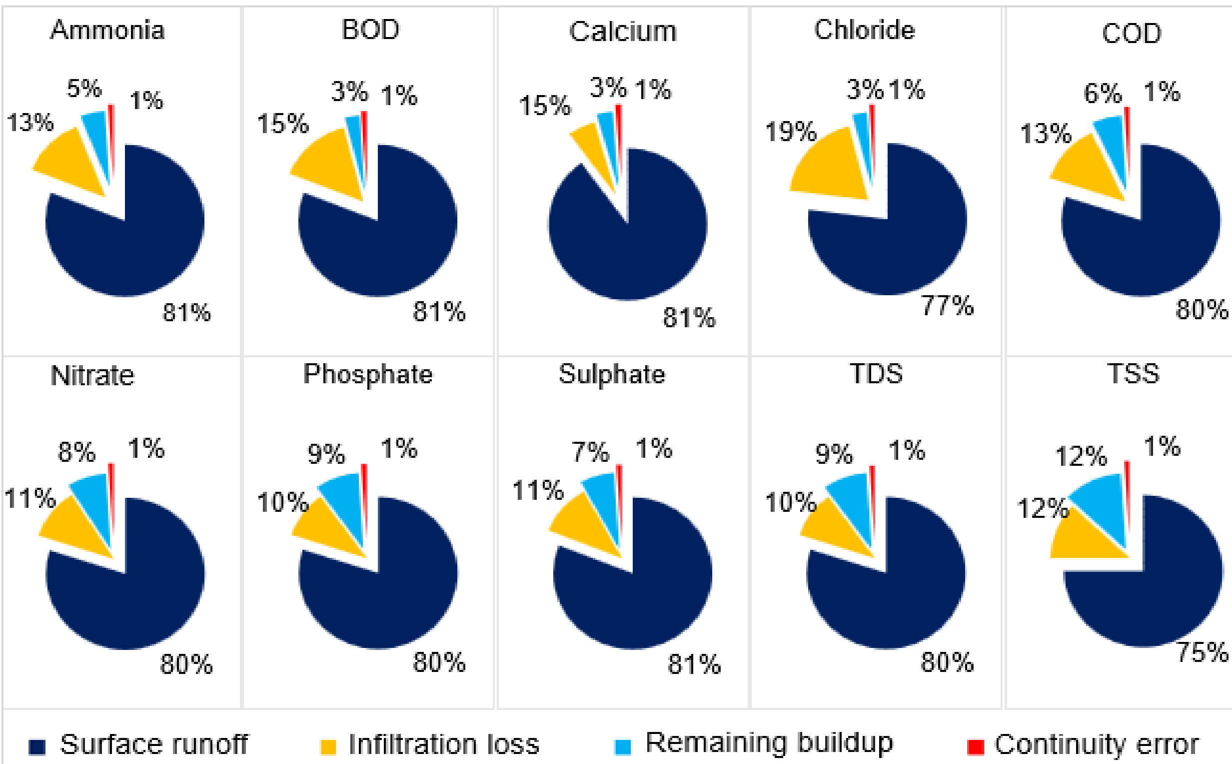

Figure 4.10: Water quality parameter balance shows the proportional contribution of each pollutant to runoff, infiltration loss, remaining buildup, and continuity error

4.3.4 Baseline Scenario Result

Under the baseline scenario, there were flooding incidences at two nodes J_{67} and J_{80}. Besides, concurrent surcharging occurred at seven nodes, namely J_{101}, J_{106}, J_{107}, J_{28}, J_{67}, J_{80}, and J_{92}. The minimum and maximum runoff were 0.0044 m^3/s and 3.6 m^3/s, with a total runoff on the order of 5 m^3/s recorded at OF1 as assigned in Fig. 4.2 of section 4.2.3, for a 2-year return period. Inability to accommodate peak flows, indicating localized exceedance of the capacity of the drainage system implying the need for further improvements in drainage infrastructure at flooding hotspots and to alleviate surcharging in the drainage system. As shown in Fig. 4.11, the baseline simulation indicates that concentrations of key water quality parameters including COD, TDS, BOD, ammonia, chloride, calcium, sulfate, nitrate, and phosphate have varied over time during the storm event, from initiation to recession. This temporal variability reflects the influence of initial washoff from different land uses—residential, commercial, asphalt-paved, and unpaved roads—on stormwater quality in the study area.

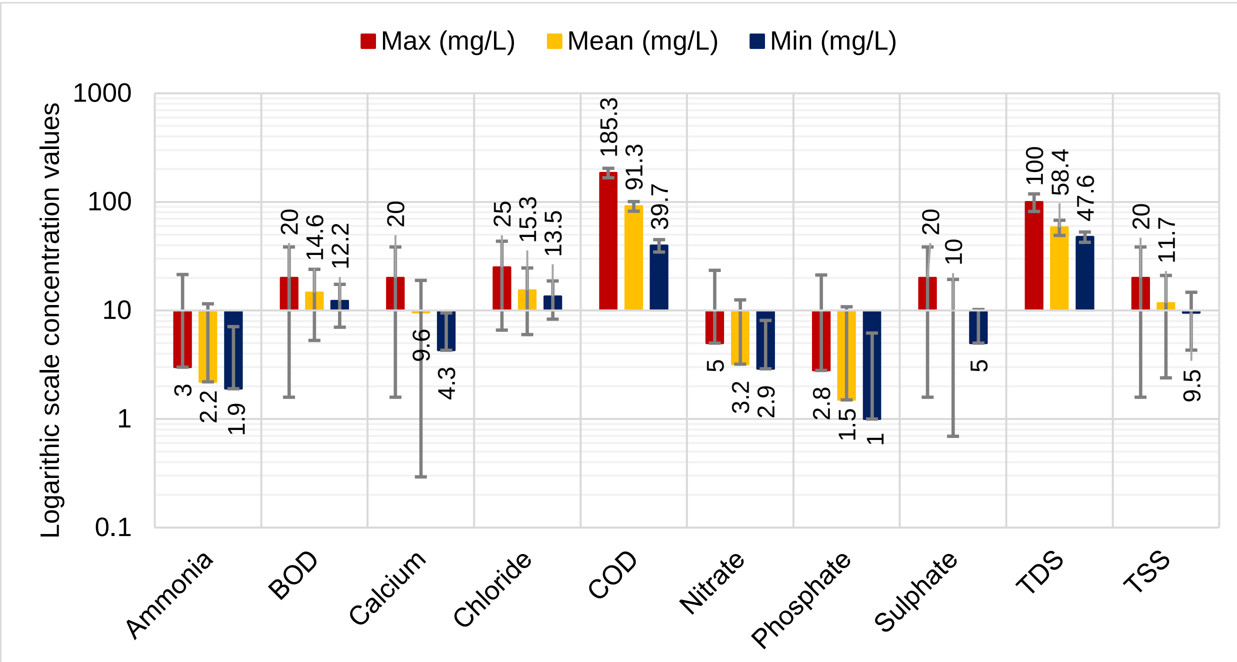

Figure 4.11: Summary of stormwater quality parameter concentrations under the baseline scenario, showing maximum, mean, and minimum concentration values

4.3.5 Impact of Climate Change on Stormwater Management System

An average increase of 1.7% across all 10 stormwater quality parameters was observed under the climate change scenario during both the near- and mid-term periods across all return intervals, indicating only a modest change in concentration levels. The result further indicated a significant increase in flooding across all return periods for both near- and mid-term horizons, with peak runoff rising substantially from the baseline scenario (3.6 m^3/s) as presented in Fig. 4.12. In the near-term (2-year return period), peak runoff increased by 5.6% under SSP2-4.5, reaching 3.8 m^3/s, and by 61.1% under SSP5-8.5, reaching 5.8 m^3/s. In the midterm, flooding intensified significantly under SSP5-8.5, with peak runoff (2-year return period) increasing from 4.7 m^3/s (a 30.6% increase) under SSP2-4.5 to 6.6 m^3/s (an 83.3% increase) under SSP5-8.5. This highlights the long-term effects of higher greenhouse gas emissions, leading to more extreme rainfall and worsening flood conditions over time. The sharply rising flood risks projected under the SSP5-8.5 scenario highlight the urgent need for proactive and integrated adaptation measures.

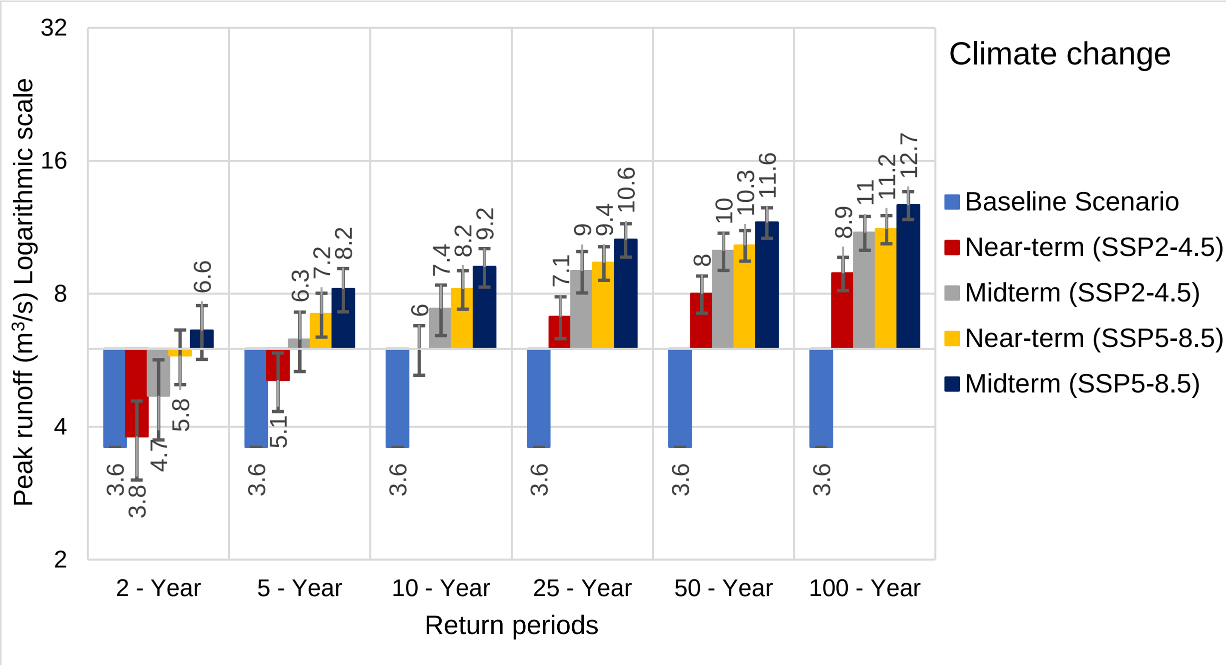

Figure 4.12: Peak runoff projections under baseline and climate change scenarios of SSP2-4.5 and SSP5-8.5 for return periods of 2-, 5-, 10-, 25-, 50-, and 100-year, and two-time horizons (the near- and mid-term) highlighting variations in runoff magnitude

4.3.6 Effect of Urbanization on Stormwater Management System

Under an urbanization scenario of 80% imperviousness, the baseline scenario with average imperviousness of 70.1%, peak runoff ranged 3.6 m^3/s to 4.1 m^3/s. This increase of 13.8% indicates the impact of impermeable surfaces on stormwater runoff. The large volumes of runoff caused flooding at various nodes, indicating that the existing drainage system is insufficient to handle intensified runoff. Under this scenario, the results of all water quality parameters showed an average increase of 7.1% in concentration. As there is more impervious surface, runoff also increases, infiltration decreases, and more pollutants are transferred to water bodies.

4.3.7 Combined Impact of Climate Change and Urbanization

The average values of the ten water quality concentration parameters obtained maximum values with increases of up to 10.3% near- and midterm for all return periods. The growth of impervious surfaces speeds up surface runoff, which lessens infiltration and increases flooding as well as the transportation of contaminants. Moreover, the results showed a peak runoff significantly increased; near-term and midterm predictions showed heavy flooding as shown in Fig. 4.13. Climate change and urbanization, steep slopes, and non-draining soils are cumulatively increasing runoff. According to climate change projections, peak runoff, which means the maximum rate of water used to be available following an extreme precipitation event, increased from 9.6 m^3/s with a 166.7% increase under SSP2-4.5 to 12 m^3/s with 233.3% increase under SSP5-8.5 for a 100-year return period. Forecasts for the midterm showed even larger increases. Peak runoff under SSP2-4.5 rises 230.6% to 11.9 m^3/s, and under SSP5-8.5 it reaches 13.5 m^3/s, which is 275% higher as expected. Flooding is confirmed to be experienced across all return periods and has been intensified due to urbanization as well as climate change. Peak runoff rates were highest in this scenario, which indicates that stormwater infrastructure will be under extreme stress.

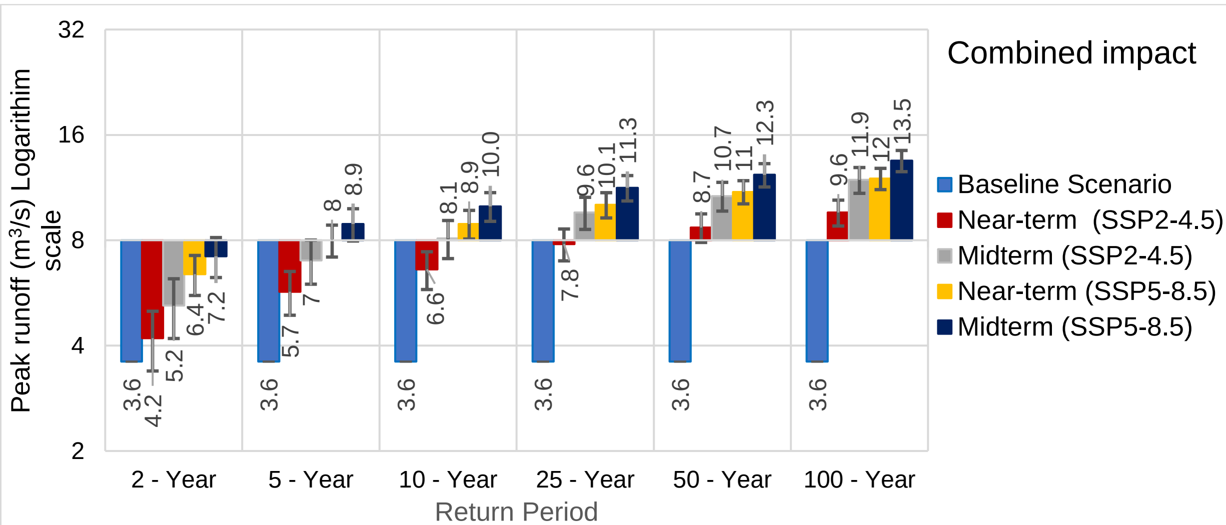

Figure 4.13: The baseline scenario and cumulative effects of climate change (SSP2-4.5 and SSP5-8.5) and urbanization on peak discharge for return periods of 2-, 5-, 10-, 25-, 50- and 100-year, for the two-time horizon (near-term and mid-term)

4.4 Discussion

4.4.1 Runoff and Pollutant Dynamics in Steep, Poorly Draining Soils

This research determined the extreme hydrologic responses that took place within a micro-watershed in Addis Ababa, which is characterized by steep slopes and low permeability soils. It was found that 72% of the rainfall turned into surface run-off. This is much higher than the typical 30–55% range reported by other researchers like Lensa et al., (2017). And on average, 80% of the pollutants were transported by the surface runoff. In accordance with Wang et al., (2017), our baseline conversion shows that urban intensification can significantly increase both flow and contaminant transport. The results show that a need exists for upstream retention and infiltration like the suggestions by McFarland et al. (2019), Speak et al. (2013), and Yang et al. (2013) to alleviate stresses at downstream conveyance zones where speedy flows and poor water quality exacerbate stormwater management challenges. Further it depicts that upstream retention, and infiltration can address both flood risk and water quality degradation because the same hydrological processes—rapid runoff from impervious surfaces, short time of concentration—generate both high peak flows and pollutant mobilization.

4.4.2 Uncertainty Analysis and Limitations

Sensitivity analysis shows the extent to which our predictions of water quality parameter loads are affected by uncertainty in the parameters. Of the ten pollutants evaluated, COD, TDS, and TSS were most sensitive to ±25% change in rain concentration, dry weather flow concentration, and initial concentration values. The changes observed in BOD, Nitrate, Ammonia, and Phosphate were moderate. Calcium, Sulfate and chloride generated a relatively stable output. The results demonstrate a high level of sensitization to the use of literature-based pollutant parameters, especially for concentration-based pollutant with dynamic urban sources like COD, TDS, and TSS. The greater impact of dry weather flow and initial concentration calls for local sampling to increase accuracy, especially in fast-urbanizing area where pollutant generation may differ from the global value cited in the report.

4.4.3 Climate Change, Urbanization, and Their Combined Impacts

The challenges posed by stormwater management are significantly aggravated by climate change and urbanization, as confirmed by the findings of this study, which are in line with those reported by Babaei et al. (2018), Hassan et al. (2017), and Hussain et al. (2022). Peak runoff steadily escalates with each projection, while midterm projection impacts intensify. The changing climate is making urban drainage systems vulnerable according to these emerging trends. Due to impervious surface expansion, urbanization is another factor that exacerbates the challenges of stormwater management challenges according to recent studies by Abd-Elhamid et al. (2020), Bibi et al. (2023), and Marhaento et al. (2018). Urbanization may increase runoff and pollutant loading, but climate change has a more dominant effect on peak runoff, particularly over longer timescales Mayou et al. (2024); Yang et al. (2024). Future stormwater infrastructure will likely experience climate-driven rainfall variability as a major stressor.

Combined impacts from climate change and urbanization are expected to be the most extreme, with flooding projected to occur at all return periods. The statement supports the accumulated flood risks identified by Sagar Kumar and Umamahesh (2024), Das and Sahoo (2025), and Saraswat et al. (2016). The result further underscores urbanization as the dominant driver of water quality degradation. Thus, it induced a 7.1% increase in pollutant loads under the urbanization-only scenario. This contrasts with the 1.7% under climate change only. A comprehensive analysis showed that asphalt pavements commercial and high-density residential areas are very important sources of key pollutants. The mobilization of sediment resulting from erosion caused TSS and calcium generating from unpaved roads and pervious surfaces principally. In commercial and residential areas that dispose of blackwater and solid waste incorrectly, BOD and COD concentrations are observed to be the highest. Residential and mixed-use areas had peak concentrations of ammonia, nitrate, and phosphate due to fertilizer application, greater runoff, and septic overflow. Chloride is mostly linked to runoff from paved roads and commercial areas where it appears that detergents and household chemicals are used. Runoff from the construction site and pavement made of cement affected the sulfate concentrations. The levels of TDS increased in both paved and unpaved areas due to various urban sources. The natural and vegetated areas delivered substantially lower pollutant loads demonstrating their buffering capacity in urban catchments (Shuster et al., 2005). Under expanding urbanization, these results signal the need for pollutant-specific, land use-targeted stormwater interventions. Calcium in runoff from unpaved roads and pervious surfaces is attributed to weathering of calcium-bearing minerals (plagioclase, calcite) in Vertisol soil (2–5% $CaCO_3$), atmospheric deposition of cement dust from construction, and leaching from decomposing organic matter. Moreover, this finding indicates that adaptation strategies focused on just one stressor are not enough. The resilience planning must be integrated and coordinate response to climatic extremes, urban expansion, and flexibility of systems. According to Hussain et al., (2022), and Wang et al., (2017), adaptive management of stormwater through multi-scenarios is the way forward to handle future threats due to the urban climate.

4.4.4 Synthesis and Roadmap for Resilient Urban Stormwater Management

Implications toward IGGI Solutions: The projected increase in runoff and pollutants in steeply sloped micro-watersheds with poorly draining soil will provide strong evidence for the need of IGGI solutions. Evidence from studies in similar settings, particularly the Moroccan case where bioretention systems and permeable pavements reduced runoff and pollutants (Ben-Daoud et al., 2024), corroborates the relevance of such an approach. In Addis Ababa, the IGGI strategies should target slope-compatible and poor-draining soil-compatible practices that are efficient in land use.

These include permeable pavements with berms for enhanced retention, which can still be used as functional parking areas and residential yards; green walls and roofs retrofitted onto buildings; an engineered rain barrel (a buried rain barrel that collects runoff from all surfaces and allows for delayed infiltration); and ornamental gardens to engineered rain gardens. Not just technically feasible and economically viable, these interventions were found to suit the city's space. The deployment should rely on localized hydrological assessments and high-resolution climate projections for effective performance.

Challenges and Solutions of IGGI Implementation: Although the strategies recommended by IGGI are elaborated in detail, implementation of the IGGI in Addis Ababa suffers from noticeable institutional and community-level challenges. Including the limited ability to plan, poor infrastructure management, regulatory bottlenecks, and limits of finances (Ijara, 2020). The community's knowledge of IGGI advantages is insufficient, which leads to limited involvement (Kemal et al., 2025). Ijara (2020) suggests that stakeholders should prepare a GIS-based green infrastructure inventory, enhance the use of their budgets, strengthen partnerships, and train their workforce. According to Gelan, (2021), the initiation of the planning councils, public participation platforms, and mechanisms of accountability across governance levels, a promising solution. Kemal et al., (2025) also urges further implementation of IGGI at household level while enabling public awareness and allocating land for retrofitting. It is vital to overcome these challenges to go from planning to effective IGGI implementation in the city of Addis Ababa.

Implication toward Stakeholders: Moreover, urban planners and policymakers should make these IGGI requirements a part of zoning codes and building regulations. Importantly, their implementation should be a priority in vulnerable, high-risk areas. Contextually suitable techniques comprise green walls and roofing in locations where they will be effective, as well as rain gardens in natural woodlands or ornamental gardens and permeable paving in parking spots and backyards. We need to retrofit drainage systems with green infrastructure to mitigate flood risk. Public awareness creation on water harvesting, and sustainable landscaping will enhance decentralized strategies. Ensuring successful long-term hydrological modeling requires improved institutional coordination, technical capacity and continual monitoring. These collectively support national climate adaptation plans and contribute to achieving the goals set out in SDGs 6, 11, and 13.

Assumptions of the Model and Limitations: Acknowledgement of the limitations of the model despite a strong performance is very important. PCSWMM did not explicitly model groundwater flow, limiting model base flow and delayed infiltration. This omission may reduce runoff estimates, particularly during wet conditions, but is likely to have limited effect in the study area as the slopes are steep, and the soils are poorly drained with low infiltration capacity. The initial values of water quality parameters or wash-off parameter were derived from literature values and applied uniformly on the land use classes. Such an approach is standard; it is noted that they may not capture the local pollutant generation processes. Dry weather flow is incorporated, but uncertainties in spatiotemporal variability exist. Soil information was generalized at the city scale, masking infiltration variability at microscale. Moreover, the calibration and validation focused on short, measured rainfall events. This might limit the model's ability to simulate the full range of hydrologic responses. The effects of prolonged storms or multiple peaks are often overlooked by this limitation of the model. Hence, the present results are probably most reliable for isolated, high-intensity runoff events and cannot be directly transferred to longer-duration storms without further recalibration. The scope of this study did not include costs and governance aspects of implementation of the proposed IGGI interventions. These will need further investigations in future research.

Comparison with Prior Studies: As with other studies, the PCSWMM model utilized in this study was well calibrated and validated both quantitatively (runoff) and qualitatively (water quality). In terms of runoff depth, the NSE varied between 0.715 and 0.809, the RMSE varied between 0.0117 and 0.019, and the RSR varied between 0.42 and 0.54, which shows good reliability of the model. NSE ranged from 0.612 to 0.901, RMSE from 0.1 to 82.6, and RSR from 0.45 to 0.62 for water quality, which also justifies acceptable predictive accuracy over parameters and periods. These findings are consistent with results from other urban catchments in the Global South. According to a study by Zakizadeh et al., 2022, runoff simulations in Tehran had an NSE range of 0.65–0.78 and an RSR range of 0.47–0.59. Additionally, the calibration of water quality in the same study had an NSE range of 0.6–0.72. The NSE values for Nyabugogo catchment, as reported by Niyonkuru et al., (2019), are in the range of 0.6-0.72, with the R^2 value of up to 0.84 for observed vs. simulated runoff. As per the Ethiopian context mentioned in the study by Bibi et al. (2023), NSE > 0.5 and RSR ≤ 0.7 are considered sufficient for stormwater modeling. Both thresholds were exceeded in our study. Furthermore, consistent with studies in Hyderabad of India, Java of

Indonesia, Phnom Penh of Cambodia, and Tehran of Iran, our findings reinforce that climate change leads to higher peak flows, while urban expansion primarily increases pollutant loads (Marhaento et al., 2018; Sagar Kumar and Umamahesh, 2024; Yim et al., 2016). To our knowledge, this is the first PCSWMM application in a steep-slope, with poorly draining soil micro-watershed in Addis Ababa. These findings provide stakeholders with evidence-based insights for planning IGGI and upgrading urban drainage systems in complex and vulnerable settings. Table 4.2 further compares the study with previous findings within different scenarios.

Table 4.2: Compares the current study and previous studies

Study (Year, Location)	Scenarios	Key Response Metrics	Our Study Result: 2-Year Return Period	Take-Home Message
(Yang et al., 2024), Calgary, Canada	Climate change	5-yr, 1-h peak Δ74.3% (2050s) / 170.7% (2080s); runoff Δ2.4–17.5%; TSS Δ2–36.1%, TN Δ3.1–21.4%, TP Δ4.1–20.7%	SSP2-4.5: +5.6% / +30.6% peak; SSP5-8.5: +61.1% / +83.3% (near-term/midterm), average pollutant Δ7.1%	Confirms that intensified precipitation under climate change drives large increases in flow and pollutant loads.
(Bibi et al., 2023), Robe, Ethiopia	Urbanization vs. climate change	Impervious 10→70% ⇒ +52% peak; CC (RCA4/RACMO22T/REMO2009) ⇒ +34.8–46.9% peaks	Imperv. 70→80% ⇒ +13.8% peak; Climate change (SSP2-4.5/SSP5-8.5) ensembled GCMs⇒ +30.6–83.3%	Steep slopes in Addis modulate urbanization's hydraulic impact; climate change remains the dominant driver of peak-flow rise.
(Hussain et al., 2022), Najaf, Iraq	Urbanization vs. climate change	LULC doubling ⇒ +83% runoff; CC (2→5-yr) ⇒ +92% runoff; flooding Δ72%	Urbanization ⇒ +13.8% peak; Climate change ⇒ +30.6–83.3%	Reinforces that climate change has a stronger influence on peak-flow increases than land-use change alone.
(Wang et al., 2017), USA	Urbanization vs. climate change	Flow and quality are more sensitive to urbanization than to climate;	Climate change>Urbanization on peak; Urbanization>Climate	Contrasts global sensitivity: in our steep catchment, climate change dominates peak flow, while

		intensification > land-use alone	change on pollutant (+7.1% vs. +1.7%)	urbanization chiefly drives pollutant loads.
(Mayou et al., 2024), Florida, USA	Climate change vs. urbanization	CC impacts > LULC for both peak and volume, especially at high recurrence intervals and in small catchments	Same pattern: Climate change has a greater effect on peaks	Confirms that in micro-watersheds, climate change outweighs land-use change in driving runoff dynamics.
(Sagar Kumar and Umamahesh, 2024), Hyderabad, India	Climate change and urbanization	Markov-CA and PCSWMM ⇒ significant increases in flooding hours and hazard areas	Combined (SSP5-8.5) ⇒ +233.3%/275% for near-term/midterm peak; +10.3% pollutants	Validates that combined stressors amplify flood risks, underscoring the need for multi-stressor adaptation.
(Das and Sahoo, 2025), Bhubaneswar, India	Climate change and urbanization	Imperv. ↑; peak depths Δ0.75→1.18 m; consistent flow increases across return periods	Combined ⇒ peak 13.5 m^3/s (SSP5-8.5 and midterm)	Aligns with global findings of escalating flood risks under joint climate-urbanization pressures.
(Ben-Daoud et al., 2024), Settat, Morocco	IGGI	Bioretention + permeable pavement ⇒ flow ↓10%; TSS↓31%, TN↓29%, TP↓40%	IGGI recommended for the assumption of achieving flow and pollutant reduction	Demonstrates the efficacy of combined green–grey interventions to mitigate both runoff and pollutant loads.

4.5 Conclusion

This study demonstrates that steep, Vertisol-dominated urban contributing zones are fundamentally different from typical urban catchments in their hydrological response. The combination of steep slopes (>7%) and low-permeability soils creates a “double constraint” that renders conventional stormwater design assumptions invalid: runoff dominates the water balance (72% of rainfall becomes surface runoff), infiltration is severely limited (<20%), and pollutant mobilization is nearly instantaneous (80% of pollutants are transported during storm events). These findings refute the common assumption that urban infiltration behavior can be approximated from literature values for loamy or sandy soils.

Two actionable insights emerge for stormwater management in challenging terrain. First, climate change and urbanization drive different risks: climate change dominates peak flow increases (up to 83% under SSP5-8.5), while urbanization is the primary driver of water quality decline (7.1% increase vs. 1.7% for climate change alone). Adaptation strategies must therefore address both stressors separately peak flow attenuation requires storage and conveyance, while pollutant control requires source reduction and treatment. Second, the combined scenario (climate change + urbanization) amplifies both risks nonlinearly, producing peak flow increases of 100–275% and a 10.3% rise in pollutant concentrations. This nonlinear amplification means that designing for climate change or urbanization in isolation will systematically undersize interventions.

For Addis Ababa and similar Global South cities, the practical implication is clear: grey infrastructure alone cannot manage future stormwater under combined stressors, and generic green infrastructure designed for gentle slopes and permeable soils will fail on steep Vertisols. IGGI solutions specifically designed for this double constraint—such as buried rain barrels for delayed infiltration, rain gardens with engineered media above native clay, permeable pavements with berms, and green roofs/walls on steep terrain—are not optional but necessary. Their implementation, however, faces socioeconomic barriers including land costs, maintenance funding, and public awareness, requiring governance-level solutions beyond technical design.

The study's limitations bound the applicability of these conclusions. Groundwater processes were not modeled, so baseflow contributions and deep percolation remain unconstrained. Water quality parameters were calibrated using event-based sampling rather than continuous monitoring, and soil data were generalized at city scale, masking microscale infiltration variability. Calibration relied on short-duration storm events (75–115 minutes) due to data constraints, limiting model applicability to isolated, high-intensity events; longer-duration or multi-peak storms would require recalibration with appropriate data. Future research should prioritize continuous monitoring networks, groundwater-surface water coupling, and socioeconomic feasibility studies to translate technical IGGI solutions into implemented infrastructure.

Chapter 5

5 Performance Evaluation of Existing Stormwater Infrastructure in a Steep-Slope Urban Watershed of Addis Ababa Using Multi-Criteria Decision Analysis

Abstract

Rapid urbanization and climate variability in Addis Ababa's steeply sloped watersheds—characterized by poorly draining Vertisol soils and high impervious cover—have increasingly overwhelmed stormwater infrastructure, resulting in frequent flooding and erosion. To address the lack of systematic performance data, this study conducted a systematic performance evaluation of 30 representative stormwater infrastructure units across five spatially delineated blocks within a 30-hectare urban micro-watershed in Addis Ababa, Ethiopia. The objective was to develop an evidence-based framework for prioritizing maintenance and green infrastructure (GI) retrofitting interventions. Six critical performance criteria—flood conveyance capacity, structural integrity, erosion control effectiveness, sediment accumulation, maintenance accessibility, and flood control effectiveness (from hydrologic modeling)—were assessed through structured field inspections and Personal Computer Storm Water Management Model (PCSWMM) simulations. The Technique for Order of Preference by Similarity to Ideal Solution (TOPSIS), integrated with expert-derived weights from the Analytic Hierarchy Process (AHP), was applied to rank the five blocks. A comprehensive sensitivity analysis tested ranking robustness against five alternative weighting scenarios. Results showed that sediment accumulation and flood conveyance capacity emerged as the most influential criteria. Spearman's rank correlation coefficients exceeded 0.92 in all cases, confirming strong ranking stability. Block 3 achieved the highest performance score (C_i = 0.7), while Block 4 ranked lowest (C_i = 0.43) due to structural deficiencies and sediment buildup. The analysis revealed that 42.3% of the study area is ready for GI retrofitting, while 57.7% requires prioritized maintenance and rehabilitation. The TOPSIS–AHP–PCSWMM framework provided a transparent, evidence-based mechanism for prioritizing interventions, offering practical insights for optimizing stormwater management in Addis Ababa and comparable data-scarce urban environments in the Global South. This work supports the United Nations Sustainable

Development Goals (UN-SDGs) 11 (Sustainable Cities), 12 (Responsible Consumption), and 13 (Climate Action).

Keywords: Stormwater infrastructure, TOPSIS, urban watershed, performance evaluation, green-grey infrastructure, Addis Ababa, flood management

5.1 Introduction

Urban stormwater management has become increasingly complex due to the accelerating effects of climate change and unregulated urban expansion worldwide. Intensified rainfall events and extended dry periods disrupt the hydrologic balance, leading to increased peak runoff, flood frequency, and degraded water quality (Nie et al., 2009; Zhou et al., 2019). As natural infiltration pathways are replaced by impervious surfaces, urban stormwater becomes a vector for pollutants—transporting sediments, nutrients, and heavy metals—into downstream water bodies (Barbosa et al., 2012; Hatt et al., 2006). These compounding risks demand integrated, adaptive, and site-specific management strategies to ensure the resilience of urban infrastructure.

In low- and middle-income countries, particularly in the Global South, stormwater management faces added constraints. Limited institutional capacity, fragmented planning, and underinvestment in infrastructure render these urban systems vulnerable (Kumar et al., 2023). Addis Ababa, the capital of Ethiopia, is emblematic of such challenges. The city's rapid spatial growth has pushed development into ecologically sensitive areas—particularly steep, erosion-prone micro-watersheds with poorly draining Vertisol soils. These physical conditions amplify hydrologic responses, increasing both surface runoff and pollutant loads (Jemberie and Melesse, 2021; McFarland et al., 2019), while overwhelming existing drainage systems. Frequent urban flooding, infrastructure degradation, and public health threats are recurring consequences in these settings (Angello et al., 2021; Jacobsen et al., 2024).

A major limitation in stormwater system management in Addis Ababa lies in the absence of structured design documentation and a systematic maintenance regime (Adugna et al., 2019). Currently, there are no regulatory requirements mandating the development of maintenance plans, regular inspections, or performance verification for stormwater infrastructure. Systems are typically constructed without any required follow-up, and design plans, if they exist, are not systematically archived or accessible to researchers and authorities. Without baseline design parameters and recorded performance data, authorities lack the means to conduct robust evaluations of system functionality. This constraint not only undermines operational efficiency but also impedes the strategic prioritization of green infrastructure (GI) retrofitting or upgrading interventions. In contrast, cities in the Global North are advancing toward integrated green-grey infrastructure (IGGI) systems, supported by robust datasets and hydrologic modeling (Zhou et al., 2019), highlighting a growing knowledge and infrastructure gap.

In this context, decision-support tools suited to data-scarce environments are essential. The Technique for Order of Preference by Similarity to Ideal Solution (TOPSIS) integrated with the Analytic Hierarchy Process (AHP)—both Multi-Criteria Decision Analysis (MCDA) methods—is valued for ranking alternatives based on their proximity to an ideal solution. Traditionally, TOPSIS-AHP has been applied to identify optimal stormwater strategies such as green infrastructure placement, rainwater harvesting zones, and sustainable drainage systems (Chiu et al., 2020; Jayasooriya et al., 2018; Wang et al., 2017; Bekiryazici and Acar, 2024; Haider et al., 2019; Zeng et al., 2021). However, its use for classifying the actual performance of existing infrastructure units, especially under physically constrained (steep slope and poorly drained soil) and data-deficient conditions, remains limited.

The novelty of this study lies in directly assessing and ranking the functional condition of existing stormwater infrastructure through a coupled TOPSIS-AHP-Personal Computer Storm Water Management Model (PCSWMM) approach. To the best of our knowledge, this represents the first application of such an integrated method for evaluating stormwater infrastructure performance within micro-watersheds in Addis Ababa. The specific objectives of this study are:

1. To characterize and evaluate the current physical condition of stormwater infrastructure across a heterogeneous urban micro-watershed using a multi-criteria field assessment protocol.
2. To quantify the hydrologic performance (peak discharge and runoff volume) of the same infrastructure under current and future climate scenarios using a calibrated PCSWMM model.
3. To integrate the field and modeled data using a TOPSIS multi-criteria analysis to rank the performance of different watershed blocks and identify priority areas for intervention.

The study area, situated on steep terrain and composed of low-infiltration Vertisols, is among the most hydrologically stressed zones in the city. Five blocks comprising 30 infrastructure units were evaluated using six performance attributes: flood conveyance capacity, structural integrity, erosion control effectiveness, sediment accumulation, maintenance accessibility, and flood control effectiveness (from PCSWMM). These attributes reflect both physical condition and functional performance. The use of expert-derived weights and on-site condition assessments ensured contextual accuracy while addressing the lack of formal design records.

Through this approach, the study develops a novel and replicable framework for infrastructure performance classification and prioritization in similarly constrained urban environments. Rather than choosing between theoretical alternatives, this method classifies real-world assets relative to their ideal performance levels, offering actionable insights for targeted maintenance and GI retrofitting. In doing so, it provides a decision-support mechanism that bridges data scarcity with evidence-based planning, contributing to the broader goals of sustainable urban water management. This framework directly contributes to several United Nations-Sustainable Development Goals (UN-SDGs), including SDG 11 (Sustainable Cities and Communities), by enhancing urban resilience and adaptive infrastructure planning; SDG 12 (Responsible Consumption and Production), through evidence-based optimization of existing infrastructure, ensuring resource-efficient GI retrofitting strategies; and SDG 13 (Climate Action), by fostering data-driven responses to increasing urban flood risks.

5.2 Materials and Methods

5.2.1 Study Area Description

The study was conducted in a 30-hectare micro-watershed within Nefas Silk Lafto sub-city, located in southwestern Addis Ababa, Ethiopia (Fig. 5.1). Geographically, Addis Ababa lies between 8°51'15"–9°4'15" N and 38°38'0"–38°55'30" E, with elevations ranging from 2,044 to 3,140 m above mean sea level. It forms part of the Little Akaki watershed and was delineated using QGIS-based overlay analysis of slope and soil data, corroborated through field validation. Regional watershed selection was performed using a 12.5 m resolution ALOS-PALSAR DEM overlaid with soil data (Vertisol/silty clay) to identify areas with slopes in the 7–15% range. The site is characterized by moderately steep slopes (7–15%) and Vertisol soils with low permeability and swelling potential—conditions that intensify surface runoff, limit infiltration, and exacerbate erosion (McFarland et al., 2019; Omitaomu et al., 2021). Land use is mixed, comprising residential, commercial, transport, and fragmented green areas, contributing to heterogeneous hydrological responses and infrastructural stress.

To support spatially structured performance analysis, the watershed was subdivided into five functional blocks, delineated based on topography, drainage direction, and infrastructure clustering. Each block aggregates multiple stormwater features and land-use elements, enabling block-level assessment and comparative scoring under the TOPSIS-AHP-PCSWMM framework. Due to the absence of formal design documentation and scheduled maintenance records, the area represents a data-scarce urban watershed, where stormwater infrastructure operates under high hydrological stress. These characteristics make it a representative setting for evaluating real-world infrastructure performance and prioritization needs in rapidly urbanizing contexts of the Global South.

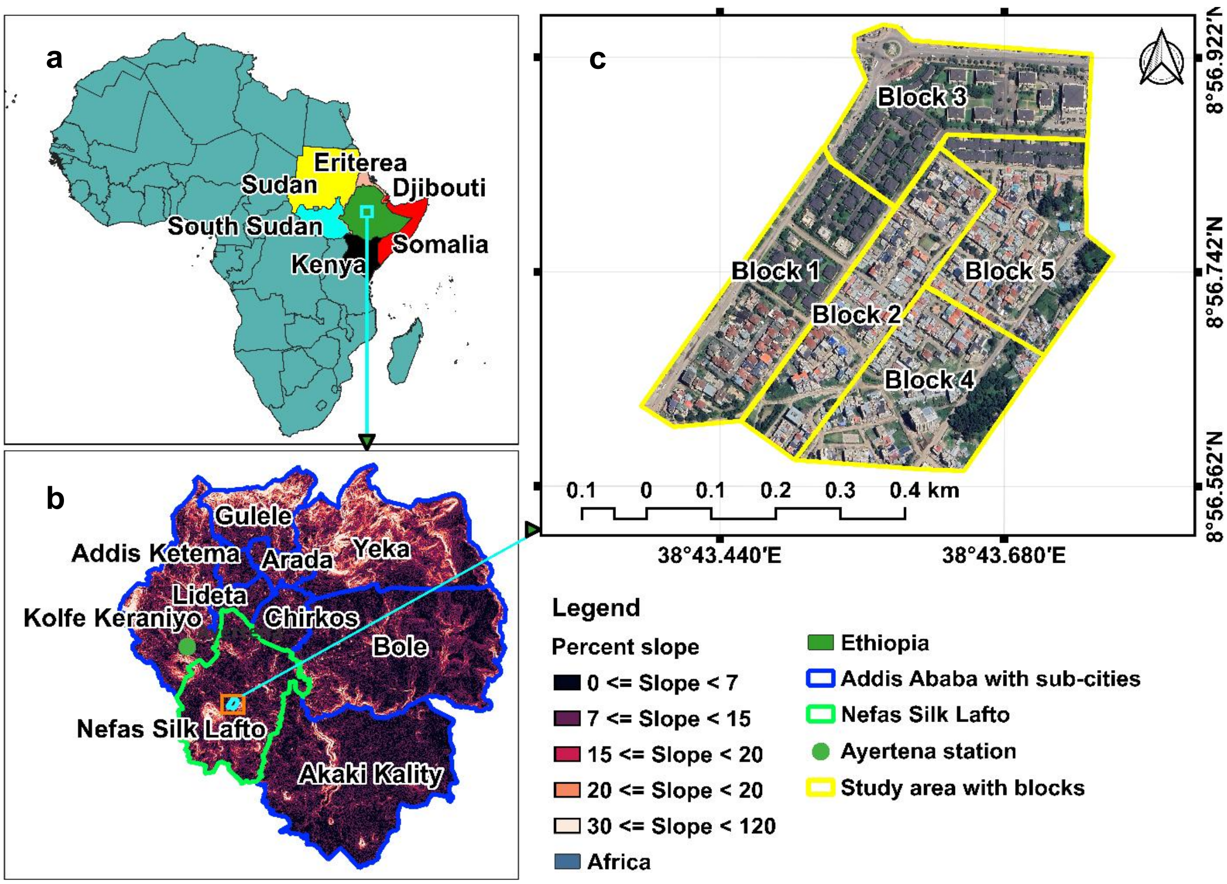

Figure 5.1: Study area location and characteristics. (a) Location of Ethiopia within Africa (base map: open.Africa, ODbL). (b) Topographic map of Addis Ababa with sub-cities showing elevation (base DEM: NASA/JAXA ALOS-PALSAR, public domain) and sub-city boundaries (base boundaries: SSGI via HDX, HDX open terms). (c) Satellite view of the 30-hectare study watershed with stormwater block boundaries overlaid (base satellite imagery: Bing Maps via QGIS, used with permission from Microsoft Corporation; block boundaries: original author data, CC BY 4.0)

This study employed a three-phase methodological framework designed to address the stated research objectives (Fig. 5.3). First, to characterize the physical condition of the infrastructure

(Objective 1), a detailed field assessment protocol was developed and implemented across five delineated watershed blocks (Sections 5.2.2 and 5.2.3). Second, to quantify hydrologic performance (Objective 2), a PCSWMM model of the watershed was constructed, calibrated, and simulated under current and future climate scenarios (Section 5.2.4). Finally, to integrate these disparate datasets and rank block-level performance (Objective 3), a TOPSIS multi-criteria decision analysis, with weights derived from the Analytic Hierarchy Process (AHP), was applied (Section 2.5). This section details each of these phases.

5.2.2 Infrastructure Selection

Five spatial blocks, each approximately 6 hectares, were delineated within the 30-hectare study area (Fig. 5.1). Blocks were delineated in PCSWMM using overlay analysis of slope gradient (1 m DEM), land use classification (Bing imagery + field verification), and soil type (Ministry of Water and Energy, 2004). Equal area (6 ha ± 5%) was achieved by iterative boundary adjustment rather than forcing exact equality, which would have fragmented hydrological coherence. Block boundaries follow drainage divides. Delineation was performed in QGIS using an overlay analysis of three key thematic layers: (1) slope gradients derived from a GPS Visualizer 1 m resolution Digital Elevation Model (DEM) (Hussain, 2020; Kemal et al., 2025b, Kemal et al., 2026) (2) Land-use classification was prepared from combined PCSWMM's Bing imagery, Google Earth Pro, and field verification, and (3) the Addis Ababa soil map (Ministry of Water and Energy, 2004). Thresholds were defined to ensure each block captured a representative range of urban conditions while maintaining hydrological coherence based on drainage direction. Blocks 3 and 4 encompass the steepest terrain (15 %, and 13.5% slope) with asphalt pavement, commercial, multi-family residential, natural/forest, single-family residential, pervious pavement, and unpaved roads. Block 2 represents the most densely urbanized area with approximately 78.26% impervious cover. Block 1 includes more gradual slopes and fragmented green spaces. Block 5 combines asphalt pavement, multi-family residential, natural/forest, single-family residential, pervious pavement, and unpaved roads. Each block aggregates multiple infrastructure features including pipes, channels, culverts, roads, and ditches, providing a holistic spatial unit for performance evaluation. Blocks were designed to capture variability in hydraulic load, urbanization intensity, slope, and soil characteristics (Table 5.1). Each block then serves as an "alternative" for prioritizing maintenance or GI retrofitting in the TOPSIS framework.

Table 5.1 presents the quantitative characteristics of each delineated block, including area, average slope, dominant soil type, and estimated imperviousness, providing essential context for interpreting subsequent performance evaluations.

Table 5.1: Quantitative characteristics of the five delineated blocks within the study watershed

Block	Area (ha)	Average Slope (%)	Dominant Soil Type	Estimated Imperviousness (%)
1	6.5852	8.6	Vertisol (Silty Clay)	75.85
2	5.5558	9.3	Vertisol (Silty Clay)	78.26
3	6.6918	15	Vertisol (Silty Clay)	75.38
4	6.122	13.9	Vertisol (Silty Clay)	64.85
5	6.0018	11.7	Vertisol (Silty Clay)	61.94

5.2.3 Infrastructure Classification Framework

The classification of stormwater infrastructure was conducted using five key attributes including type of infrastructure, slope category, drainage function, construction material, and structural condition selected for their direct relevance to hydraulic performance, structural sustainability, and vulnerability to failure under urban watershed pressures. These attributes provided a systematic basis for evaluating performance heterogeneity and informed the subsequent application of the TOPSIS multi-criteria analysis.

Type of Infrastructure: Infrastructure components were categorized into five structural typologies: (1) concrete-lined channels and pipes, (2) unlined earth ditches, (3) culverts, (4) rain gardens, and (5) overland flow roads. These types represent a spectrum of design standards and hydrological functions. Concrete-lined channels offer high durability and flow capacity but limited infiltration; unlined ditches are cost-effective but prone to erosion. Culverts serve as key conduits at crossings, while overland flow roads convey excess flow along road gradients when pipe capacity is exceeded. Classification by type enables differentiation based on flow velocity, hydraulic resistance, and sediment dynamics.

Slope Category: All classified units were located on moderately steep terrain, specifically within a slope range of 7–15%. This slope threshold is hydrologically critical; at such gradients, flow acceleration increases runoff energy, elevating the risk of channel erosion, infrastructure failure, and downstream flooding. Incorporating slope as a classification parameter enables contextual interpretation of performance under topographically stressed conditions.

Drainage Function: Each infrastructure unit was functionally categorized by its hydraulic role in the watershed network. Primary units form the drainage backbone by conveying catchment-scale flows, while secondary units serve local areas as feeder systems. Overland flow roads act as emergency conveyance when pipe capacity is exceeded, directing excess stormwater along gradients to downstream structures. This distinction calibrates performance expectations based on hydraulic role, load requirements, and systemic importance.

Construction Material: Units were further classified based on dominant construction materials—concrete, vegetative (rain gardens), and soil-based. Material type influences not only structural durability and life-cycle maintenance but also functional performance characteristics such as infiltration capacity, erosion resistance, and response to sediment load. For instance, concrete provides structural resilience, while rain gardens support bioretention but may suffer clogging or require more frequent upkeep.

Structural Condition: The structural condition of the stormwater infrastructure was evaluated through systematic field inspections to document physical integrity and maintenance accessibility. Assessing structural condition in this manner provides critical insight into the ease of maintenance access and the relationship between physical deterioration and overall system performance within the multi-criteria evaluation framework.

Each infrastructure unit was georeferenced using GPS points, these GPS points were used to verify the generated high-resolution DEM in QGIS and used to support spatial visualization, performance comparison, and data validation. High-resolution photographs were also taken to document existing conditions. The classification framework not only supports the operationalization of the integrated TOPSIS-AHP-PCSWMM model by defining relevant evaluation dimensions but also ensures the analysis reflects real-world variability typical of rapidly urbanizing, data-scarce contexts like Addis Ababa.

5.2.4 Data Collection

A hybrid data collection strategy was adopted to enable a robust, multi-criteria performance evaluation of stormwater infrastructure within the 30-hectare study area. This approach addressed the lack of design and maintenance documentation through input from direct field observation, geospatial analysis, and hydrologic model using PCSWMM. Five of the six selected performance evaluation criteria—conveyance capacity, structural integrity, flood control effectiveness, sediment accumulation, and maintenance accessibility—were each informed by tailored data collection methods described below.

5.2.4.1 Field Assessment

Within each of the five blocks, 5–7 representative infrastructure features were selected for field inspection (total n = 30). The selection aimed to capture the dominant infrastructure typologies present in each block. For example, Block 3 (high-density residential) primarily featured roadside ditches and culverts, and the sample reflected this composition. The exact distribution was Block 1 (n = 6), Block 2 (n = 6), Block 3 (n = 7), Block 4 (n = 5), and Block 5 (n = 6).

Field data were collected by two independent experts using a standardized form developed in Kobo Toolbox, which enabled systematic recording of observations, GPS coordinates, and photographic documentation. Both experts visited each site together but conducted independent assessments to reduce subjectivity. Assessments were conducted within 48 hours following storm events to capture post-event conditions accurately, with observations spanning multiple storm events of varying intensities throughout the rainy season (August to September). Signs of ponding, overflow, and erosion were documented as part of the conveyance capacity (C_1) and erosion control (C_3) assessments. Scores from the two experts were averaged to produce final unit-level scores, and individual unit scores within each block were then averaged to produce block-level scores for each performance criterion. Two experts conducted independent field assessments to reduce subjectivity while maintaining logistical feasibility within the study budget and timeframe. Scores were averaged; inter-rater agreement was high (Cohen's $\kappa = 0.82$). This approach follows precedent in infrastructure assessment studies (Jemberie et al., 2023; Omidi Arjenaki et al., 2020).

The five criteria assessed through field observation were defined as follows:

Conveyance Capacity (C_1): Evaluated based on cross-sectional area relative to expected flow, visible flow obstructions (vegetation, debris), alignment with natural slope, and structural geometry. Field teams measured pipe diameters, channel widths and depths, and recorded signs of ponding or overflow during recent storm events. Visual proxies for hydraulic efficiency, such as uninterrupted flow paths, were documented.

Structural Integrity (C_2): The physical soundness of each unit was assessed by inspecting for cracks, material degradation, joint failure, undermining, and visible deformation. Concrete-lined channels and culverts were checked for spalling, reinforcement exposure, and joint separation.

Vegetated systems (naturally grassed channels) were examined for root integrity and signs of soil erosion around structures.

Erosion Control Effectiveness (C_3): Evaluated by observing the presence, quality, and continuity of erosion control features such as riprap linings, geotextile coverings, and vegetative buffers. Units were assessed for active signs of scouring, gullying, bank failure, or detachment of surface materials. The extent of protective coverage and its functionality under recent flow conditions were recorded.

Sediment Accumulation (C_4): Sediment deposition was measured using graduated rods and depth gauges. The extent (length and width) of accumulation was visually estimated and categorized as: <25%, 25–50%, or >50% of cross-sectional area blocked. The presence of organic matter and debris was also noted, especially at inlets and outlets. As a cost criterion, lower sediment accumulation received higher scores in the analysis (i.e., 1 = minimal buildup = best; 3 = heavy accumulation = worst).

Maintenance Accessibility (C_5): Accessibility was assessed based on physical access for routine inspection and maintenance. Units located in fenced, densely vegetated, or structurally confined areas were rated as poorly accessible, as such conditions impede timely maintenance even when keys or permissions exist—secured access requires coordination that can delay responses. The assessment considered approach routes, safety risks, and feasibility for different maintenance activities (e.g., manual cleaning vs. equipment-based dredging).

All field data were recorded and transferred to a geodatabase. Photographic documentation served as visual verification for later scoring in the multi-criteria decision analysis. A copy of the field form is provided in Appendix F, and photographic examples of condition ratings are included in Appendix Figure 1.

Field site access was granted by the Nefas Silk Lafto Sub-City Administration. No specific permits were required for the non-intrusive observational field assessments conducted in this study.

5.2.4.2 PCSWMM Hydrologic Modeling

To quantitatively assess flood control effectiveness, a hydrologic model was developed using PCSWMM. The model simulated runoff response for each infrastructure unit's contributing sub-catchment under historical and forecasted rainfall data for 2–year return periods. The 2–year return period was selected in line with the study's objective of identifying blocks that require either retrofitting with GI to establish IGGI or maintenance interventions. This approach is consistent with established practice in IGGI and low-impact development (LID) studies, where measures are primarily designed to manage frequent, low-intensity storms rather than rare extreme events. Numerous peer-reviewed studies have similarly adopted the 2-year storm as a benchmark for assessing IGGI effectiveness (e.g., (Adhikari et al., 2024; Chen et al., 2023; Martínez et al., 2021; Y. Yu et al., 2023; Zahmatkesh et al., 2015). Key input parameters included:

Topographic Data: A high-resolution 1×1 m Digital Elevation Model (DEM) was generated in QGIS using GPS-based point elevation data extracted via GPS Visualizer (Hussain, 2020). This 1 m resolution DEM was verified using GPS measurements collected during field surveys and used to delineate catchment boundaries, slope gradients, and overland flow paths essential for hydrologic routing in PCSWMM.

Soil type: Soil data were sourced from the Ministry of Water and Energy's soil map of Addis Ababa (2004), as previously utilized in Feyissa et al., (2018), and Kemal et al., (2025). Prior study by Srivastava et al., (1989) and the Food and Agriculture Organization of the United Nations (FAO) world soil map identified Pellic Vertisols as the dominant soil type, characterized by poor infiltration due to >50% clay content (Berhanu, 1983). According to the USDA soil texture classification, the dominant texture is silty clay (Kemal et al., 2025). Infiltration parameters for the modified Green-Ampt method—namely suction head, saturated hydraulic conductivity, and initial moisture deficit—were collected from Rossman A., (2015) in the PCSWMM manual for Vertisol (silty clay) conditions.

Land Use and Imperviousness: Land use classification was performed using PCSWMM-integrated Bing satellite imagery, Google Earth visual inspections, and field validation. Seven categories were identified: asphalt pavement, commercial, single-family residential, multi-family residential, forested/natural, cobble stone pavement, and unpaved roads. Imperviousness estimates were assigned accordingly.

Rainfall and Climate Data: Historical climate data (1983–2024) were obtained from Ethiopia's National Meteorological Agency (NMA) (NMA, 2024). Future projections were derived from 12 precipitation and 16 temperature (maximum/minimum) General Circulation Models (GCMs) under the Coupled Model Intercomparison Project Phase 6 (CMIP6), bias-corrected and downscaled using the bias correction constructed analogues with quantile mapping reordering method (Rettie et al., 2023). The downscaling was applied to a 10 km resolution using a 5 km gridded dataset (1983–2012) for bias correction. A perfect sibling framework confirmed improved correlation, reduced bias, and lower root mean square error (RMSE). Further validation was performed using observed data (1983–2014) from the Ayertena station, selected based on Thiessen polygon analysis for its consistent long-term records. Evaluation metrics included Pearson's correlation coefficient, RMSE, Nash–Sutcliffe efficiency (NSE), percent bias (PBIAS), and Kling–Gupta efficiency (KGE). Based on performance, five precipitation, four maximum temperature, and three minimum temperature GCMs were selected and ensembled using a weighted average under two Shared Socio-economic Pathway (SSP) scenarios: SSP2-4.5 (middle-of-the-road emissions scenario) and SSP5-8.5 (high emissions scenario). Outliers in historical data were corrected, and missing values imputed using the normal ratio method (Kemal and Adeba, 2021). Due to limited access to high-resolution data in developing countries like Ethiopia, daily rainfall records are often used to develop Intensity–Duration–Frequency (IDF) curves, which are then disaggregated into sub-daily and hourly intervals (Ewea et al., 2018; Krvavica and Rubinić, 2020). For this study, daily rainfall data from the Ayertena station (1994–2023) were used to develop baseline IDF curves. Future projections were processed for near-term (2024–2053) and mid-term (2054–2083) periods, and extreme precipitation values were disaggregated into sub-daily durations for analysis.

IDF Curve Development: IDF curves were developed using the Indian Meteorological Department (IMD) method as recommended by Bibi et al., (2023) and Ashok Kumar et al., (2023), which has been widely applied in tropical climates (Al Mamun et al., 2018; R. Palaka, 2016). Maximum daily rainfall (P_{24}) was disaggregated into sub-daily durations using eq. 5.1:

$$P_t = P_{24} * \left(\frac{t}{24}\right)^{1/3} \tag{5.1}$$

where P_t (mm) is the rainfall depth for duration t (hours), and P_{24} is the maximum daily rainfall. Several probability distributions were initially considered for modeling extreme rainfall, including the Generalized Extreme Value (GEV), Log-Pearson III, and Gumbel distributions. Based on goodness-of-fit assessments using Kolmogorov–Smirnov, Anderson–Darling, and Chi-square tests, the Gumbel distribution was selected, as it provided the best overall fit for the data and is widely used for hydrological design in tropical regions. Rainfall depths for various return periods were then estimated using eq. 5.2:

$$P_T = P_{ave} + KS \tag{5.2}$$

where:

$P_{ave} = \frac{1}{n}\sum_{i=1}^{n} P_{ti}$, is the mean of value for different rainfall durations,

$K = \frac{\sqrt{2}}{\pi} + \left[0.5772 + \ln\left[ln\left[\frac{T}{(T-1)}\right]\right]\right]$, is the frequency factor, and

$S = \sqrt{\left[\frac{1}{n-1}\sum_{i=1}^{n}(P_{ti} - P_{ave})^2\right]}$, is the standard deviation.

P_{ti} represents rainfall for different durations, n is the number of years, and T denotes the return period of 2-years.

The resulting rainfall intensities (in mm/hr.) were calculated by dividing P_T by the corresponding duration. These values were used to develop the IDF curves and subsequently integrated into the PCSWMM model.

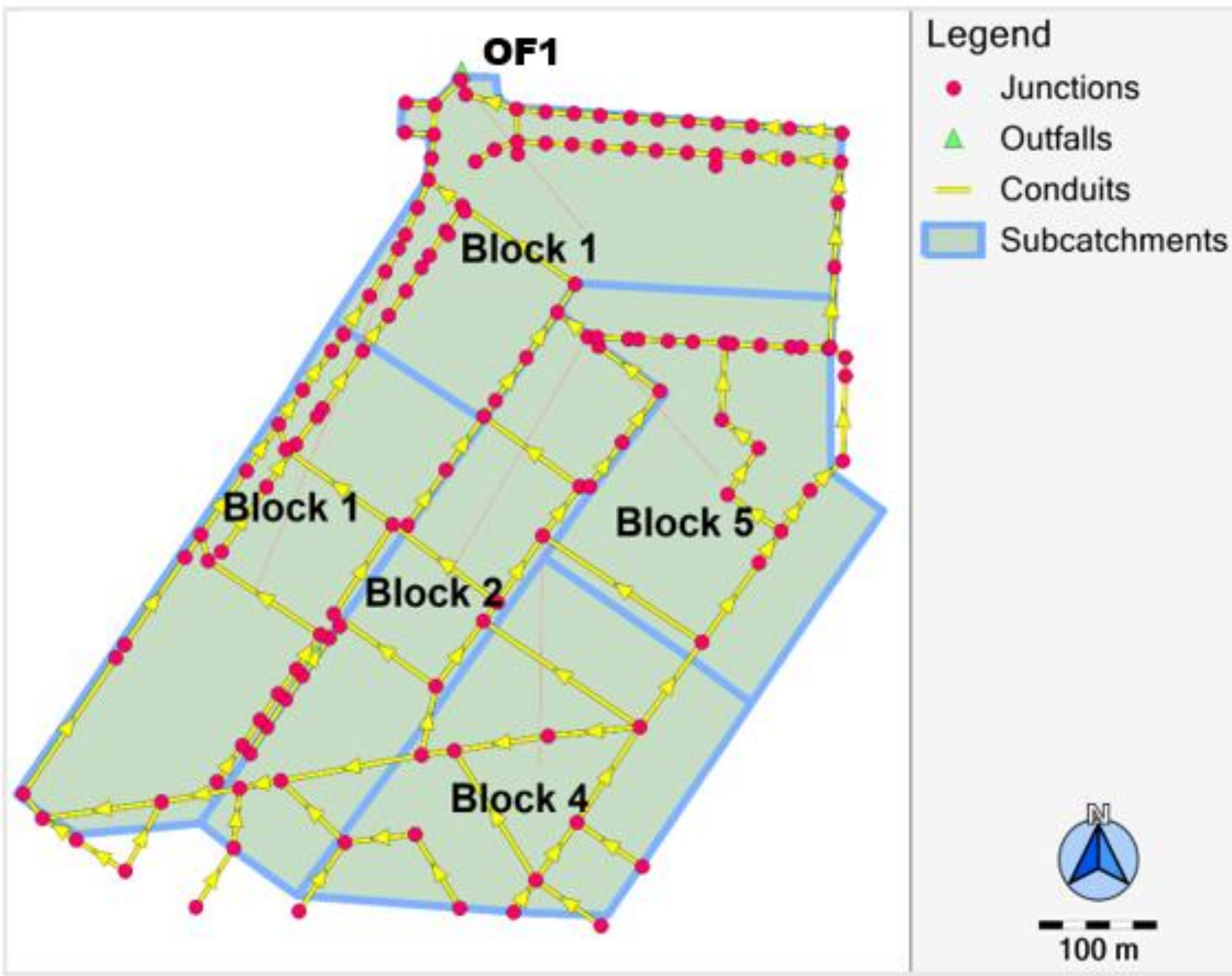

Figure 5.2: Stormwater infrastructure network in the study watershed. All data layers (stormwater network, manholes, outfalls, and sub-catchments) are original data collected by the authors through field surveys and GPS mapping, digitized in PCSWMM and QGIS (QGIS 3.40.4), and presented under CC BY 4.0

Hydraulic Configuration: PCSWMM 7.7.3910 was applied to develop, calibrate, and validate the stormwater management model. In the absence of organized municipal data, the hydraulic network was defined from field surveys, specifying conduit dimensions, slopes, Manning's *n*, and junction capacities. Elevation data were used to determine hydraulic gradients and flow patterns, while rainfall, outfalls, and inflows served as boundary conditions. The network included 5 blocks i.e., sub-catchments, 142 junctions, and 150 conduits (pipes, open channels, and roads) (Fig. 5.2). Key parameters—such as invert and rim elevations, conduit layouts, and junction coordinates—were obtained from field measurements, Google Earth Pro, and PCSWMM's Bing satellite imagery. Calibration and validation were conducted using independent datasets spanning from August to September (see Table 5.2) to ensure robustness.

Outfall Monitoring for Model Validation: To support model calibration and validation, runoff depth at Outfall 1 (OF1) presented in Fig.3 was monitored during four storm events in 2024 (Table 5.2). Monitoring periods were selected to capture peak flow dynamics despite limitations in data availability and budget constraints.

Table 5.2: Summary of storm events used for model calibration and validation

Event Purpose	Date (2024)	Storm Duration (minutes)	Monitoring Duration (minutes)	Recording Interval
Calibration 1	August 12	300	115	5-min
Validation 1	August 23	105	75	5-min
Calibration 2	September 2	360	110	5-min
Validation 2	September 23	75	60	5-min

Runoff depth was measured using a staff gauge installed at the outfall, with readings recorded at 5-minute intervals during peak flow periods. Outfall OF1 is a rectangular concrete channel (width 2.2 m, depth 2.4 m). The observed runoff depths were directly used in the Sensitivity-based Radio Tuning Calibration (SRTC) feature of PCSWMM for model calibration and validation, as PCSWMM enables direct calibration using flow depth. Rainfall and temperature data used for calibrating the PCSWMM model simulations were obtained for the same dates as the monitored events. The observed runoff depths were then compared with the corresponding PCSWMM-simulated values for these events.

5.2.4.3 Data Integration and Processing

All collected data—field-based observations, PCSWMM model outputs (using Bing satellite imagery), and Google Earth Pro assessments—were spatially referenced and analyzed to ensure alignment with the actual watershed context. Performance attributes from field assessments and hydrological modeling were normalized and structured into a decision matrix for use in the TOPSIS evaluation framework. This approach ensured that infrastructure performance was assessed comprehensively, considering both structural/visual conditions and hydraulic effectiveness.

5.2.5 Performance Criteria

Stormwater infrastructure units were evaluated against six carefully selected criteria that capture hydraulic functionality and sustainability under urban watershed stressors. These criteria were chosen based on expert consultation, and practical relevance for assessing aging infrastructure in data-limited urban settings as presented in Table 5.3:

Table 5.3: List of criterions, their descriptions and types

Code	Criterion	Description	Type
C_1	Flood conveyance capacity	The infrastructure's ability to transport stormwater without overtopping, backflow, or localized ponding under design flow conditions.	Benefit
C_2	Structural integrity	Physical condition of the unit, including presence of cracks, joint separation, collapse, or surface degradation.	Benefit
C_3	Erosion control effectiveness	Presence and condition of erosion control measures such as lining, and vegetative cover and their effectiveness in minimizing scouring.	Benefit
C_4	Sediment accumulation	Extent of sediment, organic debris, and anthropogenic waste obstructing flow paths and reducing hydraulic efficiency.	Cost
C_5	Maintenance Accessibility	Observed ease of access for maintenance, frequency of upkeep, and physical barriers affecting serviceability.	Benefit
C_6	Flood control effectiveness (PCSWMM model)	The infrastructure's capacity to attenuate peak flows, reduce flood depth and extent, and protect adjacent properties from inundation.	Benefit

Each infrastructure unit was assessed through structured field surveys conducted by two independent evaluators with expertise in urban hydrology and drainage engineering using Kobo Toolbox. A three-point ordinal scale was applied to each criterion, enabling standardized scoring while preserving interpretability:

Good (3): Fully meets or exceeds expected performance standards; no immediate issues detected.

Fair (2): Partially meets expectations; minor deficiencies observed that may require monitoring or light maintenance.

Poor (1): Falls short of functional requirements; significant damage or obstruction requiring urgent intervention.

For the cost-type criterion (C_4 – Sediment accumulation), scoring was inversely interpreted, where lower sediment levels received higher scores to maintain consistency in the benefit-oriented evaluation framework.

Scores from each evaluator were averaged to reduce subjectivity, and supporting photographic evidence was archived to validate observations and facilitate future monitoring. This approach ensured that field data collection was both systematic and suitable for integration into the multi-criteria decision analysis using TOPSIS.

5.2.6 Data Analysis: TOPSIS-AHP-PCSWMM

To synthesize multi-criteria field, hydrological and expert based data into a replicable performance ranking, this study employed the integrated TOPSIS-AHP. TOPSIS and AHP is a widely adopted method within the MCDA family, particularly valued for their conceptual simplicity, computational efficiency, and robustness in prioritization problems involving both benefit and cost criteria (Behzadian et al., 2012; Hwang and Yoon, 1981; K. Paul Yoon, 1995; Luan et al., 2019).

MCDA approaches such as ANP, MAUT, PROMETHEE, and ELECTRE differ in how they assign and aggregate decision values, yet they share foundational mathematical principles (Huang et al., 2011). TOPSIS has demonstrated strong applicability in environmental and water resource management due to its ability to incorporate expert-based weights, maintain cardinal ranking, and tolerate non-linear trade-offs (Behzadian et al., 2012; Gogate et al., 2017; Luan et al., 2019). Moreover, it does not require independence among evaluation criteria, an advantage in complex hydrological systems (Huang et al., 2011; Luan et al., 2019; Yatsalo et al., 2007).

Decision Matrix Construction: In this study, TOPSIS-AHP was applied to five spatial blocks delineated within the 30-hectare study area, each serving as an aggregated analysis unit that encapsulates multiple stormwater infrastructure features. These alternatives (i = 1, 2, ...,5) were evaluated against six criteria (j = 1, 2, ..., 6) representing stormwater infrastructure performance: flood conveyance capacity (C_1), structural integrity (C_2), erosion control effectiveness (C_3), sediment accumulation (C_4), maintenance accessibility (C_5), and flood control effectiveness (C_6, based on PCSWMM modeling).

The initial decision matrix is expressed as:

$$X = [x_{ij}]\, m \times n = \begin{bmatrix} x_{11} & x_{12} & \cdots & x_{1n} \\ x_{21} & x_{22} & \dots & x_{2n} \\ \vdots & \vdots & \ddots & \vdots \\ x_{m1} & x_{m2} & \cdots & x_{mn} \end{bmatrix}$$

where x_{ij} denotes the average performance score of blocks i under criterion j, either from field assessment or PCSWMM simulation.

Normalization of the Decision Matrix: To eliminate scale discrepancies across criteria and to standardize the matrix, vector normalization was applied using eq. 5.3:

$$r_{ij} = \frac{x_{ij}}{\left(\sqrt{\sum_{i=1}^{m} x_{ij}^2}\right)} \quad \forall i = 1, \dots, m; j = 1, \dots, n \qquad 5.3$$

This transformation yields the normalized matrix R = [r_{ij}], where each r_{ij} lies in the range [0, 1].

Weight Assignment: The relative importance of each criterion was determined through a dedicated expert elicitation process involving 12 practitioners, researchers, and academicians specializing in hydraulics, hydrology, and environmental engineering. Each expert conducted pairwise comparisons of the six evaluation criteria in accordance with the AHP framework, originally developed by (Saaty, 1980, 2008). This structured decision-making method systematically translates subjective expert judgments into a quantitative scale, facilitating the derivation of consistent and comparable weights. The chosen sample size is consistent with established practices in similar studies (Alotaibi and Anzah, 2023; Amjad et al., 2024; Asefa et al., 2021; Hisoglu et al., 2023; Kemal et al., 2025; Marzuki et al., 2023).

Ethical Considerations for Expert Participation: For the expert elicitation process involving 12 professionals who performed pairwise comparisons for the AHP, informed consent was obtained from all participants. Prior to data collection, each expert was provided with a detailed information sheet explaining the study objectives, the nature of their participation, how their data would be used, and their right to withdraw at any time without consequence. Verbal informed consent was obtained from each expert, and this consent was documented in two ways: (1) the lead investigator maintained a signed log sheet confirming each expert's agreement to participate, and (2) the date and time of consent were recorded for each participant. Experts were informed that their responses would be aggregated and anonymized in any publications, with no individual identifiers disclosed. The study procedures were reviewed and approved by the School of Civil and Environmental Engineering, Addis Ababa University, which confirmed that formal ethics committee approval was not required for this non-interventional expert consultation, provided that standard informed consent procedures were followed. All experts participated voluntarily and consented to the use of their aggregated judgments for research purposes.

The pairwise comparison process required each expert to evaluate the relative importance of one criterion over another using Saaty's fundamental 1–9 scale, where 1 indicates equal importance and 9 denotes extreme importance of one criterion over the other. Intermediate values (2, 4, 6, 8) allowed for finer distinctions. These judgments were arranged into a reciprocal comparison matrix $A = [a_{ij}]$, where aij represents the relative importance of criterion i over criterion j, and $a_{ji} = 1/a_{ij}$. From each comparison matrix, a priority vector (eigenvector) was computed by normalizing the principal eigenvector associated with the maximum eigenvalue λmax. This vector represents the relative weights of the criteria, expressed as:

w = [w1, w2, w3, w4, w5, w6] subject to the normalization condition in eq. 5.4:

$$\sum_{j=1}^{6} w_j = 1 \qquad 5.4$$

To ensure logical consistency in the expert judgments, the consistency index (CI) and consistency ratio (CR) were calculated using eq. 5.5 and eq. 5.6 respectively:

$$CI = \frac{\lambda\text{max}-1}{n-1} \qquad 5.5$$

$$CR = \frac{CI}{RI} \qquad 5.6$$

where n is the number of criteria (here, n = 6) and RI is the random index for a matrix of order n (Saaty, 2008). A CR value of 0.1 or less was considered acceptable; matrices exceeding this threshold were reviewed and adjusted to improve consistency before inclusion in the final aggregation.

The geometric mean was used because AHP operates on a ratio scale, and this method preserves the reciprocal consistency of pairwise comparisons while ensuring a balanced aggregation of expert judgments. It is the standard and recommended approach for group decision-making in AHP

(Saaty and Vargas, 2012) and is widely adopted in related MCDA studies. These weights were subsequently used to weight the normalized decision matrix.

Positive- and Negative-ideal Solutions: From the normalized weighted matrix the positive ideal solution (A^+) and negative ideal solution (A^-) were defined by selecting the best and worst values across all alternatives using eq. 5.7, and eq. 5.8:

For benefit criteria (C_1, C_2, C_3, C_5, C_6):

$$v_j^+ = \max_i v_{ij},\ if\ j\ \in \text{benefit criteria},\ v_j^+ = \min_i v_{ij} \qquad 5.7$$

For the cost criterion (C_4 – sediment accumulation):

$$v_j^- = \min_i v_{ij},\ if\ j\ \in \text{benefit criteria},\ v_j^- = \max_i v_{ij} \qquad 5.8$$

These two solution vectors defined the theoretical performance bounds for evaluating all alternatives.

Separation Measures: To quantify each alternative's proximity to the ideal and negative-ideal solutions, weighted Euclidean distances were calculated using eq. 5.9:

$$S_i^+ = \sqrt{\sum_{j=1}^n \left(v_{ij} - v_j^+\right)^2},\ S_i^- = \sqrt{\sum_{j=1}^n \left(v_{ij} - v_j^-\right)^2} \qquad 5.9$$

where S_i^+ and S_i^- represent the distances of alternative i to the ideal and anti-ideal solutions, respectively.

Relative Closeness and Ranking: The relative closeness C_i of each block to the ideal solution was computed as (eq. 5.10):

$$C_i = \frac{S_i^-}{S_i^+ + S_i^-},\ 0 \le C_i \le 1 \qquad 5.10$$

A higher C_i value indicates better performance across all criteria. The infrastructure units were subsequently ranked in descending order of C_i to prioritize maintenance or GI retrofitting needs. Classification of alternatives was derived from the statistical properties of the closeness coefficients. Specifically, alternatives were grouped into four tiers based on their relative position to the dataset's mean and standard deviation of scores:

Class I (High): $C_i \ge \bar{C}_i + S_{Ci}$

Class II: $\bar{C}_i \le C_i < \bar{C}_i + S_{ci}$

Class III: $\bar{C}_i - S_{Ci} \le C_i < \bar{C}_i$

Class IV (Low): $C_i < \bar{C}_i - S_{Ci}$

This method offers a transparent and adaptive basis for prioritizing interventions informed by peer-reviewed precedent (Hajduk and Jelonek, 2021). This enhanced formulation preserves technical rigor and interpretability, drawing on leading MCDA literature (Behzadian et al., 2012; Gogate et al., 2017; Huang et al., 2011; Hwang and Yoon, 1981; Linkov et al., 2006) while embedding the method transparently within the hydrological evaluation framework of the study.

5.2.7 Performance Metrics and Study Framework

PCSWMM Model Performance: The model was evaluated using Nash–Sutcliffe efficiency (NSE), root mean square error (RMSE), RMSE–standard deviation ratio (RSR), and integrated squared error (ISE). NSE (Eq. 5.11) assessed the agreement between observed and simulated flows, RMSE (Eq. 5.12) quantified average error magnitude, RSR (Eq. 5.13) normalized RMSE to observation variability, and ISE (Eq. 5.14) measured cumulative squared error. Rating thresholds followed established hydrologic modeling criteria (Table 5.4)

Table 5.4: Performance rating criteria for model evaluation metrics

Metric	Formula	Rating Criteria	Equation
NSE	$\mathrm{NSE} = 1 - \left(\frac{\left(\left(\sum_{i=1}^{n}(Y_{obs}^{i} - Y_{sim}^{i}\right)^2\right)}{\left(\sum_{i=1}^{n}(Y_{obs}^{i} - Y_{obs}^{mean}\right)^2}\right)$	Good: ≥ 0.8 Satisfactory: ≥ 0.6 Unsatisfactory: < 0.60	5.11
RMSE	$\mathrm{RMSE} = \frac{\sqrt{\sum_{i=1}^{n}(Y_{obs}^{i} - Y_{sim}^{i})^2}}{n}$	Very Good: < 0.5σ Good: < 0.6σ Satisfactory: < 0.7σ	5.12
RSR	$\mathrm{RSR} = \frac{\mathrm{RMSE}}{\mathrm{STDEVA_{obs}}}$	Very Good: RSR ≤ 0.5 Good: 0.5 < RSR ≤ 0.6 Satisfactory: 0.6 < RSR ≤ 0.7	5.13
ISE	$\mathrm{ISE} = \frac{\sum_{i=1}^{n}\left(Y_{obs}^{i} - Y_{sim}^{i}\right)^2}{\sum Y_{obs}^{i}} \mathrm{x}100\%$	Excellent: < 3 Very Good: 3–6 Good: 6–10 Fair: 10–25 Poor: > 25	5.14

where: STDEVAobs = standard deviation of observed value; Y_{obs}^{i} = observed value; Y_{sim}^{i} = simulated value; $\overline{Y}_{obs}$ = mean of observed values; $\sigma = \mathrm{STDEVA_{obs}}$

Sensitivity Analysis: To verify the robustness of the TOPSIS-AHP-PCSWMM-based performance rankings against subjectivity inherent in expert-derived weighting, a sensitivity analysis was conducted. In Multi Criteria Decision Making (MCDM), particularly under data-scarce or uncertain conditions, such an analysis is critical to ensure the credibility and reproducibility of prioritization outcomes. A set of alternative weighting scenarios was developed to reflect different stakeholder perspectives and planning priorities. These included: (i) the baseline expert-informed weighting scheme, (ii) a uniform weighting scenario assigning equal importance to all six performance criteria, and individual scenarios emphasizing one dominant criterion at a time such as (iii) flood conveyance capacity, (iv) structural integrity, and (v) sediment control. Each alternative weight vector was applied to the normalized decision matrix, and the full TOPSIS algorithm was re-executed to compute updated relative closeness coefficients C_i for the five spatial blocks.

To assess the consistency of block rankings across the different scenarios, Spearman's rank correlation coefficient (ρ) was calculated between the baseline ranking and each alternative. This non-parametric statistic quantifies the strength and direction of the monotonic relationship between two rank orders and is defined as (Eq. 5.15):

$$\rho = 1 - \frac{\left(6\sum_{i=1}^{n} d_i^2\right)}{n(n^2-1)} \qquad 5.15$$

where: d_i is the difference in the rank of block i between the baseline and an alternative scenario, n is the number of alternatives (here, n = 5).

Values of ρ approaching +1 indicate strong agreement between rankings, signifying model robustness against weighting variation, while lower values suggest potential ranking instability.

Furthermore, blocks that consistently appeared in the top or bottom ranks across all scenarios were flagged as high-confidence targets for immediate maintenance or retrofit planning. This dual-mode sensitivity check—quantitative (via ρ) and qualitative (via rank consistency)—ensures the performance evaluation framework remains methodologically sound, transparent, and resilient to variations in expert judgment. In conclusion, the sensitivity analysis confirms the reliability of the TOPSIS-AHP-PCSWMM-based infrastructure performance ranking and enhances the decision-making framework's adaptability for guiding urban stormwater infrastructure investments, particularly in contexts lacking design documentation or comprehensive maintenance records.

Conceptual Framework of the Study: This study integrates hydrologic modeling and multi-criteria decision analysis to evaluate the performance of existing stormwater infrastructure across five representative urban blocks (totaling 30-hectares) as presented in Fig. 5.3. Data collection encompassed soil, climate, land use, and hydraulic configuration parameters, which were integrated into PCSWMM to model flood control effectiveness. Concurrently, field assessments conducted via Kobo Toolbox evaluated five key performance criteria: conveyance capacity, structural integrity, erosion control effectiveness, sediment accumulation, and maintenance accessibility. Expert judgments for criterion prioritization were also collected through Kobo Toolbox using the AHP framework. All six performance indicators feed into the TOPSIS model, which computes a relative closeness score to the ideal solution for each block. This classification informs evidence-based decisions for maintenance prioritization and suitability for GI-based retrofitting.

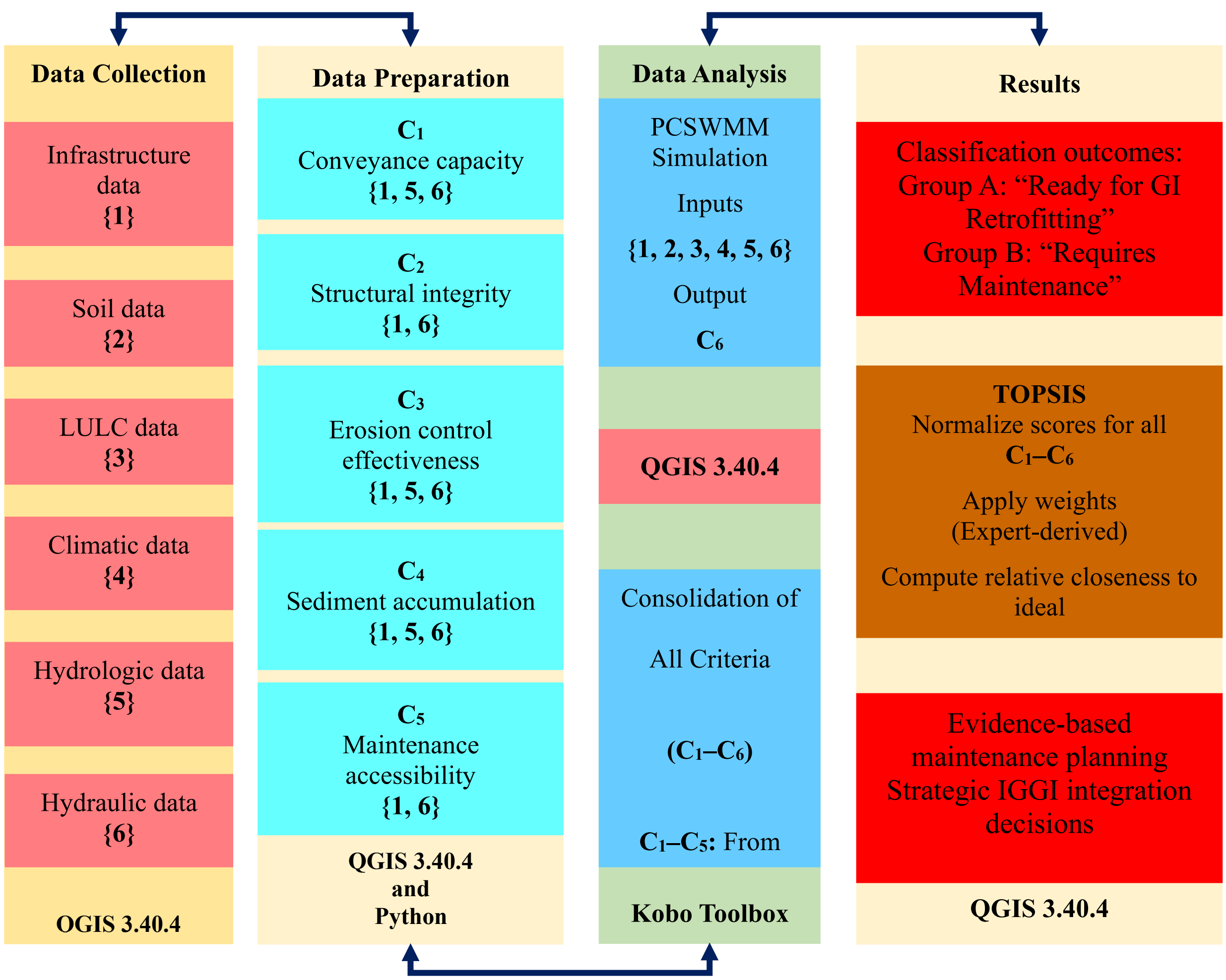

Figure 5.3: Conceptual framework designed for this study

5.3 Results

5.3.1 IDF Curve Analysis and PCSWMM Performance Evaluation

IDF Curve Result: The IDF curve developed (Fig. 5.4) from 30-years of historical and 60-years of forecasted rainfall data for a 2-year return period exhibited the expected inverse relationship between rainfall intensity and duration, with higher intensities corresponding to shorter storm durations. These curves were integrated into the PCSWMM model to evaluate infrastructure performance under frequently occurring storm conditions. Their use ensured that simulations reflected realistic rainfall patterns, supporting accurate assessment of stormwater conveyance capacity and identifying potential vulnerabilities in the system under short-return-period events for historical and forecasted scenarios.

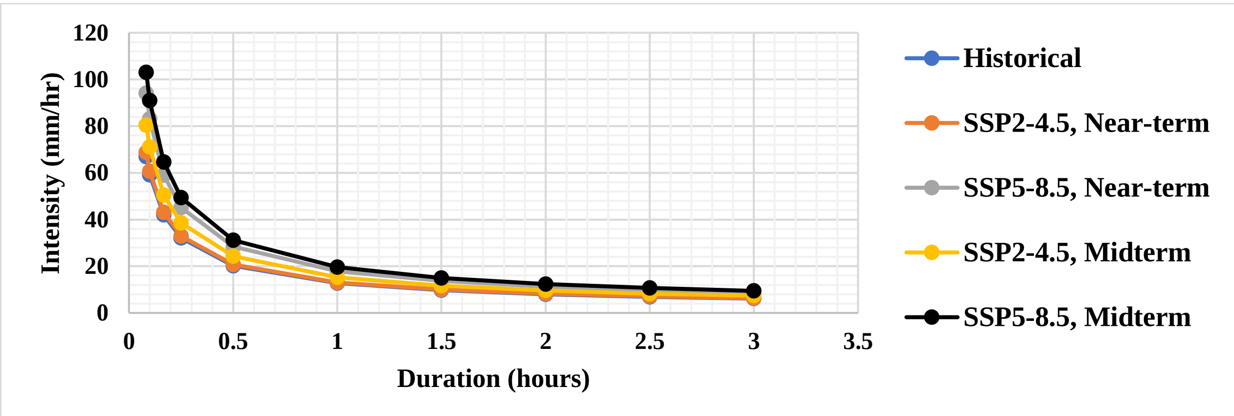

Figure 5.4: IDF curve developed using 30-years of historical (1994–2023) and 60-years of projected rainfall data under SSP2-4.5 (middle-of-the-road emissions) and SSP5-8.5 (high emissions) scenarios for near-term (2024–2053) and mid-term (2054–2083) periods, based on ensembled CMIP6 outputs for a 2-year return period. The curve was used as input for PCSWMM simulations

Performance Evaluation Result: The model performance evaluation showed that key metrics—NSE, RMSE, ISE, and RSR—fell within acceptable thresholds, indicating a strong agreement between observed and simulated runoff values. As shown in Figs. 5.5 and 5.6, the model accurately reproduced runoff depths at the monitored location OF1 (see section 5.2.4.2) during the specified storm events. These results confirmed the reliability of the model in simulating the hydrologic component of the stormwater system. Following calibration using the SRTC (Sensitivity-based Radio Tuning Calibration) tool, the final Manning's roughness values ranged from 0.011 to 0.016 for conduits and 0.01 to 0.06 for surface types (pervious and impervious areas). Imperviousness values across the 25 sub-catchments ranged from 32% to 98%, with an area-weighted average of 70.1%. Conduit geometry adjustments were limited to approximately 15% of the network, primarily affecting channel width and depth where field observations indicated underperformance. Detailed calibration parameter tables for all sub-catchments and conduits are available from the author upon request.

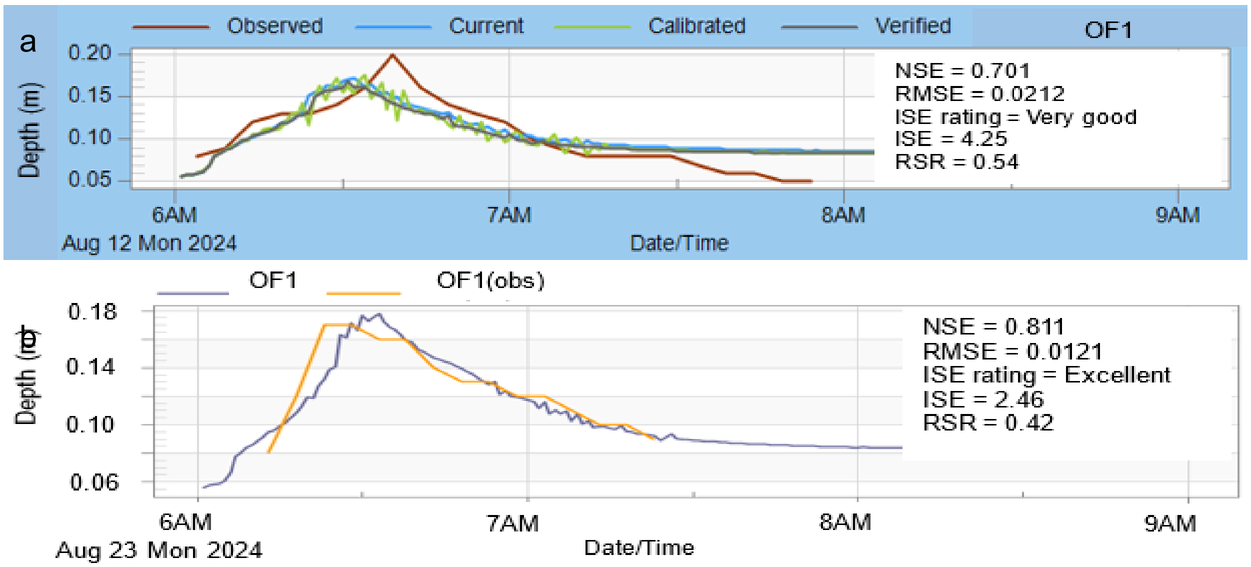

Figure 5.5: Performance evaluation metrics—NSE, RMSE, ISE, and RSR—for model calibration and validation. Results shown for Calibration 1 (August 12, 2024) and Validation 1 (August 23, 2024). Observed runoff depths (see Section 5.2.4.2 for measurement details) were directly used in PCSWMM's SRTC calibration and validation

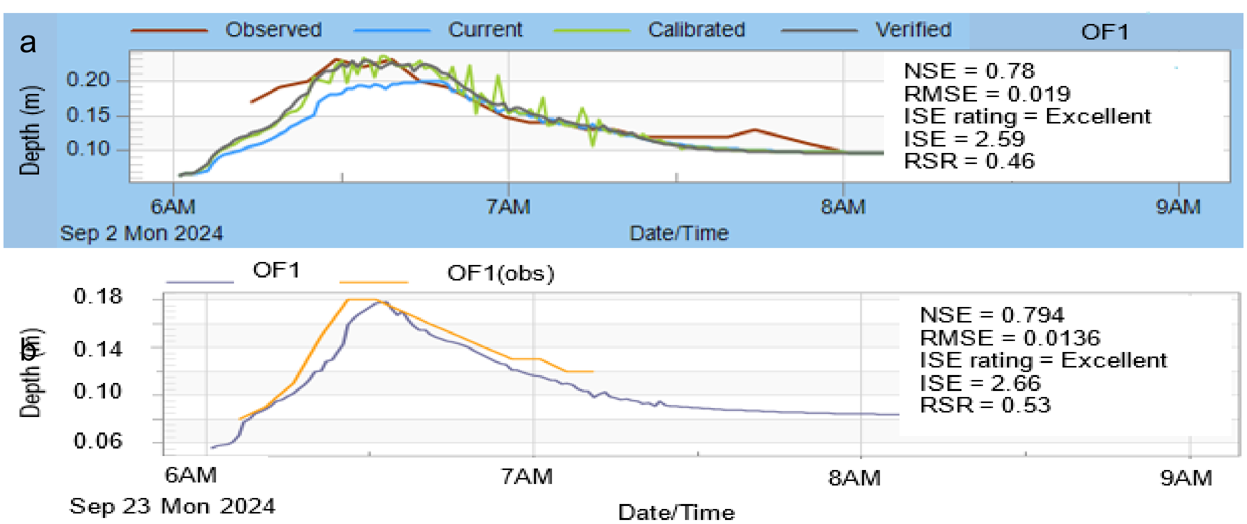

Figure 5.6: Performance evaluation metrics—NSE, RMSE, ISE, and RSR—for model calibration and validation. Results shown for Calibration 2 (September 2, 2024) and Validation 2 (September

23, 2024). Observed runoff depths (see Section 5.2.4.2 for measurement details) were directly used in PCSWMM's SRTC calibration and validation

5.3.2 Field Assessment and Block-level Aggregation

Within part of the 30-hectare micro-watershed shown in Fig. 5.2, five spatial blocks (Blocks 1–5) were delineated based on terrain slope, land use, and soil characteristics (Table 5.1). In each block, representative drainage infrastructure features were evaluated (total n = 30; exact distribution: Block 1: 6, Block 2: 6, Block 3: 7, Block 4: 5, Block 5: 6). Data were collected by two experts using a Kobo Toolbox field form (Appendix F) and then averaged at the block level for each performance criterion. Detailed unit-level scores are provided in appendix Table 11. The aggregated block-level scores are presented in appendix Table 8.

Conveyance Capacity (C_1): Conveyance capacity exhibited clear spatial differentiation. Blocks 3 and 5 recorded the highest average score (3), reflecting efficient flow conditions supported by relatively well-structured drainage layouts. Blocks 1 and 2 followed with scores of 2.67, suggesting moderate conveyance performance. Block 4 showed the lowest rating (2), attributed to narrower, partially vegetated channels that limit stormwater flow.

Structural Integrity (C_2): Structural integrity varied across the blocks. Blocks 3 and 5 achieved the highest score (3), indicating robust infrastructure with minimal signs of physical degradation. Block 1 followed with a score of 2.5. Block 2 scored moderately at 2.17. In contrast, Block 4 had the lowest integrity score (1), attributed to visible cracking, erosion, and undermined structures observed during field inspections.

Erosion Control Effectiveness (C_3): Erosion control effectiveness demonstrated notable variation. Block 3 achieved the highest score (3), reflecting well-established measures such as stabilized slopes and effective vegetation cover. Block 5 followed with a score of 2.5, indicating generally effective erosion management despite localized vulnerabilities. Blocks 1 and 2 both scored 2, suggesting moderate control with intermittent signs of soil disturbance. Block 4 received the lowest rating (1.83), corresponding with observed signs of active erosion.

Sediment Accumulation (C_4): Sediment accumulation was rated as a cost criterion, meaning lower scores indicate better condition (less blockage) and higher scores indicate worse condition (more blockage). Block 3 exhibited the best condition with a score of 1, indicating minimal sediment buildup. Block 5 followed with a score of 1.67, reflecting moderate sediment presence. Blocks 1 and 2 both scored 2, indicating moderate sediment accumulation. Block 4 exhibited the poorest condition with the highest score of 2.17, reflecting the greatest sediment accumulation among all blocks.

Maintenance Accessibility (C_5): Maintenance accessibility scores varied across blocks. Blocks 3, 4, and 5 each received the highest score of 3, indicating relatively easier physical access for maintenance personnel and equipment. Block 1 followed with a score of 2.83, reflecting moderate accessibility with some limitations. Block 2 also scored 2.83, but its lower effective accessibility results from dense vegetation and structural obstructions that impede routine inspection and repair.

5.3.3 Hydrologic Modeling for Flood Control (Criterion C_6)

PCSWMM simulations were conducted for each block's catchment under a 2-year return period storm to assess flood control effectiveness, represented by Criterion C_6. Two key hydrologic metrics were analyzed: peak discharge (m^3/s) and total runoff volume (m^3). To ensure fair comparison across blocks of different sizes, these values were normalized by the respective block areas (in hectares), allowing evaluation of flood control effectiveness per unit area as in Fig. 5.7.

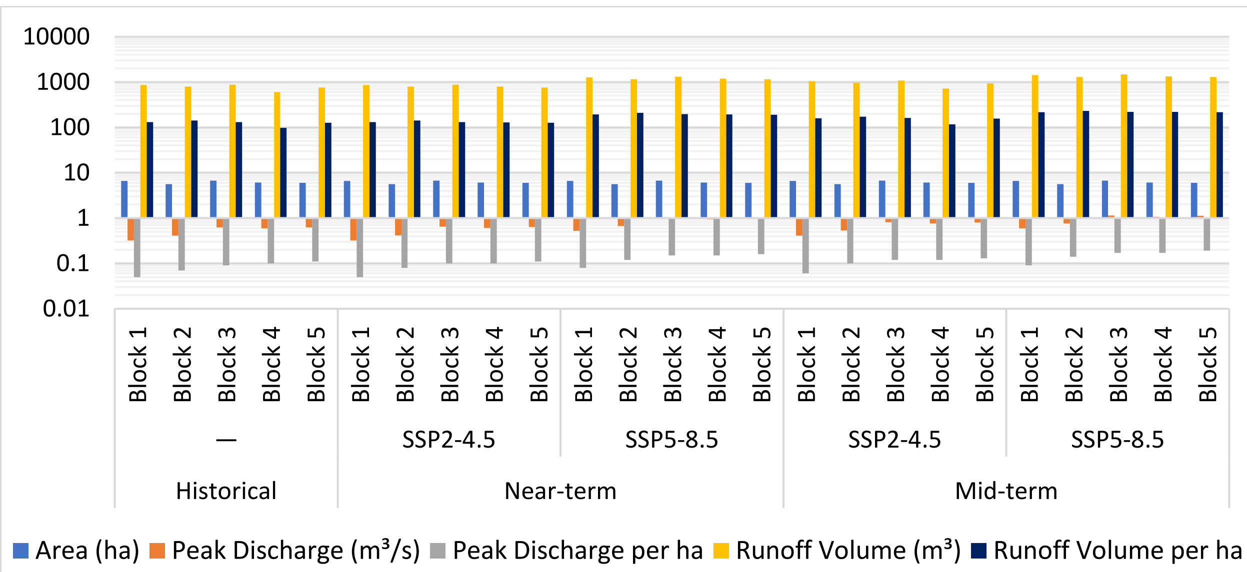

Figure 5.7: Consolidated multi-panel figure showing peak discharge per hectare ($m^3/s/ha$) and runoff volume per hectare (m^3/ha) on logarithmic scales for all five blocks: (a) Block 1, (b) Block 2, (c) Block 3, (d) Block 4, (e) Block 5. Results are shown for historical (1994–2023), near-term (2024–2053) under SSP2-4.5 (middle-of-the-road emissions), and mid-term (2054–2083) under SSP5-8.5 (high emissions) scenarios, all for a 2-year return period. Logarithmic scaling allows meaningful visualization of both metrics despite their different magnitudes

Flood control effectiveness was assessed using two key hydrologic indicators from PCSWMM simulations for a 2-year return period of historical: peak discharge per hectare and runoff volume per hectare. Peak discharge reflects the system's ability to attenuate high-intensity storm events, while runoff volume represents the infrastructure's capacity to retain or infiltrate total rainfall input. Together, these parameters provide a comprehensive measure of performance under stormwater stress conditions. All blocks were ranked accordingly, and results were cross validated with field observations of existing infrastructure.

Block 4 demonstrated the most effective performance, exhibiting the lowest runoff volume (98 m^3/ha) despite a relatively high peak discharge (0.098 $m^3/s/ha$), likely due to localized retention or infiltration features. Block 1 recorded the lowest peak discharge (0.0481 $m^3/s/ha$) and a moderate runoff volume (131 m^3/ha), indicating strong attenuation performance consistent with its well-maintained stormwater infrastructure. Block 2 showed a moderate peak discharge (0.0744 $m^3/s/ha$) but the highest runoff volume (142.37 m^3/ha), suggesting limited volume retention capacity. Block 3 exhibited a high runoff volume (131.21 m^3/ha) and elevated peak discharge (0.0947 $m^3/s/ha$); however, field observations confirmed the presence of functional drainage systems with limited capacity, underscoring the need for targeted GI retrofitting rather than complete replacement. Block 5 performed poorest in both indicators, with the highest peak discharge (0.1045 $m^3/s/ha$) and elevated runoff volume (125.77 m^3/ha), signaling an urgent requirement for infrastructural intervention. These results were synthesized into a normalized ranking of flood control effectiveness (Table 5.5), providing data-driven guidance for prioritizing blocks for immediate upgrades or GI retrofitting measures.

Table 5.5: Normalized flood control performance ranking based on peak discharge and runoff volume

Block	Peak discharge ($m^3/s/ha$)	Runoff volume (m^3/ha)	Flood control rank	Aggregated criterion C_6
1	0.048	131	Good	3
2	0.074	142.37	Fair	2
3	0.095	131.21	Fair	2
4	0.098	98	Good	3
5	0.105	125.77	Poor	1

The final ranking closely aligns with site-based infrastructure assessments and highlights spatial disparities in flood mitigation capacity. These insights are essential for prioritizing maintenance and retrofits and guiding sustainable urban drainage upgrades in similarly complex, rapidly urbanizing areas. The aggregated findings, reflecting infrastructure quality and maintenance across blocks, are summarized in Table 5.6.

Table 5.6: Color-coded table presenting aggregated field and model-based scores by criterion and blocks. Scores range from 1 to 3 and are represented by a gradient color scale evolving from green (1, best performance) through intermediate shades to red (3, poorest performance)

Block	C_1 (Benefit)	C_2 (Benefit)	C_3 (Benefit)	C_4 (Cost)	C_5 (Benefit)	C_6 (Benefit)
1	2.67	2.5	2	2	2.83	3
2	2.67	2.17	2	2	2.83	2
3	3	3	3	1	3	2
4	2	1	1.83	2.17	3	3
5	3	3	2.5	1.67	3	1

5.3.4 TOPSIS-AHP-PCSWMM-based Performance Ranking

A decision matrix was constructed for five spatial blocks using the six evaluation criteria (C_1–C_6). To standardize heterogeneous data, vector normalization was applied. Criteria weights were derived via AHP pairwise comparison from 12 experts, yielding a consistent weighting scheme (CR = 0.06): C_1 = 0.25, C_6 = 0.2, C_2 = 0.2, C_3 = 0.15, C_4 = 0.1, and C_5 = 0.1. These weights informed the weighted normalized decision matrix used in the TOPSIS analysis. The positive ideal (A^+) and negative ideal (A^-) solutions were defined by maximizing benefit criteria (C_1, C_2, C_3, C_5, C_6) and minimizing the cost criterion (C_4—sediment accumulation). Euclidean distances to these ideals were computed to calculate each block's relative closeness coefficient (C_i) presented in Table 5.7.

Table 5.7: Closeness to ideal positive and negative solution

Block	Closeness Coefficient (Ci)	Category	Description
Block 3	0.7	Class I – High	Significantly above the mean; top-performing block with strong alignment to the ideal solution.
Block 1	0.66	Class II – Upper Medium	Above the mean but within one standard deviation; good performance with potential for optimization.

Block 5	0.5	Class III – Lower Medium	Slightly below the mean; moderate performance requiring targeted improvements.
Block 2	0.48	Class III – Lower Medium	Slightly below the mean; moderate performance requiring targeted improvements.
Block 4	0.43	Class IV – Low	More than one standard deviation below the mean; weakest performance, priority for intervention.

Block 3 exhibited the highest overall performance (C_i = 0.7), followed by Block 1. Blocks 5 and 2 showed moderate performance, while Block 4 ranked lowest, primarily due to deficiencies in sediment and infrastructural integrity.

5.3.5 Sensitivity Analysis

To evaluate the robustness of the TOPSIS-AHP-PCSWMM-derived block performance rankings against uncertainties in the weighting of criteria, a comprehensive sensitivity analysis was conducted by systematically varying the weights across five distinct scenarios.

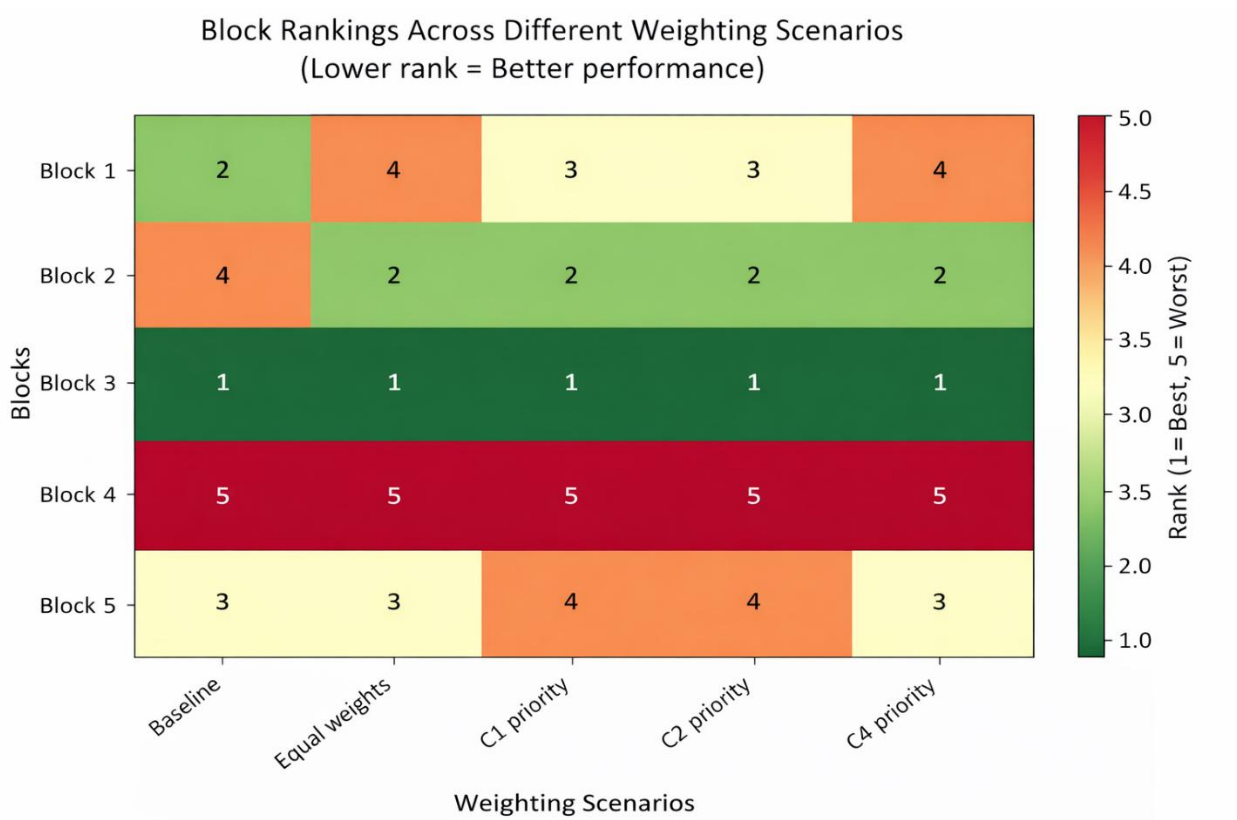

Figure 5.8: Sensitivity analysis of block rankings under five weighting scenarios. Baseline column (AHP weights) shows rank order consistent with table 5: Block 3 (1), Block 1 (2), Block 5 (3), Block 2 (4), Block 4 (5). Blocks 3 and 4 remain stable as top and bottom performers across all

scenarios. Block 2 improves to rank 2 in all other scenarios, while Block 5 drops to rank 4 when C_1 or C_2 are prioritized

The baseline scenario reflected AHP-based expert consensus with weights assigned as follows: $C_1 = 0.25$, $C_2 = 0.2$, $C_3 = 0.15$, $C_4 = 0.1$, $C_5 = 0.1$, and $C_6 = 0.2$. The subsequent scenarios included equal weighting (0.2 for all criteria), flood conveyance prioritization ($C_1 = 0.5$ with proportional reduction in other weights), structural integrity prioritization ($C_2 = 0.5$), and sediment accumulation minimization ($C_4 = 0.4$).

For each scenario, the TOPSIS methodology was applied to recalculate block rankings, which were then compared to the baseline using Spearman's rank correlation coefficient (ρ). The results demonstrated a high degree of stability in the rankings across all scenarios, with correlation coefficients exceeding 0.92. Notably as presented in (Fig. 5.8), block 3 consistently maintained its position as the top ranked block, while block 4 remained the lowest ranked throughout all weight variations. Block 2 exhibited sensitivity to weighting changes, improving from rank 4 under the baseline scenario to rank 2 across all alternative weighting scenarios, where it remained stable. Blocks 1 and 5 exhibited greater positional variability under the equal-weight and sediment-focused scenarios, indicating that mid-performing blocks may be more sensitive to changes in criteria weighting.

Whereas Fig. 5.8 presents composite scenarios in which multiple criteria weights were adjusted simultaneously to reflect distinct policy priorities, Table 5.8 was derived from a separate sensitivity exercise in which each criterion weight was varied individually while holding all others constant at their baseline values. This complementary approach enables identification of criteria that exert the greatest individual influence on ranking outcomes. Higher ranks indicate greater impact of weight variation on ranking outcomes. This supports the robustness analysis by identifying which performance parameters most affect decision outcomes when their weights are altered.

Table 5.8: Relative sensitivity of the criterion

Rank	Criterion	Relative sensitivity
1	Sediment accumulation	High
2	Flood conveyance capacity	Moderate-high
3	Flood control effectiveness	Moderate
4	Structural integrity	Moderate
5	Maintenance accessibility	Low-moderate

6	Erosion control effectiveness	Low

These findings affirm the robustness of the ranking framework in reliably distinguishing between the highest- and lowest-performing blocks (Blocks 3 and 4), which remained stable across all weighting scenarios. However, the observed sensitivity among mid-ranked blocks (Blocks 1, 2, and 5) underscores the importance of careful weight assignment when prioritizing interventions for blocks with intermediate performance. However, the observed sensitivity among mid-ranked blocks underscores the critical importance of carefully assigning weights to criteria in decision-making processes. This variability suggests that such blocks may benefit from more detailed, context-specific evaluations to inform prioritization of maintenance and GI retrofitting interventions. The high sensitivity of sediment accumulation (C_4) in the individual tuning analysis reflects its low baseline weight (0.1), such that proportional increases produced substantial shifts in ranking outcomes. In composite scenarios, however, the simultaneous reduction of other criteria weights dampened this effect, explaining the muted visual impact in Fig. 5.8.

5.3.6 Recommendations for GI Retrofitting and Maintenance

Based on the integrated results of the TOPSIS-AHP-PCSWMM ranking and corroborating field data, targeted recommendations for GI retrofitting and maintenance were developed to enhance the sustainability of stormwater management infrastructure within the study area. Block 3 (C_i = 0.7, Class I – High): Block 3 exhibits high conveyance capacity (C_1 = 3), structural integrity (C_2 = 3), and erosion control (C_3 = 3), indicating that the existing gray infrastructure is fundamentally sound. However, its moderate flood control performance (C_6 = 2) with high peak discharge (0.095 $m^3/s/ha$) suggests that the system is hydraulically stressed during storm events. This combination makes Block 3 an ideal candidate for GI retrofitting (e.g., rain barrels, rain gardens, bioretention cells, permeable pavements) to augment the existing concrete-lined channels by facilitating localized infiltration and runoff storage. These interventions would reduce peak flows and pollutant loads while enhancing climate resilience. Maintenance should focus on preserving the high structural quality of existing assets while strategically implementing GI at source areas.

Block 1 (C_i = 0.66, Class II – Upper Medium): Block 1 shows moderate performance across most criteria but exhibits concerning deficiencies in conveyance capacity (C_1 = 2.67), structural integrity (C_2 = 2.5), and erosion control (C_3 = 2). These issues make some portions of the existing gray infrastructure unreliable. Its moderate runoff volume (131 m^3/ha) suggests that strategic GI implementation—specifically bio-retention systems and permeable pavements tailored to site-specific conditions—could help manage runoff at source areas while the most problematic drainage segments undergo targeted rehabilitation. A combined approach of rehabilitation and strategic GI is recommended.

Block 5 (C_i = 0.5, Class III – Lower Medium): Block 5 demonstrates well-maintained, structurally sound infrastructure (C_2 = 3, C_3 = 2.5) but exhibits the poorest flood control performance (C_6 = 1) with the highest peak discharge (0.105 $m^3/s/ha$) and elevated runoff volume (125.77 m^3/ha). This indicates that while the physical infrastructure is in good condition, its hydraulic capacity is insufficient for current and projected storm events. Block 5 is therefore an ideal candidate for GI retrofitting specifically focused on volume reduction, such as rain gardens, vegetated swales, and constructed wetlands, to augment system capacity without replacing functional gray infrastructure.

Blocks 2 and 4 (C_i = 0.48 and 0.43, Classes III and IV): These blocks require focused maintenance and rehabilitation prior to any GI retrofitting. Block 2 exhibits moderate structural deterioration (C_2 = 2.17) and sediment accumulation (C_4 = 2), necessitating sediment removal, repair of channel defects, and improvements in maintenance access (C_5 = 1.17). Block 4, identified as the lowest performing block overall (C_i = 0.43), demands comprehensive rehabilitation beginning with emergency maintenance to restore conveyance capacity (C_1 = 2) and structural stability (C_2 = 1). Only after these foundational improvements can phased green infrastructure retrofits be effectively introduced, adapted to the slope and soil characteristics of each block.

5.4 Discussion

5.4.1 TOPSIS-AHP-PCSWMM-based Performance Implications

The integration of the PCSWMM hydrologic modeling framework with the TOPSIS-AHP multi-criteria decision-making approach provided a robust and comprehensive platform for evaluating the performance of stormwater infrastructure across spatially delineated blocks within the study watershed. By simulating key hydrologic variables such as peak runoff and flood volume under different rainfall scenarios, PCSWMM outputs were converted into quantifiable performance indicators. These were then integrated with infrastructural field data and objectively evaluated using the TOPSIS method. The AHP contributed criterion weights based on expert consensus, ensuring that the multi-dimensional aspects of infrastructure performance—both hydraulic and structural—were appropriately prioritized in the evaluation. The results demonstrated that block 3 consistently achieved higher ranking, which translated into its highest preference score of 0.92. This suggests that the stormwater management features in block 3 are better maintained to attenuate peak flows and reduce flood risks, which unfortunately was not the case due to the undersized infrastructure design of the infrastructures in the block. In contrast, blocks 4 and 2 ranked lowest, likely due to the under designed or under maintenance and suboptimal drainage network configurations, which reduce their capacity to manage stormwater effectively. The marked volumetric disparity between blocks—such as the runoff volume of 142.37 m^3/ha in Block 5 compared to 98 m^3/ha in Block 4—reflects tangible differences in stormwater retention and conveyance capabilities. This hybrid evaluation framework, combining process-based hydrological modeling with multi-criteria decision analysis, exemplifies a powerful approach to identify and prioritize sustainable IGGI solutions tailored to micro-watershed scale urban flood management challenges.

The juxtaposition of Block 4's high maintenance accessibility score (3) with its poor sediment accumulation (C_4 = 2.17, where higher indicates worse condition) and low structural integrity (C_2 = 1) is particularly instructive. This pattern suggests that while the infrastructure in Block 4 is physically easy for personnel and equipment to reach, this accessibility has not translated into effective or timely maintenance activities. The high sediment buildup indicates that routine cleaning and upkeep are not occurring at sufficient frequency or intensity. This points not merely to physical constraints but to a potential failure in the maintenance regime or scheduling itself—a finding that underscores the need for performance-based maintenance plans rather than relying on ease of access as a proxy for maintenance effectiveness.

5.4.2 Sensitivity Analysis Implications

The sensitivity analysis conducted in this study further illuminated the robustness and limitations of the integrated assessment framework. Five alternative weighting schemes were tested, ranging from equal weighting to hydrologically focused prioritizations and expert judgment-based scenarios, to explore how variations in criterion importance influence block rankings. Blocks 3 and 4 demonstrated remarkable stability in their relative rankings regardless of weight adjustments, indicating their stormwater performance assessments are resilient to subjective biases in criteria prioritization. Such stability lends confidence that these blocks represent reliable targets for maintenance and GI retrofitting actions. On the other hand, blocks 1 and 5 showed notable fluctuations in their rankings across scenarios, signaling that their performance is contingent on specific criteria such as infiltration capacity and localized ponding potential. This variability highlights the importance of transparent and iterative weighting processes, as well as the potential need for adaptive management that can accommodate uncertainty in decision parameters. Overall, the sensitivity analysis confirms that while the integrated TOPSIS-AHP-PCSWMM approach is robust, its application benefits from careful consideration of weighting schemes and the contextual relevance of each criterion to local hydrological dynamics.

5.4.3 Policy and Municipal Planning Implications

The findings of this study carry significant implications for urban stormwater management policy and municipal infrastructure planning in Addis Ababa and other rapidly urbanizing cities in the Global South facing similar hydrological challenges. Firstly, the identification of high-performing blocks with superior stormwater attenuation capacity provides a valuable evidence base for developing design guidelines and best practice standards for IGGI deployment, especially in flood-vulnerable micro-watershed contexts. Such data-driven design guidance can promote replication of effective infrastructure typologies and enhance resilience to increasing urban runoff volumes driven by climate change and urban expansion.

Secondly, the prioritized ranking of spatial blocks according to hydrologic and structural performance offers municipal planners a strategic framework for targeted resource allocation. This enables more efficient investment and maintenance scheduling, focusing limited financial and technical capacity on areas exhibiting suboptimal performance or urgent rehabilitation needs. Thirdly, the transparent coupling of PCSWMM hydrological simulation with TOPSIS-AHP multi-criteria decision analysis delivers a replicable, data-driven decision support system that enhances cross-sectoral coordination and participatory urban planning processes. This integrated framework supports evidence-based policymaking aligned with Ethiopia's national green development agenda and global efforts toward building climate-resilient, sustainable urban infrastructure under SGD 11 (sustainable cities and communities), 12 (responsible consumption and production), and 13 (climate action) (United Nations, 2015). Ultimately, the study's approach demonstrates the potential to bridge scientific modeling with practical governance tools, facilitating proactive, adaptive management of urban stormwater systems under uncertain and changing environmental conditions. The TOPSIS-AHP-PCSWMM framework is scalable to city level because the methodology uses transferable inputs: slope from DEM, land use from satellite imagery and field observation, soil from national maps, and field-observable performance criteria. Application to other sub-cities and the city at large would require block re-delineation and local field assessment but not methodological redesign.

5.4.4 Study Limitations

Despite the methodological rigor, several limitations should be acknowledged. First, the model inputs relied primarily on available surface and spatial data, which may not fully capture subsurface complexities such as buried utilities, soil heterogeneity at depth, and localized preferential infiltration pathways—potentially affecting hydrologic simulation precision. Second, although criterion weights were derived through structured expert elicitation using AHP pairwise comparisons, and both consistency checks and sensitivity analysis were performed ($CR = 0.06$, $\rho > 0.92$), the inherent subjectivity of expert judgment may still introduce bias and variability into the prioritization outcomes. Third, the analysis emphasized technical performance criteria without incorporating economic considerations (e.g., capital costs, operational and maintenance expenses) or social dimensions (e.g., stakeholder preferences, acceptance), limiting the sustainability assessment from a broader financial and community perspective. Future research should incorporate higher-resolution datasets that capture subsurface conditions, apply complementary or mixed methods to reduce reliance on subjective expert judgment and broaden the evaluation framework to include economic and social dimensions alongside technical performance, thereby enabling more comprehensive, balanced, and context-responsive stormwater management strategies.

5.4.5 Comparison with Previous Studies

The novelty of this study lies in its integration of PCSWMM and the TOPSIS-AHP multi-criteria decision-making method to spatially classify stormwater infrastructure blocks based on readiness for GI retrofitting, need for maintenance, or requirement for complete development. Unlike many previous studies, this research was conducted within a contributing zone of a micro-watershed, characterized by steep slopes and poorly draining soils, making the results particularly relevant for topographically challenging urban contexts.

Prior studies such as Yu et al., (2013) primarily focused on the performance and cost-efficiency of various Best Management Practices (BMPs) across Korea’s River basins, emphasizing pollutant removal and operational cost without explicit hydrologic modeling or spatial prioritization of GI retrofitting zones. Mani et al., (2019) combined SWMM and TOPSIS within a multi-objective optimization framework, identifying optimal zones for low impact development in Tehran; however, their focus remained on broader catchment-level stormwater control measures planning rather than block-scale GI retrofitting prioritization performed on steep sloped, poorly draining soil, contributing zone of urban micro-watershed.

Similarly, Luan et al., (2019) applied SWMM-TOPSIS to assess green stormwater infrastructure performance under various land-use and cost-weighted scenarios. Their study emphasized comparative strategy performance but did not address block-scale heterogeneity or operational readiness for implementation. Akhter et al., (2020) and Yao et al., (2022) highlighted the cost and hydraulic performance trade-offs between conventional and hybrid stormwater systems, contributing valuable economic insights but lacking an integrated MCDM evaluation framework. Of particular relevance is the work by Omidi Arjenaki et al., (2020), which coupled SWMM and TOPSIS to prioritize sub-catchments in Shahrekord city. While their results demonstrated 80% overlap between high-runoff and high-risk areas, their scale of analysis remained limited to sub-catchments and did not incorporate retrofit readiness or classify infrastructure performance into operational categories, as this study does. Furthermore, it does not focus on steeply sloped, poorly draining contributing zone of urban micro-watershed.

Therefore, the current research advances the field by offering a spatially-resolved, simulation-supported MCDM approach that not only evaluates hydrologic performance but also categorizes each block based on actionable recommendations—GI retrofitting, maintenance, or development, focusing on steeply sloped, poorly draining soil contributing zone of urban micro-watershed. This operational framing makes the method more directly applicable to urban planning and infrastructure renewal efforts under climate-uncertain and resource-constrained settings. Table 5.9 summarizes a comparative assessment of the previous studies and the current study.

Table 5.9: Comparison with previous studies based on their focus, methods and findings

Study	Focus	Methods	Scale/Area	Key Findings
This Study (2025)	Categorizing IGGI retrofit readiness by block using TOPSIS-AHP-PCSWMM	PCSWMM + TOPSIS+AHP	Contributing zone of micro-watershed with steep slope and poorly draining soils (5 blocks)	Novel classification into retrofit, maintenance or development categories; sensitive to mid-block variation

Yu et al., (2013)	Performance and cost evaluation of BMPs in Korea	Monitoring + Cost Analysis	Four major river basins in Korea	Constructed wetlands cost-effective; media filters efficient but expensive
Mani et al., (2019)	Optimization of urban runoff management using LID stormwater control measure and TOPSIS	SWMM + Multi-Objective Ant Lion Optimization Algorithm (MOALOA) + TOPSIS	Urban district in Tehran	TOPSIS ranks stormwater control measures with MOALOA optimization providing efficient runoff reduction
Luan et al., (2019)	Green stormwater infrastructure strategy evaluation in a rapidly urbanizing catchment using SWMM-TOPSIS	SWMM + TOPSIS + MCDA	Western New City, Zhuhai, China	Distributed-centralized green stormwater infrastructures perform best; cost weight shifts influence rankings
Akhter et al., (2020)	Cost comparison of conventional vs hybrid stormwater systems	DRAINS Model + Cost Estimation	Greenfield residential site, Australia	Hybrid systems reduce cost by 18% while ensuring performance
Zhang et al., (2021)	Effectiveness of Sponge City strategies in stormwater management	SWMM + Interdisciplinary low impact development approach	Old residential community, Suzhou, China	Sponge facilities capture 91% runoff; improve resilience in older developments
Omidi Arjenaki et al., (2020)	SWMM simulation and critical sub-catchment prioritization using TOPSIS	SWMM + TOPSIS + Sensitivity	Urban catchments in Shahrekord city	Critical sub-catchments identified with 80% compliance between SWMM and TOPSIS

Yao, Hu, et al., (2022)	Performance and cost-effectiveness analysis of stormwater measures in Sponge City context	AHP + Regret Theory + Cost Analysis	Gui'an New District, China	Combined measures outperform single ones; cost-effective multi-criteria evaluation

5.5 Conclusion

This study introduced a novel integrated framework combining PCSWMM hydrological modeling with the TOPSIS-AHP multi-criteria decision-making method to evaluate and prioritize stormwater infrastructure within a steep-slope, poorly draining soil contributing zone of urban micro-watershed. The block-level classification effectively distinguishes infrastructure that is ready for GI retrofitting (42.3%) from areas requiring maintenance or further development (57.7%), enabling targeted, data-driven interventions. Sensitivity analysis demonstrated strong robustness of the ranking results (Spearman's $\rho > 0.92$), confirming the reliability of the prioritization across alternative weighting schemes. Sediment accumulation and flood conveyance capacity emerged as the most influential performance criteria, while mid-ranked blocks showed greater sensitivity to weighting variations, underscoring the importance of transparent and context-specific decision frameworks.

Compared to previous studies, this approach advances urban stormwater management by integrating hydraulic performance and maintenance criteria at a fine spatial and analytical scale—assessing infrastructure block-by-block within a 30-hectare micro-watershed—tailored to challenging topographic (steep slope) and soil conditions (poorly draining soil) often overlooked in conventional planning. The framework offers municipal and policy-level guidance for prioritizing retrofit investments, optimizing maintenance scheduling, and enhancing flood resilience in rapidly urbanizing areas. While focused on a single micro-watershed, the methodology is scalable and adaptable, with potential application across diverse urban contexts of the Global South.

Despite the methodological rigor, several limitations should be acknowledged. First, the model inputs relied primarily on available surface and spatial data, which may not fully capture subsurface complexities such as buried utilities, soil heterogeneity, and localized infiltration pathways—potentially affecting hydrologic simulation precision. Second, although criterion weights were derived through structured expert elicitation using AHP pairwise comparisons, and both consistency checks and sensitivity analysis were performed, the inherent subjectivity of expert judgment may still introduce bias and variability into the prioritization outcomes. Third, the analysis emphasized technical performance criteria without incorporating economic considerations (e.g., capital costs, operational and maintenance expenses) or social dimensions (e.g., stakeholder preferences, acceptance), limiting the sustainability assessment from a broader financial and community perspective. Future research should incorporate higher-resolution datasets that capture subsurface conditions, apply complementary or mixed methods to reduce reliance on subjective expert judgment, and broaden the evaluation framework to include economic and social dimensions alongside technical performance, thereby enabling more comprehensive, balanced, and context-responsive stormwater management strategies. This framework supports UN-SDGs by providing evidence-based prioritization of stormwater infrastructure interventions: SDG 11 (Sustainable Cities) through flood risk reduction; SDG 12 (Responsible Consumption) through extending infrastructure life via targeted maintenance; SDG 13 (Climate Action) through climate-responsive retrofitting. These contributions are evidenced by the ranking of blocks and the identification of 42.3% of the study area as ready for GI retrofitting.

Chapter 6

6 A Novel Integration of Green-Grey Infrastructure in Steep Slope Micro-Watersheds: PCSWMM Modeling for Non-Draining Soils in Addis Ababa

Abstract

Urban watersheds with steep slopes and poorly draining soils are increasingly prone to flooding and water quality decline under rapid urbanization and climate change. This study assessed the hydrological and water quality performance of IGGI using a PCSWMM-based model in a micro-watershed of Addis Ababa, Ethiopia. The analysis considered historical data, projected climate change, and land use change as indicators of future urbanization. A novel IGGI setup was developed by integrating buried RBs with conventional RGs within contributing zones—an approach seldom applied in stormwater design. While RBs and RGs are established practices, burying the barrels enhanced stormwater retention by capturing runoff from rooftops and impervious areas and allowing delayed subsurface infiltration. Model calibration and validation showed good performance (NSE = 0.6-0.9; RSR = 0.3-0.6) with acceptable integral square error values. Under baseline conditions, runoff peaked at 3.6 m^3/s (5,179 m^3 total volume) with pollutant loads of ammonia 18.5 kg, BOD 109.8 kg, COD 1,363.1 kg, nitrate 19.3 kg, and phosphate 21.3 kg. Urbanization increased runoff and pollutant loads by 9–12%, while climate change raised them by 41.5–45%. The combined scenario yielded the highest runoff (7.2 m^3/s; 9,897 m^3) and pollutant loads of ammonia 35.4 kg, BOD 208.8 kg, COD 2,591.4 kg, nitrate 36.8 kg, and phosphate 40.3 kg. Post-IGGI implementation for the baseline, peak runoff and total volume declined by 43.5% and 36.7%, with pollutant loads reduced by 37.2–42.4%. The IGGI framework enhances infiltration, mitigates hydrological and water quality impacts, and supports SDGs 6, 11, and 13 through climate-resilient urban drainage.

Key words: IGGI, Urban stormwater management, Steep-slope watersheds, Climate change adaptation, Water quality improvement, PCSWMM modeling.

6.1 Introduction

At present, stormwater management is shifting from conventional grey infrastructure to sustainable and integrated methods with the increase in urban floods and water quality deterioration (Qiao et al., 2020; Y. Yang et al., 2024). According to research from Madakumbura et al., (2021), Pour et al., (2020), and Jiang et al., (2023), climate change and rapid urbanization are significant contributors. Climate change alters the intensity and temporal distribution of rainfall Jiang et al., (2023). In addition, urbanization increases imperviousness, which results in an increase in runoff and pollutants (Pour et al., 2020). According to Zahmatkesh et al., (2015), conventional drainage systems are not adequate to deal with these changes as they were designed under the hydrological stationary assumption.

Some of the most difficult challenges are faced by cities with complex topography and rapid urbanization. Urban watersheds with steep slopes, and poorly draining soil (Vertisols or Clay) are highly susceptible to flash flooding and cause pollution (Jemberie and Melesse, 2021; McFarland et al., 2019). In plenty of rapidly growing Global South cities like Nairobi of Kenya, Dar es Salaam of Tanzania, Warangal of India, and Addis Ababa of Ethiopia, their expanding urbanization outpaces the development of infrastructure. This leads to ongoing piling up of runoff water and poor water quality (Kumar et al., 2023; Mguni et al., 2015; Parkinson and Mark, 2015).

(i) Climate and Urbanization Pressures: Steep slopes accelerate overland flow, while low-permeability soils limit infiltration, causing higher peak discharges and pollutant export (Osman, 2018; Omitaomu et al., 2021). Uncontrolled urban expansion further disrupts natural drainage pathways, replacing vegetated surfaces with impervious materials, reducing baseflow recharge, and increasing flood peaks (J. Wang et al., 2022).

(ii) Limitations of Existing Green Infrastructure: Globally, IGGI—also termed SuDS, LID, WSUD, or sponge city systems—has emerged as a sustainable alternative (Bai et al., 2018; Fletcher et al., 2015; Hua et al., 2020). However, existing GI designs often assume flat topography and permeable soils, which limit their effectiveness in steep, poorly draining environments like Addis Ababa's Vertisol-dominated catchments (EPA, 2014; Berhanu, 1983). Consequently, conventional measures such as bioretention cells, grass swales, and permeable pavements are difficult to apply or fail to perform effectively under such conditions.

(iii) Need for IGGI in Steep-Slope Areas: Recent simulation–optimization studies have enhanced IGGI design using tools such as SWMM, SUSTAIN, and metaheuristic algorithms (e.g., NSGA-II, SMA, MOPSO) to improve hydraulic and economic efficiency (Nazari et al., 2021; Eskandaripour and Soltaninia, 2024; Sun et al., 2020). Yet, few address the unique constraints of steep micro-watersheds with low-infiltration soils, where contributing zones—areas generating most runoff—hold untapped potential for attenuation (Marsh, 2010; McFarland et al., 2019). The limited focus on such settings has resulted in recurring urban flooding and poor pollutant control (Angello et al., 2021; Zhang and Chui, 2018).

Research Gap and Novelty: This study addresses these gaps by introducing a novel IGGI configuration that integrates buried RBs with RGs within contributing zones of steep, poorly drained micro-watersheds. Unlike standard GI systems—where RBs are aboveground and used primarily for rooftop runoff collection and reuse (Eroksuz and Rahman, 2010; Jones and Hunt, 2010; J. Xu et al., 2023)—the RBs in this study are buried and encased in permeable sand, enabling temporary storage and delayed subsurface infiltration. The uniqueness lies in capturing runoff from both rooftops and adjacent impervious surfaces, improving capture efficiency and infiltration under challenging hydrogeological conditions. Implementing this configuration within Addis Ababa's steep, Vertisol-dominated watershed further enhances its scientific and practical novelty.

Hypothesis and Study Objective: The hypothesis tested is that the designed IGGI system can reduce stormwater runoff volume, peak flow, and pollutant loads by approximately 30% under a typical 2-year return-period design storm, relative to baseline conditions. This study aims to (a) evaluate the hydrological and water-quality performance of the proposed IGGI under baseline, urbanization, climate change, and combined scenarios using a PCSWMM-based model, (b) quantify the capacity of buried RBs integrated with RGs to reduce peak runoff, total runoff volume, and pollutant loads, and (c) demonstrate the applicability of IGGI for steep, poorly drained urban catchments.

Aligned with Addis Ababa's strategic development framework (World Bank, 2021) and policy brief 3: Green and blue infrastructure (Dereje Fekadu et al., 2022) and reinforced by academic evidence on urban green infrastructure (GI) (Azagew and Worku, 2020; Jemberie and Melesse, 2021), this IGGI approach supports the city's transition toward nature-based, decentralized stormwater management solutions. It further advances understanding of IGGI performance under complex urban, topographic, and climatic conditions, offering a replicable, site-specific framework that contributes to SDGs 6, 11, and 13 by promoting climate-resilient and sustainable stormwater management in steep, poorly draining urban environments. While IGGI integration has been published previously, the novelty of this chapter is threefold: (1) buried RBs (rather than above-ground) that capture runoff from multiple impervious surfaces; (2) integration with RGs specifically designed for steep slopes (>7%) and Vertisol soils; (3) field implementation in a data-scarce Global South context with local materials.

6.2 Materials and Methods

6.2.1 Study Area Description

The target study area is found in Nefas Silk Lafto Sub-City in southwestern Addis Ababa, Ethiopia, within Little Akaki watershed as shown in Fig 6.1. covering an area of about 30 ha which has mixed urban land use such as residential, commercial, and road on poorly draining Vertisol soils.

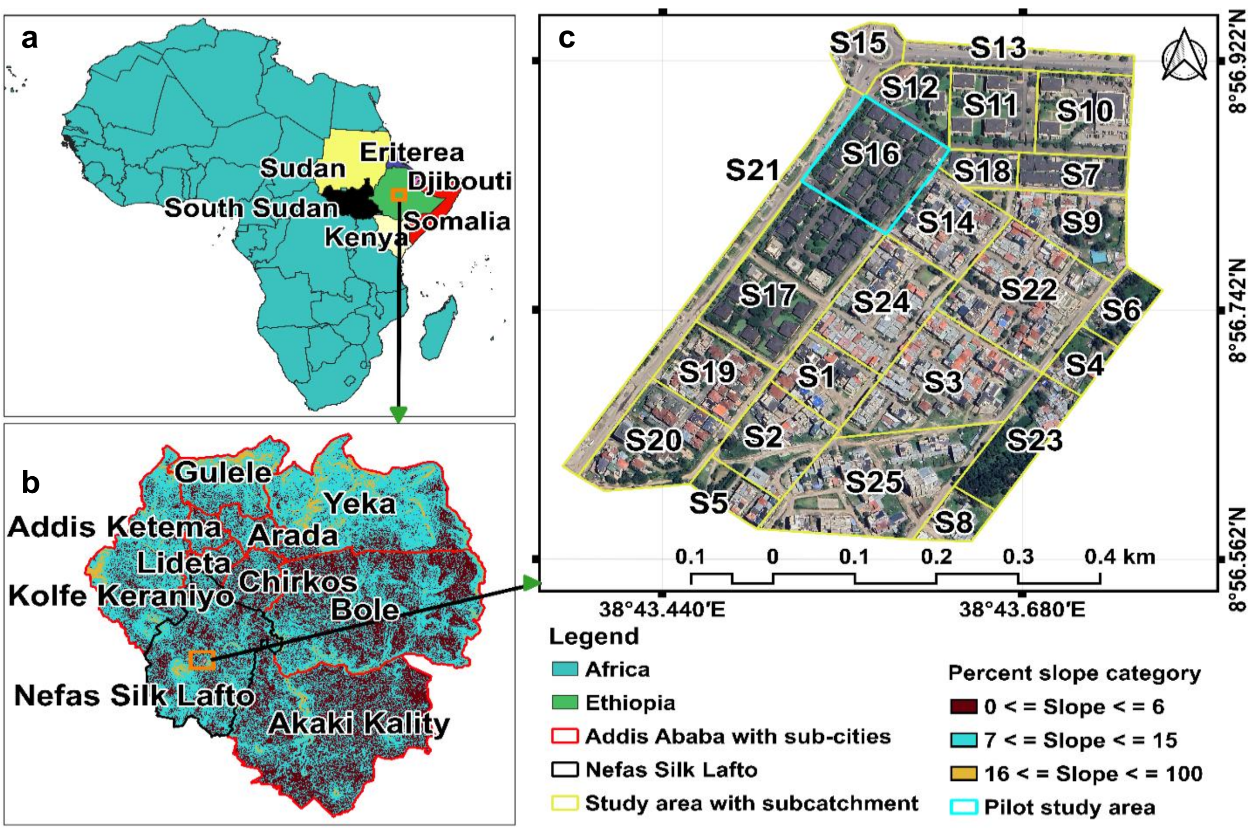

Figure 6.1: Study area showing (a) Africa, (b) Addis Ababa slope with sub-cities, and (c) study area sub-catchments with sub-catchment (S_{16}) as the pilot intervention site

According to terrain analysis, the area with slope < 7% is about 16.9% and 79.7% with slope between 7 – 30% and 3.4% with slope above 30%. Thus, the area is characterized by a predominantly moderately steep terrain (Atinafu et al., 2024, FAO, 2006). These slopes, which are moderate geomorphologically, are functionally steep for IGGI because of design and infiltration limitations of inclined surfaces (Liu et al., 2021, EPA, 2014; McFarland et al., 2019). The shape of the terrain has a huge influence on runoff, and it restricts infiltration-based IGGI application. Therefore, the watershed may be representative of IGGI analysis under sloped urban conditions.

Within this watershed, sub-catchment S_{16} (2.09 ha) was selected for on-ground IGGI implementation because its soil and slope typify the broader hydrological challenges. Due to financial and institutional constraints, full-scale GI installation wasn't feasible for the entire 30 ha.

6.2.2 Data Sources and Preparation

Topographical and Soil Data: A 1 m-resolution DEM was produced in QGIS using GPS Visualizer–based elevation points (Hussain, 2020; Kemal et al., 2025b). The DEM accurately represented site topography and guided sub-catchment delineation. Soil data were derived from the Addis Ababa soil map (Ministry of Water and Energy, 2004) which was verified using the FAO Digital Soil Map, and used in previous studies by Feyissa et al., (2018); Moisa et al., (2023); Kemal et al., (2025a). The study area is dominated by Pellic Vertisols with >50% clay, <10% sand, and 40% silt (Berhanu, 1983; Srivastava et al., 1989), corresponding to a silty clay texture. Infiltration parameters for the modified Green–Ampt method—suction head, hydraulic conductivity, and moisture deficit—were adopted from the PCSWMM manual (Rossman, 2015) for silty clay soil due to field-testing constraints.

Climate Data: From the National Meteorological Agency, historical records of climatic data (1983-2023) sourced from the Ayertena station were selected by using Thiessen polygon analysis since it has long time series data, and it has been used in this study. Future climate projections used 12 precipitation and 16 temperature GCMs from CMIP6, bias-corrected and downscaled with the BCCAQ method to 10 km resolution, referencing a 5 km gridded dataset for calibration (Kemal et al., 2025b; Rettie et al., 2023). Validation against observed Ayertena data (1983–2014) using a perfect-sibling framework showed high performance (r = 0.83–0.94, RMSE = 0.74–1.28 mm/day, NSE = 0.71–0.88, PBIAS ±8%, KGE = 0.79–0.91). Based on their performance five precipitation (CMCC-CM2, GFDL-ESM4, INM-CM4-8, MIROC6, MPI-ESM1-2-LR), four maximum temperatures (GFDL-ESM4, INM-CM4-8, MIROC6, MPI-ESM1-2-LR), and three minimum temperature (INM-CM4-8, IPSL-CM6A-LR, MPI-ESM1-2-LR) GCMs were selected and ensembled using a weighted average under SSP2-4.5 and SSP5-8.5 scenarios. Historical gaps and outliers were corrected via the normal-ratio method (Kemal and Adeba, 2021), and daily rainfall was disaggregated into sub-daily series for IDF curve development (Ewea et al., 2018).

IDF Curve Development: The Indian Meteorological Department (IMD) equation (Eq. 6.1) (Bibi et al., 2023; Kumar et al., 2023) was applied in Addis Ababa's tropical–highland context (Al Mamun et al., 2018; Nwaogazie et al., 2021; R. Palaka, 2016):

$$P_t = P_{24} * \left(\frac{t}{24}\right)^{1/3} \quad (6.1)$$

where P_t (mm) is rainfall depth for duration t (hours), and P_{24} is the 24-hour maximum rainfall. Among several tested probability distributions (GEV, GPD, Log-Pearson III, and Gumbel), the Gumbel distribution best fitted the data (Badou et al., 2021; Delian Akpen et al., 2020; Lau and Behrangi, 2022; Silas et al., 2022). Rainfall depths for 2- and 10-year return periods were estimated using Eq. 6.2:

$$P_T = P_{ave} + KS \quad (6.2)$$

where K is the frequency factor, S the standard deviation, and P_{ave} the mean rainfall.

The 2-year return period, commonly used for LID/IGGI design, represents frequent storms that dominate annual runoff (Adhikari et al., 2024; Chen et al., 2023; Martínez et al., 2021; Yu et al., 2023; Zahmatkesh et al., 2015), while the 10-year event provides insight into system resilience under more extreme conditions.

Land Use: Land use classification based on PCSWMM Bing Imagery and Google Earth Pro and Field Verification. The researchers assigned seven categories to the mapped surfaces specifically: asphalt pavement, commercial, multi-family residential, natural/forest, single-family residential, cobble stone pavement, unpaved roads. The assessed sub-catchments received area-weighted proportions of each land-use type with additional categories for percent pervious and impervious, which accounted for various surfaces such as rooftop, vegetation, asphalt pavement, unpaved road and cobblestone pavement. The classification accuracy was validated using a total of 60 georeferenced field points spread across all land-use category and cross-verified with the help of field observation, high-resolution imagery in Google Earth Pro, and Bing (PCSWMM). The reliability metrics in Python 3.11.4 led to the following results: AUC = 0.92 (excellent, ≥ 0.75) RMSE = 0.08 (good agreement, ≤ 0.2) implying strong spatial classification performance The Event Mean Concentration (EMC) method was used to estimate the pollutant washoff parameters through literature-derived values. From previous works by Chow et al., (2012), Fernández et al., (2019), Gaut et al., (2019), Temprano et al., (2006), Tu and Smith, (2018), and Zakizadeh et al., (2022) we have made use of literature-derived estimations.

Selecting Pollutant: For selection of pollutants, ammonia (NH_3), biochemical oxygen demand (BOD), chemical oxygen demand (COD), nitrate (NO_3^-) and phosphate (PO_4^{3-}) were selected as they are toxicants in runoff from urban areas. These denote a flora-rich eutrophication and oxygen depletion pollution risk common in built-up catchments.

Data for In-situ Calibration: For the calibration, nine rainfall events were sampled in June – September 2024 and 2025 considering the usual issues of data scarcity and cost for monitoring continuous real time data in developing countries (Feyissa et al., 2018). Event based monitoring of runoff flow depths utilizing staff gauges for stormwater quantity calibration and collection of water samples for stormwater quality analysis. The quantitative analysis of ammonia, nitrate, and phosphate by colorimetry, BOD (5 days incubation) and COD (dichromate oxidation) was carried out using HI83399 COD Multiparameter Laboratory Photometer (Hanna Instruments Inc., USA) at the laboratories of Addis Ababa Science and Technology University and Addis Ababa University. These field-derived concentrations were used to calibrate pollutant parameters in PCSWMM.

Grey Infrastructure Data: Because no municipal records were available, hydraulic data (pipe diameters, slopes, manhole depths, and channel geometries) were obtained via field surveys and Google Earth Pro. The existing system comprises concrete pipes (0.125–1.375 m diameter, 1–28% slope) and rectangular channels (0.75–3.75 m depth, 0.5–2.2 m width), with manholes at ≈50 m spacing. Sub-catchments were delineated in PCSWMM using DEM, drainage divides, and land-use data to support hydrologic and pollutant-load modeling.

6.2.3 Model Development (PCSWMM)

Model setup, calibration, and validation were performed in PCSWMM 7.7.3910. The stormwater network included 25 sub-catchments, 142 junctions, 150 conduits, and two outfalls (OF1 and OF2). The configuration mirrors the actual drainage layout (Fig. 6.2). Further datasets used in the model development are summarized under Table 6.1.

Table 6.1: Summary of datasets used for model development

Dataset	Source / Method	Application
DEM	GPS Visualizer, QGIS	Topography, sub-catchment delineation
Soil	Ministry of Water and Energy (2004)	Infiltration parameters
Climate (historical)	NMA (1983–2023)	Rainfall and temperature input
Climate (projected)	CMIP6 GCMs (2024–2083)	Scenario analysis (SSP2-4.5, SSP5-8.5)
Land use	Bing imagery + Field survey	Runoff and pollutant assignment
Grey infrastructure	Field survey, Google Earth Pro	Hydraulic network setup
Pollutant data	Field sampling (2024, 2025)	Calibration and validation

Grey Infrastructure Setup: Hydraulic properties such as conduit geometry, slope, Manning's n, and junction elevations were defined from field and satellite measurements. Boundary conditions were set using rainfall and inflow data to simulate real-world hydrologic responses.

Model Calibration and Validation: Two sequential calibrations were undertaken including grey-infrastructure-only scenario to benchmark existing conditions, and IGGI scenario to assess IGGI performance. Independent datasets were used for each calibration phase. The model was evaluated using standard statistical indicators (NSE, RMSE, and ISE) to ensure hydrologic and pollutant-load simulation reliability.

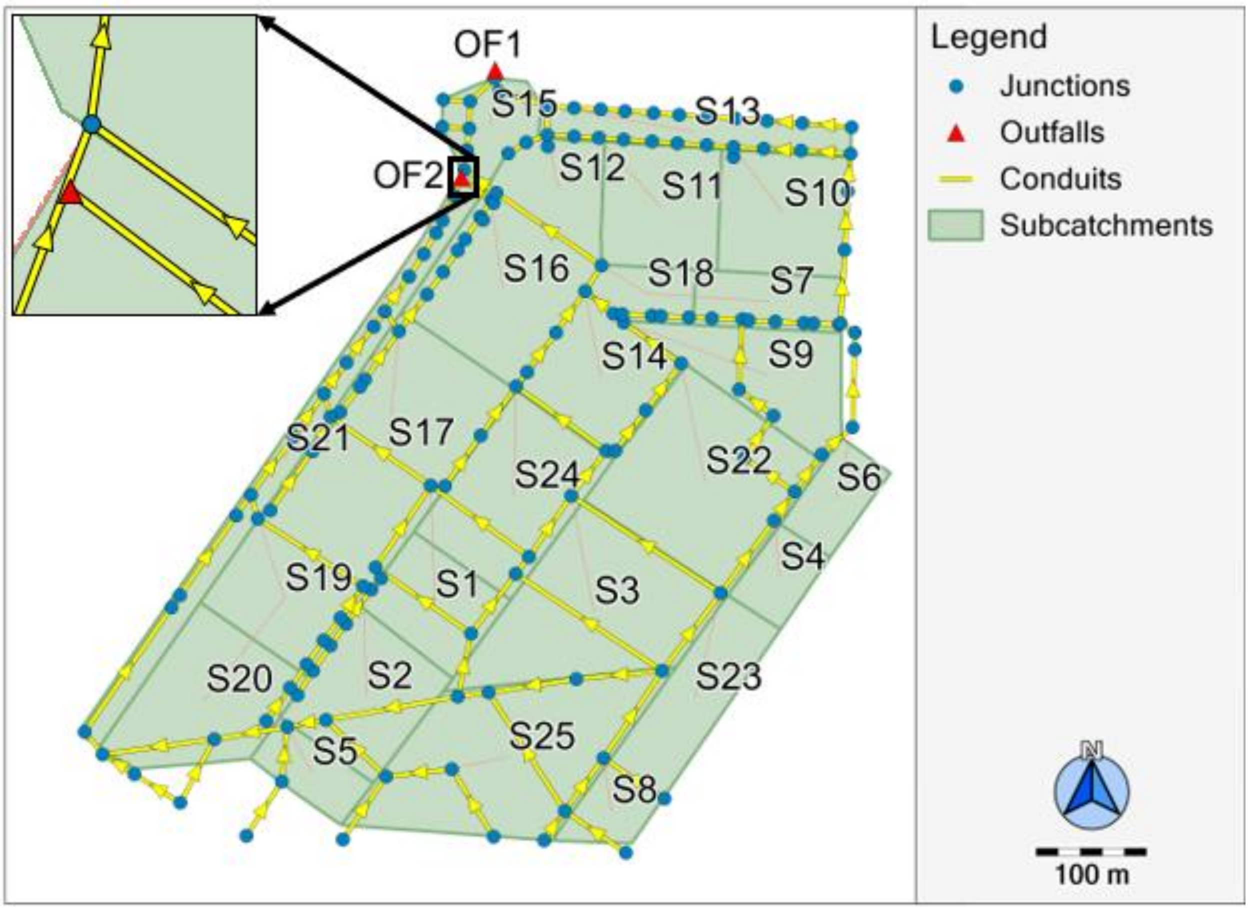

Figure 6.2: Study area hydraulic configuration of a) the junctions, outfalls, conduits and sub-catchments and b) zoomed in picture of OF2 the outfall which receives outflow only from S_{16}

6.2.4 IGGI Integration in the Pilot Intervention for Enhanced Stormwater Management

RBs and RG were selected over alternatives (green walls, green roofs, permeable pavements, and others) because: (1) RGs provide proven bioretention at lower cost; (2) buried RBs capture runoff from multiple surfaces; (3) permeable pavements require full-depth reconstruction unsuitable for retrofitting within budget constraints; (4) both use locally available materials and can be implemented incrementally.

RG: RG with a surface area of 0.1 ha, representing approximately 5% of the S_{16} sub-catchment, was constructed upstream to enhance stormwater retention, filtration, and infiltration. The RG has a total depth of 0.6 m, consisting of a 0.2 m surface ponding zone, a 0.3 m engineered sandy-loam filter layer, and a 0.1 m gravel drainage layer placed above the native Vertisol subgrade. The engineered filter media was assigned a conservative infiltration rate of 35 mm/h (Aboukarima et al., 2018) and an effective porosity of 0.2 for active water storage and transmission (Frings et al., 2011; Nimmo, 2004), while the gravel layer porosity was taken as 0.25, consistent with fluvial sand–gravel mixtures (Frings et al., 2011). Locally adapted wet–dry-tolerant vegetation was planted to promote evapotranspiration and pollutant removal (Fig. 6.4a).

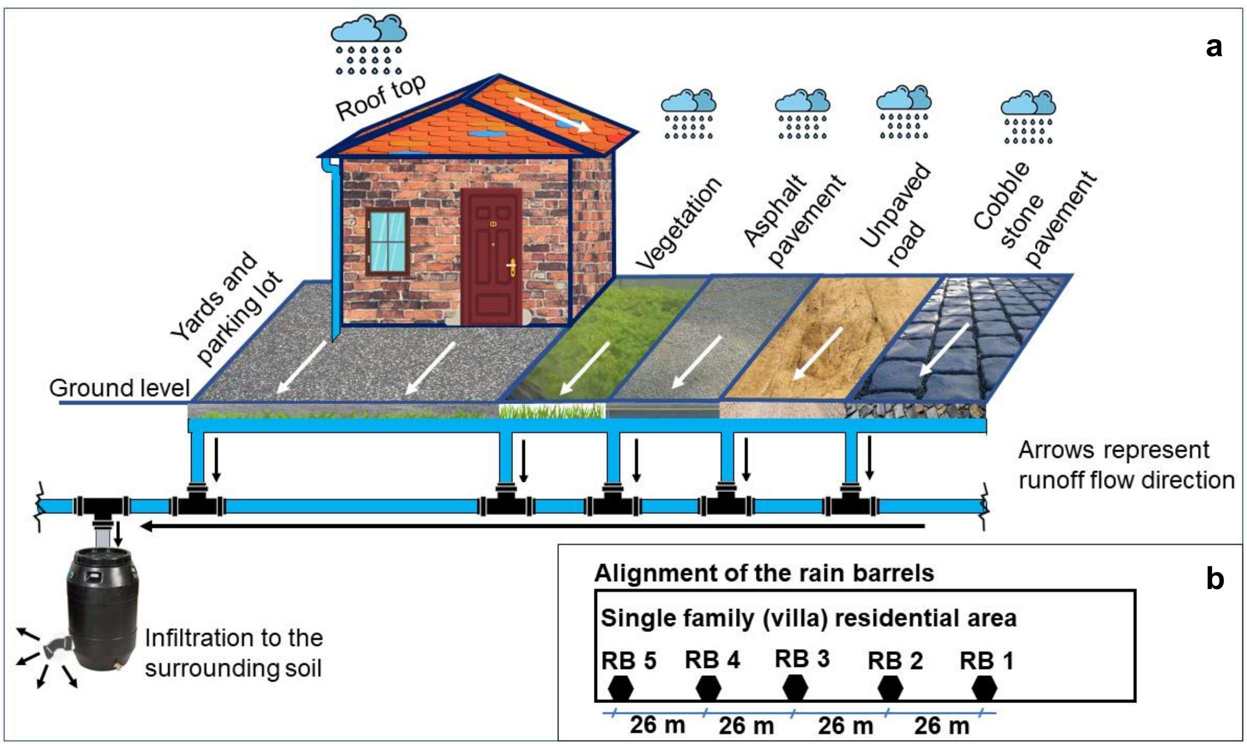

Figure 6.3: (a) Schematic of the buried RBs system showing runoff from multiple land covers (roof, parking lots, yards, vegetation, unpaved roads, asphalt, cobblestone) directed to the barrel via a T-junction; excess water bypasses the barrel (b) Top view of five RBs (RB_1 – RB_5) aligned at 26 m intervals along the 130 m side of the 2.09 ha pilot sub-catchment. Key components labeled

Buried RBs: Five buried RBs were installed along the lower boundary to provide secondary detention and water-quality polishing (Fig. 6.3, 6.4b). Each barrel has a total capacity of 0.42 m^3

(effective 0.4 m^3) and is spaced 26 m apart, collectively providing ≥ 2 m^3 of distributed detention. The barrels are embedded in a sand filtration bed, with ball-tanker check valves regulating inflow and outflow. Downstream pipe doubling begins after the first barrel, terminating in a 75 cm outlet with a 45° elbow to control discharge over the underlying low-permeability Vertisol. The RBs capture residual runoff from roofs, roads, vegetation, yards, and parking areas, complementing the RG by providing additional temporary storage and polishing. Five RBs (one every 26 m along the 130 m lower boundary) were installed to provide distributed detention (total ≥2 m^3). The 0.4 m^3 effective capacity per barrel was sized using PCSWMM simulation of the 2-year, 3-hour design storm (86 m^3 30% of the total runoff volume). The target was to capture the initial 2–3% of runoff (first flush) and pollutant removal.

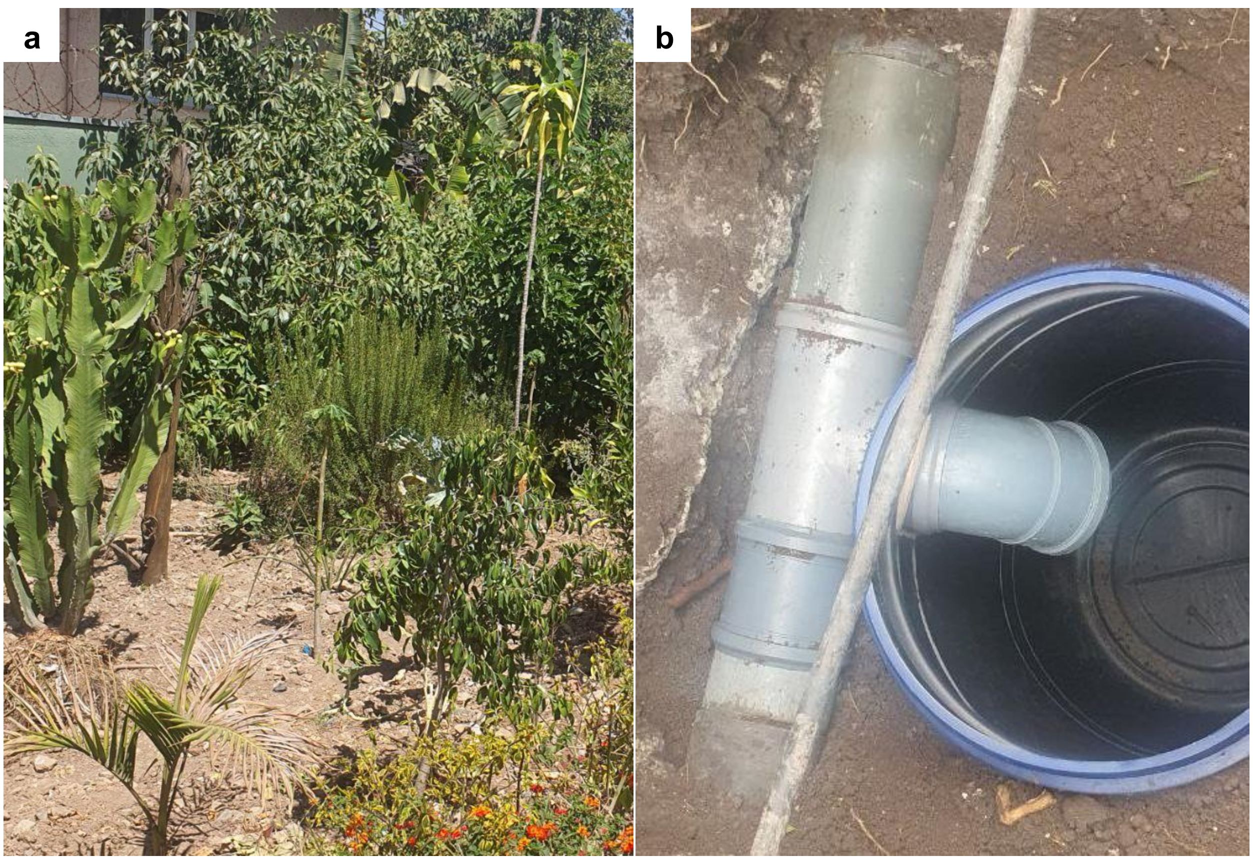

Figure 6.4: Sample picture of a) RG development on the field and b) RB installation

RG-RB Integration: The RG and buried RBs were designed as an IGGI system to manage runoff from a 2-year return-period, 3-hour Chicago hyetograph. PCSWMM simulations for the S_{16} sub-catchment produced 286.1 m^3 of runoff with a peak discharge of 0.1236 m^3/s. The IGGI system was hypothesized to reduce total runoff volume and associated pollutant loads by approximately

30% (86 m^3), through infiltration, temporary storage, and distributed detention. Pollutant load reduction arises from both the lower runoff volume and removal processes within the engineered sandy-loam media and vegetation.

Subsurface storage in the RG was estimated from the porosity of the engineered sandy-loam (0.3 m × 1,000 m^2 × 0.2) and gravel (0.1 m × 1,000 m^2 × 0.25) layers, yielding 85 m^3. Combined with 2 m^3 in the RBs, this configuration allows controlled percolation to the native Vertisol, rapid infiltration within the filter media, and minimal surface ponding, reducing health and nuisance risks. The total depth (0.6 m) follows bioretention design guidelines (Davis et al., 2009): 0.2 m ponding for design storm storage, 0.3 m engineered media for infiltration and pollutant removal, 0.1 m gravel drainage for underdrain function. These thicknesses are standard for rain gardens in clay soils (Sharma and Malaviya, 2021). Furthermore, the piloted IGGI system is designed for neighborhood scale (0.8–2 ha contributing area). Household-scale (individual rain barrels) and catchment-scale (>30 ha) applications would require modification of RB density and RG sizing.

Field Implementation, Collaboration, and Economic Assessment: The system was implemented from September 2024 to August 30, 2025, through collaboration among researchers, field technicians, excavation workers, local Woreda officials, and neighborhood committee members.

The overall cost for the five RBs, which includes the barrels, fittings, and excavation, was 14,100 ETB per unit. The RG with 0.1 ha size and 0.6 m depth required excavation, sandy loam backfill, and vegetation/landscaping, costing a total of 400,000 ETB. The costs were standardized per hectare. Also, the costs were translated into USD (1 USD = 143.31 ETB). This shows an easier-to-implement and economical city stormwater management method.

6.2.5 Model Execution

Simulation Parameters: The model is designed for improved incorporation of IGGI in a contributing zone of a micro-watershed which is characterized by steep slope and poorly draining soil. Simulations were performed with 3-hour Chicago hyetographs in the baseline scenario, derived from 30-years of daily rainfall data used to develop the IDF curves. We selected the Chicago hyetograph method, which is commonly applied to urban drainage design, particularly in areas that receive heavy rainfall over short time periods (Back, 2024; Balbastre-Soldevila et al., 2019; Liao et al., 2021; J. Yang et al., 2022; Zhou et al., 2019). This technique is known for its easy and efficient estimation of peak runoff, which is important in designing stormwater systems in urban catchments that have fast responses. The dynamic wave routing method was applied using a computational time step of 5 seconds. The modeling specified a mass-balance error tolerance of ≤10%, which is in line with SWMM-based simulation recommendations (Rossman, 2010). It made sure of stability and well-continuous performance. The simulation structure for various activities spanned rainfall-runoff model, flow routing, and water quality model for IGGI efficiency evaluation. The modified Green-Amp method was employed for simulating the infiltration process, while routing was handled using the dynamic wave approach. The performance of IGGI strategies was quantified through the analysis of hydrologic and water quality outputs. The hydrologic outputs being considered are runoff volume (m^3) and peak flow rate (m^3/s). Outputs related to water quality concentrated on pollutant concentrations (mg/L) and pollutant loads (kg). IGGI has the potential to significantly reduce stormwater runoff and improve water quality in urban areas.

6.2.6 Scenario Design

Four scenarios were developed to assess the performance of IGGI in handling stormwater under changing conditions: baseline, climate change, urbanization, and combined impact. As outlined in Table 6.2, these scenarios simulate hydrological responses and water-quality outcomes pertaining to climate, land use, or infrastructure change. The RG incursions and buried RBs enacted IGGI strategies, as discussed in Section 6.2.4.

The four simulated conditions of the baseline scenario using the historical climate series of 2-year and 10-year return period, with existing land uses. The 2-year return period represents frequent storms (50% annual exceedance probability) that dominate annual runoff volume and is the standard design event for LID/IGGI (Zahmatkesh et al., 2015; Adhikari et al., 2024). The 10-year return period (10% annual exceedance probability) tests IGGI performance under moderately extreme events. The first two conditions were on the pilot sub-catchment (S_{16}, 20,900 m^2), where GI was physically installed, and without IGGI. The actual footprint of RG installed (1,000 m^2) as well as the five standard 400 l buried RBs (which have an equivalent footprint of 2 m^2) is less than 10% of the sub-catchment. The “percent of area treated” input in PCSWMM was set to 40%. This is the percentage of pervious and impervious surfaces impacted by the IGGI system that was determined through trial-and-error to provide optimum runoff and pollutant load reduction. Because of practical constraints related to land access, funding, and stakeholder engagement, the 2.09ha sub-catchment was selected. The performance of the system was subsequently calibrated and validated against observed stream flow and pollutant data at the site outlet (OF2; Fig. 6.2, Section 6.2.3).

The third and fourth baseline conditions simulated the whole 30 ha study area: one without any GI intervention (which was already calibrated and validated at the OF1, the contributing zone of the micro-watershed outlet), and one with simulated IGGI covering 40% of the total area for treatment (not a physical installation). By presenting possible outcomes, they can be used to judge those of broader GI.

The climate change scenario assesses how the system reacts to climatic changes projected using SSP2-4.5 and SSP5-8.5 for near- and mid-term (2024-2053 and 2054-2083) periods at a 2-year and 10-year return period. The present status of land use was maintained, and the scenario was simulated with and without 40% IGGI treatment coverage that helped quantify IGGI mitigation under future climate scenarios.

The Urbanization Scenario models the impact of increased imperviousness of 80% over two years to represent a more urbanized solution from baseline 70% (3.8% urbanization rate, UN-Habitat, 2017). Model simulations were conducted using historical climate data for a 2-year return period of storms, without and with 40% IGGI treatment, to estimate the potential of IGGI to offset urbanization impacts.

Ultimately, the Combined Impact Scenario refers to the most unfavorable conditions in which the climate change of a 2-year return period and 80% imperviousness is used. As per SSP2-4.5 and SSP5-8.5 in the provincial cities would be considered. This scenario was run with and without 40% IGGI overlay to observe the effectiveness of integrated infrastructure approaches under simultaneous climate and land use pressures.

Table 6.2: Summarizes four scenarios, their design, and their main characteristics.

Scenario	Infrastructure	Climate Data	Land Use	GI Coverage	Implementation Type
Baseline (Entire area and S_{16})	Grey	Historical	Existing	None	Simulated
	IGGI	Historical	Existing	40%	Actual (S_{16}) and Simulated (entire micro-watershed)
Climate Change (Entire area)	Grey	SSP2-4.5, SSP5-8.5	Existing	None	Simulated

	IGGI	SSP2-4.5, SSP5-8.5	Existing	40%	Simulated
Urbanization (Entire area)	Grey	Historical	Projected (80% impervious)	None	Simulated
	IGGI	Historical	Projected (80% impervious)	40%	Simulated
Combined Impact (Entire area)	Grey	SSP2-4.5, SSP5-8.5	Projected (80% impervious)	None	Simulated
	IGGI	SSP2-4.5, SSP5-8.5	Projected (80% impervious)	40%	Simulated

6.2.7 Model Performance

Analysis of Sensitivity: Some key parameters affecting model outputs were identified using SRTC which included the sub-catchment area, width, imperviousness, and Manning roughness of both the pervious and impervious areas. A one factor at a time (OAT) approach was then applied to GI elements (e.g., RBs and RGs) to quantify their effect on peak flow attenuation and pollutant removal efficiency. The uncertainty ranges for these parameters are summarized in Table 6.3, as suggested by (Akhter and Hewa, 2016; James, 2005; Kemal et al., 2025b).

Table 6.3: Sensitivity analysis parameter for calibration of stormwater runoff

Compartment	Notation	Calibration parameter	Uncertainty value (%)
Surface	Area	Sub-catchment area	±10
	Width	Sub-catchment width	±100
	Imperv. %	Impervious Percentage	±25
	N perv	Manning roughness for pervious area	±25
	N Imperv	Manning roughness for impervious area	±25
Transport	Geom 1	Geometry and maximum depth of conduits	±25
	Roughness	Manning roughness of conduits	±25
RB	Capacity	Storage capacity	±20
	Drainage time	Emptying time	±25
RG	Depth	Soil depth	±25

Calibration and Validation: The stormwater model was calibrated and validated sequentially for flow and pollutant loads using PCSWMM's SRTC module, first optimizing hydrologic parameters and then adjusting water-quality parameters. Pre-IGGI calibration covered the entire study area and sub-catchment S_{16}, while post-IGGI calibration focused on S_{16} only, using observed streamflow depths and laboratory-analyzed pollutant concentrations from representative samples collected at the outlet. Grey infrastructure calibration used storm events on August 12 and September 2, 2024, with validation on August 23 and September 23, 2024. IGGI scenario calibration used events on June 22, June 28, and July 30, 2025, with validation on July 15 and August 10, 2025, after RB installation and RG construction (September 2024–February 2025). Rainfall inputs were matched to observed event dates for hydrological consistency. The results and performance of the models were assessed by comparing the simulated runoff depth and pollutant concentrations at OF1 (pre-IGGI, whole area) and OF2 (pre- and post-IGGI, S_{16}) locations with the observed runoff depth and pollutant concentrations.

Metrices of Performance: The model performance was evaluated using three statistical parameters, which include the Nash-Sutcliffe Efficiency (NSE; Eq. 6.3), the RMSE-standard deviation ratio (RSR; Eq. 6.6), and the Integral Square Error (ISE; Eq. 6.7). A NSE equal to or greater than 0.8 is indicative of good fit for the model, while an RSR equal to or less than 0.5 indicates an adequate fit. For ISE, values < 3 represent "Excellent" performance, whereas values > 25 reflect "Poor" performance. Although these deterministic metrics provide robust performance evaluation, they do not include uncertainty bands or confidence intervals.

$$\mathrm{NSE} = 1 - \left(\frac{\left(\sum_{i=1}^{n}\left(\boldsymbol{Y}_{obs}^{i} - \boldsymbol{Y}_{sim}^{i}\right)^{2}\right)}{\sum_{i=1}^{n}\left(\boldsymbol{Y}_{obs}^{i} - \overline{\boldsymbol{Y}_{obs}}\right)^{2}}\right) \tag{6.3}$$

$$\mathrm{RMSE} = \frac{\sqrt{\sum_{i=1}^{n}\left(Y_{obs}^{i} - Y_{sim}^{i}\right)^{2}}}{n} \tag{6.4}$$

$$S_{obs} = \left[\sum_{i=1}^{n}\left(Y_{i}^{obs} - Y^{mean}\right)^{2}\right] \tag{6.5}$$

$$RSR = \frac{RMSE}{STDEVA_{obs}} \tag{6.6}$$

$$ISE = \frac{\left(\sqrt{\sum\left(y_{obs}^{i} - y_{sim}^{i}\right)^{2}}\right)}{\sum y_{obs}^{i}} x\ 100\ \% \tag{6.7}$$

where: $y_{obs}^{i} =$ the observed value for the i^{th} observation, y_{sim}^{i} = the simulated value for the i^{th} observation, n = the number of observed/computed values.

IGGI Performance Evaluation: The effectiveness of IGGI implementation was assessed by comparing baseline (pre-IGGI) and IGGI-enhanced scenarios using simulated hydrologic and water quality outputs at outlet OF1 (representing the entire watershed) and outlet OF2 (representing Sub-catchment S_{16}), as shown in Fig. 6.2 of Section 6.2.3. The same evaluation procedure was applied to all remaining scenarios.

Hydrologic effectiveness: percentage reduction in total runoff volume (eq. 6.8).

$$\mathrm{R}_{\text{runoff}} = \left(\frac{V_{baseline} - V_{IGGI}}{V_{baseline}}\right) * 100 \tag{6.8}$$

Peak runoff reduction: percentage reduction in peak flow rate (eq. 6.9).

$$\mathrm{R}_{\text{peak}} = \left(\frac{Q_{baseline} - Q_{IGGI}}{Q_{baseline}}\right) * 100 \tag{6.9}$$

Pollutant removal efficiency: percentage reduction in pollutant concentration (eq. 6.10).

$$\mathrm{R}_{\text{pollutant (C)}} = \left(\frac{C_{baseline} - C_{IGGI}}{C_{baseline}}\right) * 100 \tag{6.10}$$

Pollutant removal efficiency: percentage reduction in pollutant load (eq. 6.11).

$$R_{\text{pollutant (L)}} = \left(\frac{L_{baseline} - L_{IGGI}}{L_{baseline}}\right) * 100 \tag{6.11}$$

Where $V_{baseline}$ and V_{IGGI} are the total runoff volumes before and after IGGI implementation, respectively; $Q_{baseline}$ and Q_{IGGI} are the peak flow rates under baseline and IGGI scenarios; $L_{baseline}$ and L_{IGGI} are the total pollutant loads before and after IGGI integration; and $C_{baseline}$ and C_{IGGI} are before and after IGGI implementation.

6.2.8 Conceptual Framework

The conceptual framework of this study presented in Fig. 6.5 follows four core phases: data collection, preparation, analysis, and comparative evaluation. Data were gathered from diverse sources, including historical and CMIP6-GCM-projected climate data, land use/land cover, a high-resolution DEM, soil properties, stormwater depth observations, stormwater quality samples, and detailed hydraulic configurations. These datasets were preprocessed within a GIS environment to delineate the micro-watershed (30-hectares) and define the 2.09-hectare pilot contributing zone. The PCSWMM platform was employed to simulate four scenarios: (1) baseline (calibrated and validated), (2) future climate change, (3) projected urbanization, and (4) combined climate-urban scenarios—each assessed with and without the IGGI intervention. The analysis compared conventional grey infrastructure to a novel IGGI design integrating buried RBs and RGs. Outputs, including runoff volume, peak flow, pollutant concentration, and pollutant loads, were evaluated to determine the hydrological and water quality performance and resilience contribution of the IGGI system.

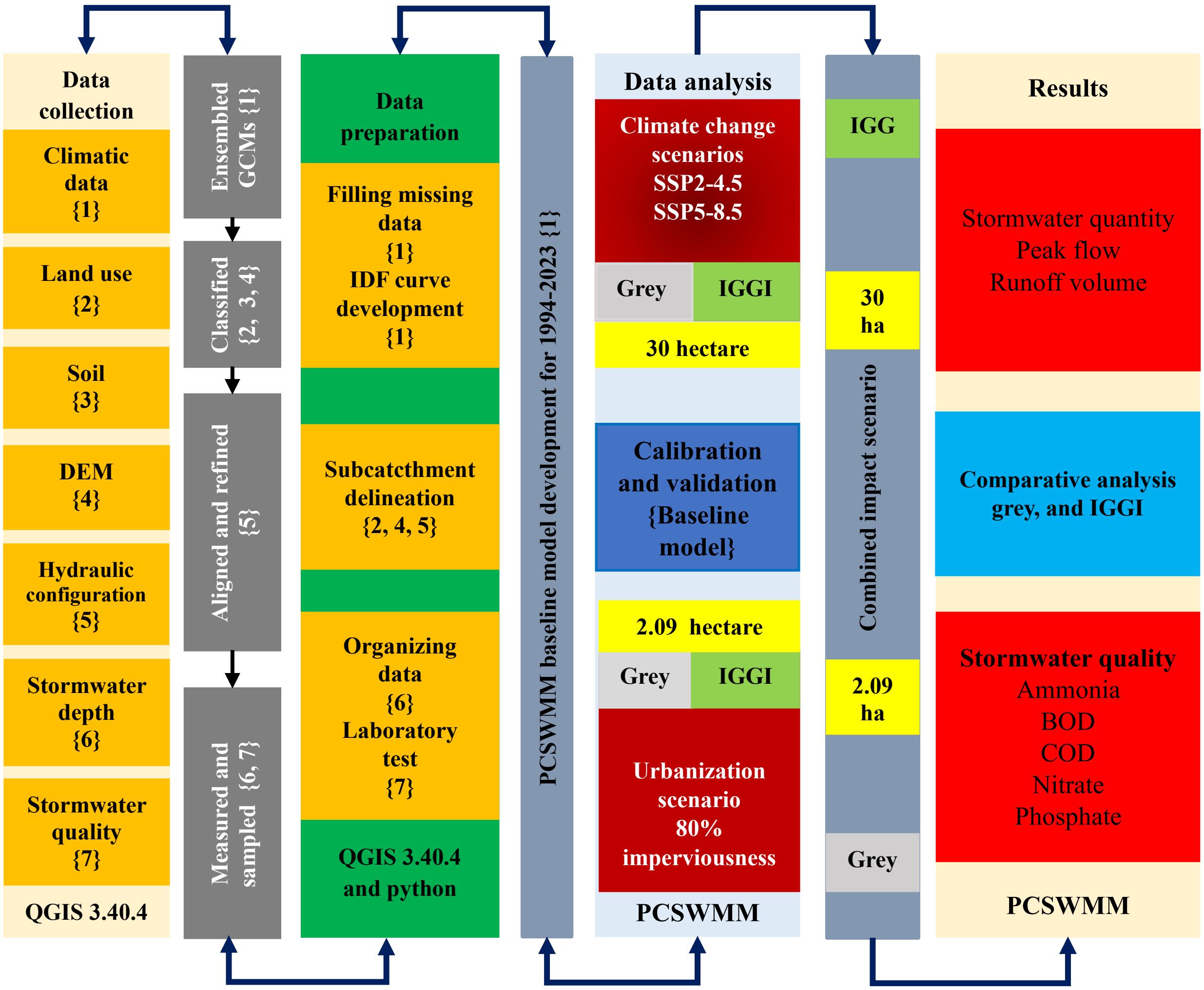

Figure 6.5: Conceptual framework designed for this study

6.3 Results

The result section includes the finding of the model pre- and post IGGI implementation in an effort to improve the integration mechanism of IGGI. This section included 2-year return period IDF curve for the baseline and climate scenarios, model performance evaluation result, pre- and post-IGGI runoff (peak and volume), and pre- and post-IGGI pollutant (concentration and load) for baseline (for the entire area, and S_{16} only), climate change (entire area), urbanization (entire area) and combined impact scenario (entire area).

6.3.1 IDF Curves and Performance Evaluation

IDF Curve Result: The IDF curves generated from both historical data for 2- and 10-year return period and ensembled CMIP6-GCM projections for 2-year return period, are presented in Fig. 6.6. These curves illustrate an increase in rainfall intensity under future climate scenarios, with intensities rising progressively from the historical baseline to the near-term and mid-term projections.

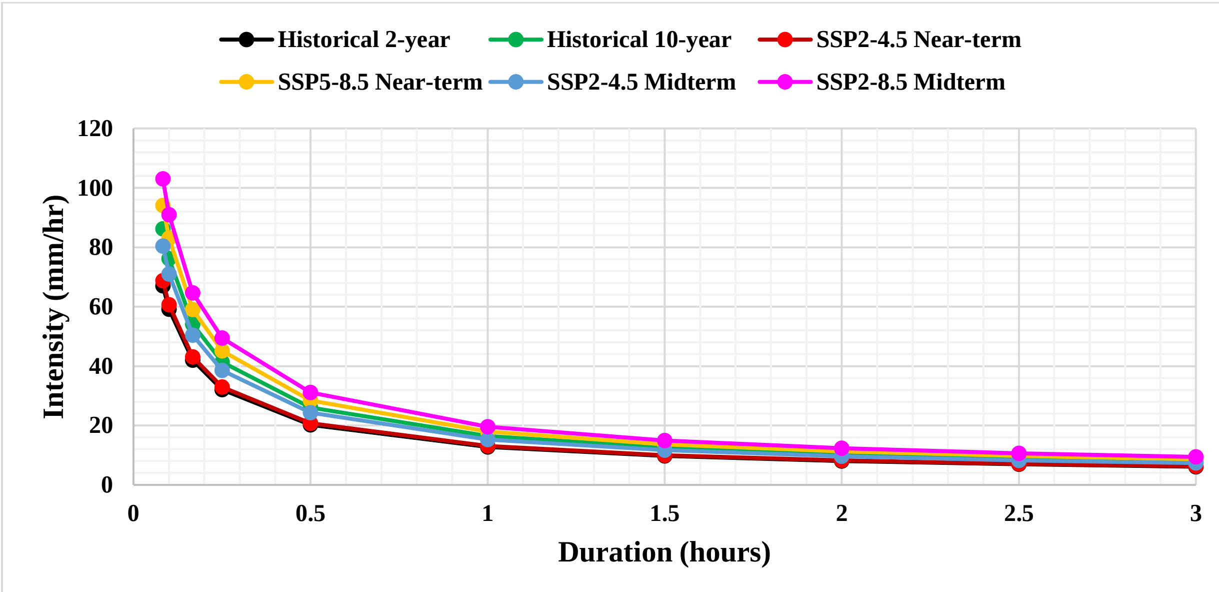

Figure 6.6: IDF curves for the Ayertena station, showing 2-, and 10-year return period historical rainfall data (1994–2023) and projected rainfall under SSP2-4.5 and SSP5-8.5 scenarios for the near-term (2023–2052) and midterm (2053–2082) periods

Performance Evaluation Results: Runoff quantity calibration using stormwater runoff depth for the S_{16} sub-catchment (pre-IGGI) using data from August 12 and September 2, 2024 yielded NSE = 0.76, 0.82, RSR = 0.49, 0.36, and ISE = 6.2, 5.2; validation on August 23 and September 23 gave NSE = 0.71, 0.73, RSR = 0.56, 0.41, and ISE = 8.7, 6.5. Post-IGGI calibration (June 22, June 28, and July 30, 2025) showed improvements with NSE = 0.81–0.84, RSR = 0.44–0.41, and ISE = 4.8–3.6; validation (July 15 and Aug 10) gave NSE = 0.78–0.8, RSR = 0.48–0.45, and ISE = 5.3–4.2. For the 30-ha watershed (pre-IGGI only), calibration and validation showed NSE = 0.7–0.9, RSR = 0.42–0.54, and ISE = 2.46–4.25, as presented in Fig. 6.7, and 6.8.

Stormwater quality for stormwater parameter including ammonia, BOD, COD, nitrate, and phosphate in S_{16} pre-IGGI showed calibration ranges of NSE = 0.68–0.75, RSR = 0.51–0.59, and ISE = 6.9–9.8; validation gave NSE = 0.64–0.72, RSR = 0.54–0.6, and ISE = 7.4–10.3. Post-IGGI quality calibration gave NSE = 0.77–0.83, RSR = 0.42–0.49, and ISE = 4.1–6.3; validation resulted in NSE = 0.73–0.8, RSR = 0.44–0.51, and ISE = 4.7–6.9. In the 30-ha watershed (pre-IGGI only), quality calibration showed NSE = 0.61–0.8, RSR = 0.45–0.62, and ISE = 4.31–6.2 as presented in Fig. 6.9.

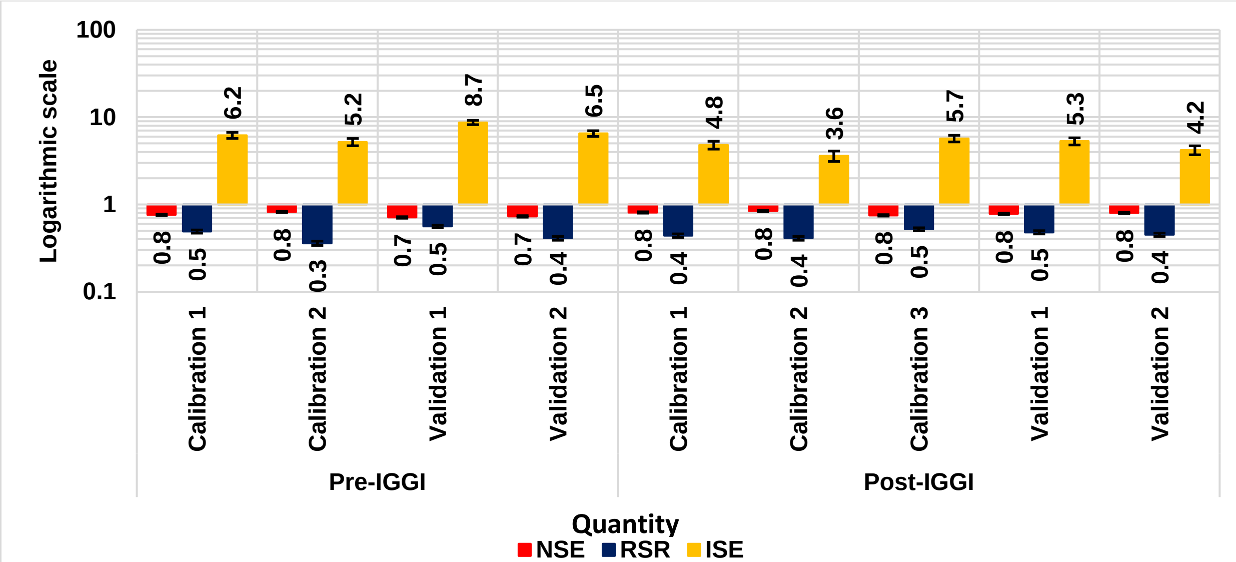

Figure 6.7: Evaluation of water quantity of S_{16} during the pre-IGGI period includes calibration 1 on August 12, validation 1 on August 23, calibration 2 on September 2, and validation 2 on September 23, 2024. The post-IGGI evaluation includes calibration 1 on June 22, calibration 2 on June 28, validation 1 on July 15, calibration 3 on July 30, and validation 2, August 10, 2025

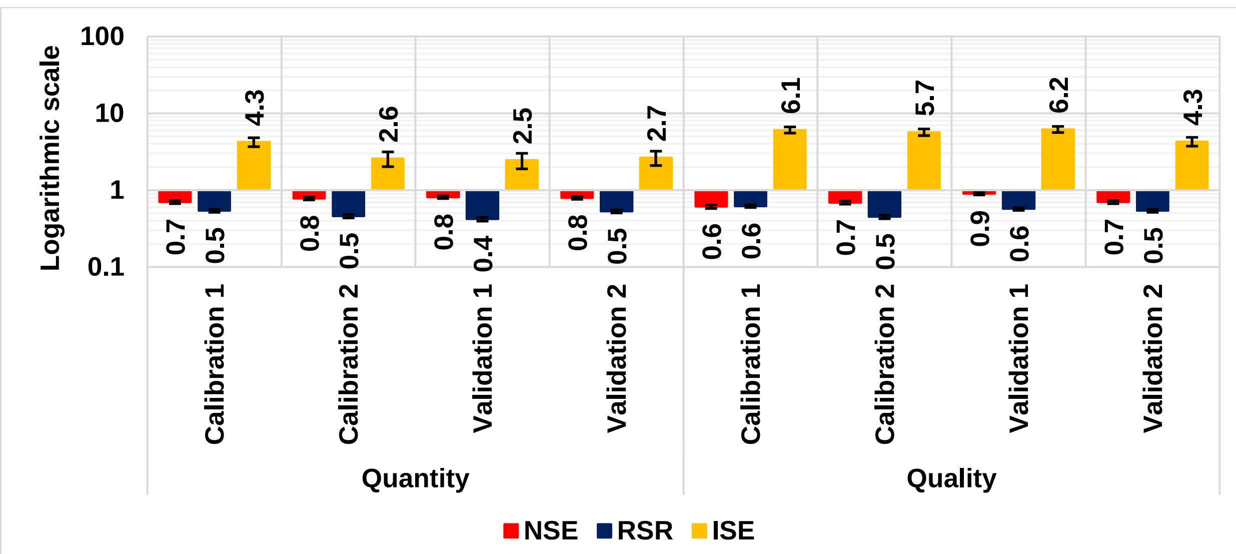

Figure 6.8: Evaluation of entire area during the pre-IGGI period includes calibration 1 on August 12, validation 1 on August 23, calibration 2 on September 2, and validation 2 on September 23, 2024

Evaluation of IGGI Effectiveness: The IGGI system markedly improved stormwater management performance across both the pilot sub-catchment (S_{16}) and the entire area under 2-year and 10-year return periods. Under the 2-year event, total runoff volume decreased by 23.2% for S_{16} (286.1 →

219.8 m^3) and 29.6% for the entire area (5,179 → 3,648 m^3), with peak runoff reductions of 41.1% and 43.5%, respectively. Load reductions of pollutant were found to be in the range of 30.9–33.7% in S_{16} and up to 36.4–41.1% at the watershed scale. Phosphate showed the maximum (41.1%) and COD showed the minimum (36.4%) reductions.

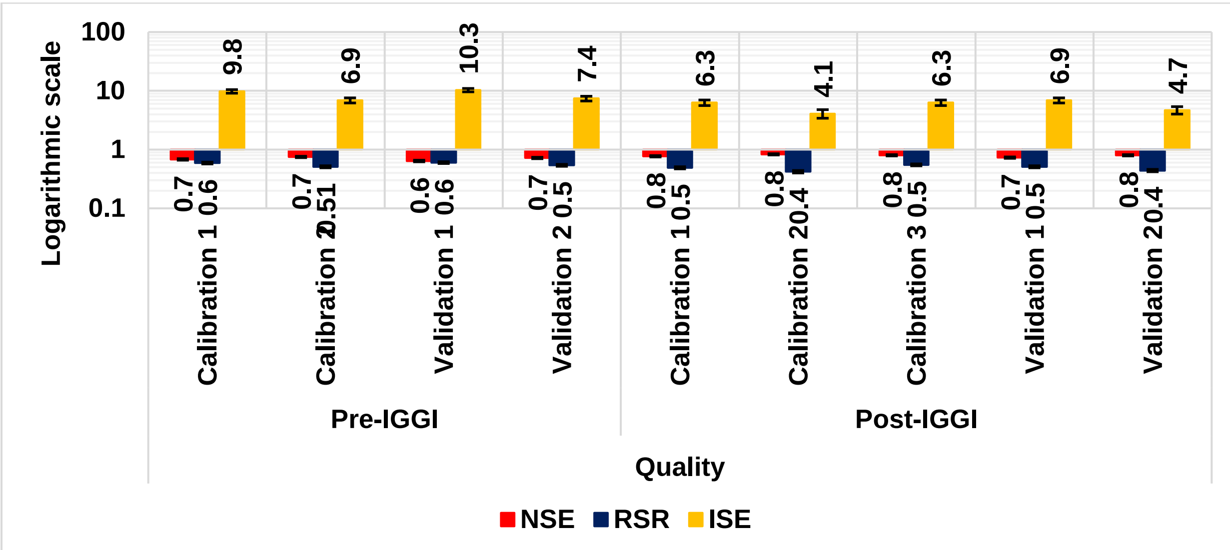

Figure 6.9: Evaluation of water quality of sub-catchment S_{16} during the pre-IGGI period includes calibration 1 on August 12, validation 1 on August 23, calibration 2 on September 2, and validation 2 on September 23, 2024. The post-IGGI evaluation includes calibration 1 on June 22, calibration 2 on June 28, validation 1 on July 15, calibration 3 on July 30, and validation 2, August 10, 2025

For the more extreme 10-year event, IGGI maintained substantial effectiveness, achieving a 30.6% reduction in peak runoff (from 5.183 to 3.042 m^3/s) and 28.3% in total volume (from 7,143 to 5,126 m^3) over the total watershed. The reductions in relevant pollutant loads were 36.4%–41.1% (Table 6.4). The increase in scale and reliability of IGGI to reduce runoff quantity and runoff pollutant loads was evident from these results. However, it was also seen that rare extremes may require additional grey infrastructure support.

Table 6.4: The efficiency of reduction of pollutant loads, with reference to the baseline, in percentage values

Pollutant	S_{16} (2-y)	S_{16} (10-y)	Entire area (2-y)	Entire area (10-y)
Ammonia	33.4	40.9	33.4	40.9
BOD	33.5	40	33.5	40
COD	30.9	36.4	30.9	36.4

Nitrate	33	39.4	33	39.4
Phosphate	33.7	41.1	33.7	41.1

A pre- and post-implementation stormwater balance check confirmed the model's hydrologic consistency, with continuity errors ≤10%. IGGI lowered surface runoff, increased temporary storage, and improved pollutant retention (water balance results are shown in Appendix L, Appendix Table 14).

6.3.2 Cost Analysis

As per the report, the total capital cost of the IGGI System for 0.836 ha without operation and maintenance (OandM) cost was about 3,283 USD, with each hectare costing 3,928 USD. Table 6.5 shows that RBs were considerably cheaper (589 USD/ha) than RG, as RG needs higher material and soil preparation costs compared to RG. The findings suggest the IGGI deployment cost is reasonable compared to the costs of conventional IGGI. Future studies must consider O&M costs to provide an overall economic assessment.

Table 6.5: The cost involved in implementing IGGI components (RBs and RG)

Component	Unit cost (ETB/unit or m^3/lump sum)	Quantity / Volume	Total cost (ETB)	Total cost (USD)	Area treated (ha)	Cost per ha (USD)
RBs (5 units incl. fittings and excavation)	14,100 ETB/barrel	5 barrels	70,500	492	—	—
RG (Sandy loam)	Excavation: 200 ETB/m^3, Backfill: 250 ETB/m^3, Vegetation lump sum: 40,000 ETB	800 m^3 over 0.1 ha	400,000	2,791	—	—
Combined IGGI (0.836 ha)	—	—	**470,500**	**3,283**	**0.836**	**3,928**

Exchange rate: 1 USD = 143.31 ETB, Date: December 2024

Total capital cost was 3,283 USD for 0.836 ha (3,928 USD/ha). This is lower than reported costs for conventional GI in developed countries (5,000–15,000 USD/ha for bioretention; Vineyard et al., 2015).

6.3.3 Baseline Scenario Findings Pre- and Post- IGGI

IGGI system implementation improved hydrological and water quality performance at sub-catchment (S_{16}) scale and entire area scale for 2-year and 10-year return periods of the baseline scenario (Table 6.6). For the 2-year return period, peak flow and total runoff volume declined by 40% (0.1236 → 0.07415) and 46% (286.1 → 154.5) at S_{16}, and by 43.5% (3.64 → 2.058) and 36.7% (5,179 → 3,276) across the entire area, respectively. In accordance with this, total pollutant loads were cut back by 47–57% at S_{16} and by 37–42% at watershed scale, with phosphate and BOD showing the highest removal efficiencies. The concentrations of pollutants experienced minor variances (indicating stable background levels), while the mass of the total pollutant value reduced significantly, indicating the effectiveness of IGGI in improving detention, infiltration, and trapping of pollutants.

In the baseline scenario for a return period of 10 years, the IGGI system recorded adequate performance despite a higher rainfall intensity. Peak flow decreased by 30.6% (5.183 → 3.042 m^3/s) and total runoff volume by 28.3% (7,143 → 5,126 m^3) across the entire area. The peak flow at S_{16} reduced by 1.6% (0.1796 → 0.1768 m^3/s), whereas the total runoff reduced by 23.1% (388.3 → 298.3 m^3). Major parameters showed pollutant load reductions of 36.4 to 41.1%, for entire area. The highest removal efficiencies for COD and phosphate again indicate the IGGI's robustness and scalability for reducing stormwater volume and quality impacts but may require additional grey infrastructure in rare extreme events. Pollutant load reduction (36.4–41.1%) results from three mechanisms: (1) volume reduction (36.7%) – less runoff means less total pollutant mass exported; (2) sedimentation – RBs and RG ponding zones allow settling of particle-bound pollutants; (3) filtration and adsorption – engineered RG media (sandy-loam) filters TSS and adsorbs phosphorus.

Table 6.6: The hydrological and pollutant load reduction from baseline scenarios due to IGGI implementation, the comparison involved different catchment areas over 2- and 10-year return periods.

Parameter	Return period	S_{16} pre-IGGI	S_{16} post-IGGI	Reduction (%)	Entire area pre-IGGI	Entire area post-IGGI	Reduction (%)
Peak flow in m^3/s	2-y	0.1236	0.07415	40	3.64	2.058	43.5
Peak flow in m^3/s	10-y	0.1796	0.1768	1.6	5.183	3.042	30.6

Total runoff in m^3	2-y	286.1	154.5	46	5,179	3,276	36.7
Total runoff in m^3	10-y	388.3	298.3	23.1	7,143	5,126	28.3
Pollutant concentration in mg/L							
Ammonia	2-y	3.2	2.8	11.6	3	3	0
	10-y	3.2	3.1	2.7	3.01	3	0.3
BOD	2-y	21	18.5	11.9	20	20	0
	10-y	21	20.4	2.8	20.01	20	0.05
COD	2-y	262	258.3	1.4	185.3	153.3	17.3
	10-y	262	261.1	0.3	202.9	179	11.8
Nitrate	2-y	3.7	3.3	10	5	5	0
	10-y	3.7	3.6	2.4	5	5	0
Phosphate	2-y	3.3	2.9	12.4	2.8	2.07	26.3
	10-y	3.3	3.2	2.9	3.1	2.7	10.4
Pollutant load in kg							
Ammonia	2-y	0.9	0.4	55.4	18.5	10.7	42.1
	10-y	1.3	0.9	26.3	25.6	16.9	33.9
BOD	2-y	6	2.7	56.1	109.8	64.5	41.2
	10-y	8.2	6	26.5	151.5	101.7	32.9
COD	2-y	75.4	39.8	47.2	1,363.1	855.9	37.2
	10-y	102.3	78.2	23.6	1,879.7	1,339.7	28.7
Nitrate	2-y	1	0.5	55.1	19.33	11.5	40.6
	10-y	1.4	1	26	26.7	18.1	32.2
Phosphate	2-y	0.9	0.4	56.8	21.3	12.3	42.4
	10-y	1.3	0.9	26.7	29.3	19.4	33.9

Differences of less than 5% are described as “unchanged” in the text.

The lower percentage reduction for the 10-year return period occurred because storage capacity (RBs: 2 m^3; RG effective storage: 85 m^3) is fixed while runoff volume increases with storm intensity. The absolute volume reduced is similar, but percentage reduction declines due to larger denominator.

6.3.4 Climate Change Impact Pre- and Post- IGGI

Climate change scenario increased the peak runoff by 45% (3.6 → 6.6 m^3/s), and runoff volume by 42% (5,365 m^3 → 9,178 m^3). The introduction of IGGI led to a decrease in the peak flow rate and the runoff volume in all climate scenarios. Under the midterm SSP5-8.5 scenario, the peak runoff decreased by 36% (6.6 → 4.2 m^3/s) and the total runoff volume declined by 22% (9,178 → 7,151 m^3) for a return period of 2 years. Similar trends were observed in the near-term scenarios, with peaks of runoff reduction of 24% and total volume reduction of runoff of 9% Fig. 6.10. The results show that IGGI can manage increasing flood risk by reducing runoff even under the enhanced rainfall scenario used in midterm climate models with 40% GI treatment.

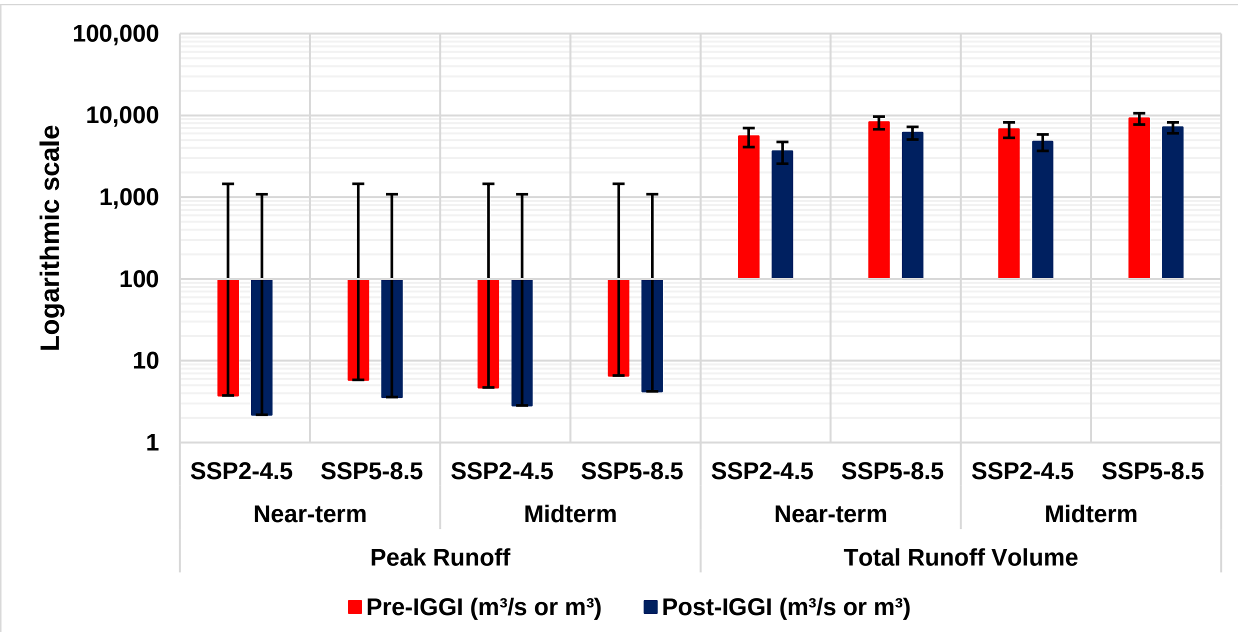

Figure 6.10: The hydrological performance (Pre- vs. Pos-IGGI) for a 2-year return period under climate change scenarios

The effect of IGGI on pollutant concentrations differed by parameter. COD and Phosphate exhibited notable reductions: COD decreased by 28.1% (213.2 → 153.3 mg/L under midterm SSP5-8.5), while Phosphate concentrations dropped by 35.31% (3.2 → 2.07 mg/L). Conversely, concentrations of ammonia, nitrate, and BOD showed no changes after IGGI (ammonia went from 3.1 to 3 mg/L, nitrate remained at 5 mg/L, and BOD remained at 20 mg/L), as shown in Fig. 6.11. The design of the IGGI seems to favor the reduction of runoff volume over changed inherent concentrations of individual pollutants of certain parameters. When looking at the effects of climate change as well, this seems like the intention.

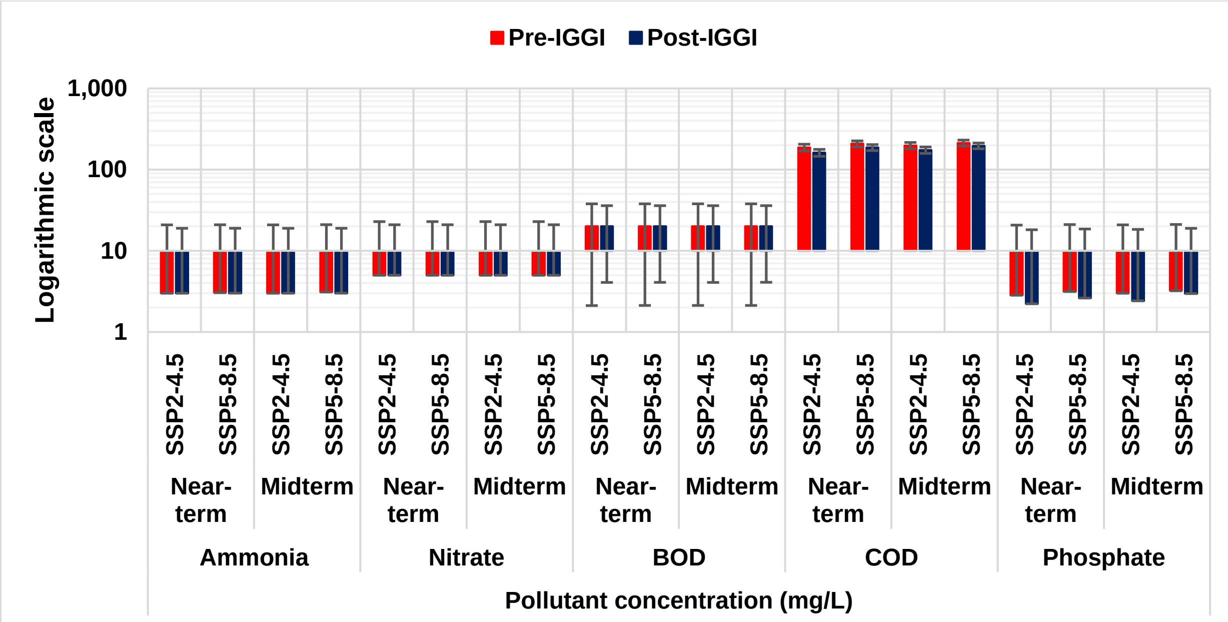

Figure 6.11: Concentration cut of pollutant under climate change scenario of 2-year return period

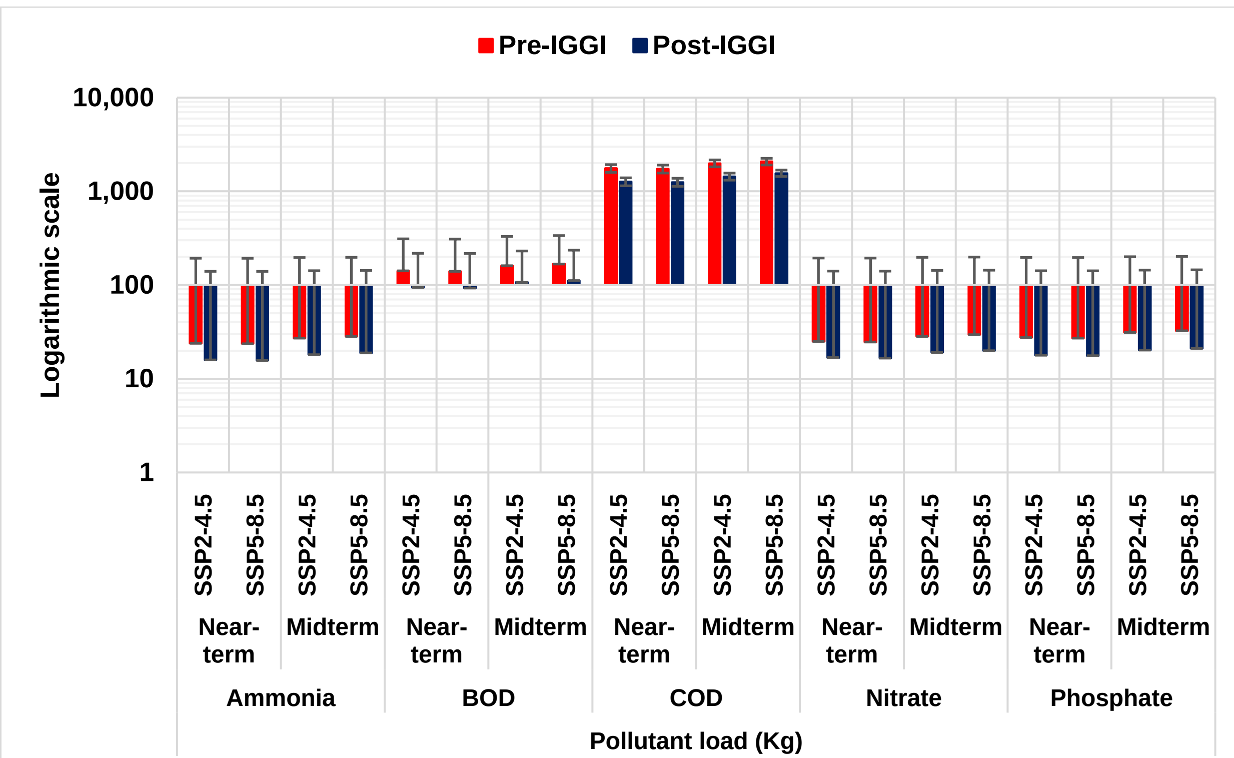

Figure 6.12: Pollutant load reductions under climate change scenarios of a 2-year return period

As illustrated in Fig. 6.12, under the climate change impact scenario, pollutant loads increased by 41.8% for ammonia (19.07 → 32.74 kg), 41.6% for BOD (113.44 → 194.23 kg), 41.5% for COD

(1,405.8 → 2,404.74 kg), 41.6% for nitrate (19.9 → 25.1 kg), and 41.6% for phosphate (21.9 → 26.94 kg). After implementation of IGGI, all pollutants decreased significantly: ammonia reduced by 28.3 percent, BOD by 27.35 percent, COD by 22.93 percent, nitrate by 26.6 percent, and phosphate by 28.35 percent. The findings indicate that IGGI is effective in enhancing water quality by reducing runoff volume and providing delayed infiltration through its controlled release mechanism, resulting in a lower total pollutant load discharged into receiving water bodies.

6.3.5 Effect of Urbanization, Pre- and Post-IGGI

The simulation result under the urbanization scenario (historical climatic data with 80% imperviousness) shows the peak runoff increased by 13.8% (3.6 → 4.1 m^3/s) and the total runoff volume increased by 10.6% (5,179 → 5,794 m^3) with an average increase in pollutant loads of 9–12%. The output also shows that IGGI can effectively reduce hydrological and water quality impacts. The IGGI systems reduced peak runoff and total runoff volume substantially, indicating better detention and infiltration capacity. The load of total pollutants was noted to have reduced significantly even though the concentrations of certain pollutants (ammonia, BOD, nitrate) did not change. This indicates that IGGI intercepted, detained, and partially treated the urban runoff before it was released into receiving water bodies. As can be seen from Appendix L, Appendix Table 14, the reductions for soluble pollutants like COD and phosphate were proportionally greater, suggesting the treatment efficacy of the IGGI system implemented.

6.3.6 Combined Impact Analysis Pre- and Post- IGGI

Under the co-occurring stresses of a 2-year return period (SSP5-8.5 midterm) and 80% imperviousness, peak runoff and runoff volume increased by 100% and 93%, respectively. The incorporation of IGGI led to a marked decrease in peak runoff and total runoff volume. The peak runoff was reduced by 29% (from 7.2 to 5.1 m^3/s under the SSP5-8.5 midterm), and the total runoff volume was reduced by 21% (from 9,897 to 7,775 m^3 under the SSP5-8.5 midterm). As presented in Fig. 6.13. IGGI is proven to be effective in managing stormwater discharge under very urbanized and climatic conditions.

IGGI resulted in a 7.4% and 8.9% reduction of COD and phosphate concentrations (COD from 216.4 to 200.4 mg/L, phosphate from 3.25 to 2.96 mg/L under SSP5-8.5 midterm). Minor reductions were observed for ammonia (3.17 to 3.01 mg/L) and BOD (20.09 to 20.04 mg/L) while the nitrates' concentrations remained constant, as shown in Fig. 6.14. IGGI is effective at removing many particulate and organic contaminants, despite stable levels of dissolved nutrients.

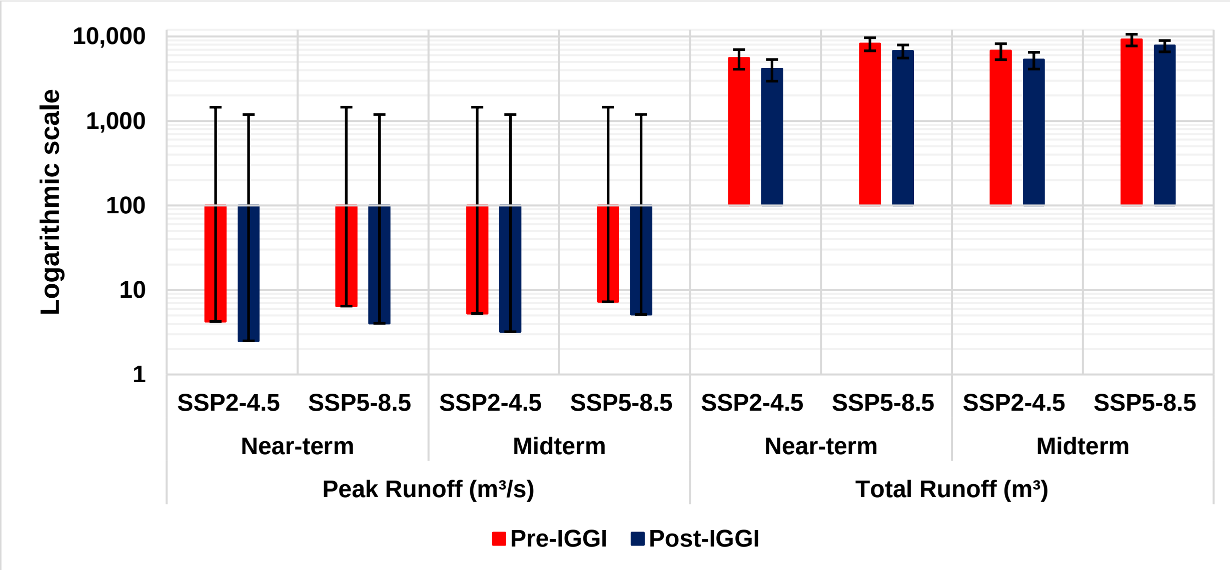

Figure 6.13: Hydrological performance under combined stressors

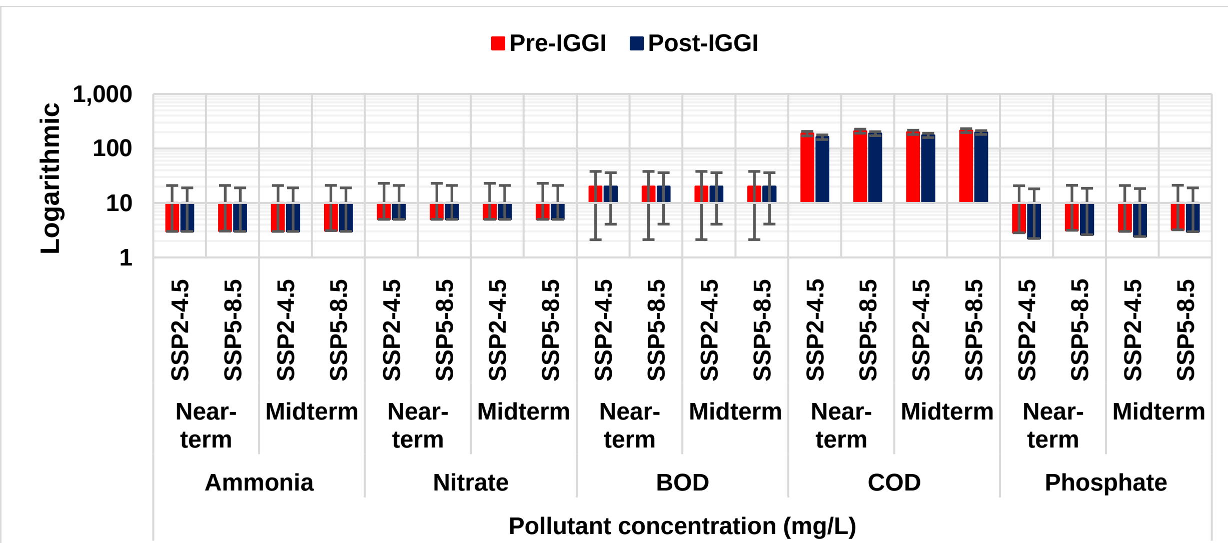

Figure 6.14: Pollutant concentration changes under combined stressors

All pollutant loads increased under the combined impact scenario: Ammonia by 46.2% (from 19.1 to 35.4 kg), BOD by 45.7% (from 113.8 to 208.8 kg), COD by 45.8% (from 1,405.8 to 2,591.4 kg), Nitrate by 45.7% (from 19.9 to 36.8 kg), and Phosphate by 45.5% (from 21.9 to 40.3 kg). With the implementation of IGGI, however, pollutant loads decreased substantially as a result of reduced runoff volumes and improved pollutant concentrations. Ammonia loads fell by 27.4% (from 35.4 to 25.7 kg), BOD by 26.3% (from 208.8 to 153.8 kg), COD by 22% (from 2,591.4 to 2,021.2 kg), Nitrate by 25.6% (from 36.8 to 27.4 kg), and Phosphate by 27.3% (from 40.3 to 29.3

kg), as presented in Fig. 6.15. These reductions emphasize IGGI's dual role in addressing both water quantity and quality challenges under compounded environmental pressures.

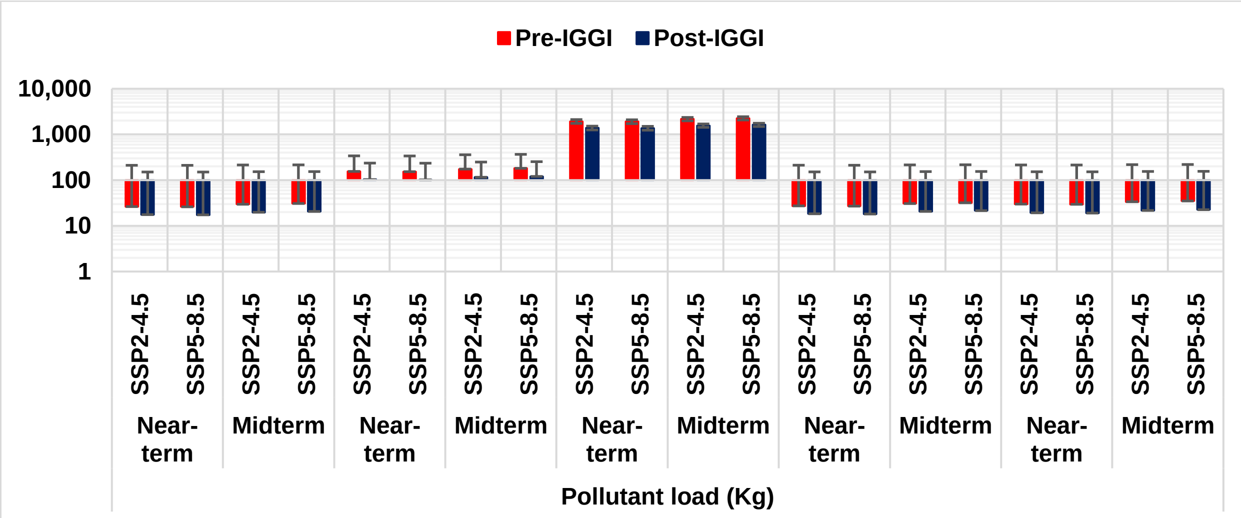

Figure 6.1: Pollutant load reductions under combined stressors

6.3.7 Integrated Comparison of Hydrologic and Pollutant Reductions

Overall result presented in Table 6.7 shows that IGGI significantly reduces runoff and pollutant loads from both common and moderate extreme storms under future urban and climate change conditions. Across the entire catchment, peak runoff reductions were 28.6–41.9% and reductions in total runoff volume were 34.2–34.8% for the 2-year and 10-year baseline events, demonstrating the ability of IGGI to moderate flow extremes, both at design and higher events. The pollutant loads of COD, BOD, ammonia, phosphate, and nitrate decreased in the order of 25–41%, and the 2-year event reduced higher than other events. Ammonia, nitrate, and BOD get diluted and treated constantly, so their concentrations remain more or less constant. On the other hand, the COD and phosphate concentrations get diluted in the final outfall by 17.7–25.3% and 24.2–24.6%, respectively, so IGGI continues to be effective.

Table 6.7: Comparison of hydrologic and pollutant reduction as a result of implementation of IGGI

Parameter	Scenario (Entire Area)	Pre-IGGI	Post-IGGI	Reduction (%)
Peak Runoff	Baseline (2-year)	3.6	2.2	41.9
(m^3/s)	Baseline (10-year)	5.2	3	41.3
	Climate change (SSP5–8.5 Midterm)	6.6	4.2	36
	Urbanization	4.1	3.2	23.5
	Combined (Climate + Urbanization)	7.2	5.1	29.4
	Baseline (2-year)	5,547	3,649	34.2

Total Runoff volume (m^3)	Baseline (10-year)	7,143	5,126	28.2
	Climate change (SSP5–8.5 Midterm)	9,178	7,126	22.3
	Urbanization	5,961	4,320	27.5
	Combined (Climate + Urbanization)	9,897	7,775	21
Ammonia Load (kg)	Baseline (2-year)	23.9	15.9	33.5
	Baseline (10-year)	25.6	18.7	26.7
	Climate change (SSP5–8.5 Midterm)	28.3	18.9	33.3
	Urbanization	21.4	12.6	41.2
	Combined (Climate + Urbanization)	30.9	20.6	33.2
BOD Load (kg)	Baseline (2-year)	141.9	94.2	33.6
	Baseline (10-year)	151.5	108.4	28.4
	Climate change (SSP5–8.5 Midterm)	167.8	111.6	33.5
	Urbanization	125.75	75.3	40.1
	Combined (Climate + Urbanization)	181.5	120.5	33.6
COD Load (kg)	Baseline (2-year)	1,761.3	1,271	27.8
	Baseline (10-year)	1,879.7	1,428.5	24
	Climate change (SSP5–8.5 Midterm)	2,082	1,564.9	24.9
	Urbanization	1,567.5	996.9	36.4
	Combined (Climate + Urbanization)	2,258.5	1,624.7	28.1
Nitrate Load (kg)	Baseline (2-year)	24.9	16.8	32.7
	Baseline (10-year)	26.7	19.9	25.2
	Climate change (SSP5–8.5 Midterm)	29.5	19.9	32.5
	Urbanization	22.2	13.4	39.6
	Combined (Climate + Urbanization)	31.9	21.5	32.7
Phosphate Load (kg)	Baseline (2-year)	27.5	17.8	35.1
	Baseline (10-year)	29.3	21.7	26
	Climate change (SSP5–8.5 Midterm)	32.5	21.1	35
	Urbanization	24.3	14.3	41.1
	Combined (Climate + Urbanization)	35	22.6	35.6

6.4 Discussions

6.4.1 Hydrologic Performance

IGGI system successfully reduced the volume of runoff and peak flow of all the return periods investigated in the study. Under baseline scenario, the total runoff was decreased by 46% for sub-catchment S_{16} and 36.7% for catchment as a whole for 2-year return period. Peak flow reduced from 0.1236 m^3/s to 0.07415 m^3/s (S_{16}) and from 3.64 m^3/s to 2.058 m^3/s (watershed). For 10-year return period entire area, total runoff and peak flow reduced by 28.2% and 41.3% respectively, indicating IGGI possessed considerable mitigation capacity even for moderately extreme events. The findings of reductions are consistent with those obtained from research pertaining to GI systems in other countries, Lin et al. (2023) and Oberascher et al. (2019), that have found IGGI can enhance infiltration and detention and moderate peak discharges.

The system designed in this study i.e., the buried RBs and with the conventional raingarden provided superior hydraulic performance. Aves (2022) found minimal runoff reductions between 5.3 and 7.7% using conventional RBs. In contrast, this study IGGI being flexible in infiltration and conveyance gave greater flood attenuation and stability to the system, thus supporting Sharma and Malaviya (2021) finding for the efficiency of RGs in runoff and pollutant abatement.

Compared to other projects, the IGGI project in this study reduced the watershed-scale peak runoff in the 2-year event by 43.5%. This reduction was greater than that achieved by RGs (29–36%; Lin et al., 2023) and city-scale RB application (12%; Ghodsi et al., 2021). The total reduction in runoff of 32% was greater than the conventional RGs (12.7–19.4%; Autixier et al., 2014) and similar to what IoT was able to achieve RBs (18–40%; Oberascher et al., 2019). The IGGIs 10-year analysis reinforces the storm resilience of the system as it was able to maintain effective hydrologic performance in both design and stress conditions during higher intensity storms due to its integrated and adaptive configuration.

6.4.2 Pollutant Removal

The IGGI system designed and implemented in this study was effective in reducing pollutant loads for the 2-year and 10-year return periods over the entire area, but the removal efficiency varied for parameters. In the 2-year event, there was a 37.2%–42.4% reduction of total pollutant loads. The reduction of overall pollutant load reduced 28.7%–33.9% under baseline 10-year events. The higher-intensity storm produces a lower efficiency because of the reduced hydraulic retention and contact time. Such patterns are common in GI systems when flow volumes exceed design. The concentrations of dissolved nutrients, including nitrate and ammonia, were found to be largely stable during both events, indicating that IGGI mainly seeks to attenuate runoff volume instead of a strong chemical treatment, which would be similar to flood GI designs (Autixier et al., 2014; Sharma and Malaviya, 2021).

IGGI's phosphate removal (42.4%) under the 2-year event is lower than that of high-conductivity RGs (77-90%; Imteaz et al., 2022) or laboratory biphasic systems (97.6-99.3%; Wadzuk et al., 2021). This is likely due to factors of scale, such as the heterogeneity of the field-scale implementation, limited adsorption capacity in the sediment, and diffuse phosphate inputs. The COD removal (37.2%) is similarly lower than that found in enhanced biogeochemical RGs (~89%; Fajardo-Herrera et al., 2019) with additional filtration layers. The absence of a denitrification medium and advanced reactive substrate from the tested IGGI configuration visibly corroborates the findings (Sharma and Malaviya, 2021).

The reductions in pollutant loads confirm the ability of IGGI to mitigate non-point source pollution at the catchment scale. Nevertheless, removal efficiency does drop for the 10-year event. This shows that performance may be variable with larger events. In the foreseeable future, stormwater management practices can include the implementation of bioremediation layers, the use of biochar-based media, or amended substrates for better nutrient retention and microbial denitrification to enable a better control of pollutants under a higher range of storm intensities.

6.4.3 Climate and Urban Resilience

The IGGI system showed strong resilience to climate change and urbanization. Under the SSP5–8.5 climate scenario (2-year return period), IGGI reduced peak runoff by 36% and total runoff by 22%, while conventional GIs only achieve 18% total runoff under similar extreme events (Ghodsi et al., 2020). The recent results from Yang et al. (2022) indicated that RCP scenarios do not yield a reduction in IGGI performance, and there is a consistent mitigation potential under increased future rainfall.

With an imperviousness of approximately 80% (urbanization), IGGI provided a 23.5% peak runoff reduction that mitigated the performance limitations of GI systems owing to space constraints in densely built environments due to limited RG areas and RB storage capacities (Jennings et al., 2013). In the combined scenario of climate and urbanization stressors, a runoff reduction of 21% was observed. The reduction was lower than Neupane (2018), who noted a 26.8% reduction. The combined scenario's resilience to runoff was still high compared to the resilient to runoff standalone systems.

The robustness of the IGGI system is due to the decentralized retention-conveyance coupling of its infrastructure. More specifically, the RGs buffer the first peaks, while buried RBs delay discharge. The grey system then safely discharges pollutants and excess flow. As per Lin et al., 2023, this allows the hybrid design to overcome the limitations of classical GI in long-term storms. Bibi and Kara (2023) emphasized that the designs should be hybrid to help consist performance where climate and urbanization are both compounding.

6.4.4 Cost Implications

The economic evaluation showed that IGGI configured and implemented in this study is a cost-effective and sustainable solution for stormwater. The cost of buried RBs was approximately 589 USD/ha, while RGs was 2,791 USD/ha, which were a total of 3,928 USD/ha for the IGGI case. This investment has provided a total reduction in runoff of 27.4%, peak reduction of 39.2% and pollutant load reduction of 30%. The cost-effective ratios for this investment are 1,040 USD per 1% total runoff reduction, 727 USD per 1% peak reduction and 950 USD per 1% pollutant load reduction. The figures reveal that the new IGGI configuration is economically viable compared to other GI systems that often require bigger capex for limited hydrologic gain (Lin et al., 2023). Though, OandM costs were not included so a long-term life-cycle cost analysis will be needed to check sustainability. Shamsi (2015) indicates that OandM, can greatly impact the total life-cycle costs of GI. As a result, future research must include both economic and environmental accounting to sustain implementation strategies in resource-limited towns.

6.4.5 Synthesis and Implications

The IGGI system shows scalability, multi-functionality, and resiliency in stormwater management. Total runoff was reduced by 36.7% at the watershed scale, and peak flows were reduced by 43.5%. Furthermore, 2-year return period pollutant load reductions were 37.2%–42.4%. These findings contribute directly to achieving SDG 6 (Clean Water and Sanitation) by reducing pollution from urban non-point sources, as well as to SDG 11 (Sustainable Cities and Communities) by lowering flood risk and improving urban resilience under climate change and high imperviousness scenarios (SSP5–8.5; 80% urbanization), with peak runoff reduced by 29.4%, and the combined stressors resulted in 21% runoff reduction.

The IGGI configuration is more efficient in terms of space and modular than conventional IGGIs (bioretention cells, permeable pavements) and well suited for compact urban areas, allowing for a phased approach and interaction with grey infrastructure (Ghodsi et al., 2021). In addition to hydrologic and pollutant benefits, IGGI also reaps additional benefits such as urban cooling, aesthetics, and ecology that further enhance the contributions to SDGs.

From a policy perspective, the IGGI can be adopted in rapidly urbanizing Global South cities using local materials, modular deployment, and performance-based municipal regulations, presenting a cost-effective, climate-responsive opportunity to implement multifunctional greenery stormwater solutions. To conclude, IGGI's hybrid design connects measurable hydrologic and water quality improvements to urban resilience and SDG-aligned environmental co-benefits, providing a practical and scalable solution for dense urban contexts.

6.4.6 Limitations and Future Research

This study, although promising, has some limitations. The underlying soil properties were assumed to be uniform, and long-term clogging or degradation of the media was not considered (Amur et al., 2020). Over time, the performance of an IGGI system will depend on how often maintenance is carried out. Lowering the frequency of maintenance may reduce the runoff reduction efficiency and increase lifecycle costs. This will also impact the performance of the IGGI. The simulations did not take account of site-specific interactions with groundwater, which are especially important in Vertisol soils. Soil swelling and high-water tables will constrain infiltration. A geotechnical assessment is recommended to assess site suitability and adaptation.

In the water quality modeling, the resuspension and microbial dynamics in the sewer did not get considered, which underrepresented nutrient mobilization (Autixier et al., 2014). The analysis of costs did not include operation, maintenance, and ongoing down depreciation, and the possibility of reusing buried RB water was not examined, although reuse of rooftop rainwater is of better quality. During the field implementation stage, the challenges posed by community engagement and awareness were not overly significant. However, it has been determined that more outreach and training are necessary to achieve proper system use. Requirement of standardized guidelines for performing operations to homogenize performances is another area which needs improvement. Monitoring for clogging with time will help in assessing media degradation along with hydraulic performance for periodical maintenance. Integrating rooftop rainwater harvesting could facilitate water reuse. In addition, the life-cycle cost analysis, uncertainty quantification, and adaptive maintenance strategies will allow for a robust assessment of the hydrologic, water quality, and economic performance of IGGI in complex urban contexts. Additional limitation not examined is the risk of groundwater pollution from buried RB outflow. While Vertisols have low permeability and high adsorption capacity for most pollutants, nitrate is mobile and could potentially reach groundwater. The study area has no groundwater wells used for drinking water within 500 m, reducing immediate human health risk.

6.5 Conclusion

This study demonstrates that IGGI is an effective and scalable nature-based solution for stormwater management in steep-slope, poorly draining soil urban micro-watersheds. By integrating decentralized retention (buried RBs) with infiltration-based practices (RGs), IGGI achieved peak runoff reductions of 43.5%, total runoff reductions of 36.7%, and pollutant load reductions of 37.2% – 42.4% under baseline scenario. Under the 10-year return period, IGGI maintained substantial mitigation capacity, with peak flow and total runoff reduced by 41.3% and 28.2%, respectively, demonstrating its resilience under moderately extreme storms. Overall, these results confirm IGGI's capacity to enhance urban hydrologic resilience and stormwater quality, particularly when strategically implemented in source-contributing zones.

IGGI's modular and adaptive design enables phased and budget-conscious implementation, allowing municipalities to start with high-priority areas and expand over time. The use of locally available materials and tailored maintenance schedules reduces operational costs while maintaining long-term efficiency. This makes IGGI especially suitable for resource-limited cities in the Global South, aligning with SDG 6 (clean water), SDG 11 (sustainable cities), and SDG 13 (climate action).

Beyond stormwater control, IGGI provides co-benefits including urban cooling, aesthetic enhancement, and support for urban biodiversity, which further strengthens its case for municipal adoption. Limitations of this study include simplified soil and pollutant assumptions, the exclusion of long-term clogging and maintenance effects, and the absence of groundwater interactions. Future work should address these through life-cycle cost analyses, long-term monitoring, and integration with rooftop rainwater reuse, providing a more comprehensive evaluation of hydrologic, environmental, and economic performance.

IGGI offers a resilient, multifunctional, and cost-effective strategy. Policymakers and planners should integrate it into design standards, launch pilot projects, and foster interdisciplinary collaboration to enhance hydrologic performance, social acceptance, and sustainability. Municipalities can adopt IGGI gradually using local materials and tailored maintenance for scalable implementation under budget constraints.

Chapter 7

7 Conclusion and Recommendation

7.1 Conclusion

This dissertation concludes that IGGI constitutes a viable, resilient, and scalable paradigm for sustainable urban stormwater management in rapidly urbanizing cities such as Addis Ababa. Based on the collective results and discussions across the four specific objectives, the study demonstrates that effective stormwater governance in such contexts cannot rely on isolated grey infrastructure upgrades or generic green solutions, but requires spatially targeted, system-informed, and performance-validated hybrid interventions.

First, the study concludes that Addis Ababa possesses substantial and spatially heterogeneous potential for IGGI deployment. Suitability is not uniformly distributed but is strongly governed by terrain slope, soil drainage capacity, urban density, and infrastructural accessibility. Accounting for interdependencies among these factors significantly improves spatial decision reliability, confirming that network-based weighting approaches provide more realistic guidance for urban stormwater planning than linear, assumption-independent models. This establishes spatial prioritization as a necessary precursor for effective IGGI implementation rather than an optional planning exercise.

Second, the dissertation concludes that steep, Vertisol-dominated urban micro-watersheds are intrinsically hydrologically vulnerable and will experience disproportionate increases in runoff and pollutant mobilization under projected climate and urbanization pressures. Conventional drainage systems alone are insufficient to address these compounded risks. The results demonstrate that future stormwater challenges in Addis Ababa will be driven more by system sensitivity and land-surface transformation than by rainfall increase alone, underscoring the urgency of integrating infiltration, storage, and treatment functions within urban drainage systems.

Third, the study concludes that infrastructure performance and retrofit decisions must be informed by integrated hydraulic behavior and field-condition evidence. The combination of hydrologic simulation with multi-criteria decision analysis enables transparent, stable, and defensible prioritization of maintenance and retrofit needs. This approach bridges the gap between model outputs and actionable municipal decision-making, demonstrating that data-driven prioritization is both technically feasible and operationally valuable in resource-constrained urban contexts.

Fourth, the dissertation concludes that hybrid IGGI systems—specifically those integrating buried rain barrels with rain gardens—deliver sustained hydrological and water-quality benefits across present and future scenarios. Even under intensified climate–urban stress conditions, IGGI maintains meaningful reductions in runoff, peak flow, and pollutant loads, confirming its functional resilience. The cost-effectiveness analysis further supports IGGI as a financially realistic alternative to conventional infrastructure expansion, particularly when co-benefits such as urban cooling, ecological enhancement, and improved urban livability are considered.

Taken together, the dissertation demonstrates that IGGI is a viable, context-sensitive approach to urban stormwater management in steep, Vertisol-dominated environments—one that integrates spatial planning, hydrologic modeling, infrastructure performance evaluation, and targeted intervention within a unified framework. By integrating GIS-based suitability analysis, calibrated hydrologic modeling, multi-criteria prioritization, and intervention-level performance evaluation, this research provides a scientifically grounded and context-sensitive pathway for transitioning toward climate-resilient, nature-based urban stormwater systems in Addis Ababa and comparable cities across the Global South.

Three surprising findings emerged. First, ANP classified 59.86% of Addis Ababa as suitable for IGGI—substantially higher than expected given the city's topographic and soil constraints. Second, under different scenarios, urbanization was the dominant driver of water quality decline (7.1% increase vs. 1.7% for climate change alone). Third, buried RBs captured runoff from multiple surfaces in the steep, Vertisol pilot, achieving 43.5% peak reduction—comparable to much larger GI systems. The IGGI framework is applicable at the national level to Ethiopian cities with similar biophysical conditions (Adama, Debre Birhan, Dessie, Jimma). Adaptation would require local calibration. For Addis Ababa city-level application, confidence is high for sub-cities with comparable topography (Nefas Silk Lafto, Akaki Kality, Kolfe Keraniyo) but moderate for flat, well-drained areas (Bole, Yeka).

7.2 Recommendation

7.2.1 Policy and Governance Level

Establish an IGGI Implementation and Monitoring Framework: The city should create a dedicated Green-Grey Infrastructure Council to coordinate stakeholders across environmental, construction, and planning departments, ensuring long-term maintenance, performance monitoring, and community involvement.

Promote Financial and Policy Incentives: Incentivize IGGI adoption through tax rebates, development bonuses, and stormwater fee credits for households and developers implementing green roofs, permeable paving, or rainwater harvesting systems.

Integrate IGGI into Climate Resilience and SDG Strategies: Embed IGGI into Ethiopia's National Adaptation Plan (NAP) and urban climate action frameworks, aligning with SDGs 6, 11, and 13 to access climate finance and international support mechanisms.

7.2.2 Managerial and Technical Level

Adopt a Phased Implementation Approach: Prioritize highly suitable areas (e.g., Akaki Kality, Bole) for initial IGGI pilots, followed by expansion to moderately suitable zones, ensuring early demonstration of benefits and iterative learning.

Enhance Hydrological and Pollutant Monitoring: Establish continuous runoff, infiltration, and water quality monitoring at reasonably representative sites to generate high-resolution local datasets for calibration, validation, and adaptive management.

Standardize Design and Maintenance Protocols: Develop localized design templates for IGGI typologies using locally available materials, coupled with periodic maintenance schedules to ensure long-term functionality and prevent clogging.

Integrate Hydrologic Simulation into Planning Tools: Institutionalize the use of models such as PCSWMM, coupled with MCDA frameworks (AHP/ANP, TOPSIS), in routine infrastructure planning to facilitate evidence-based prioritization and scenario testing.

7.2.3 Community and Socioeconomic Level

Enhance Public Awareness and Participation: Implement sustained awareness campaigns through schools, community centers, and media on the benefits of IGGI, encouraging household-level practices such as rain gardens, barrels, and green roofs.

Strengthen Capacity Building and Training: Provide technical training for municipal engineers, contractors, and local artisans on IGGI design, construction, and maintenance to promote local job creation and reduce dependency on imported expertise.

Encourage Private Sector and Academic Collaboration: Promote partnerships among universities, research institutes, and private developers for innovation, performance assessment, and the development of low-cost IGGI materials.

Incorporate Socioeconomic Evaluation: Future studies should assess the cost–benefit ratio and community willingness-to-pay for IGGI systems to ensure socio-economic feasibility and equitable access.

7.2.4 Future Research Directions

Integrate Dynamic Hydrologic–Economic Modeling: Combine PCSWMM with economic optimization and cost–benefit analysis to evaluate life-cycle performance and financial viability of IGGI typologies.

Explore Coupled Groundwater–Surface Water Interactions: Model subsurface hydrology and baseflow to capture IGGI's long-term effects on groundwater recharge, especially under Vertisol conditions.

Expand Socio-institutional Research: Investigate governance, land tenure, and behavioral drivers of IGGI adoption to inform participatory and inclusive urban stormwater governance.

Evaluate Long-Term Maintenance and Clogging Dynamics: Conduct longitudinal field studies to assess IGGI performance degradation, maintenance costs, and adaptive design improvements under real-world conditions.

Integrate Corridor and Riverside Development with Stormwater Management: Given that the Addis Ababa Riverside Development Project has already incorporated some GI elements, future research should evaluate whether these align with the IGGI framework developed in this dissertation and contextualized global approach and assess their hydrological performance.

7.2.5 Scientific and Research Level

Advance Integrated Modeling and Theory Development: Future research should focus on advancing coupled hydro–geomorphic–water quality models that explicitly capture steep-slope processes, Vertisol behavior, and infrastructure–landscape feedback, thereby strengthening the theoretical foundations of IGGI performance in non-conventional urban settings.

Promote Methodological Standardization and Transferability: Comparative multi-city studies are recommended to test the transferability of the integrated GIS–MCDA–PCSWMM–TOPSIS framework across different climatic, topographic, and institutional contexts, contributing to the development of standardized scientific protocols for hybrid stormwater infrastructure assessment.

Strengthen Experimental and Data-Driven Research: Establish long-term experimental IGGI observatories to generate high-resolution datasets for model refinement, uncertainty reduction, and validation of emerging data-driven and hybrid physics–machine learning approaches in urban stormwater science.

References

Abd-Elhamid, H. F., Zeleňáková, M., Vranayová, Z., and Fathy, I. (2020). Evaluating the impact of urban growth on the design of storm water drainage systems. *Water*, 12(6), 1-22. https://doi.org/10.3390/W12061572

Abebe, M. T., and Megento, T. L. (2017). Urban green space development using GIS-based multi-criteria analysis in Addis Ababa metropolis. *Applied Geomatics*, 9(4), 247-261. https://doi.org/10.1007/s12518-017-0198-7

Abebe, Y., and Tesfamariam, S. (2019). Climate change impact and adaptation for urban drainage systems. In *Climate Adaptation Engineering: Risks and Economics for Infrastructure Decision-Making* (pp. 73-98). Elsevier. https://doi.org/10.1016/B978-0-12-816782-3.00003-6

Aboukarima, A. M., Al-Sulaiman, M. A., and El Marazky, M. S. A. (2018). Effect of sodium adsorption ratio and electric conductivity of the applied water on infiltration in a sandy-loam soil. *Water SA*, 44(1), 105-110. https://doi.org/10.4314/wsa.v44i1.12

Achu, A. L., Thomas, J., and Reghunath, R. (2020). Multi-criteria decision analysis for delineation of groundwater potential zones in a tropical river basin using remote sensing, GIS and analytical hierarchy process (AHP). *Groundwater for Sustainable Development*, 10, 100365. https://doi.org/10.1016/j.gsd.2020.100365

Addis Ababa City Administration. (2020). *Resilience Strategy Addis Ababa*.

Adhikari, U., Broekhuizen, I., Pons, V., Sun, Z., Sjöman, J. D., Randrup, T. B., Viklander, M., and Blecken, G. T. (2024). Comparing the hydrological performance of blue green infrastructure design strategies in urban/semi-urban catchments for stormwater management. *Water Science and Technology*, 90(9), 2696-2712. https://doi.org/10.2166/wst.2024.346

Adugna, D., Lemma, B., Jensen, M. B., and Gebrie, G. S. (2019). Evaluating the hydraulic capacity of existing drain systems and the management challenges of stormwater in Addis Ababa, Ethiopia. *Journal of Hydrology: Regional Studies*, 25. https://doi.org/10.1016/j.ejrh.2019.100626

Adugna, D., Lemma, B., Sahilu Gebrie, G., Larsen, L., Yeshitela, K., and Bergen Jensen, M. (2019). Stormwater impact on water quality of rivers subjected to point sources and urbanization – the case of Addis Ababa, Ethiopia. *Water and Environment Journal*, 33(1), 98-110. https://doi.org/10.1111/wej.12381

Akhter, F., Hewa, G. A., Ahammed, F., Myers, B., and Argue, J. R. (2020). Performance evaluation of stormwater management systems and its impact on development costing. *Water*, 12(2). https://doi.org/10.3390/w12020375

Akhter, M. S., and Hewa, G. A. (2016). The use of PCSWMM for assessing the impacts of land use changes on hydrological responses and performance of WSUD in managing the impacts at Myponga catchment, South Australia. *Water*, 8(11). https://doi.org/10.3390/w8110511

Al Mamun, A., bin Salleh, M. N., and Noor, H. M. (2018). Estimation of short-duration rainfall intensity from daily rainfall values in Klang Valley, Malaysia. *Applied Water Science*, 8(7), 1-10. https://doi.org/10.1007/s13201-018-0854-z

Allende-Prieto, C., Roces-García, J., and Sañudo-Fontaneda, L. Á. (2024). The high-resolution calibration of the topographic wetness index using PAZ satellite radar data to determine the optimal positions for the placement of smart sustainable drainage systems (SuDS) in urban environments. *Sustainability*, 16(2). https://doi.org/10.3390/su16020598

Almaliki, A. H., Zerouali, B., Santos, C. A. G., Almaliki, A. A., Silva, R. M. da, Ghoneim, S. S. M., and Ali, E. (2023). Assessing coastal vulnerability and land use to sea level rise in Jeddah province, Kingdom of Saudi Arabia. *Heliyon*, 9(8). https://doi.org/10.1016/j.heliyon.2023.e18508

Alotaibi, O. S., and Anzah, F. (2023). Applying an AHP-GIS model to hybrid wind-solar energy site selection in a hot desert region: A case study of the Kuwaiti desert. *Geografisk Tidsskrift-Danish Journal of Geography*, (1), 25-41. https://doi.org/10.1080/00167223.2023.2218891

Alves, A., Gersonius, B., Kapelan, Z., Vojinovic, Z., and Sanchez, A. (2019). Assessing the co-benefits of green-blue-grey infrastructure for sustainable urban flood risk management. *Journal of Environmental Management*, 239, 244-254. https://doi.org/10.1016/j.jenvman.2019.03.036

Amjad, F., Agyekum, E. B., and Wassan, N. (2024). Identification of appropriate sites for solar-based green hydrogen production using a combination of density-based clustering, Best-Worst Method, and spatial GIS. *International Journal of Hydrogen Energy*, 68, 1281-1296. https://doi.org/10.1016/j.ijhydene.2024.04.310

Amur, A., Wadzuk, B., and Traver, R. (2020). Analyzing the performance of a rain garden over 15 years: How predictable is the rain garden's response?

Angello, Z. A., Behailu, B. M., and Tränckner, J. (2021). Selection of optimum pollution load reduction and water quality improvement approaches using scenario based water quality modeling in Little Akaki River, Ethiopia. *Water*, 13(5). https://doi.org/10.3390/w13050584

Anteneh, M. B., Damte, D. S., Abate, S. G., and Gedefaw, A. A. (2023). Geospatial assessment of urban green space using multi-criteria decision analysis in Debre Markos City, Ethiopia. *Environmental Systems Research*, 12(1). https://doi.org/10.1186/s40068-023-00291-x

Arch Students. (2023, July 21). Best Resource Provider for Modern Architectural Facts, Designs Ideas Architecture Design Portfolios and Competitions for Students in India and Worldwide. https://archistudent.net/wp-content/uploads/2018/07/Infiltration-trench.jpg

Arnbjerg-Nielsen, K., Willems, P., Olsson, J., Beecham, S., Pathirana, A., Bülow Gregersen, I., Madsen, H., and Nguyen, V. T. V. (2013). Impacts of climate change on rainfall extremes and urban drainage systems: A review. *Water Science and Technology*, 68(1), 16-28. https://doi.org/10.2166/wst.2013.251

Asefa, E. M., Damtew, Y. T., and Barasa, K. B. (2021). Landfill site selection using GIS based multicriteria evaluation technique in Harar City, Eastern Ethiopia. *Environmental Health Insights*, 15. https://doi.org/10.1177/11786302211053174

Ashok Kumar, K., Sudheer, K. V. S., Pavani, K., Umadevi, G. D., Reddy, C. V. C. M., and Sahadeva Reddy, B. (2023). Extreme rainfall analysis for development of rainfall intensity duration frequency curves for semiarid region of Andhra Pradesh in India. *National Academy Science Letters*. https://doi.org/10.1007/s40009-023-01360-6

Asnake, K., Worku, H., and Argaw, M. (2021). Assessing the impact of watershed land use on Kebena River water quality in Addis Ababa, Ethiopia. *Environmental Systems Research*, 10(1). https://doi.org/10.1186/s40068-020-00208-y

Atinafu, M., Getnet, K., and Gojjam, A. (2024). Effects of physical soil and water conservation practices and slope gradient on soil physicochemical properties in northwestern Ethiopia. *Arabian Journal of Geosciences*, 17(3). https://doi.org/10.1007/s12517-024-11909-4

Autixier, L., Mailhot, A., Bolduc, S., Madoux-Humery, A. S., Galarneau, M., Prévost, M., and Dorner, S. (2014). Evaluating rain gardens as a method to reduce the impact of sewer overflows in sources of drinking water. *Science of the Total Environment*, 499, 238-247. https://doi.org/10.1016/j.scitotenv.2014.08.030

Autodesk. (2023). *InfoWorks ICM (Integrated Catchment Modeling) [Computer software]*. Autodesk, Inc.

Aves, F. A. (2022). Rain barrel implementation for urban runoff mitigation. *International Research Journal of Advanced Engineering and Science*, 7(2), 255-260.

Azagew, S., and Worku, H. (2020). Accessibility of urban green infrastructure in Addis Ababa city, Ethiopia: current status and future challenge. *Environmental Systems Research*, 9(1), 1-20. https://doi.org/10.1186/S40068-020-00187-0

Azizi, A., Malekmohammadi, B., Jafari, H. R., Nasiri, H., and Amini Parsa, V. (2014). Land suitability assessment for wind power plant site selection using ANP-DEMATEL in a GIS environment: case study of Ardabil province, Iran. *Environmental Monitoring and Assessment*, 186(10), 6695-6709. https://doi.org/10.1007/s10661-014-3883-6

Babaei, S., Ghazavi, R., and Erfanian, M. (2018). Urban flood simulation and prioritization of critical urban sub-catchments using SWMM model and PROMETHEE II approach. *Physics and Chemistry of the Earth*, 105, 3-11. https://doi.org/10.1016/j.pce.2018.02.002

Back, Á. J. (2024). Applying the Chicago hyetograph for intense rainfall equations of the LnLn type. *Revista Brasileira de Recursos Hídricos*, 29. https://doi.org/10.1590/2318-0331.292420240017

Badou, D. F., Adango, A., Hounkpè, J., Bossa, A., Yira, Y., Biao, E. I., Adounkpè, J., Alamou, E., Sintondji, L. O. C., and Afouda, A. A. (2021). Heavy rainfall frequency analysis in the Benin section of the Niger and Volta Rivers basins: Is the Gumbel's distribution a one-size-fits-all model? *Proceedings of the International Association of Hydrological Sciences*, 384, 187-194. https://doi.org/10.5194/piahs-384-187-2021

Bagheri, M., Masoudian, M., and Afrous, A. (2025). Investigation of hydromorphological changes of river corridor using satellite images. *International Journal of Environmental Science and Technology*, 22(7), 5289-5308. https://doi.org/10.1007/s13762-024-06126-1

Bai, Y., Zhao, N., Zhang, R., and Zeng, X. (2018). Storm water management of low impact development in urban areas based on SWMM. *Water*, 11(1). https://doi.org/10.3390/w11010033

Bakolo, C., Kayitete, L., de Dieu Tuyizere, J., Tomlinson, J., Fawcett, J., and Alfaro, R. F. (2024). Identification of optimal locations for green space initiatives through GIS-based multi-criteria analysis and the analytical hierarchy process. *Environmental Systems Research*, 13(1). https://doi.org/10.1186/s40068-024-00377-0

Balbastre-Soldevila, R., García-Bartual, R., and Andrés-Doménech, I. (2019). A comparison of design storms for urban drainage system applications. *Water*, 11(4). https://doi.org/10.3390/w11040757

Balkan Sewer and Drain Cleaning Inc. (2023). *Dry Wells Have Various Helpful Uses - Balkan Drain Cleaning*. https://www.balkandraincleaning.com/dry-wells-uses-purpose-construction/

Barbosa, A. E., Fernandes, J. N., and David, L. M. (2012). Key issues for sustainable urban stormwater management. *Water Research*, 46(20), 6787-6798. https://doi.org/10.1016/j.watres.2012.05.029

Beganskas, S., Ryan, R. J., Walters, E., Soro, M., Cushman, E., and Toran, L. (2021). Coupling PCSWMM and WASP to evaluate green stormwater infrastructure impacts to storm sediment loads in an urban watershed. *Journal of the American Water Resources Association*, 57(1), 134-153. https://doi.org/10.1111/1752-1688.12896

Behzadian, M., Khanmohammadi Otaghsara, S., Yazdani, M., and Ignatius, J. (2012). A state-of the-art survey of TOPSIS applications. *Expert Systems with Applications*, 39(17), 13051-13069. https://doi.org/10.1016/j.eswa.2012.05.056

Bekiryazici, F., and Acar, C. (2024). Determining the most appropriate stormwater management strategies within the development of urban landscape infrastructure using the TOPSIS method: applications to Rize city. *Water Science and Technology*, 89(10), 2746-2762. https://doi.org/10.2166/wst.2024.157

Ben-Daoud, A., Chokhmane, M. G., Moroșanu, G. A., and M'Rabet, S. (2024). Modeling the effect of land-use change on runoff water quality in the urban watershed: a case study of Settat city, Morocco. *Water Science and Technology*, 90(9), 2554-2571. https://doi.org/10.2166/wst.2024.353

Benedict, M. A., and McMahon, E. (2006). *Green infrastructure: linking landscapes and communities*. Island Press.

Berhanu, D. (1983). The Vertisols of Ethiopia: Their properties, classification and management. *5th Meeting of the Eastern African Soil Correlation and Land Evaluation Subcommittee*, 5-10 December.

Beven, K. J., and Kirkby, M. J. (1979). A physically based, variable contributing area model of basin hydrology. *Hydrological Sciences Bulletin*, 24(1), 43-69. https://doi.org/10.1080/02626667909491834

Bibi, T. S., and Kara, K. G. (2023). Evaluation of climate change, urbanization, and low-impact development practices on urban flooding. *Heliyon*, 9(1). https://doi.org/10.1016/j.heliyon.2023.e12955

Bibi, T. S., Kara, K. G., Bedada, H. J., and Bededa, R. D. (2023). Application of PCSWMM for assessing the impacts of urbanization and climate changes on the efficiency of stormwater drainage systems in managing urban flooding in Robe town, Ethiopia. *Journal of Hydrology: Regional Studies*, 45, 101291. https://doi.org/10.1016/j.ejrh.2022.101291

Birhanu, D., Kim, H., Jang, C., and Park, S. (2016). Flood risk and vulnerability of Addis Ababa City due to climate change and urbanization. *Procedia Engineering*, 154, 696-702. https://doi.org/10.1016/j.proeng.2016.07.571

Blecken, G. T., Hunt, W. F., Al-Rubaei, A. M., Viklander, M., and Lord, W. G. (2017). Stormwater control measure (SCM) maintenance considerations to ensure designed functionality. *Journal of Environmental Management*, 193, 93-107. https://doi.org/10.1016/j.jenvman.2017.02.015

Brattebo, B. O., and Booth, D. B. (2003). Long-term stormwater quantity and quality performance of permeable pavement systems. *Water Research*, 37(18), 4369-4376. https://doi.org/10.1016/S0043-1354(03)00410-X

Brezonik, P. L. (1976). Nutrients and other biologically active substances in atmospheric precipitation. *Journal of Great Lakes Research*, 2, 166-186. https://doi.org/10.1016/S0380-1330(76)72325-6

Browne, S., Lintern, A., Jamali, B., Leitão, J. P., and Bach, P. M. (2021). Stormwater management impacts of small urbanising towns: The necessity of investigating the 'devil in the detail.' *Science of the Total Environment*, 757, 143835. https://doi.org/10.1016/J.SCITOTENV.2020.143835

Butler, D., and Davies, J. W. (2011). *Urban Drainage* (3rd ed.). CRC Press.

Chan, F. K. S., Griffiths, J. A., Higgitt, D., Xu, S., Zhu, F., Tang, Y. T., and Thorne, C. R. (2018). "Sponge City" in China—A breakthrough of planning and flood risk management in the urban context. *Land Use Policy*, 76, 772-778. https://doi.org/10.1016/j.landusepol.2018.03.005

Charbeneau, R. J., and Barrett, M. E. (1998). Evaluation of methods for estimating stormwater pollutant loads. *Water Environment Research*, 70(7), 1295-1302. https://doi.org/10.2175/106143098x123679

Chen, W., Wang, W., Huang, G., Wang, Z., Lai, C., and Yang, Z. (2021). The capacity of grey infrastructure in urban flood management: A comprehensive analysis of grey infrastructure and the green-grey approach. *International Journal of Disaster Risk Reduction*, 54, 102045. https://doi.org/10.1016/j.ijdrr.2021.102045

Chen, X., Davitt-Liu, I., Erickson, A. J., and Feng, X. (2023). Integrating the spatial configurations of green and gray infrastructure in urban stormwater networks. *Water Resources Research*, 59(12). https://doi.org/10.1029/2023WR034796

Cheng, T., Huang, B., Yang, Z., Qiu, J., Zhao, B., and Xu, Z. (2022). On the effects of flood reduction for green and grey sponge city measures and their synergistic relationship—Case study in Jinan sponge city pilot area. *Urban Climate*, 42, 101058. https://doi.org/10.1016/j.uclim.2021.101058

CHI (Computational Hydraulics International). (2023). *PCSWMM Water Quality Modeling*. PCSWMM Professional Version. Computational Hydraulics International.

Chiteculo, V., Abdollahnejad, A., Panagiotidis, D., and Surový, P. (2022). Effects, monitoring and management of forest roads using remote sensing and GIS in Angolan Miombo woodlands. *Forests*, 13(4). https://doi.org/10.3390/f13040524

Chiu, Y. R., Aghaloo, K., and Mohammadi, B. (2020). Incorporating rainwater harvesting systems in Iran's potable water-saving scheme by using a GIS-simulation based decision support system. *Water*, 12(3). https://doi.org/10.3390/w12030752

Cho, J. H., and Seo, H. J. (2007). Parameter optimization of SWMM for runoff quantity and quality calculation in a eutrophic lake watershed using a genetic algorithm. *Water Science and Technology: Water Supply*, 7(5-6), 35-41. https://doi.org/10.2166/ws.2007.114

Chocat, B., Krebs, P., Marsalek, J., Rauch, W., and Schilling, W. (2001). Urban drainage redefined: from stormwater removal to integrated management. *Water Science and Technology*, 43(5), 61-68.

Chow, M. F., Yusop, Z., and Toriman, M. E. (2012). Modelling runoff quantity and quality in tropical urban catchments using Storm Water Management Model. *International Journal of Environmental Science and Technology*, 9(4), 737-748. https://doi.org/10.1007/s13762-012-0092-0

Chow, V. T. (1988). *Applied Hydrology*. McGraw-Hill.

Czemiel Berndtsson, J. (2010). Green roof performance towards management of runoff water quantity and quality: A review. *Ecological Engineering*, 36(4), 351-360. https://doi.org/10.1016/j.ecoleng.2009.12.014

Dagenais, D., Thomas, I., and Paquette, S. (2016). Siting green stormwater infrastructure in a neighbourhood to maximise secondary benefits: lessons learned from a pilot project. *Landscape Research*, 42(2), 195-210. https://doi.org/10.1080/01426397.2016.1228861

Das, A., and Sahoo, S. N. (2025). Impact of land use and climate change on urban flooding: a case study of Bhubaneswar city in India. *Natural Hazards*. https://doi.org/10.1007/s11069-025-07130-5

Das, S., Morshed, M. M., and Rafizul, I. M. (2024). Investigating landfill site suitability integrating GIS and multicriteria decision-making approaches in Khulna, Bangladesh. *International Journal of Environmental Science and Technology*. https://doi.org/10.1007/s13762-024-06249-5

Davis, A. P., Hunt, W. F., Traver, R. G., and Clar, M. (2009). Bioretention technology: Overview of current practice and future needs. *Journal of Environmental Engineering*, 135(3), 109-117. https://doi.org/10.1061/(ASCE)0733-9372(2009)135:3(109)

Davis, A. P., Shokouhian, M., Sharma, H., and Minami, C. (2001). Laboratory study of biological retention for urban stormwater management. *Water Environment Research*, 73(1), 5-14. https://doi.org/10.2175/106143001X138624

Davis, A. P., Traver, R. G., Hunt, W. F., Lee, R., Brown, R. A., and Olszewski, J. M. (2012). Hydrologic performance of bioretention storm-water control measures. *Journal of*

Hydrologic Engineering, 17(5), 604-614. https://doi.org/10.1061/(ASCE)HE.1943-5584.0000467

Debele, T., and Deressa, H. (2016). Integrated management of Vertisols for crop production in Ethiopia: A review. *Journal of Biology, Agriculture and Healthcare*, 6(24), 26-36.

DeBusk, K., Hunt, W. F., and Carolina Water, N. (2012). Rainwater harvesting: A comprehensive review of literature.

Deely, J., Hynes, S., Barquín, J., Burgess, D., Finney, G., Silió, A., Álvarez-Martínez, J. M., Bailly, D., and Ballé-Béganton, J. (2020). Barrier identification framework for the implementation of blue and green infrastructures. *Land Use Policy*, 99, 105108. https://doi.org/10.1016/j.landusepol.2020.105108

Degefu, M. A., and Asefa, W. (2024). Municipal solid waste management practices and sanitary landfill site selection using the AHP approach for emerging industrial zones. *Environmental Systems Research*, 13(58). https://doi.org/10.1186/s40068-024-00387-y

Delian Akpen, G., Omale, D., and Ekwule, R. (2020). Frequency modeling of rainfall intensities for Abuja Metropolis, Nigeria. *Usak University Journal of Engineering*, 2020(1).

Dereje Fekadu, Philipp Rode, Elias Yitbarek Alemayehu, Elleni Ashebir, Ricky Burdett, Anka Derichs, et al. (2022). *Policy Brief: Green and Blue Infrastructure: Working with Nature: Next generation green and blue infrastructure for Addis Ababa*.

Dietz, M. E. (2007). Low impact development practices: A review of current research and recommendations for future directions. *Water, Air, and Soil Pollution*, 186(1-4), 351-363. https://doi.org/10.1007/s11270-007-9484-z

DHI (Danish Hydraulic Institute). (2020). *MIKE URBAN (Version 2020) [Computer software]*. DHI Group.

Dile, Y. T., Berndtsson, R., and Setegn, S. G. (2018). Hydrological response to climate change for Gilgel Abay River, Lake Tana Basin, Ethiopia. *Journal of Hydrology: Regional Studies*, 15, 47-61. https://doi.org/10.1016/j.ejrh.2017.12.002

Dong, X., Yuan, P., Song, Y., and Yi, W. (2021). Optimizing green-gray infrastructure for non-point source pollution control under future uncertainties. *International Journal of Environmental Research and Public Health*, 18(14). https://doi.org/10.3390/ijerph18147586

Dunne, T., and Black, R. D. (1970). An experimental investigation of runoff production in permeable soils. *Water Resources Research*, 6(2), 478-490. https://doi.org/10.1029/WR006i002p00478

Emagnu, Y. M. (2018). *Performance Evaluation of Addis Ababa City Road Network*. https://doi.org/10.13140/RG.2.2.30164.09607

EPA (U.S. Environmental Protection Agency). (2014). *Addressing Green Infrastructure Design Challenges in the Pittsburgh Region: Steep Slopes*.

Eroksuz, E., and Rahman, A. (2010). Rainwater tanks in multi-unit buildings: A case study for three Australian cities. *Resources, Conservation and Recycling*, 54(12), 1449-1452. https://doi.org/10.1016/j.resconrec.2010.06.010

Eshetu, S. B., Yeshitela, K., and Sieber, S. (2021). Urban green space planning, policy implementation, and challenges: The case of Addis Ababa. *Sustainability*, 13(20). https://doi.org/10.3390/su132011344

Eskandaripour, M., and Soltaninia, S. (2024). Optimal low-impact development facility design in urban environments: A multidimensional optimization approach employing slime mould and nondominated sorting genetic algorithms. *Urban Climate*, 55, 101963. https://doi.org/10.1016/j.uclim.2024.101963

ESS (Ethiopian Statistical Service). (2023). *Population Size by Sex, Region, Zone and Wereda as of July 2023*.

Ewea, H. A., Elfeki, A. M., Bahrawi, J. A., and Al-Amri, N. S. (2018). Modeling of IDF curves for stormwater design in Makkah Al Mukarramah region, the Kingdom of Saudi Arabia. *Open Geosciences*, 10(1), 954-969. https://doi.org/10.1515/geo-2018-0076

Eyring, V., Bony, S., Meehl, G. A., Senior, C. A., Stevens, B., Stouffer, R. J., and Taylor, K. E. (2016). Overview of the Coupled Model Intercomparison Project Phase 6 (CMIP6) experimental design and organization. *Geoscientific Model Development*, 9(5), 1937-1958. https://doi.org/10.5194/gmd-9-1937-2016

Fajardo-Herrera, R. J., Valdelamar-Villegas, J. C., and Mouthon Bello, J. (2019). Un jardín de lluvia para la remoción de nitrógeno de la escorrentía en ciudades tropicales. *Revista de Ciencias Ambientales*, 53(2), 132-146. https://doi.org/10.15359/rca.53-2.7

FAO (Food and Agriculture Organization). (2006). *Plant nutrition for food security: a guide for integrated nutrient management*. FAO.

FAO-UN. (2006). *World Reference Base for Soil Resources*. FAO.

FAO-UNESCO. (1977). *Soil map of the world, volume 6 Africa*.

Fernandez, A., Ghobrial, T. R., Zhang, W., Zhu, D. Z., Loewen, M. R., van Duin, B., Mahmood, K., and Chen, L. (2019). PCSWMM modeling of storm runoff and sediment and nutrients loading to stormwater wetlands in Calgary, Alberta. *Proceedings, Annual Conference - Canadian Society for Civil Engineering*, 2019-June.

Feyissa, G., Zeleke, G., Gebremariam, E., and Bewket, W. (2018). GIS based quantification and mapping of climate change vulnerability hotspots in Addis Ababa. *Geoenvironmental Disasters*, (1). https://doi.org/10.1186/s40677-018-0106-4

Fletcher, T. D., Andrieu, H., and Hamel, P. (2013). Understanding, management and modelling of urban hydrology and its consequences for receiving waters: A state of the art. *Advances in Water Resources*, 51, 261-279. https://doi.org/10.1016/j.advwatres.2012.09.001

Fletcher, T. D., Shuster, W., Hunt, W. F., Ashley, R., Butler, D., Arthur, S., Trowsdale, S., Barraud, S., Semadeni-Davies, A., Bertrand-Krajewski, J. L., Mikkelsen, P. S., Rivard, G., Uhl, M., Dagenais, D., and Viklander, M. (2015). SUDS, LID, BMPs, WSUD and more – The evolution and application of terminology surrounding urban drainage. *Urban Water Journal*, 12(7), 525-542. https://doi.org/10.1080/1573062X.2014.916314

Folke, C., Carpenter, S. R., Walker, B., Scheffer, M., Chapin, T., and Rockström, J. (2010). Resilience thinking: Integrating resilience, adaptability and transformability. *Ecology and Society*, 15(4), 20. https://doi.org/10.5751/ES-03610-150420

Frings, R. M., Schüttrumpf, H., and Vollmer, S. (2011). Verification of porosity predictors for fluvial sand-gravel deposits. *Water Resources Research*, 47(7). https://doi.org/10.1029/2010WR009690

Gado, T. A., Salama, A. M., and Zeidan, B. A. (2021). Selection of the best probability models for daily annual maximum rainfalls in Egypt. *Theoretical and Applied Climatology*, 144(3-4), 1267-1284. https://doi.org/10.1007/s00704-021-03594-0

Garg, V., Nikam, B. R., Thakur, P. K., and Aggarwal, S. P. (2013). Assessment of the effect of slope on runoff potential of a watershed using NRCS-CN method. *International Journal of Hydrology Science and Technology*, 3(2), 141-159.

Gaut, J., Chua, L. H., Irvine, K. N., and Le, S. H. (2019). Modelling the washoff of pollutants in various forms from an urban catchment. *Journal of Environmental Management*, 246, 374-383. https://doi.org/10.1016/j.jenvman.2019.05.118

Gebrechorkos, S. H., Hülsmann, S., and Bernhofer, C. (2019). Regional climate projections for impact assessment studies in East Africa. *Environmental Research Letters*, 14(4), 044031. https://doi.org/10.1088/1748-9326/ab055a

Gelan, E. (2021). GIS-based multi-criteria analysis for sustainable urban green spaces planning in emerging towns of Ethiopia: the case of Sululta town. *Environmental Systems Research*, 10(1). https://doi.org/10.1186/s40068-021-00220-w

Ghangrekar, M. M. (2022). Quantity estimation of sanitary sewage and storm water. In *Wastewater to Water* (pp. 21-58). https://doi.org/10.1007/978-981-19-4048-4_2

Ghodsi, S. H., Zahmatkesh, Z., Goharian, E., Kerachian, R., and Zhu, Z. (2020). Optimal design of low impact development practices in response to climate change. *Journal of Hydrology*, 580. https://doi.org/10.1016/j.jhydrol.2019.124266

Ghodsi, S. H., Zhu, Z., Gheith, H., Rabideau, A. J., Torres, M. N., and Meindl, K. (2021). Modeling the effectiveness of rain barrels, cisterns, and downspout disconnections for reducing combined sewer overflows in a city-scale watershed. *Water Resources Management*, 35(9), 2895-2908. https://doi.org/10.1007/s11269-021-02875-7

Gill, S. E., Handley, J. F., Ennos, A. R., and Pauleit, S. (2007). Adapting cities for climate change: The role of the green infrastructure. *Built Environment*, 33(1), 115-133. https://doi.org/10.2148/benv.33.1.115

Girma, Y., Terefe, H., Pauleit, S., and Kindu, M. (2019). Urban green infrastructure planning in Ethiopia: The case of emerging towns of Oromia special zone surrounding Finfinne. *Journal of Urban Management*, 75-88. https://doi.org/10.1016/J.JUM.2018.09.004

Gogate, N. G., Kalbar, P. P., and Raval, P. M. (2017). Assessment of stormwater management options in urban contexts using multiple attribute decision-making. *Journal of Cleaner Production*, 142, 2046-2059. https://doi.org/10.1016/j.jclepro.2016.11.079

Gomi, T., Sidle, R. C., and Richardson, J. S. (2002). Understanding processes and downstream linkages of headwater systems. *BioScience*, 52(10), 905-916. https://doi.org/10.1641/0006-3568(2002)052[0905:UPADLO]2.0.CO;2

Görener, A. (2012). Comparing AHP and ANP: An application of strategic decisions making in a manufacturing company. *International Journal of Business and Social Science*, 3(11), 194-208.

Gregory, J. H., Dukes, M. D., Jones, P. H., and Miller, G. L. (2006). Effect of urban soil compaction on infiltration rate. *Journal of Soil and Water Conservation*, 61(3), 117-124.

Grigg, N. S. (2024). Stormwater management: An integrated approach to support healthy, livable, and ecological cities. *Urban Science*, 8(3). https://doi.org/10.3390/urbansci8030089

Gule, T. T., Hailu, B. T., and Lemma, B. (2024). The ripple effect of climate change: Assessing the impacts on water quality and hydrology in Addis Ababa City (Akaki Catchment). *Scientifica*, 2024. https://doi.org/10.1155/2024/8824622

Gule, T. T., Lemma, B., and Hailu, B. T. (2023). Implications of land use/land cover dynamics on urban water quality: Case of Addis Ababa city, Ethiopia. *Heliyon*, 9(5). https://doi.org/10.1016/j.heliyon.2023.e15665

Haasnoot, M., Kwakkel, J. H., Walker, W. E., and ter Maat, J. (2013). Dynamic adaptive policy pathways: A method for crafting robust decisions for a deeply uncertain world. *Global Environmental Change*, 23(2), 485-498. https://doi.org/10.1016/j.gloenvcha.2012.12.006

Haggard, B. E., Moore, P. A., and Brye, K. R. (2005). Effect of slope on runoff from a small variable slope box-plot. *Journal of Environmental Hydrology*, 13(25).

Haider, H., Ghumman, A. R., Al-Salamah, I. S., Ghazaw, Y., and Abdel-Maguid, R. H. (2019). Sustainability evaluation of rainwater harvesting-based flood risk management strategies: A multilevel decision-making framework for arid environments. *Arabian Journal for Science and Engineering*, 44(10), 8465-8488. https://doi.org/10.1007/s13369-019-03848-0

Hailemariam, B. A. (2021). Suitable site selection for urban green space development using geographic information system and remote sensing based on multi criterion analysis. *International Journal of Human Capital in Urban Management*, 6(1), 97-110. https://doi.org/10.22034/IJHCUM.2021.01.08

Hailu, T., Assefa, E., and Zeleke, T. (2024). Urban expansion induced land use changes and its effect on ecosystem services in Addis Ababa, Ethiopia. *Frontiers in Environmental Science*, 12. https://doi.org/10.3389/fenvs.2024.1454556

Hajduk, S., and Jelonek, D. (2021). A decision-making approach based on TOPSIS method for ranking smart cities in the context of urban energy. *Energies*, 14(9). https://doi.org/10.3390/en14092691

Harlis, T. A., and Seo, S. B. (2024). Land suitability analysis for blue-green infrastructure implementation in an urban stormwater management system in Surabaya, Indonesia. *Water Science and Technology*, 90(5), 1501-1519. https://doi.org/10.2166/wst.2024.265

Hassan, W. H., Nile, B. K., and Al-Masody, B. A. (2017). Climate change effect on storm drainage networks by storm water management model. *Environmental Engineering Research*, 22(4), 393-400. https://doi.org/10.4491/eer.2017.036

Hatt, B. E., Deletic, A., and Fletcher, T. D. (2006). Integrated treatment and recycling of stormwater: A review of Australian practice. *Journal of Environmental Management*, 79(1), 102-113. https://doi.org/10.1016/j.jenvman.2005.06.003

Hisoglu, S., Tuominen, A., and Huovila, A. (2023). An approach for selecting optimal locations for electric vehicle solar charging stations. *IET Smart Cities*, 5(2), 123-134. https://doi.org/10.1049/smc2.12058

Holling, C. S. (1973). Resilience and stability of ecological systems. *Annual Review of Ecology and Systematics*, 4(1), 1-23. https://doi.org/10.1146/annurev.es.04.110173.000245

Hordofa, T., Alemu, M., and Eshetu, M. (2024). Land suitability analysis and mapping using geospatial technique and multi criteria decision analysis for urban green area of Goba Town, Oromia, Ethiopia. *Landscape Architecture and Regional Planning*, 9(2), 25-37. https://doi.org/10.11648/j.larp.20240902.11

Horton, R. E. (1933). The role of infiltration in the hydrologic cycle. *Eos, Transactions American Geophysical Union*, 14(1), 446-460.

Hua, P., Yang, W., Qi, X., Jiang, S., Xie, J., Gu, X., Li, H., Zhang, J., and Krebs, P. (2020). Evaluating the effect of urban flooding reduction strategies in response to design rainfall and low impact development. *Journal of Cleaner Production*, 242, 118515. https://doi.org/10.1016/j.jclepro.2019.118515

Huang, I. B., Keisler, J., and Linkov, I. (2011). Multi-criteria decision analysis in environmental sciences: Ten years of applications and trends. *Science of the Total Environment*, 409(19), 3578-3594. https://doi.org/10.1016/j.scitotenv.2011.06.022

Huang, Z., Sun, Y., Fan, Y., Guan, R., Zhang, H., Zhao, L., and Zhang, B. (2025). Toward urban micro-renewal: Integrating "BMP-Plan" and "LID-Design" for enhanced stormwater control – A case study. *Water*, 17(7). https://doi.org/10.3390/w17070992

Huber, W. C., Heaney, J. P., Smolenyak, K. J., and Aggidis, D. A. (1979). *Urban rainfall-runoff-quality data base update with statistical analysis*. Research report Jun 74-Nov 78.

Hunt, W. F., Davis, A. P., and Traver, R. G. (2012). Meeting hydrologic and water quality goals through targeted bioretention design. *Journal of Environmental Engineering*, 138(6), 698-707. https://doi.org/10.1061/(ASCE)EE.1943-7870.0000504

Hussain, S. N., Zwain, H. M., and Nile, B. K. (2022). Modeling the effects of land-use and climate change on the performance of stormwater sewer system using SWMM simulation: case study. *Journal of Water and Climate Change*, 13(1), 125-138. https://doi.org/10.2166/wcc.2021.180

Hussain. (2020). Derivation of earth geoid model for Mosul city in Iraq. *IOP Conference Series: Materials Science and Engineering*, 870(1). https://doi.org/10.1088/1757-899X/870/1/012093

Hwang, C.-L., and Yoon, K. (1981). *Methods for Multiple Attribute Decision Making*. Lecture Notes in Economics.

Ijara, T. M. (2020). Financing green infrastructure development and maintenance in Addis Ababa City, Ethiopia. *International Journal of Social Science and Economic Research*, 5(11), 3678-3694. https://doi.org/10.46609/ijsser.2020.v05i11.025

Imteaz, M. A., Boulomytis, V. T. G., Yilmaz, A. G., and Shanableh, A. (2022). Water quality improvement through rainwater tanks: A review and simulation study. *Water*, 14(9). https://doi.org/10.3390/w14091411

IPCC. (2023). *Climate Change 2023: Synthesis Report. Contribution of Working Groups I, II and III to the Sixth Assessment Report of the Intergovernmental Panel on Climate Change*. Cambridge University Press.

Jacobsen, K., Hollander, J. B., Sternlieb, S. R., Yimere, A., Naegele, A. C., and Schwalm, C. (2024). Urban policy responses to climate hazards in Addis Ababa, Ethiopia. *City and Environment Interactions*, 24. https://doi.org/10.1016/j.cacint.2024.100162

Jacobson, C. R. (2011). Identification and quantification of the hydrological impacts of imperviousness in urban catchments: A review. *Journal of Environmental Management*, 92(6), 1438-1448. https://doi.org/10.1016/j.jenvman.2011.01.018

James, W. (2005). *Rules for Responsible Modeling* (4th ed.). Computational Hydraulics International.

James, W., and Rossman, L. A. (2010). *User's Guide to SWMM5*.

Jayasooriya, V. M., Muthukumaran, S., Ng, A. W. M., and Perera, B. J. C. (2018). Multi criteria decision making in selecting stormwater management green infrastructure for industrial areas Part 2: A case study with TOPSIS. *Water Resources Management*, 32(13), 4297-4312. https://doi.org/10.1007/s11269-018-2052-z

Jemberie, M. A., and Melesse, A. M. (2021). Urban flood management through urban land use optimization using LID techniques, city of Addis Ababa, Ethiopia. *Water*, 13(13). https://doi.org/10.3390/w13131721

Jemberie, M. A., Melesse, A. M., and Abate, B. (2023). Urban drainage: The challenges and failure assessment using AHP, Addis Ababa, Ethiopia. *Water*, 15(5). https://doi.org/10.3390/w15050957

Jennings, A. A., Adeel, A. A., Hopkins, A., Litofsky, A. L., and Wellstead, S. W. (2013). Rain barrel–urban garden stormwater management performance. *Journal of Environmental Engineering*, 139(5), 757-765. https://doi.org/10.1061/(asce)ee.1943-7870.0000663

Jha, A. K., Bank, W., Lamond, J. E., Proverbs, D., and Bhattacharya-Mis, N. (2012). *Cities and Flooding: A guide to integrated urban flood risk management for the 21st Century*. https://doi.org/10.1596/978-0-8213-8866-2

Jia, H., Wang, Z., Zhen, X., Clar, M., and Yu, S. L. (2017). China's sponge city construction: A discussion on technical approaches. *Frontiers of Environmental Science and Engineering*, 11(4), 1-9. https://doi.org/10.1007/s11783-017-0984-4

Jiang, A., McBean, E., Zeng, P., Wang, Y., Chen, H., Binns, A., and Gharabaghi, B. (2023). Understanding changes in the timing of heavy storms: a regional case study of climate change impacts. *Climatic Change*, 176(12), 172. https://doi.org/10.1007/s10584-023-03644-8

Jiang, Y., Zevenbergen, C., and Ma, Y. (2018). Urban pluvial flooding and stormwater management: A contemporary review of China's challenges and "sponge cities" strategy. *Environmental Science and Pollution Research*, 25(16), 15333-15345. https://doi.org/10.1007/s11356-018-1829-1

Jones, M. P., and Hunt, W. F. (2010). Performance of rainwater harvesting systems in the southeastern United States. *Resources, Conservation and Recycling*, 54(10), 623-629. https://doi.org/10.1016/j.resconrec.2009.11.002

Ju. (2023). *Rainwater Harvesting -Process, Advantages and Disadvantages*. https://byjus.com/biology/rainwater-harvesting/

Kabisch, N., Korn, H., Stadler, J., and Bonn, A. (2017). *Nature-based Solutions to Climate Change Adaptation in Urban Areas*. Springer.

Kadlec, R. H., and Wallace, S. D. (2009). *Treatment Wetlands* (2nd ed.). CRC Press.

Karamoutsou, L., Veliou, E., Kvernberg, E. B., and Psilovikos, A. (2024). Urban stormwater management: A sustainable approach. *Water*, 16(15). https://doi.org/10.3390/w16152089

Kaur, R., and Gupta, K. (2022). Blue-green infrastructure (BGI) network in urban areas for sustainable storm water management: A geospatial approach. *City and Environment Interactions*, 16, 100087. https://doi.org/10.1016/j.cacint.2022.100087

Kawabata, Y., Takimoto, K., Nishida, T., Koshikawa, Y., and Aizawa, A. (2025). Integration of green and gray infrastructures – Conceptualization from the perspective of gray engineers. *Structural Engineering International*, 35(1), 125-133. https://doi.org/10.1080/10168664.2024.2398791

Kemal, B., and Adeba, D. (2021). Surface water potential assessment and water demand evaluation (A case of Dabus Watershed, Blue Nile Basin). *Computational Water, Energy, and Environmental Engineering*, 10(04), 155-168. https://doi.org/10.4236/cweee.2021.104012

Kemal, B., Hailu, D., Fekersillassie, D., Seyoum, S., and Sahilu, G. (2025a). Assessing green and grey infrastructure suitability in Addis Ababa, Ethiopia using GIS-based multi-criteria analysis. *Environmental Earth Sciences*, 84(16), 455. https://doi.org/10.1007/s12665-025-12441-8

Kemal, B., Hailu, D., Fekersillassie, D., Seyoum, S., Sahilu, G., and Tariq, A. (2025b). Stormwater modeling in a steep, poorly drained contributing micro-watershed zone of Addis Ababa. *Earth Systems and Environment*. https://doi.org/10.1007/s41748-025-00765-1

Khan, S. T., Chapa, F., and Hack, J. (2020). Highly resolved rainfall-runoff simulation of retrofitted green stormwater infrastructure at the micro-watershed scale. *Land*, 9(9). https://doi.org/10.3390/LAND9090339

Kirkby, M. J. (Ed.). (1978). *Hillslope Hydrology*. John Wiley and Sons.

Koroso, N. H., Lengoiboni, M., and Zevenbergen, J. A. (2021). Urbanization and urban land use efficiency: Evidence from regional and Addis Ababa satellite cities, Ethiopia. *Habitat International*, 117. https://doi.org/10.1016/j.habitatint.2021.102437

Krvavica, N., and Rubinić, J. (2020). Evaluation of design storms and critical rainfall durations for flood prediction in partially urbanized catchments. *Water*, 12(7). https://doi.org/10.3390/w12072044

Kumar, A., Button, C., Gupta, S., and Amezaga, J. (2023). Water sensitive planning for the cities in the Global South. *Water*, 15(2). https://doi.org/10.3390/w15020235

Lau, A., and Behrangi, A. (2022). Understanding intensity–duration–frequency (IDF) curves using IMERG sub-hourly precipitation against dense gauge networks. *Remote Sensing*, 14(19). https://doi.org/10.3390/rs14195032

Le Coustumer, S., Fletcher, T. D., Deletic, A., Barraud, S., and Lewis, J. F. (2009). Hydraulic performance of biofilter systems for stormwater management: Influences of design and operation. *Journal of Hydrology*, 376(1-2), 16-23. https://doi.org/10.1016/j.jhydrol.2009.07.012

Lee, J. G., Nietch, C. T., and Panguluri, S. (2018). Drainage area characterization for evaluating green infrastructure using the Storm Water Management Model. *Hydrology and Earth System Sciences*, 22(5), 2615-2635. https://doi.org/10.5194/hess-22-2615-2018

Lee, J. G., Selvakumar, A., Alvi, K., Riverson, J., Zhen, J. X., Shoemaker, L., and Lai, F. H. (2012). A watershed-scale design optimization model for stormwater best management practices. *Environmental Modelling and Software*, 37, 6-18. https://doi.org/10.1016/j.envsoft.2012.04.011

Lemes de Oliveira, F., Bezerra, M. do C. de L., Nunes, O. V. R., Duarte, E. D. A., Castaldo, A. G., and Almeida, D. N. de. (2025). Nature-based solutions for stormwater management: Co-creating a multiscalar proposal in the Global South. *Land*, 14(4). https://doi.org/10.3390/land14040740

Liao, D., Zhang, Q., Wang, Y., Zhu, H., and Sun, J. (2021). Study of four rainstorm design methods in Chongqing. *Frontiers in Environmental Science*, 9. https://doi.org/10.3389/fenvs.2021.639931

Lin, J., Taguchi, H., and Nakamura, H. (2023). Comprehensive assessment of the role of rain barrels and rain gardens in densely built-up residential areas near Tokyo. https://ssrn.com/abstract=5030434

Lindsey, G., Roberts, L., and Page, W. (1992). Inspection and maintenance of infiltration facilities. *Journal of Soil and Water Conservation*, 47(6), 481-486.

Linkov, I., Satterstrom, F. K., Kiker, G., Batchelor, C., Bridges, T., and Ferguson, E. (2006). From comparative risk assessment to multi-criteria decision analysis and adaptive management: Recent developments and applications. *Environment International*, 32(8), 1072-1093. https://doi.org/10.1016/j.envint.2006.06.013

Liu, T., Lawluvy, Y., Shi, Y., and Yap, P. S. (2021). Low impact development (LID) practices: A review on recent developments, challenges and prospects. *Water, Air, and Soil Pollution*, 232(9). https://doi.org/10.1007/s11270-021-05262-5

Liu, Y., Xiong, Z., Wang, M., Zhang, M., Adnan, R. M., Fu, W., Sun, C., and Tan, S. K. (2025). Decentralized coupled grey–green infrastructure for resilient and cost-effective stormwater management in a historic Chinese district. *Water*, 17(15). https://doi.org/10.3390/w17152325

Lourdes, K. T., Hamel, P., Gibbins, C. N., Sanusi, R., Azhar, B., and Lechner, A. M. (2022). Planning for green infrastructure using multiple urban ecosystem service models and multicriteria analysis. *Landscape and Urban Planning*, 226. https://doi.org/10.1016/j.landurbplan.2022.104500

Luan, B., Yin, R., Xu, P., Wang, X., Yang, X., Zhang, L., and Tang, X. (2019). Evaluating green stormwater infrastructure strategies efficiencies in a rapidly urbanizing catchment using SWMM-based TOPSIS. *Journal of Cleaner Production*, 223, 680-691. https://doi.org/10.1016/j.jclepro.2019.03.028

Madakumbura, G. D., Thackeray, C. W., Norris, J., Goldenson, N., and Hall, A. (2021). Anthropogenic influence on extreme precipitation over global land areas seen in multiple observational datasets. *Nature Communications*, 12(1). https://doi.org/10.1038/s41467-021-24262-x

Mailhot, A., Beauregard, I., Talbot, G., Caya, D., and Biner, S. (2012). Future changes in intense precipitation over Canada based on a regional climate model ensemble. *Journal of Climate*, 25(19), 6724-6745. https://doi.org/10.1175/JCLI-D-11-00447.1

Mallin, M. A., Johnson, V. L., and Ensign, S. H. (2009). Comparative impacts of stormwater runoff on water quality of an urban, a suburban, and a rural stream. *Environmental Monitoring and Assessment*, 159(1-4), 475-491. https://doi.org/10.1007/s10661-008-0644-4

Mallin, M. A., Williams, K. E., Esham, E. C., and Lowe, R. P. (2000). Effect of human development on bacteriological water quality in coastal watersheds. *Ecological Applications*, 10(4), 1047-1056. https://doi.org/10.1890/1051-0761(2000)010[1047:EOHDOB]2.0.CO;2

Mani, M., Bozorg-Haddad, O., and Loáiciga, H. A. (2019). A new framework for the optimal management of urban runoff with low-impact development stormwater control measures considering service-performance reduction. *Journal of Hydroinformatics*, 21(5), 727-744. https://doi.org/10.2166/hydro.2019.126

Marhaento, H., Booij, M. J., and Hoekstra, A. Y. (2018). Hydrological response to future land-use changes and climate change in a tropical catchment. *Hydrological Sciences Journal*, 63(9), 1368-1385. https://doi.org/10.1080/02626667.2018.1511054

Marsalek, J. (2006). *Urban Water Cycle Processes and Interactions*. CRC Press. https://doi.org/10.1201/9781482288544

Marsh, W. M. (2010). *Landscape Planning: Environmental Applications* (5th ed.). John Wiley and Sons.

Martínez, C., Vojinovic, Z., and Sanchez, A. (2021). Multi-objective model-based assessment of green-grey infrastructures for urban flood mitigation. *Hydrology*, 8(3). https://doi.org/10.3390/hydrology8030110

Marzuki, A., Bagheri, M., Ahmad, A., Masron, T., and Akhir, M. F. (2023). Establishing a GIS-SMCDA model of sustainable eco-tourism development in Pahang, Malaysia. *Episodes*, 46(3), 375-387. https://doi.org/10.18814/epiiugs/2022/022037

Mayou, L. A., Alamdari, N., Ahmadisharaf, E., and Kamali, M. (2024). Impacts of future climate and land use/land cover change on urban runoff using fine-scale hydrologic modeling. *Journal of Environmental Management*, 362, 121284. https://doi.org/10.1016/j.jenvman.2024.121284

McFarland, A. R., Larsen, L., Yeshitela, K., Engida, A. N., and Love, N. G. (2019). Guide for using green infrastructure in urban environments for stormwater management. *Environmental Science: Water Research and Technology*, 5(4), 643-659. https://doi.org/10.1039/c8ew00498f

McGrane, S. J. (2016). Impacts of urbanisation on hydrological and water quality dynamics, and urban water management: a review. *Hydrological Sciences Journal*, 61(13), 2295-2311. https://doi.org/10.1080/02626667.2015.1128084

McGuire, K. J., and McDonnell, J. J. (2006). A review and evaluation of catchment transit time modeling. *Journal of Hydrology*, 330(3-4), 543-563. https://doi.org/10.1016/j.jhydrol.2006.04.020

Meerow, S., Newell, J. P., and Stults, M. (2016). Defining urban resilience: A review. *Landscape and Urban Planning*, 147, 38-49. https://doi.org/10.1016/j.landurbplan.2015.11.011

Mekuria, D. M., Kassegne, A. B., and Asfaw, S. L. (2021). Assessing pollution profiles along Little Akaki River receiving municipal and industrial wastewaters, Central Ethiopia: implications for environmental and public health safety. *Heliyon*, 7(7). https://doi.org/10.1016/j.heliyon.2021.e07526

Mensah, C. A. (2014). Urban green spaces in Africa: Nature and challenges. *International Journal of Ecosystem*, 2014(1), 1-11. https://doi.org/10.5923/j.ije.20140401.01

Mentens, J., Raes, D., and Hermy, M. (2006). Green roofs as a tool for solving the rainwater runoff problem in the urbanized 21st century? *Landscape and Urban Planning*, 77(3), 217-226. https://doi.org/10.1016/j.landurbplan.2005.02.010

Mguni, P., Herslund, L., and Jensen, M. B. (2015). Green infrastructure for flood-risk management in Dar es Salaam and Copenhagen: Exploring the potential for transitions towards sustainable urban water management. *Water Policy*, 17(1), 126-142. https://doi.org/10.2166/wp.2014.047

Millennium Ecosystem Assessment. (2005). *Ecosystems and Human Well-being: Synthesis*. Island Press.

Milly, P. C. D., Betancourt, J., Falkenmark, M., Hirsch, R. M., Kundzewicz, Z. W., Lettenmaier, D. P., and Stouffer, R. J. (2008). Stationarity is dead: Whither water management? *Science*, 319(5863), 573-574. https://doi.org/10.1126/science.1151915

Mitchell, V. G. (2006). Applying integrated urban water management concepts: A review of Australian experience. *Environmental Management*, 37(5), 589-605. https://doi.org/10.1007/s00267-004-0252-1

Mobarak, B., Shrahily, R., Mohammad, A., and Alzandi, A. A. (2022). Assessing green infrastructures using GIS and the multi-criteria decision-making method: The case of the Al Baha Region (Saudi Arabia). *Forests*, 13(12). https://doi.org/10.3390/f13122013

Moisa, M. B., Dejene, I. N., Roba, Z. R., and Gemeda, D. O. (2022). Impact of urban land use and land cover change on urban heat island and urban thermal comfort level: a case study of Addis Ababa City, Ethiopia. *Environmental Monitoring and Assessment*, 194(10). https://doi.org/10.1007/s10661-022-10414-z

Moisa, M. B., Merga, B. B., Deribew, K. T., Feyissa, M. E., Gurmessa, M. M., and Gemeda, D. O. (2023). Urban green space suitability analysis using geospatial techniques: a case study of Addis Ababa, Ethiopia. *Geocarto International*, 38(1). https://doi.org/10.1080/10106049.2023.2213674

Moriasi, D. N., Arnold, J. G., Van Liew, M. W., Bingner, R. L., Harmel, R. D., and Veith, T. L. (2007). Model evaluation guidelines for systematic quantification of accuracy in watershed simulations. *Transactions of the ASABE*, 50(3), 885-900.

Mouhoumed, R. M., Ekmekcioğlu, Ö., Başakın, E. E., and Özger, M. (2023). Integrated Fuzzy AHP-TOPSIS model for assessing managed aquifer recharge potential in a hot dry region: A case study of Djibouti at a country scale. *Water*, 15(14). https://doi.org/10.3390/w15142534

Mugiyo, H., Chimonyo, V. G., Sibanda, M., Kunz, R., Nhamo, L., Masemola, C. R., and Mabhaudhi, T. (2021). Multi-criteria suitability analysis for neglected and underutilised crop species in South Africa. *PLoS ONE*, 16(1), e0244734.

Mukhtar, M. A., Shangguan, D., Ding, Y., Anjum, M. N., Banerjee, A., Butt, A. Q., Yadav, N., Li, D., Yang, Q., Khan, A. A., Muhammad, A., and He, B. B. (2024). Integrated flood risk assessment in Hunza-Nagar, Pakistan: Unifying big climate data analytics and multi-criteria decision-making with GIS. *Frontiers in Environmental Science*, 12. https://doi.org/10.3389/fenvs.2024.1337081

Mulligan, J., Bukachi, V., Clause, J. C., Jewell, R., Kirimi, F., and Odbert, C. (2020). Hybrid infrastructures, hybrid governance: New evidence from Nairobi (Kenya) on green-blue-grey infrastructure in informal settlements. *Anthropocene*, 29, 100227. https://doi.org/10.1016/j.ancene.2019.100227

Nazari, A. H., Roozbahani, A., and Hashemy Shahdany, S. M. (2021). Urban stormwater management by optimizing low impact development techniques and integration of SWMM and SUSTAIN models. *Journal of Water and Wastewater*, 32(4), 136-151. https://doi.org/10.22093/wwj.2021.285296.3138

Nguyen, T. T., Ngo, H. H., Guo, W., Wang, X. C., Ren, N., and Li, G. (2019). Implementation of a specific urban water management – Sponge City. *Science of the Total Environment*, 652, 147-162. https://doi.org/10.1016/j.scitotenv.2018.10.168

Nie, L., Lindholm, O., Lindholm, G., and Syversen, E. (2009). Impacts of climate change on urban drainage systems - a case study in Fredrikstad, Norway. *Urban Water Journal*, 6(4), 323-332. https://doi.org/10.1080/15730620802600924

Nimmo, J. R. (2004). Porosity and pore size distribution. In D. Hillel (Ed.), *Encyclopedia of Soils in the Environment* (Vol. 3, pp. 295-303). Elsevier.

Niyonkuru, P., Sang, J. K., Nyawada, M. O., and Munyaneza, O. (2019). Calibration and validation of EPA SWMM for stormwater runoff modelling in Nyabugogo catchment, Rwanda. *Journal of Sustainable Research in Engineering*, 4(4), 152-159.

Novotny, V., Sung, H. M., Bannerman, R., and Baum, K. (1985). Estimating nonpoint pollution from small urban watersheds. *Journal of the Water Pollution Control Federation*, 57(4), 339-348.

Nwaogazie, I. L., Sam, M. G., and Ikebude, C. (2021). Improving Indian meteorological department method for 24-hourly rainfall downscaling to shorter durations for IDF modelling. *International Journal of Hydrology*, 5(2), 72-82. https://doi.org/10.15406/ijh.2021.05.00268

Oberascher, M., Zischg, J., Palermo, S. A., Kinzel, C., Rauch, W., and Sitzenfrei, R. (2019). Smart rain barrels: Advanced LID management through measurement and control. *Green Energy and Technology*, 777-782. https://doi.org/10.1007/978-3-319-99867-1_134

Oberndorfer, E., Lundholm, J., Bass, B., Coffman, R. R., Doshi, H., Dunnett, N., Gaffin, S., Köhler, M., Liu, K. K. Y., and Rowe, B. (2007). Green roofs as urban ecosystems: Ecological structures, functions, and services. *BioScience*, 57(10), 823-833. https://doi.org/10.1641/B571005

O'Donnell, E. C., Lamond, J. E., and Thorne, C. R. (2017). Recognising barriers to implementation of blue-green infrastructure: a Newcastle case study. *Urban Water Journal*, 14(9), 964-971. https://doi.org/10.1080/1573062X.2017.1279190

Omidi Arjenaki, M., Zarif Sanayei, H. R., and Heidarzadeh, H. (2020). Urban surface runoff simulation and prioritization of critical sub catchments using SWMM model and TOPSIS method (Case study: Shahrekord City). *Journal of Water and Wastewater*, 31(4), 99-113. https://doi.org/10.22093/wwj.2020.209846.2957

Omitaomu, O. A., Kotikot, S. M., and Parish, E. S. (2021). Planning green infrastructure placement based on projected precipitation data. *Journal of Environmental Management*, 279, 111718. https://doi.org/10.1016/j.jenvman.2020.111718

O'Neill, B. C., Tebaldi, C., van Vuuren, D. P., Eyring, V., Friedlingstein, P., Hurtt, G., Knutti, R., Kriegler, E., Lamarque, J. F., Lowe, J., Meehl, G. A., Moss, R., Riahi, K., and Sanderson, B. M. (2016). The Scenario Model Intercomparison Project (ScenarioMIP) for CMIP6. *Geoscientific Model Development*, 9(9), 3461-3482. https://doi.org/10.5194/gmd-9-3461-2016

Osman, K. T. (2018). Soils on steep slopes. In *Management of Soil Problems* (pp. 185-217). Springer. https://doi.org/10.1007/978-3-319-75527-4_8

Ou, J., Li, J., Li, X., and Zhang, J. (2024). Planning and design strategies for green stormwater infrastructure from an urban design perspective. *Water*, 16(1). https://doi.org/10.3390/w16010029

Oudin, L., Salavati, B., Furusho-Percot, C., Ribstein, P., and Saadi, M. (2018). Hydrological impacts of urbanization at the catchment scale. *Journal of Hydrology*, 559, 774-786. https://doi.org/10.1016/j.jhydrol.2018.02.064

Özkan, B., Özceylan, E., and Sarıçiçek, İ. (2019). GIS-based MCDM modeling for landfill site suitability analysis: A comprehensive review of the literature. *Environmental Science and Pollution Research*, 26(30), 30711-30730. https://doi.org/10.1007/s11356-019-06298-1

Parkinson, J., and Mark, O. (2015). *Urban Stormwater Management in Developing Countries*. IWA Publishing. https://doi.org/10.2166/9781780402574

Pathan, A. I., Agnihotri, P. G., and Patel, D. (2022). Integrated approach of AHP and TOPSIS (MCDM) techniques with GIS for dam site suitability mapping: a case study of Navsari City, Gujarat, India. *Environmental Earth Sciences*, 81(18), 1-19. https://doi.org/10.1007/s12665-022-10568-6

Piran, H., Maleknia, R., Akbari, H., Soosani, J., and Karami, O. (2013). Site selection for local forest park using analytic hierarchy process and geographic information system (case study: Badreh County). *International Journal of Science and Basic Applied Research*, 6(7), 930-935.

Pitt, R., Lantrip, J., Harrison, R., Henry, C., and Xue, D. (1999). *Infiltration through Disturbed Urban Soils*. USEPA.

Pour, S. H., Wahab, A. K. A., Shahid, S., Asaduzzaman, M., and Dewan, A. (2020). Low impact development techniques to mitigate the impacts of climate-change-induced urban floods: Current trends, issues and challenges. *Sustainable Cities and Society*, 62. https://doi.org/10.1016/j.scs.2020.102373

Qiao, X. J., Liao, K. H., and Randrup, T. B. (2020). Sustainable stormwater management: A qualitative case study of the Sponge Cities initiative in China. *Sustainable Cities and Society*, 53, 101963. https://doi.org/10.1016/j.scs.2019.101963

Qin, H. P., Li, Z. X., and Fu, G. (2013). The effects of low impact development on urban flooding under different rainfall characteristics. *Journal of Environmental Management*, 129, 577-585. https://doi.org/10.1016/j.jenvman.2013.08.026

Qu, Y., and Duffy, C. J. (2007). A semidiscrete finite volume formulation for multiprocess watershed simulation. *Water Resources Research*, 43(8). https://doi.org/10.1029/2006WR005752

R. Palaka. (2016). Development of intensity duration frequency curves for Narsapur Mandal, Telangana State, India. *International Journal of Research in Engineering and Technology*, 05(06), 109-113. https://doi.org/10.15623/ijret.2016.0506022

Redshaw, P., Boon, D., Campbell, G., Willis, M., Mattai, J., Free, M., Jordan, C., Kemp, S. J., Morley, A., and Thomas, M. (2019). The 2017 Regent landslide, Freetown Peninsula, Sierra Leone. *Quarterly Journal of Engineering Geology and Hydrogeology*, 52(4), 435-444. https://doi.org/10.1144/qjegh2018-187

Regional Plan. (2023, July 21). *Vegetated Swales | Better Town Toolkit (Regional Plan Association and Orange County Planning Department*. http://designyourtown.org/design_detail/vegetated-swales/

Rejani, R., Rao, K. V., Osman, M., Chary, G. R., Pushpanjali, Reddy, K. S., and Rao, C. S. (2015). Spatial and temporal estimation of runoff in a semi-arid microwatershed of Southern India. *Environmental Monitoring and Assessment*, 187(8). https://doi.org/10.1007/s10661-015-4772-3

Rettie, F. M., Gayler, S., Weber, T. K. D., Tesfaye, K., and Streck, T. (2023). High-resolution CMIP6 climate projections for Ethiopia using the gridded statistical downscaling method. *Scientific Data*, 10(1). https://doi.org/10.1038/s41597-023-02337-2

Rezaei, A. R., Ismail, Z., Niksokhan, M. H., Dayarian, M. A., Ramli, A. H., and Shirazi, S. M. (2019). A quantity-quality model to assess the effects of source control stormwater management on hydrology and water quality at the catchment scale. *Water*, 11(7). https://doi.org/10.3390/w11071415

Riahi, K., van Vuuren, D. P., Kriegler, E., Edmonds, J., O'Neill, B. C., Fujimori, S., Bauer, N., Calvin, K., Dellink, R., Fricko, O., Lutz, W., Popp, A., Cuaresma, J. C., Kc, S., Leimbach, M., Jiang, L., Kram, T., Rao, S., Emmerling, J., Ebi, K., Hasegawa, T., Havlik, P., Humpenöder, F., Da Silva, L. A., Smith, S., Stehfest, E., Bosetti, V., Eom, J., Gernaat, D., Masui, T., Rogelj, J., Strefler, J., Drouet, L., Krey, V., Luderer, G., Harmsen, M., Takahashi, K., Baumstark, L., Doelman, J. C., Kainuma, M., Klimont, Z., Marangoni, G., Lotze-Campen, H., Obersteiner, M., Tabeau, A., and Tavoni, M. (2017). The Shared Socioeconomic Pathways and their energy, land use, and greenhouse gas emissions implications: An overview. *Global Environmental Change*, 42, 153-168. https://doi.org/10.1016/j.gloenvcha.2016.05.009

Ridolfi, E., Mondino, E., and Di Baldassarre, G. (2021). Hydrological risk: Modeling flood memory and human proximity to rivers. *Hydrology Research*, 52(1), 241-252. https://doi.org/10.2166/NH.2020.195

Rodriguez, M., Fu, G., Butler, D., Yuan, Z., and Sharma, K. (2021). Exploring the spatial impact of green infrastructure on urban drainage resilience. *Water*, 13(13), 1-21. https://doi.org/10.3390/w13131789

Rossman, L. A. (2010). *Storm Water Management Model User's Manual Version 5.0*. USEPA.

Rossman, L. A. (2015). *Storm Water Management Model User 's Manual Version 5.1* (EPA/600/R-14/413b). U.S. Environmental Protection Agency.

Rossman, L. A., and Huber, W. C. (2016). *Storm Water Management Model Reference Manual Volume III – Water Quality*. USEPA.

Saaty, T. L. (1980). *The Analytic Hierarchy Process*. McGraw-Hill.

Saaty, T. L. (2005). *Theory and Applications of the Analytic Network Process*. RWS Publications.

Saaty, T. L. (2008). Decision making with the analytic hierarchy process. *International Journal of Services Sciences*, 1(1), 83. https://doi.org/10.1504/IJSSCI.2008.017590

Saaty, T. L., and Vargas, L. G. (2012). The possibility of group choice: Pairwise comparisons and merging functions. *Social Choice and Welfare*, 38(3), 481-496. https://doi.org/10.1007/s00355-011-0541-6

Sagar Kumar, M., and Umamahesh, N. V. (2024). Integrated assessment of future climate and land use changes on urban floods: A Markov chain and PCSWMM-based approach for Hyderabad case study. *Water Science and Technology*, 89(4), 1003-1027. https://doi.org/10.2166/wst.2024.034

Saget, A., Chebbo, G., and Bertrand-Krajewski, J. L. (1996). The first flush in sewer systems. *Water Science and Technology*, 33(9), 101-108. https://doi.org/10.2166/wst.1996.0185

Saha, P., Mitra, R., Das, J., and Mandal, D. K. (2024). Urban flash flood prediction modelling using probabilistic and statistical approaches. *Results in Earth Sciences*, 2, 100032. https://doi.org/10.1016/j.rines.2024.100032

Saraswat, C., Kumar, P., and Mishra, B. K. (2016). Assessment of stormwater runoff management practices and governance under climate change and urbanization: An analysis of Bangkok, Hanoi and Tokyo. *Environmental Science and Policy*, 64, 101-117. https://doi.org/10.1016/J.ENVSCI.2016.06.018

Scholz, M., and Grabowiecki, P. (2007). Review of permeable pavement systems. *Building and Environment*, 42(11), 3830-3836. https://doi.org/10.1016/j.buildenv.2006.11.016

Seidu, S., Chan, D. W. M., and Taiwo, R. (2025). Integrating green and grey infrastructure systems in dense urban regions: a synthesis of critical barriers and effective implementation guidelines. *Clean Technologies and Environmental Policy*. https://doi.org/10.1007/s10098-025-03309-3

Senay, S. D., and Worner, S. P. (2019). Multi-scenario species distribution modeling. *Insects*, 10(3). https://doi.org/10.3390/insects10030065

Senes, G., Ferrario, P. S., Cirone, G., Fumagalli, N., Frattini, P., Sacchi, G., and Valè, G. (2021). Nature-based solutions for storm water management – creation of a green infrastructure suitability map as a tool for land-use planning at the municipal level in the province of Monza-Brianza (Italy). *Sustainability*, 13(11). https://doi.org/10.3390/su13116124

Shamsi, U. (Sam). (2015). Modeling to quantify the benefits of LID for CSO reduction. In *Low Impact Development Technology: Design Methods and Case Studies* (pp. 136-140). https://doi.org/10.1061/9780784413883.015

Sharma, R., and Malaviya, P. (2021). Management of stormwater pollution using green infrastructure: The role of rain gardens. *Wiley Interdisciplinary Reviews: Water*, 8(2), e1507. https://doi.org/10.1002/wat2.1507

Shawky, M., Moussa, A., Hassan, Q. K., and El-Sheimy, N. (2019). Pixel-based geometric assessment of channel networks/orders derived from global spaceborne digital elevation models. *Remote Sensing*, 11(3). https://doi.org/10.3390/rs11030235

Shrestha, A., Chaosakul, T., Priyankara, D. P. M. P., Chuyen, L. H., Myat, S. S., Syne, N. K., Irvine, K., Koottatep, T., and Babel, M. S. (2014). Application of PCSWMM to explore possible climate change impacts on surface flooding in a peri-urban area of Pathumthani, Thailand. *Journal of Water Management and Modeling*, 1-7. https://doi.org/10.14796/jwmm.c377

Shrestha, S., Bhatta, B., Shrestha, M., and Shrestha, P. K. (2018). Integrated assessment of the climate and land use change impact on hydrology and water quality in the Songkhram River Basin, Thailand. *Science of the Total Environment*, 643, 1610-1622. https://doi.org/10.1016/j.scitotenv.2018.06.306

Shuster, W. D., Bonta, J., Thurston, H., Warnemuende, E., and Smith, D. R. (2005). Impacts of impervious surface on watershed hydrology: A review. *Urban Water Journal*, 2(4), 263-275. https://doi.org/10.1080/15730620500386529

Silas, E. O., Onwuka, D. O., and Njoku, F. C. (2022). Factorial model prediction for performance of ordinary Portland cement blended with metakaolin and sawdust ash for oil well cementing. *NIPES Journal of Science and Technology Research*, 4(2), 64-78. https://doi.org/10.37933/nipes.e/4.2.2022.7

Silva, C. de M., and Silva, G. B. L. da. (2020). Cumulative effect of the disconnection of impervious areas within residential lots on runoff generation and temporal patterns in a small urban area. *Journal of Environmental Management*, 253, 109719. https://doi.org/10.1016/j.jenvman.2019.109719

Singh, J., Knapp, H. V., and Demissie, M. (2004). *Hydrologic Modeling of the Iroquois River Watershed Using HSPF and SWAT*.

Singh, V. P., and Woolhiser, D. A. (2002). Mathematical modeling of watershed hydrology. *Journal of Hydrologic Engineering*, 7(4), 270-292. https://doi.org/10.1061/(ASCE)1084-0699(2002)7:4(270)

Solomon, T., Yeshitela, K., and Abebe, W. T. (2024). Potential of ecological water treatment elements to reduce pollution of river water used for urban agriculture in Addis Ababa, Ethiopia. *Discover Water*, 4(1). https://doi.org/10.1007/s43832-024-00118-5

Soonthornnonda, P., and Christensen, E. R. (2008). A load model based on antecedent dry periods for pollutants in stormwater. *Water Environment Research*, 80(2), 162-171. https://doi.org/10.2175/106143007x220888

Sørup, H. J. D., Fryd, O., Liu, L., Arnbjerg-Nielsen, K., and Jensen, M. B. (2019). An SDG-based framework for assessing urban stormwater management systems. *Blue-Green Systems*, 1(1), 102-118. https://doi.org/10.2166/bgs.2019.922

Spahr, K. M., Bell, C. D., McCray, J. E., and Hogue, T. S. (2020). Greening up stormwater infrastructure: Measuring vegetation to establish context and promote cobenefits in a diverse set of US cities. *Urban Forestry and Urban Greening*, 48, 126548. https://doi.org/10.1016/j.ufug.2019.126548

Speak, A. F., Rothwell, J. J., Lindley, S. J., and Smith, C. L. (2013). Rainwater runoff retention on an aged intensive green roof. *Science of the Total Environment*, 461-462, 28-38. https://doi.org/10.1016/j.scitotenv.2013.04.085

Srivastava, K. L., Abebe, M., Astatke, A., Haile, M., and Regassa, H. (1989). Distribution and importance of Ethiopian Vertisols and location of study sites. In *Management of Vertisols for Improved Agricultural Production*.

Stagge, J. H., Davis, A. P., Jamil, E., and Kim, H. (2012). Performance of grass swales for improving water quality from highway runoff. *Water Environment Research*, 84(10), 1705-1716. https://doi.org/10.2175/106143012X13373550427075

Stovin, V. (2010). The potential of green roofs to manage urban stormwater. *Water and Environment Journal*, 24(3), 192-199. https://doi.org/10.1111/j.1747-6593.2009.00174.x

Sun, N., Hall, M., Hong, B., and Zhang, L. (2014). Impact of SWMM catchment discretization: Case study in Syracuse, New York. *Journal of Hydrologic Engineering*, 19(1), 223-234. https://doi.org/10.1061/(asce)he.1943-5584.0000777

Sun, Y., Deng, L., Pan, S.-Y., Chiang, P.-C., Sable, S. S., and Shah, K. J. (2020). Integration of green and gray infrastructures for sponge city: Water and energy nexus. *Water-Energy Nexus*, 3, 29-40. https://doi.org/10.1016/j.wen.2020.03.003

Tansar, H., Li, F., Zheng, F., and Duan, H. F. (2024). A critical review on optimization and implementation of green-grey infrastructures for sustainable urban stormwater management. *AQUA - Water Infrastructure, Ecosystems and Society*, 73(6), 1135-1150. https://doi.org/10.2166/aqua.2024.310

Tavakol-Davani, H. E., Tavakol-Davani, H., Burian, S. J., McPherson, B. J., and Barber, M. E. (2019). Green infrastructure optimization to achieve pre-development conditions of a semiarid urban catchment. *Environmental Science: Water Research and Technology*, 5(6), 1157-1171. https://doi.org/10.1039/c8ew00789f

Taylor, C. H. (1982). The effect on storm runoff response of seasonal variations in contributing zones in small watersheds. *Nordic Hydrology*, 13(3), 165-182.

Taylor, G. D., Fletcher, T. D., Wong, T. H., Breen, P. F., and Duncan, H. P. (2005). Nitrogen composition in urban runoff – implications for stormwater treatment. *Journal of Environmental Engineering*, 131(4), 622-632. https://doi.org/10.1061/(ASCE)0733-9372(2005)131:4(622)

Temprano, J., Arango, Ó., Cagiao, J., Suárez, J., and Tejero, I. (2006). Stormwater quality calibration by SWMM: A case study in Northern Spain. *Water SA*, 32(1), 55-63. https://doi.org/10.4314/wsa.v32i1.5240

Teston, A., Scolaro, T. P., Maykot, J. K., and Ghisi, E. (2022). Comprehensive environmental assessment of rainwater harvesting systems: A literature review. *Water*, 14(17), 2716. https://doi.org/10.3390/w14172716

Tripathi, A. K., Agrawal, S., and Gupta, R. D. (2021). Comparison of GIS-based AHP and fuzzy AHP methods for hospital site selection: a case study for Prayagraj City, India. *GeoJournal*, 1-22.

Trupti, L., Kote, A., and Mali, S. (2020). Integration of GIS and AHP-ANP modeling for landfill site selection for Nagpur City, India. In *Recent developments in waste management: Select proceedings of Recycle 2018* (pp. 499-510). Springer.

Tu, M. C., and Smith, P. (2018). Modeling pollutant buildup and washoff parameters for SWMM based on land use in a semiarid urban watershed. *Water, Air, and Soil Pollution*, 229(4). https://doi.org/10.1007/s11270-018-3777-2

Tucker, C. J. (1979). Red and photographic infrared linear combinations for monitoring vegetation. *Remote Sensing of Environment*, 8(2), 127-150. https://doi.org/10.1016/0034-4257(79)90013-0

Tzoulas, K., Korpela, K., Venn, S., Yli-Pelkonen, V., Kaźmierczak, A., Niemela, J., and James, P. (2007). Promoting ecosystem and human health in urban areas using green infrastructure: A literature review. *Landscape and Urban Planning*, 81(3), 167-178. https://doi.org/10.1016/j.landurbplan.2007.02.001

UN-Habitat. (2017). *The state of Latin American and Caribbean cities 2012: towards a new urban transition*.

UN-Habitat. (2021). *Cities and Climate Change*.

United Nations. (2014). *World Urbanization Prospects: The 2014 Revision, Highlights* (ST/ESA/SER.A/352).

United Nations. (2015). *Global Sustainable Development Report*.

USACE (U.S. Army Corps of Engineers). (2022). Hydrologic Modeling System HEC-HMS User 's Manual Version 4.11 (CPD-74A). Hydrologic Engineering Center, U.S. Army Corps of Engineers.

USEPA (U.S. Environmental Protection Agency). (1983). *Results of the Nationwide Urban Runoff Program. Vol. I*.

USEPA. (1993). *Handbook: Urban Runoff Pollution Prevention and Control Planning*.

USEPA (U.S. Environmental Protection Agency). (2009). *SUSTAIN – A Framework for Placement of Best Management Practices for Urban Stormwater Management*. National Risk Management Research Laboratory, Office of Research and Development, U.S. Environmental Protection Agency.

USEPA. (2025). *Urbanization and Stormwater Runoff*.

van Rooijen, D. J., Biggs, T. W., Smout, I., and Drechsel, P. (2010). Urban growth, wastewater production and use in irrigated agriculture: A comparative study of Accra, Addis Ababa and Hyderabad. *Irrigation and Drainage Systems*, 24(1-2), 53-64. https://doi.org/10.1007/s10795-009-9089-3

Vasconcelos, A. F., Barbassa, A. P., dos Santos, M. F. N., and Imani, M. A. (2022). Barriers to sustainable urban stormwater management in developing countries: The case of Brazil. *Land Use Policy*, 112. https://doi.org/10.1016/j.landusepol.2021.105821

Venkataramanan, V., Packman, A. I., Peters, D. R., Lopez, D., McCuskey, D. J., McDonald, R. I., Miller, W. M., and Young, S. L. (2019). A systematic review of the human health and social well-being outcomes of green infrastructure for stormwater and flood management. *Journal of Environmental Management*, 246, 868-880. https://doi.org/10.1016/j.jenvman.2019.05.028

Vijayaraghavan, K., Biswal, B. K., Adam, M. G., Soh, S. H., Tsen-Tieng, D. L., Davis, A. P., Chew, S. H., Tan, P. Y., Babovic, V., and Balasubramanian, R. (2021). Bioretention systems for stormwater management: Recent advances and prospects. *Journal of Environmental Management*, *292*(April), 112766. https://doi.org/10.1016/j.jenvman.2021.112766

Vineyard, D., Ingwersen, W. W., Hawkins, T. R., Xue, X., Demeke, B., and Shuster, W. (2015). Comparing green and grey infrastructure using life cycle cost and environmental impact: A rain garden case study in Cincinnati, OH. *Journal of the American Water Resources Association*, 51(5), 1342-1360. https://doi.org/10.1111/1752-1688.12320

Vymazal, J. (2011). Constructed wetlands for wastewater treatment: Five decades of experience. *Environmental Science and Technology*, 45(1), 61-69. https://doi.org/10.1021/es101403q

Wadzuk, B., DelVecchio, T., Sample-Lord, K., Ahmed, M., and Welker, A. (2021). Nutrient removal in rain garden lysimeters with different soil types. *Journal of Sustainable Water in the Built Environment*, 7(1). https://doi.org/10.1061/jswbay.0000924

Wagener, T., and Wheater, H. S. (2006). Parameter estimation and regionalization for continuous rainfall-runoff models including uncertainty. *Journal of Hydrology*, 320(1-2), 132-154. https://doi.org/10.1016/j.jhydrol.2005.07.015

Wagesho, N., and Yohannes, M. (2021). Analysis of rainfall extremes and its implications on water resources management in Ethiopia. *Journal of Water and Climate Change*, 12(5), 1823-1842. https://doi.org/10.2166/wcc.2020.318

Waheeb, S. A., Zerouali, B., Elbeltagi, A., Alwetaishi, M., Wong, Y. J., Bailek, N., AlSaggaf, A. A., Abd Elrahman, S. I. M., Santos, C. A. G., and Majrashi, A. A. (2023). Enhancing sustainable urban planning through GIS and multiple-criteria decision analysis: A case study of green space infrastructure in Taif Province, Saudi Arabia. *Water*, 15(17). https://doi.org/10.3390/w15173031

Walker, B., Holling, C. S., Carpenter, S. R., and Kinzig, A. (2004). Resilience, adaptability and transformability in social–ecological systems. *Ecology and Society*, 9(2), 5. https://doi.org/10.5751/ES-00650-090205

Walker, W. E., Rahman, S. A., and Cave, J. (2001). Adaptive policies, policy analysis, and policy-making. *European Journal of Operational Research*, 128(2), 282-289. https://doi.org/10.1016/S0377-2217(00)00071-0

Walsh, C. J., Roy, A. H., Feminella, J. W., Cottingham, P. D., Groffman, P. M., and Morgan, R. P. (2005). The urban stream syndrome: current knowledge and the search for a cure. *Journal of the North American Benthological Society*, 24(3), 706-723. https://doi.org/10.1899/04-028.1

Wang, J., Liu, J., Mei, C., Wang, H., and Lu, J. (2022). A multi-objective optimization model for synergistic effect analysis of integrated green-gray-blue drainage system in urban inundation control. *Journal of Hydrology*, 609, 127725. https://doi.org/10.1016/j.jhydrol.2022.127725

Wang, L., Zhao, J., Xiong, Z., Zhuang, J., and Wang, M. (2025). Integrating grey–green infrastructure in urban stormwater management: A multi-objective optimization framework for enhanced resilience and cost efficiency. *Applied Sciences*, 15(7). https://doi.org/10.3390/app15073852

Wang, M., Liu, M., Zhang, D., Qi, J., Fu, W., Zhang, Y., Rao, Q., Bakhshipour, A. E., and Tan, S. K. (2023). Assessing and optimizing the hydrological performance of grey-green infrastructure systems in response to climate change and non-stationary time series. *Water Research*, 232, 119720. https://doi.org/10.1016/j.watres.2023.119720

Wang, M., Liu, M., Zhang, D., Zhang, Y., Su, J., Zhou, S., Bakhshipour, A. E., and Tan, S. K. (2023). Assessing hydrological performance for optimized integrated grey-green infrastructure in response to climate change based on shared socio-economic pathways. *Sustainable Cities and Society*, 91, 104436. https://doi.org/10.1016/j.scs.2023.104436

Wang, M., Zhang, D. Q., Su, J., Trzcinski, A. P., Dong, J. W., and Tan, S. K. (2017). Future scenarios modeling of urban stormwater management response to impacts of climate change and urbanization. *Clean – Soil, Air, Water*, 45(10). https://doi.org/10.1002/clen.201700111

Weiler, M. (2017). Macropores and preferential flow – a love-hate relationship. *Hydrological Processes*, 31(1), 3-11. https://doi.org/10.1002/hyp.11074

Weiss, P. T., Kayhanian, M., Gulliver, J. S., and Khazanovich, L. (2017). Permeable pavement in northern North American urban areas: research review and knowledge gaps. *International Journal of Pavement Engineering*, 20(2), 1-16. https://doi.org/10.1080/10298436.2017.1279482

Wilson, J. P., and Gallant, J. C. (2000). *Terrain Analysis: Principles and Applications*. John Wiley and Sons.

Woldegerima, T., Yeshitela, K., and Lindley, S. (2016). Characterizing the urban environment through urban morphology types (UMTs) mapping and land surface cover analysis: The case of Addis Ababa, Ethiopia. *Urban Ecosystems*, 19(2), 245-263. https://doi.org/10.1007/s11252-016-0590-9

World Bank. (2015). *Ethiopia Urbanization Review: Urban Institutions for A Middle-Income Ethiopia*.

World Bank. (2021). *Addis Ababa's Strategic Development Framework*.

Xu, J., Dai, J., Wu, X., Wu, S., Zhang, Y., Wang, F., Gao, A., and Tan, Y. (2023). Urban rainwater utilization: A review of management modes and harvesting systems. *Frontiers in Environmental Science*, 11. https://doi.org/10.3389/fenvs.2023.1025665

Yang, H., Dick, W. A., McCoy, E. L., Phelan, P. L., and Grewal, P. S. (2013). Field evaluation of a new biphasic rain garden for stormwater flow management and pollutant removal. *Ecological Engineering*, 54, 22-31. https://doi.org/10.1016/j.ecoleng.2013.01.005

Yang, J., Xiang, Y., Xu, X., and Sun, J. (2022). Design hyetograph for short-duration rainstorm in Jiangsu. *Atmosphere*, 13(6). https://doi.org/10.3390/atmos13060899

Yang, W., and Zhang, J. (2021). Assessing the performance of gray and green strategies for sustainable urban drainage system development: A multi-criteria decision-making analysis. *Journal of Cleaner Production*, 293, 126191. https://doi.org/10.1016/j.jclepro.2021.126191

Yang, W., Zhang, J., and Krebs, P. (2022). Low impact development practices mitigate urban flooding and non-point pollution under climate change. *Journal of Cleaner Production*, 347, 131320. https://doi.org/10.1016/j.jclepro.2022.131320

Yang, Y., Zhu, D. Z., Loewen, M. R., Zhang, W., van Duin, B., and Mahmood, K. (2024). Impacts of climate change on urban stormwater runoff quantity and quality in a cold region. *Science of the Total Environment*, 954. https://doi.org/10.1016/j.scitotenv.2024.176439

Yao, Y., Hu, C., Liu, C., Yang, F., Ma, B., Wu, Q., Li, X., and Soomro, S. e. hyder. (2022). Comprehensive performance evaluation of stormwater management measures for sponge city construction: A case study in Gui'an New District, China. *Journal of Flood Risk Management*, 15(4). https://doi.org/10.1111/jfr3.12834

Yao, Y., Li, J., lv, P., Li, N., and Jiang, C. (2022). Optimizing the layout of coupled grey-green stormwater infrastructure with multi-objective-oriented decision making. *Journal of Cleaner Production*, 367, 133061. https://doi.org/10.1016/j.jclepro.2022.133061

Yatsalo, B. I., Kiker, G. A., Kim, J., Bridges, T. S., Seager, T. P., Gardner, K., Satterstrom, F. K., and Linkov, I. (2007). Application of multicriteria decision analysis tools to two contaminated sediment case studies.

Yim, S., Aing, C., Men, S., and Sovann, C. (2016). Applying PCSWMM for stormwater management in the Wat Phnom sub catchment, Phnom Penh, Cambodia. *Journal of Geography, Environment and Earth Science International*, 5(3), 1-11. https://doi.org/10.9734/jgeesi/2016/23525

Yu, J., Min, K. S., and Kim, Y. (2011). Development of EMC-based empirical model for estimating spatial distribution of pollutant loads. *Desalination and Water Treatment*, 27(1-3), 175-188. https://doi.org/10.5004/dwt.2011.2736

Yu, J., Yu, H., and Xu, L. (2013). Performance evaluation of various stormwater best management practices. *Environmental Science and Pollution Research*, 20(9), 6160-6171. https://doi.org/10.1007/s11356-013-1655-4

Yu, Y., Li, Z., Yu, T., Guo, S., Zhou, Y., Li, X., and Zhang, W. (2023). Hydrologic and water quality modelling of bioretention columns in cold regions. *Hydrological Processes*, 37(4). https://doi.org/10.1002/hyp.14871

Yüksel, I., and Dağdeviren, M. (2007). Using the analytic network process (ANP) in a SWOT analysis – A case study for a textile firm. *Information Sciences*, 177(16), 3364-3382. https://doi.org/10.1016/j.ins.2007.01.001

Zahmatkesh, Z., Burian, S. J., Karamouz, M., Tavakol-Davani, H., and Goharian, E. (2015). Low-impact development practices to mitigate climate change effects on urban stormwater runoff: Case study of New York City. *Journal of Irrigation and Drainage Engineering*, 141(1). https://doi.org/10.1061/(asce)ir.1943-4774.0000770

Zakizadeh, F., Moghaddam Nia, A., Salajegheh, A., Sañudo-Fontaneda, L. A., and Alamdari, N. (2022). Efficient urban runoff quantity and quality modelling using SWMM model and field data in an urban watershed of Tehran Metropolis. *Sustainability*, 14(3). https://doi.org/10.3390/su14031086

Zambrano, K. T., Poleto, C., and Oliveira, J. N. (2017). A comparative analysis on water quality in an urban micro watershed. *Management of Environmental Quality*, 28(4), 566-578. https://doi.org/10.1108/MEQ-07-2015-0141

Zeng, J., Lin, G., and Huang, G. (2021). Evaluation of the cost-effectiveness of green infrastructure in climate change scenarios using TOPSIS. *Urban Forestry and Urban Greening*, 64. https://doi.org/10.1016/j.ufug.2021.127287

Zerouali, B., Elbeltagi, A., Al-Ansari, N., Abda, Z., Chettih, M., Santos, C. A. G., Boukhari, S., and Araibia, A. S. (2022). Improving the visualization of rainfall trends using various innovative trend methodologies with time–frequency-based methods. *Applied Water Science*, 12(9), 1-19. https://doi.org/10.1007/s13201-022-01722-3

Zevenbergen, C., Fu, D., and Pathirana, A. (2018). Transitioning to sponge cities: Challenges and opportunities to address urban flooding in China. *Water*, 10(5), 569. https://doi.org/10.3390/w10050569

Zhang, B., Shrestha, N. K., Daggupati, P., Rudra, R., Shukla, R., Kaur, B., and Hou, J. (2018). Quantifying the impacts of climate change on streamflow dynamics of two major rivers of the Northern Lake Erie basin in Canada. *Sustainability*, 10(8). https://doi.org/10.3390/su10082897

Zhang, K., and Chui, T. F. M. (2018). A comprehensive review of spatial allocation of LID-BMP-GI practices: Strategies and optimization tools. *Science of the Total Environment*, 621, 915-929. https://doi.org/10.1016/j.scitotenv.2017.11.281

Zhang, Y., Yin, H., Liu, M., Kong, F., and Xu, J. (2025). Evaluating the effectiveness of environmental sustainability indicators in optimizing green-grey infrastructure for sustainable stormwater management. *Water Research*, 272, 122932. https://doi.org/10.1016/j.watres.2024.122932

Zhang, Y., Zhao, W., Chen, X., Jun, C., Hao, J., Tang, X., and Zhai, J. (2021). Assessment on the effectiveness of urban stormwater management. *Water*, 13(1), 1-20. https://doi.org/10.3390/w13010004

Zheng, Q., Hao, L., Huang, X., Sun, L., and Sun, G. (2020). Effects of urbanization on watershed evapotranspiration and its components in southern China. *Water*, 12(3). https://doi.org/10.3390/w12030645

Zhou, Q. (2014). A review of sustainable urban drainage systems considering the climate change and urbanization impacts. *Water*, 6(4), 976-992. https://doi.org/10.3390/w6040976

Zhou, Q., Leng, G., Su, J., and Ren, Y. (2019). Comparison of urbanization and climate change impacts on urban flood volumes: Importance of urban planning and drainage adaptation. *Science of the Total Environment*, 658, 24-33. https://doi.org/10.1016/j.scitotenv.2018.12.184

Zhran, M., Ghanem, K., Tariq, A., Alshehri, F., Jin, S., Das, J., Pande, C. B., Pramanik, M., Hasher, F. F. Ben, and Mousa, A. (2024). Exploring a GIS-based analytic hierarchy process for spatial flood risk assessment in Egypt: a case study of the Damietta branch. *Environmental Sciences Europe*, 36(1), 184. https://doi.org/10.1186/s12302-024-01001-9

Appendixes

Appendix A: Computational Formulas for Spatial Attributes

A1: Slope (Eq. A.1):

$$S = \left(\frac{\Delta Z}{d}\right) x100 \quad (A.1)$$

Where: S = slope (%), ΔZ = elevation difference (m), d = horizontal distance (m).

A2: Topographic Wetness Index (TWI) (Eq. A.2):

$$TWI = \ln\left(\frac{A_{\mathrm{upslope}}}{\tan(S)}\right) \quad (A.2)$$

Where: $A_{upslope}$ = upslope contributing area per unit contour length (m^2/m), S = slope (radians).

A3: Topographic Position Index (TPI) (Eq. A.3):

$$\mathrm{TPI} = Z_i - \left(\frac{\sum_{i=1}^{n} Z_i}{n}\right) \quad (A.3)$$

Where: Z_i = elevation of target cell (m), Z_j = elevation of neighboring cell (m), n = number of neighboring cells.

A4: Topographic Ruggedness Index (TRI) (Eq. A.4):

$$\mathrm{TRI} = \sqrt{\frac{1}{n}\sum_{i=1}^{n}(Z_i - \bar{Z})^2} \quad (A.4)$$

Where: Z_i = elevation of target cell (m), $\bar{Z}$ = mean elevation in neighborhood (m).

A5: Hillshade (Eq. A.5):

$$\mathrm{HS} = 255\mathrm{xCos}(Z_a)\mathrm{xCos}(Z_e) + 255\mathrm{xSin}(Z_a)\mathrm{xCos}(Z_e)\mathrm{xCos}(A - A_s) \quad (A.5)$$

Where: Z_a = zenith angle, Z_e = slope (radians), A = azimuth angle, A_s = aspect (radians).

A6: Normalized Difference Vegetation Index (NDVI) (Eq. A.6):

$$\mathrm{NDVI} = \frac{\mathrm{NIR-RED}}{\mathrm{NIR+RED}} \quad (A.s6)$$

Where: NIR = near-infrared reflectance, RED = red reflectance.

Appendix B: Expert's Demographics Summary

Appendix Table 1: Expert's demographics summary in pseudonyms

Expert ID	Affiliation	Field of Expertise	Years of Experience
E1	Addis Ababa University	Civil and Environmental Engineering	15

E2	Addis Ababa University	Water and Environmental Engineering	10
E3	Ethiopian Civil Service University	Hydrologist and Hydraulic Engineer	20
E4	Ministry of Water and Energy	Civil Engineer	26
E5	Debre Birhan University	Civil and Environmental Engineering	8
E6	Bahir Dar University	Hydrology	8
E7	College of Technology and Built Environment, Addis Ababa University	Civil and Environmental Engineering	10
E8	College of Technology and Built Environment, Addis Ababa University	Hydraulic Engineering	9
E9	College of Technology and Built Environment, Addis Ababa University	Water Supply Engineering	10
E10	Debre Birhan University	Hydrology	10
E11	Florida International University	Hydrology	11
E12	College of Technology and Built Environment, Addis Ababa University	Hydraulic Engineering	13

Appendix C: AHP and ANP Pair-Wise Comparison Matrix

Appendix Table 2: AHP pair-wise comparison matrix

Pair wise comparison between attributes

	S	**TWI**	**EN**	**TPI**	**TRI**	**LULC**	**SL**	**NDVI**	**HS**	**PW**	**PR**	**PD**
S	1	3	7	5	3	2	1	5	3	3	3	3
TWI	1/3	1	1/2	1	1	1	1/2	1	1	2	3	1/2
EN	1/7	2	1	1	1/5	1	1/3	3	1	2	1/2	1/2
TPI	1/5	1	1	1	1	1	1/2	1	2	1	1	1/3
TRI	1/3	1	5	1	1	1	1/3	3	3	3	3	1
LULC	1/2	1	1	1	1	1	1/3	3	1	1	½	2

SL	1	2	3	2	3	1/3	1	5	3	3	3	3
NDVI	1/5	1	1/3	1	1/3	1/3	1/5	1	1	1	1/3	1/3
HS	1/3	1	1	1/2	1/3	1	1/3	1	1	1/3	1/2	1/2
PW	1/3	1/2	1/2	1	1/3	1	1/3	1	3	1	3	1/3
PR	1/3	1/3	2	1	1/3	2	1/3	3	2	1/3	1	1/2
PD	1/3	1/3	2	3	1	1/2	1/3	3	2	3	2	1

Appendix Table 3: Intra-cluster comparison matrices: ANP

Intra-luster														
TH Cluster						**LUV Cluster**					**SSA Cluster**			
-	**S**	**TWI**	**EN**	**TPI**	**TRI**	-	**LULC**	**SL**	**NDVI**	**HS**	-	**PW**	**PR**	**PD**
S	1	3	7	2	3	**LULC**	1	3	3	7	**PW**	1	3	5
TWI	1/3	1	1/2	1	3	**SL**	1/3	1	3	5	**PR**	1/3	1	3
EN	1/7	2	1	2	3	**NDVI**	1/3	1/3	1	3	**PD**	1/5	1/3	1
TPI	1/2	1	1/2	1	1	**HS**	1/7	1/5	1/3	1	-	-	-	-
TRI	1/3	1/3	1/3	1	1	-	-	-	-	-	-	-	-	-

Appendix Table 4: Cluster-wise comparison matrix: ANP

Between clusters			
	TH	**LUV**	**SSA**
TH	1	3	5
LUV	1/3	1	3
SSA	1/5	1/3	1

Appendix D: LULC Classification Summary

Appendix Table 5: Esri's LULC classification summary

Class Code	Class Name	Validation Points	Coverage Percentage (%)
7	Urban Area	142	69.6
5	Crops	44	21.6
2	Trees	12	5.9
11	Rangeland	6	2.9
1	Water	0	0

4	Flooded Vegetation	0	0
8	Bare ground	0	0
9	Snow/Ice	0	0
10	Clouds	0	0

Appendix E: Overall Attributes Summary

Appendix Table 6: Summary of attribute suitability ranges

Attribute	Highly Suitable (Score 1-2)	Unsuitable (Score 4-5)
Slope (%)	<5% (24.2% of area)	>10% (42.6% of area)
TWI	>6.83 (21.3% of area)	<5.63 (34.7% of area)
Elevation (m)	<2,264 (38.4% of area)	>2,704 (20.7% of area)
LULC	Water, trees, vegetation (8.4% of area)	Urban (69.6% of area)
Soil	Eutric Nitisols (21.2% of area)	Vertisols (61.0% of area)
NDVI	>0.2658 (12.3% of area)	<0.1658 (58.5% of area)
Proximity to river (m)	<500 (40.7% of area)	>1,500 (16.8% of area)
Proximity to road (m)	<500 (56.9% of area)	>1,500 (17.2% of area)
Population density (persons/km^2)	<6,664 (74.8% of area)	>12,757 (7.8% of area)

Note: Scores based on five-level classification (1 = very high suitability, 5 = very low suitability). Full detailed table available from the author upon request.

Appendix F: Stormwater Infrastructure Performance Evaluation – Kobo Toolbox Form

🔗 **Form Link**: https://ee.kobotoolbox.org/x/uhHl3y1w

F1: Purpose

This form is designed for expert data collectors to evaluate and document the functional condition of stormwater management infrastructure in the field. The assessment supports performance benchmarking and prioritization for maintenance or GI retrofitting.

F2: Assessment Coverage

Each expert is expected to assess **two to four distinct stormwater infrastructure units** per session. Each unit should be clearly identified using a unique code (e.g., $\mathbf{I_1}$, $\mathbf{I_2}$, $\mathbf{I_3}$, … $\mathbf{I_n}$) in the **Infrastructure Unit ID** field.

F3: Form Components (Five Blocks)

The evaluation includes the following five structured blocks:

1. **Metadata**

Surveyor Name, Date of Assessment (auto), Start/End Time (auto), and Infrastructure Unit ID.

2. **Location**

Auto-captured GPS coordinates and at least one photo of the infrastructure.

3. **Infrastructure Characteristics**

Type of structure, drainage function, material composition, slope category, and observed maintenance status.

4. **Performance Criteria Evaluation**: Each criterion is rated on a **1 to 3 ordinal scale**, where:

3 = Good

2 = Fair

1 = Poor

The five performance criteria are:

C_1: Flood Conveyance Capacity

C_2: Structural Integrity

C_3: Erosion Control Effectiveness

C_4: Sediment Accumulation *(Cost criterion: lower score is better)*

C_5: Maintenance Accessibility

5. **Additional Observations (Optional)**

Space for expert notes and additional images, as needed.

Appendix G: Field Protocol for Infrastructure Assessment

The following protocol was followed by the two experts who collected field-based infrastructural data:

1. At each designated block, identify and register 5–7 representative infrastructure units covering dominant typologies present.
2. For each unit, complete all five of the six performance criteria (C1–C5) ratings based on expert judgment using the standardized Kobo Toolbox form.
3. Capture GPS coordinates and at least two photographs per unit (upstream and downstream views).
4. Assign a unique identifier code for each infrastructure unit (e.g., B1-I1, B1-I2, ... B5-I6).

5. Record any qualitative notes, anomalies, or context-specific observations in the comments field.
6. Conduct assessments within 48 hours following a storm event to capture post-event conditions accurately.
7. Both experts should assess units independently; scores will be averaged to reduce subjectivity.

Appendix H: AHP Expert Weight Assignments from Kobo Toolbox

H1: Expert Demographic Background with Pseudonyms

Appendix Table 7: Expert demographics summary with pseudonyms

Expert ID	Affiliation	Field of expertise	Years of experience
Expert 1	Addis Ababa University	Civil and environmental engineering	15
Expert 2	Addis Ababa University	Water and environmental engineering	10
Expert 3	Ethiopian Civil Service University	Hydrologist and hydraulic engineering	20
Expert 4	Ministry of Water and Energy	Civil engineering	26
Expert 5	Debre Birhan University	Civil and environmental Engineering	8
Expert 6	Bahir Dar University	Hydrology	8
Expert 7	Addis Ababa University	Civil and environmental engineering	10
Expert 8	College of Technology and Built Environment	Hydraulic engineering	9
Expert 9	College of Technology and Built Environment	Water supply engineering	10
Expert 10	Debre Birhan University	Hydrology	10
Expert 11	Florida International University	Hydrology	11
Expert 12	Addis Ababa University	Hydraulic engineering	13

H2: Expert Based Decision Matrix

Appendix Table 8: Aggregated pairwise comparison matrix of six criteria based on judgments from the 12 experts. The matrix was derived by geometric averaging of individual expert pairwise comparisons, resulting in the weights

	C_1	C_2	C_3	C_4	C_5	C_6
C_1	1	1.25	1.67	2.5	2.5	1.25
C_2	0.8	1	1.33	2	2	1
C_3	0.6	0.75	1	1.5	1.5	0.75
C_4	0.4	0.5	0.67	1	1	0.5
C_5	0.4	0.5	0.67	1	1	0.5
C_6	0.8	1	1.33	2	2	1

H3: Normalized Expert-based Decision Matrix

Appendix Table 9: Normalized expert-based decision matrix

	C_1	C_2	C_3	C_4	C_5	C_6	Rows average (Weight)
C_1	0.25	0.25	0.25	0.25	0.25	0.25	0.25
C_2	0.2	0.2	0.2	0.2	0.2	0.2	0.2
C_3	0.15	0.15	0.15	0.15	0.15	0.15	0.15
C_4	0.1	0.1	0.1	0.1	0.1	0.1	0.1
C5	0.1	0.1	0.1	0.1	0.1	0.1	0.1
C_6	0.2	0.2	0.2	0.2	0.2	0.2	0.2
Total							1

Appendix I: TOPSIS-AHP-PCSWMM-based Performance Ranking

I1: Positive- and Negative-ideal Solutions, Separation Measures, and Relative Closeness and Ranks

Appendix Table 10: Positive- and negative-ideal solutions, separation measures, and relative closeness

Blocks	S+	S-	S_+ + S-	Ci	Rank
Block 1	0.050725	0.097741	0.148466	0.66	2
Block 2	0.070559	0.063907	0.134467	0.48	4

Block 3	0.043891	0.10297	0.146861	0.7	1
Block 4	0.099777	0.075887	0.175665	0.43	5
Block 5	0.086252	0.086451	0.172704	0.5	3
Mean		-	-	0.55	-
STDEVA		-	-	0.12	-

I2: Detailed Field Inspection Scores for all 30 Stormwater Infrastructure Units

Appendix Table 11: Detailed field inspection scores for all 30 stormwater infrastructure units, including block assignment, infrastructure typology, and scores for criteria C_1–C_5

Block	Unit ID	Infrastructure Typology	C_1	C_2	C_3	C_4	C_5
Block 1	B1-I1	Concrete-lined channel	3	3	2	2	3
Block 1	B1-I2	Concrete-lined channel	3	3	2	2	3
Block 1	B1-I3	Pipe	3	2	2	2	3
Block 1	B1-I4	Pipe	2	2	2	2	3
Block 1	B1-I5	Unlined earth ditch	2	2	2	2	2
Block 1	B1-I6	Culvert	3	3	2	2	3
Block 1 Average			**2.67**	**2.5**	**2**	**2**	**2.83**
Block 2	B2-I1	Concrete-lined channel	3	3	2	2	3
Block 2	B2-I2	Concrete-lined channel	3	2	2	2	3
Block 2	B2-I3	Pipe	3	2	2	2	3
Block 2	B2-I4	Pipe	2	2	2	2	3
Block 2	B2-I5	Unlined earth ditch	2	2	2	2	2
Block 2	B2-I6	Culvert	3	2	2	2	3
Block 2 Average			**2.67**	**2.17**	**2**	**2**	**2.83**
Block 3	B3-I1	Rain garden	3	3	3	1	3
Block 3	B3-I2	Rain garden	3	3	3	1	3
Block 3	B3-I3	Concrete-lined channel	3	3	3	1	3
Block 3	B3-I4	Concrete-lined channel	3	3	3	1	3
Block 3	B3-I5	Pipe	3	3	3	1	3
Block 3	B3-I6	Culvert	3	3	3	1	3
Block 3	B3-I7	Unlined earth ditch	3	3	3	1	3
Block 3 Average			**3**	**3**	**3**	**1**	**3**

Block 4	B4-I1	Unlined earth ditch	2	1	2	2	3
Block 4	B4-I2	Unlined earth ditch	2	1	2	2	3
Block 4	B4-I3	Unlined earth ditch	2	1	2	2	3
Block 4	B4-I4	Culvert	2	1	1	2	3
Block 4	B4-I5	Pipe	2	1	2	3	3
Block 4 Average			**2**	**1**	**1.8**	**2.2**	**3**
Block 5	B5-I1	Concrete-lined channel	3	3	3	1	3
Block 5	B5-I2	Concrete-lined channel	3	3	3	1	3
Block 5	B5-I3	Concrete-lined channel	3	3	2	2	3
Block 5	B5-I4	Pipe	3	3	2	2	3
Block 5	B5-I5	Pipe	3	3	2	2	3
Block 5	B5-I6	Culvert	3	3	3	2	3
Block 5 Average			**3**	**3**	**2.5**	**1.67**	**3**

Note: Scores are on a 3-point scale: 3 = Good, 2 = Fair, 1 = Poor. For C_4 (Sediment accumulation), scores are inverted: 1 = minimal buildup (best), 3 = heavy accumulation (worst).

Appendix J: Detailed Design and Hydrological Parameters of IGGI Components

Appendix Table 12: Design and hydrological parameters of IGGI components

Component	Parameter	Value	Source / Design Basis
RG	Location	Upstream	Field layout
	Area	0.1 ha (1,000 m^2)	Field layout
	Soil profile	0.2 m surface ponding + 0.3 m sandy loam + 0.1 m gravel (total 0.6 m)	Al-Sulaiman and Elmarazky (2018); Cui et al., 2020
	Infiltration rate	35 mm/h	Al-Sulaiman and Elmarazky (2018); Cui et al., 2020
	Porosity (*n*)	0.2 (Sandy loam), and 0.25 (Gravel)	Typical sandy loam
	Effective retention (design target)	85 m^3	Surface ponding + subsurface infiltration + RBs
Buried RBs	Location	Downstream	Field layout
	Quantity	5 units	Field observation

	Volume per unit	0.4 m^3	Field layout
	Total storage	2 m^3	Secondary detention / polishing
IGGI System	Design storm	3-hour Chicago hyetograph	Hydrological design criterion
	30% of modeled runoff volume	86 m^3	PCSWMM (used for sizing and comparison)
	Peak flow	0.1236 m^3/s	PCSWMM
	Service area	0.836 ha (40 % of S_{16})	Site survey

Appendix K: The Whole Area Parameter Value Before and After Calibration for Both the First (August 12, 2024) and Second (September 2, 2024) Calibration: Surface Parameter.

Appendix Table 13: S_{16} final calibrated parameters (pre- and post-IGGI)

Parameter	Pre-IGGI Final	Post-IGGI Final	Remarks
Area (ha)	2.092	2.092	Unchanged (GIS-based)
Width (m)	12.8	12.6	Slight reduction to improve Tc
Impervious (%)	72	58	Post-IGGI reduction via GI
N perv	0.06	0.058	Slight roughening from GI
N imperv	0.01	0.01	Unchanged
C61 (geom1, m)	0.95	0.95	Unchanged (no structural works)
C27-29 (geom1, m)	0.48-0.6	0.48-0.6	Minor routing adjustments
Roughness (C61)	0.0116	0.0116	Unchanged
RB capacity (m^3)	—	2.01	Added post-IGGI
RG depth (m)	—	1.0	Added post-IGGI

Note: Pre-IGGI calibration used storm events on August 12 and September 2, 2024. Post-IGGI calibration used events on June 22, June 28, July 15, July 30, and August 10, 2025. Performance metrics are reported in Section 6.3.1.

Appendix L: Detailed Stormwater Quantity and Quality Balance Pre- and Post-IGGI

Appendix Table 14: Summary of stormwater quantity and quality balance

Parameter	Pre-IGGI (2-y)	Pre-IGGI (10-y)	Post-IGGI (2-y)	Post-IGGI (10-y)
Water Balance				
Total Precipitation (m^3)	6,870	8,850	6,870	8,850
Surface Runoff (m^3, %)	4,850 (71%)	6,690 (76%)	3,080 (45%)	4,820 (54%)
Infiltration Loss (m^3, %)	1,550 (23%)	1,580 (18%)	1,430 (21%)	1,460 (16%)
Evaporation + Storage (m^3, %)	560 (8%)	580 (7%)	2,510 (37%)	2,870 (32%)
Continuity Error (%)	-1.42	-1.62	-1.11	-2.63
Pollutant Load Reduction (%)				
Ammonia	—	—	42.1	33.9
BOD	—	—	41.2	32.9
COD	—	—	37.2	28.7
Nitrate	—	—	40.6	32.2
Phosphate	—	—	42.4	33.9

Appendix M: Photographic Examples of the Infrastructural Data Collected

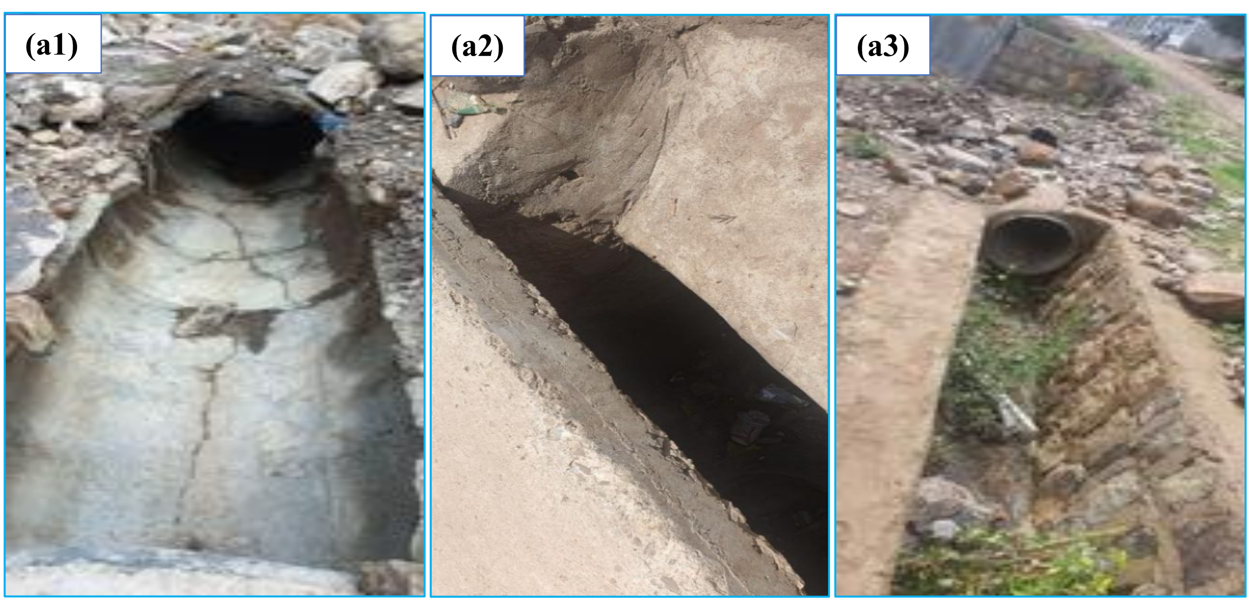

Appendix Figure 1: Photographic examples of "Good," "Fair," and "Poor" conditions for key performance criteria. (a) Structural integrity (C_2): a1 = Good (intact concrete, no cracks), a2 = Fair (minor cracking), a3 = Poor (severe cracking, spalling). (b) Erosion control effectiveness (C_3): b1 = Good (well-vegetated, stable banks), b2 = Fair (minor scouring), b3 = Poor (severe gullying, bank failure). (c) Sediment accumulation (C_4): c1 = Good (<25% blockage), c2 = Fair (25-50% blockage), c3 = Poor (>50% blockage).